

GASEOUS MOTOR FUELS. AN ASSESSMENT OF THE CURRENT AND FUTURE STATUS.
S. S. Sorem, Shell Oil Co., San Francisco, Calif., et al.

The Engine Fuels Subcommittee of the API Committee of Environmental Affairs undertook an assessment of published information on the potential impact of adoption of gaseous fuels to reduce automotive emissions from existing and future motor vehicles as a means of achieving improved air quality in the 1975-80 period. The major considerations of vehicle emissions, fuel and equipment costs and availability, and overall impact on emissions from all sources provided the basis for the report. This study found that with favorable costs for the gaseous fuels and favorable fuel tax consideration coupled with fuel availability, and inherently lower maintenance, converted fleets can show an economic advantage. Conversion of older models to gaseous fuels can result in reduced emissions for those vehicles, but will not realize significant benefit for the current (1973) model vehicles, nor those anticipated to meet the 1975-76 Federal standards. Therefore, the impact of such conversion on air quality is expected to have marginal impact in the 1975-80 period. If the gasoline engine can meet or even approach the 1975-76 emissions limits, conversion of earlier models to gaseous fuels will not provide improved air quality during the next decade except under very special environmental and economic conditions.

FUEL VOLATILITY AS AN ADJUNCT TO AUTO EMISSION CONTROL. R. W. Hurn, Dennis B. Eccleston, and Barton H. Eccleston, U.S. Department of Interior, Bureau of Mines, P.O. Box 1398, Bartlesville, Okla. 74003

Late-model vehicles were used in an experimental study of the interaction of fuel volatility with emissions and associated fuel economy. Volatility characteristics of the test fuels ranged between 7 and 14 pounds Reid vapor pressure; between 130° and 240° F 50% point; and between 190° and 370° F 90% point. Choke settings of each vehicle were adjusted as needed for choke action appropriate to each fuel's volatility.

Midrange and back-end volatility were found to influence emissions significantly. The principal influence is upon emissions during cold start and warmup. Results show that, in general, hydrocarbon and carbon monoxide emissions are reduced by increasing either, or both, midrange and back-end volatility. Fuel economy during starting and warmup also was improved by increasing volatility in the midrange and back-end portion of the boiling curve. Within the vapor pressure limits traditional of U.S. fuels, vapor pressure and fuel front-end volatility were found to have only slight effect upon either emissions or fuel economy.

Pre-engine Converter

N. Y. Chen and S. J. Lucki

Mobil Research and Development Corporation
Princeton and Paulsboro Laboratories
Princeton and Paulsboro, N. J.

I. INTRODUCTION

During the past decade, efforts to reduce vehicular pollutant emission have included suggestions for the removal of lead from gasoline or for use of alternative fuels such as H₂ and low molecular weight hydrocarbons which are known to have high octane values and good burning characteristics (1), (2). Lead removal, which is already being implemented, raises the octane requirement of the fuel. The increased severity required in refining to produce such high octane gasoline decreases the gasoline yield per barrel of crude and, therefore, increases crude oil consumption and demands more refining capacity in the face of an impending energy crisis. Use of low molecular weight hydrocarbons is difficult to implement because of safety hazards and lack of nationwide storage and distribution systems.

The concept of attaching a catalytic reactor to an internal combustion engine converting liquid hydrocarbons to gaseous fuel was disclosed in a patent issued to Cook (3) in 1940. Recently, it has received some renewed attention. Newkirk *et al* (2) described their concept of an on-board production of CO₂/H₂ mixture by steam reforming of gasoline fuel. A U.S. patent was issued to W. R. Grace Company in 1972 (4) on a mobile catalytic cracking unit in conjunction with a mobile internal combustion engine. In 1973, Siemens Company (5) of Germany announced a "splitting carburetor" which breaks up gasoline and related fuels into burnable gases. The jet propulsion laboratory of NASA (6) is investigating the concept of the generation of hydrogen for use as an additive to gasoline in internal combustion engines.

While little technical data are available, these developments appear to represent different approaches of adapting established industrial catalytic processes designed for a narrow range of operating conditions to moving vehicles which must operate from idling to full throttle.

To design a reactor system capable of operating satisfactorily under full throttle conditions requires either a large reactor or an unusually active and efficient catalyst. A standard 300 cu. in. automotive engine at full throttle consumes fuel at a rate of about 10 cc/sec. If the reactor were operating at 1-2 LHSV (vol/vol/hr.), i.e., at the throughput of an average industrial reactor, the engine would require a catalyst bed volume of 18-36 liters (4.8 - 9.5 gallons) - far larger than the carburetor it replaces. The necessity of a multi-reactor system for continuous operation plus accessory devices including the fuel preheater, etc., would make the system impractically bulky and too slow to warm up. Therefore, a workable system clearly depended on the discovery of new catalysts of high activity. To reduce the size of the reactor to that of a carburetor, an increase in catalytic activity by a factor of at least 50-100 is necessary.

In addition to the problem of the catalytic reactor volume, the life of the catalyst is also of critical importance. Most industrial catalysts require periodic oxidative regeneration in a matter of minutes after operation to maintain their effectiveness. A catalytic cracking catalyst, such as that proposed in the patent issued to Grace (4), requires frequent regeneration. An example described in this patent states that with a zeolite-containing catalyst, 2% of the fuel was converted to coke in the catalytic converter. We estimate that under the proposed operating conditions, each volume of catalyst could process no more than 10 volumes of fuel before sufficient coke (20%) would have deposited on the catalyst to deactivate it. Thus, even if the catalyst were active enough to operate at 100 LHSV, no more than 6 minutes of continuous operation between oxidative regenerations would be feasible.

In this paper we present experimental studies with a catalyst that overcomes many of these limitations.

II. EXPERIMENTAL

1. Equipment

To demonstrate the performance of the new catalyst system, the catalytic reactor was attached to a standard motor knock Test Engine, Method IP44/60 (7), bypassing the carburetor. Figure 1 shows a schematic diagram of the catalytic unit. The reactor consisted of two 3/4 inch O.D. x 18 inches stainless steel cylinders mounted vertically, one on top of the other, and connected in series. The top chamber serving as the preheater contained 82 cc of 3 mm diameter glass beads; the catalyst bed (5 inches long) in the bottom chamber consisted of 24 cc of 20/30 mesh catalyst mixed with 12 cc of 8/14 mesh Vycor chips. During thermal runs, Vycor chips were substituted for the catalyst.

Both cylinders were electrically heated. Liquid fuel flow was metered with a rotameter. Air-fuel ratio was monitored by Orsat analysis of the exhaust.

2. Test Fuels

Two types of feedstocks were used: (1) an 86 research octane (R+O) and 79.5 motor octane (M+O) reformat obtained from Mobil's Paulsboro Refinery containing: 23.4 wt. % n-paraffins, 33.9% branched paraffins, 1.2% olefins, 1.0% naphthenes and 40.5% aromatics, and (2) a Kuwait naphtha of 40.5 clear motor octane (M+O).

III. RESULTS AND DISCUSSIONS

(1) Upgrading of a C₅-400°F reformat

The experiments were carried out by charging the liquid fuel stored in a pressurized reservoir (4500 cc) at 38 cc/min. continuously for about 2 hours through the catalytic converter during which time the motor octane number of the reactor effluent was determined every 30 minutes. At the end of 2 hours, the reactor was cooled to 800°F with purge nitrogen while the fuel reservoir was being refilled. The experiment was then repeated. Two catalysts were examined, viz., a

new stable zeolite catalyst (12 gms) and a commercial zeolite cracking catalyst (16 gms), which had previously been aged for 2 hours in a test described later. The feed rate corresponds to a weight hourly space velocity of 140 and 93, respectively. The reactor was maintained at between 910 and 920°F. Octane rating of the reactor effluent as a function of the cumulative on-stream time is shown in Figure 2. During the first 2 hours, the stable zeolite raised the octane number from the thermal value of 79.6 to 85 M+O. The octane dropped 2 numbers during the next two hours and maintained above 82 M+O for the next seven hours. The aged commercial zeolite catalyst, on the other hand, produced no appreciable conversion under the experimental conditions, i.e., at this high space velocity.

(2) Upgrading of a C₆-350 Kuwait naphtha

After 12 hours of operation without regeneration using reformat as the feed, the fuel was switched to the low octane virgin naphtha and the test continued over the aged stable zeolite catalyst for an additional two 2-hours runs before the experiment was terminated due to a mechanical malfunction. The result of the naphtha test is summarized in Figure 3. Shown in the same figure are the results over a fresh Durabead 8 catalyst and the thermal run. It is interesting to note that a boost of 22 motor octane numbers was registered by the aged stable zeolite catalyst while the fresh commercial zeolite cracking catalyst and the thermal run recorded a gain of only 10 and 6 numbers, respectively.

(3) Shape Selective Cracking

In addition to their excellent burning qualities, i.e., non-polluting combustion, light hydrocarbons have volume blending octane ratings ranged between 100 and 150 research clear numbers (R+O). Thus low octane liquids such as virgin naphtha and mildly reformed reformat can be upgraded by partially converting them to light hydrocarbons in the pre-engine converter, and feeding the entire reactor effluent directly into the engine.

A typical distribution of reaction products is shown in Table I for three samples collected when a blend of C₆ hydrocarbons was passed over the stable zeolite catalyst at 1 atm. and 900°F. The results clearly show that the catalyst exhibited preferential shape selective cracking in the order of n- > monomethyl- > dimethyl-paraffins. Thus isomers having the lower octane ratings are preferentially cracked. The C₄ minus cracked products are highly olefinic and some C₇⁺ aromatics are formed by secondary reactions.

The added advantage of shape selective cracking in the order of octane rating is illustrated by the cracking of a 61 research octane Udex raffinate, a low octane product from the solvent extraction of aromatics from a reformat. In Figure 4, curve I shows the calculated octane number of the reactor effluent vs. wt. % liquid cracked to C₄⁻ light hydrocarbons. To produce a 91 R+O fuel, about 49% of the liquid is cracked. Examination of the composition of the raffinate shows that the straight chain paraffins having an average octane rating of 17 R+O represent 27% of the liquid. Curve II shows that when these n-paraffins are selectively cracked, the octane rating of the fuel can be boosted to ~ 90 R+O with only 27% conversion. An ideal shape selective cracking

would yield curve III which represents the most efficient route of upgrading. The octane rating of the fuel is boosted to 100 R+O with less than 40% conversion.

(4) Catalyst life and stability toward oxidative regeneration

Preliminary data obtained in bench scale micro-reactor (8) studies using the reformat over both the fresh catalysts and the regenerated catalysts showed that the catalyst was stable toward air regeneration and catalyst activity was restored after regeneration. At 100 WHSV, the catalyst appeared to have a useful cycle life of about 7 hours, corresponding to processing 700 pounds of fuel per pound of catalyst. At lower space velocities, the cycle life appeared to be much longer than 7 hours, although the amount of fuel processed over the same length of operating hours was less than that at 100 WHSV.

IV. CONCLUSIONS

A highly active, stable and shape selective zeolite cracking catalyst overcomes a major problem in the application of the concept of pre-engine conversion to a moving vehicle. The catalyst is active enough to operate at above 100 LHSV and 900°F. The volume of a catalyst bed for a 300 cu. in. engine capable of operating satisfactorily at full throttle would be less than 360 cc - a manageable volume from both size and warm-up considerations. The catalyst has the capacity of processing more than 700 volumes of fuel per volume of catalyst. For a 360 cc catalyst bed, this corresponds to processing 66.5 gallons of fuel or about a driving range of 800 to 1000 miles before air regeneration would be necessary. The catalyst appears stable toward oxidative regeneration and its catalytic activity can be fully restored. Since the required volume of catalyst bed is small enough, segmented or multiple reactors could be used to accomplish cracking operation and regeneration at all times.

LITERATURE CITED

1. Corbeil, R. J. and Griswold, S. S., Proc. Int. Clean Air Congr., 2nd 1970, p. 624 (1971).
2. Newkirk, M. S. and Abel, J. L., paper No. 720670 presented at New England Section Meeting, Society of Automotive Engineers, November 2, 1971. Also U.S. Patent 3,682,142 assigned to International Materials Corp., August 8, 1972.
3. U.S. Patent 2,201,965 to John T. Cook, May 21, 1940.
4. U.S. Patent 3,635,200 assigned to W. R. Grace and Company, January 18, 1972.
5. New York Times, February 11, 1973.
6. New York Times, September 17, 1973.
7. IP Standard for Petroleum and its Products, Part II, 2nd Ed. Inst. Petrol., London, 1960.
8. Chen, N. Y. and Lucki, S. J., Ind. Eng. Chem. Process Des. Develop. 10, 71 (1971).

TABLE I
Product Distribution at 900°F

Wt. %	Feed	WHSV			% Conversion		
		55	100	200	55	100	200
Methane	--	0.6	0.4	0.2			
Ethane, Ethene	--	3.3	2.5	0.8			
Propane	--	9.7	6.1	1.1			
Propene	--	7.0	5.8	3.6			
Butanes	--	2.1	1.5	0.3			
Butenes	--	3.1	2.6	2.0			
2,2-Dimethylbutane	9.1	8.6	8.6	8.6	5.5	5.5	5.5
2,3-Dimethylbutane	5.4	5.4	5.4	5.4	0.0	0.0	0.0
2-Methylpentane	13.5	8.5	10.7	11.7	37.0	20.7	13.3
Hexane, 1-hexene	24.5	6.9	10.4	16.1	71.8	57.6	34.3
Benzene	47.5	38.1	40.8	44.4	19.8	14.1	6.5
C ₇ ⁺ Aromatics	--	6.7	5.1	5.6			
R+O	77.1	96.8	92.0	84.5			
ΔON	--	19.7	14.9	7.4			
C ₄ ⁻ % Conversion	--	25.8	18.9	8.0			
ΔON/ % Conversion	--	0.76	0.79	0.93			

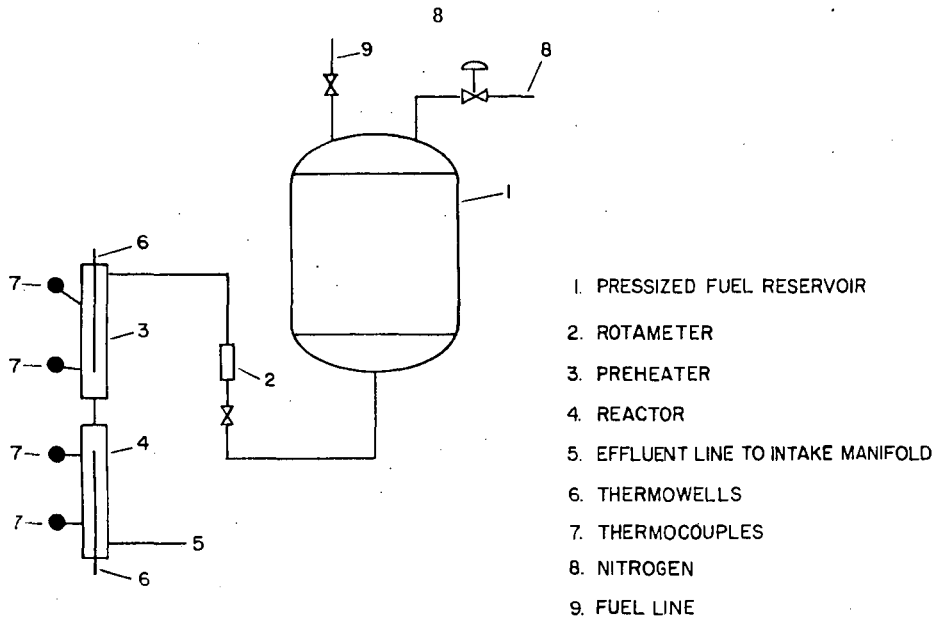


Fig. 1 SCHEMATIC DIAGRAM OF UNIT

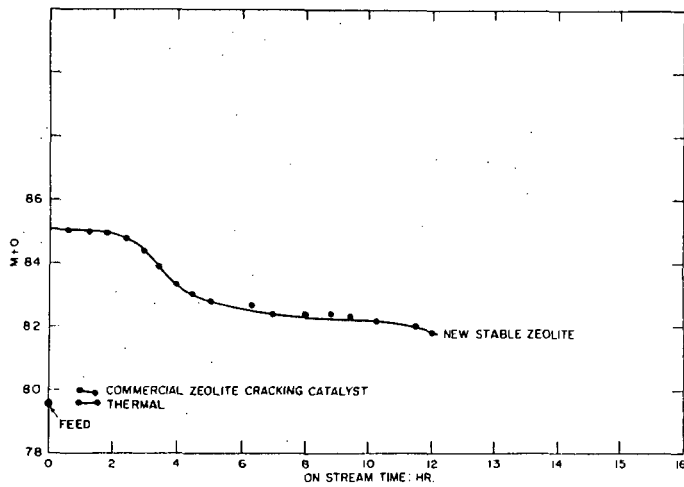


Fig 2 EFFECT OF ON STREAM TIME ON OCTANE RATING - KNOCK TEST ENGINE
 79.5 M+O C₂-400 REFORMATE
 915°F 95 LHSV

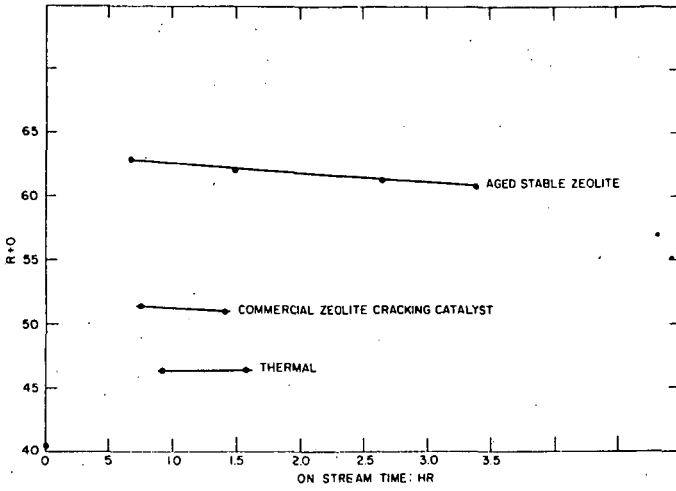


Fig 3 EFFECT OF ON STREAM TIME ON OCTANE RATING
 405 M+O KUWAIT NAPHTHA
 915°F 95 LHSV

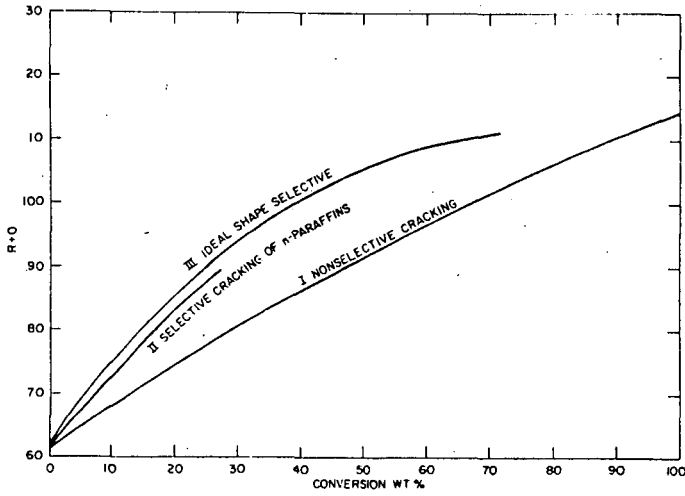


Fig 4 OCTANE RATING vs. CONVERSION LEVEL

Emission Control and Fuel Economy

L. E. Furlong, E. L. Holt, and L. S. Bernstein

Esso Research and Engineering Company
Linden, New Jersey

Extended Abstract

For at least the near term future, the conventional piston engine will continue to be the dominant automobile power plant. The two major factors to which it must respond are emission standards and fuel economy. Since these two factors are closely linked, we have made a theoretical and experimental study of fuel economy as a function of emission standards for a variety of catalytic and thermal control systems applied to the piston engine.

Theoretical Considerations

Factors affecting fuel economy and emissions can be divided into those external to the engine and those internal. For this paper, all external factors will be assumed constant, with vehicle weight, the most important of these, held at 4000 lbs.

Internal factors having significant effects include air-fuel ratio, compression ratio, spark timing, exhaust gas recycle, and load factor. Each will be discussed in turn and the entire discussion summarized by relating fuel economy to emission standards for several emission control systems.

Peak fuel economy is obtained at air-fuel ratios slightly leaner than the stoichiometric value. The region of 16-16.5 lbs. of air per lb. of fuel generally is the optimum. Richer mixtures release less of the fuel's available heat of combustion while leaner mixtures are increasingly difficult to burn at the optimum time. Additionally, dilution with fuel or air lowers peak flame temperature. Maximum production of nitrogen oxides occurs at about the same air-fuel ratio as maximum fuel economy, since both are functions of peak flame temperature. Carbon monoxide and unburned hydrocarbon emissions decrease with increasing air-fuel ratio, although a practical limit is reached with conventional systems at about 18, where mis-fire begins and hydrocarbon emissions turn up again.

Increasing compression ratio allows more efficient use to be made of the heat energy in fuel. For example, at constant performance, an increase in C. R. from 8:1 to 9:1 would improve fuel economy 5 - 6 %. However, the higher peak flame temperatures associated with this change would also produce an increase in nitrogen oxide production.

Engine load is another important parameter affecting fuel economy. The greatest relative economy is obtained at wide open throttle operation. At any reduced load (reduced intake manifold pressure) the engine must work harder to pump the air-fuel charge into the cylinders. These pumping losses are a minimum at full-load operation. In practice, maximum fuel economy is not obtained at a vehicle's top speed, since increased wind resistance and road friction losses more than compensate for increased engine efficiency. However, for a given vehicle weight at a given speed, a small engine operating closer to full load will have better fuel economy than a large engine throttled back.

Exhaust gas recycle is commonly used to reduce nitrogen oxide formation. It functions by lowering peak flame temperatures and thus might be expected to harm fuel economy. However, because EGR requires an increased intake manifold pressure (wider throttle opening) to maintain constant power output, the engine has less pumping and throttling losses and can compensate for most of the efficiency lost by lower peak flame temperatures. In order to take maximum advantage of this trade-off, it must be borne in mind that EGR also decreases flame speed. Therefore, spark tim-

ing must be advanced to allow proper combustion time. Spark timing must also be adjusted for changes in air-fuel ratio as flame speed also changes with this parameter.

The foregoing has discussed peak flame temperature as related to fuel economy and nitrogen oxide formation. It is also necessary to consider a related parameter, exhaust gas temperature, and its relation to emission control. Generally, the higher the peak flame temperature, the more heat energy which can be extracted from the combustion chamber, hence the lower the exhaust gas temperature. However, in order to control emissions by homogeneous or heterogeneous reactions outside of the engine, high temperatures are desirable. Thus we must examine the balance between temperature and emission control.

Thermal reactors require temperatures in excess of 1500°F to achieve satisfactory homogeneous control of carbon monoxide and hydrocarbons to the most stringent statutory levels. Normal exhaust gas temperatures are in the 1000°F range. Therefore, a substantial increase in exhaust temperature or in available heat of combustion in the exhaust is required for these devices. The most fuel economical method of supplying the needed heat is to richen the air-fuel ratio. This will supply excess carbon monoxide and hydrocarbons, which, when combusted in the reactor, will maintain it at its operating temperature.

Practical considerations militate against using this approach solely, so a combination of enrichment and spark retard, which also increases exhaust temperature, but at a greater fuel economy penalty, is necessary. A third method, lowering the compression ratio, imposes a still higher fuel penalty. Fuel economy debits of 20 - 25% compared to uncontrolled cars are typical for thermal reactors controlling emissions to the stringent statutory levels of 3.4 g/mi. of CO and 0.41 g/mi. of HC.

On the other hand, catalytic oxidation of carbon monoxide and hydrocarbons proceeds efficiently at temperatures associated with normal exhaust temperatures. Thus fuel economy debits of the type associated with thermal reactors are not necessary. The engine can be tuned for maximum operating efficiency without regard to exhaust temperatures. Therefore, oxidation catalysts allow decoupling of emission control from engine operation.

Unfortunately, catalytic reduction of nitrogen oxide is not as independent of engine operation as is catalytic oxidation of carbon monoxide and hydrocarbons. The reduction catalyst requires a reducing atmosphere, hence the engine must be run at an air-fuel ratio richer than stoichiometric. This means a fuel penalty will be incurred compared to an uncontrolled car even if all other engine parameters are optimized. In addition, most reduction catalysts require operating temperatures in excess of normal exhaust levels, so further inefficiencies would be necessary. It would be desirable to have a reduction catalyst capable of efficient conversion at normal exhaust gas temperatures. Ruthenium-containing catalysts have this potential, but to date neither they nor their high temperature base metal counterparts have exhibited satisfactory durability.

In summarizing all of these considerations, we can compare a pre-control, 1967, 4000 lb. vehicle in fuel economy with that predicted for vehicles equipped with thermal or catalytic control systems to meet several emission standards. First, a 1974 vehicle relying on engine modifications only, including a compression ratio of 8.2:1, to meet this year's standards shows approximately a 14% debit in fuel economy. Thermal reactor vehicles, which can tolerate leaded fuel and therefore operate at compression ratios of 10:1, could meet the 1974 standards with about a 6% debit and the 1975 United States interim standards for carbon monoxide and hydrocarbons with about a 12% debit. In meeting the more stringent California interim and future U. S. standards, rich thermal reactors are required and the debit should rise to the 20 - 22% level. Finally, if the statutory 1977 nitrogen oxide level of 0.4 g/mi. is to be achieved with a thermal system, the debit should reach approximately 25%.

Catalytic systems on the other hand, cannot use leaded fuels. They will therefore be designed with compression ratios in the range of 8:1 to accommodate lower octane unleaded fuels. Even so, their lower operating temperatures should result in better fuel economy. Thus the 1975 interim standards for carbon monoxide and hydrocarbons should be achievable at a fuel economy debit of only about 6% from pre-controlled levels. The more stringent 1976 standards should cause a rise to only

about 8%, and even the 1977 standard for nitrogen oxide will produce only about a 12% debit.

Experimental Results

The relationship between fuel economy and exhaust emissions has been studied with two types of systems. The first uses a noble metal monolithic oxidation catalyst to control hydrocarbon and carbon monoxide emissions and exhaust gas recycle to limit nitrogen oxide emissions. The second system is a dual catalyst configuration, with a reduction catalyst for nitrogen oxide control followed by the oxidation catalyst. Air is injected between the two catalysts to convert the exhaust gas to a net oxidizing composition.

The oxidation catalyst-EGR system was mounted on a 1973 vehicle with a 350 in³ displacement engine. The stock vehicle, equipped with a non-proportional EGR system, gave emissions, in g/vehicle mile as tested on the 1975 Federal Test Procedure, of 21.4 CO, 1.3 HC, and 3.3 NO_x. Its fuel economy over the same test cycle was 10.40 miles per gallon. As modified with oxidation catalysts and a proportional EGR system, that is one responding directly to the exhaust gas flow rate, the test vehicle easily met the 1976 statutory CO and HC standards of 3.4 and 0.41 g/mile respectively. With the timing advanced for good fuel economy, not only was the stock NO_x emission level matched, but a 7% gain in fuel economy was achieved. Retarding the timing lowered NO_x emissions further, but at some cost in fuel economy. Work is continuing in an effort to optimize the factors influencing the NO_x emission-fuel economy trade-off with this system.

The dual catalyst system was mounted in a 1973 vehicle similar to the base car described above. In this case, no EGR was used on the modified car. The reduction catalyst was the GEM reinforced Ni-Cu material made by Gould, Inc. With the dual catalyst configuration, as described earlier, catalyst temperature is the primary determinant of fuel economy and NO_x emissions. The temperature was varied by a combination of air-fuel ratio and spark timing control. The statutory 1976 standards for CO and HC emissions were met at all temperatures, but NO_x was dependent on catalyst temperature. At an average catalyst temperature around 1100°F., an emission level of 1.7 g/mile was achieved, with fuel economy comparable to the unmodified vehicle. At 1200°F., NO_x emissions were controlled to 0.9 g/mile, but a fuel economy debit of 4% was incurred. Finally, the 1977 statutory standard of 0.4 g/mile was reached at 1300°F., with a fuel economy debit of 10%.

IMPACT OF AUTOMOTIVE TRENDS AND EMISSIONS REGULATIONS ON GASOLINE DEMAND. Dayton H. Clewell, Mobil Oil Corporation, 150 East 42nd Street, New York, N. Y., 10017. William J. Koehl, Mobil Research and Development Corporation, Research Department, Paulsboro Laboratory, Paulsboro, N. J., 08066.

Gasoline demand has increased steadily in recent years because of growth in vehicle registrations and miles traveled and because of trends in vehicle designs and equipment, among which emission controls are most notable. Through 1985, gasoline demand is projected to increase about 50%, and maybe substantially more depending on the emission controls required. In view of increasing demand and tightening supplies for energy in all forms, four alternatives are explored for moderating the growth in demand for gasoline. These alternatives are: (1) optimizing the energy cost of vehicle emission standards against the emissions reduction needed to achieve the ambient air quality standards; (2) increasing the use of smaller, more economical cars; (3) using more efficient engines; and (4) increasing the use of public transportation. Each can contribute to energy conservation; no one is the whole answer. The benefits of optimum standards can be assured by prompt government action. The trend toward smaller cars is already growing. Introduction of alternate engines requires a long lead time. Mass transportation could be most beneficial in metropolitan areas.

INFLUENCE OF FUEL COMPOSITION ON TOTAL ENERGY RESOURCES

W. A. Bailey, Jr. and G. P. Hinds, Jr.

Shell Development Company, MTM Process R&D Laboratory, P.O.Box 100, Deer Park, Tx 77536

Combustion fuels are essentially limited to compounds of carbon, hydrogen and oxygen by the requirement that combustion products be non-offensive and biodegradable. Properties of these compounds are determined by their chemical structure, but can often be related in a gross way to their hydrogen to carbon ratio. The quality of fuels for continuous combustion decreases with the hydrogen to carbon ratio, and the hydrogen content of a crude petroleum limits the amounts of preferred fuel oils that can be made from it. Also, the removal of impurities such as sulfur, nitrogen, etc., from fuels at present requires the use of hydrogen. Other potential raw materials - shale, coal, etc. - are poorer in hydrogen, and thus future fuel manufacture will require the manufacture of this element in relatively pure form.

The production of hydrogen from water, the most probable source, requires the expenditure of energy, and thus improving fuel quality reduces the total energy resources availability. For various specific situations, e.g., coal conversion, the magnitude of this effect can be calculated, and these calculations may aid in emphasizing areas of desirable compromises among fuel quality, combustor or engine design, and emission regulations.

Low Emissions Combustion Engines
for Motor Vehicles

Henry K. Newhall

Chevron Research Company
Richmond, California 94802

During the past 10-15 years, very significant advances in controlling exhaust emissions from automobile power plants have been made. Initially, emissions reductions were achieved through careful readjustment and control of engine operating conditions (1). More recently, highly effective exhaust treatment devices requiring a minimum of basic modification to the already highly developed internal combustion engine have been demonstrated. These are based on thermal and/or catalytic oxidation of hydrocarbons (HC) and carbon monoxide (CO) in the engine exhaust system (2,3,4). Nitrogen oxide (NO_x) emissions have been reduced to some extent through a combination of retarded ignition timing and exhaust gas recirculation (EGR), both factors serving to diminish severity of the combustion process temperature-time history without substantially altering design of the basic engine (5).

Basic combustion process modification as an alternative means for emissions control has received less attention than the foregoing techniques, though it has been demonstrated that certain modified combustion systems can in principle yield significant pollutant reductions without need for exhaust treatment devices external to the engine. Additionally, it has been demonstrated that when compared with conventional engines controlled to low emissions levels, modified combustion processes can offer improved fuel economy.

Nearly all such modifications involve engine designs permitting combustion of fuel-air mixtures lean beyond normal ignition limits. As will be shown, decreased mean combustion temperatures associated with extremely lean combustion tend to limit the rate of nitric oxide (NO) formation and, hence, the emission of NO_x. At the same time, the relatively high oxygen content of lean mixture combustion products tends to promote complete oxidation of unburned HC and CO provided that combustion gas temperatures are sufficiently high during late portions of the engine cycle.

The purpose of this paper is to present an overall review of the underlying concepts and current status of unconventional engines employing modified combustion as a means for emissions control. Detailed findings related to specific power plants or to specific applications will be treated by the papers which follow.

Throughout the paper exhaust emissions will be compared with emissions standards legislated for the years 1975 and 1976. As a result of Environmental Protection Agency (EPA) actions suspending the 1975 HC and CO standards and the 1976 NO_x standard, several sets of values exist. These are listed in Table I and in the text will be referenced either as statutory (original standards as set by the Clean Air Act Amendment of 1970) or as interim standards as set by the EPA.

Theoretical Basis for
Combustion Modification

Figure 1 has been derived from experimental measurements (6) of the rate of NO formation in combustion processes under conditions typical of engine operation. This figure demonstrates two major points related to control of NO_x emissions: First, the slow rate of NO formation relative to the rates of major combustion reactions responsible for heat release and, second, the strong influence of fuel-air equivalence ratio on the rate of NO formation.

Experimental combustion studies (7) employing "well-stirred reactors" have shown that hydrocarbon-air combustion rates can be correlated by an expression of the form

$$\frac{N}{V p^{1.8}} = 48 \frac{\text{Gram-Moles/Liter-Second}}{\text{Atm}^{1.8}}$$

where:

N = moles reactants consumed per second
V = combustion volume
p = total pressure

For conditions typical of engine operation, this expression yields a time of approximately 0.1 ms for completion of major heat release reactions following ignition of a localized parcel of fuel-air mixture within the combustion chamber. Comparison with Figure 1 shows that the time required for formation of significant amounts of NO in combustion gases is at least a factor of 10 greater. Thus, in principle, energy conversion can be effected in times much shorter than required for NO formation. In the conventional spark ignition engine, the relatively lengthy flame travel process permits combustion products to remain at high temperatures sufficiently long that considerable NO formation occurs.

Figure 2, which consolidates the data of Figure 1, indicates that maximum rates of NO formation are observed at fuel-air equivalence ratios around 0.9 (fuel lean). For richer mixtures, the concentrations of atomic and diatomic oxygen, which participate as reactants in the formation of NO in combustion gases, decrease. On the other hand, for mixtures leaner than approximately 0.9 equivalence ratio, decreasing combustion temperatures result in lower NO formation rates.

Figure 2 serves as a basis for combustion process modification. Operation with extremely rich fuel-air mixtures (Point A of Figure 2), of course, results in low NO_x emissions since the maximum chemical equilibrium NO level is greatly reduced under such conditions. However, the resultant penalties in terms of impaired fuel economy and excessive HC and CO emissions are well known. An alternative is operation with extremely lean mixtures (Point B), lean beyond normal ignition limits. Combustion under such conditions can lead to low NO_x emissions while at the same time providing an excess of oxygen for complete combustion of CO and HC.

Operation of internal combustion engines with extremely lean overall fuel-air ratios has been achieved in several ways, employing a number of differing combustion chamber configurations. One approach

involves ignition of a very small and localized quantity of fuel-rich and ignitable mixture (Point A of Figure 2), which in turn serves to inflame a much larger quantity of surrounding fuel-air mixture too lean for ignition under normal circumstances. The bulk or average fuel-air ratio for the process corresponds to Point B of Figure 2; and, as a consequence, reduced exhaust emissions should result.

A second approach involves timed staging of the combustion process. An initial rich mixture stage in which major combustion reactions are carried out is followed by extremely rapid mixing of rich mixture combustion products with dilution air. The transition from initial Point A to final Point B in Figure 2 is, in principle, sufficiently rapid that little opportunity for NO formation exists. Implicit here is utilization of the concept that the heat release reactions involved in the transition from Point A to Point B can be carried out so rapidly that time is not available for formation of significant amounts of NO.

Reciprocating spark ignition engines designed to exploit the foregoing ideas are usually called stratified charge engines, a term generally applied to a large number of designs encompassing a wide spectrum of basic combustion processes.

Open-Chamber Stratified Charge Engines

Stratified charge engines can be conveniently divided into two types: open-chamber and dual-chamber engines. The open-chamber stratified charge engine has a long history of research interest. Those engines reaching the most advanced stages of development are probably the Ford-programmed combustion process (PROCO) (8) and Texaco's controlled combustion process (TCCS) (9). Both engines employ a combination of inlet air swirl and direct timed combustion chamber fuel injection to achieve a local fuel-rich ignitable mixture near the point of ignition. The overall mixture ratio under most operating conditions is fuel lean.

The Texaco TCCS engine is illustrated schematically in Figure 3. During the engine inlet stroke, an unthrottled supply of air enters the cylinder through an inlet port oriented to promote a specified level of air swirl within the cylinder and combustion chamber. As the subsequent compression stroke nears completion, fuel is injected into and mixes with an element of swirling air charge. This initial fuel-air mixture is spark ignited, and a flame zone is established downstream from the nozzle. As injection continues, fuel-air mixture is continuously swept into the flame zone. The total quantity of fuel consumed per cycle and, hence, engine power output, are controlled by varying the duration of fuel injection. Under nearly all engine operating conditions, the total quantity of fuel injected is on the lean side of stoichiometric. The TCCS system has been under development by Texaco since the 1940's. To date, this work has involved application of the process to a wide variety of engine configurations.

Like the TCCS engine, the PROCO system (Figure 4) employs timed combustion chamber fuel injection. However, in contrast to the TCCS system, the PROCO system is based on formation of a premixed fuel-air mixture prior to ignition. Fuel injection and inlet air swirl are coordinated to provide a small portion of rich mixture near the point of ignition surrounded by a large region of increasingly fuel-lean

mixture. Flame propagation proceeds outward from the point of ignition through the leaner portions of the combustion chamber.

Both the TCCS and PROCO engines are inherently low emitters of CO, primarily a result of lean mixture combustion. Unburned HC and NO_x emissions have been found to be lower than those typical of uncontrolled conventional engines, but it appears that additional control measures are required to meet statutory 1976 Federal emissions standards.

The U.S. Army Tank Automotive Command has sponsored development of low emissions TCCS and PROCO power plants for light-duty Military vehicles. These power plants have been based on conversion of the 4-cylinder, 70-hp L-141 Jeep engine. The vehicles in which these engines were placed were equipped with oxidizing catalysts for added control of HC and CO emissions, and EGR was used as an additional measure for control of NO_x.

Results of emissions tests on Military Jeep vehicles equipped with TCCS and PROCO engines are listed in Table II (10). At low mileage these vehicles met the statutory 1976 emissions standards. Deterioration problems related to HC emission would be expected to be similar to those of conventional engines equipped with oxidizing catalysts. This is evidenced by the increase in HC emissions with mileage shown by Table II. NO_x and CO emissions appear to have remained below 1976 levels with mileage accumulation.

Table III presents emissions data at low mileage for several passenger car vehicles equipped with PROCO engine conversions (10). These installations included noble metal catalysts and EGR for added control of HC and NO_x emissions, respectively. All vehicles met the statutory 1976 standards at low mileage. Fuel consumption data, as shown in Table III, appear favorable when contrasted with the fuel economy for current production vehicles of similar weight.

Fuel requirements for the TCCS and PROCO engines differ substantially. The TCCS concept was initially developed for multifuel capability; as a consequence, this engine does not have a significant octane requirement and is flexible with regard to fuel requirements. In the PROCO engine combustion chamber, an end gas region does exist prior to completion of combustion; and, as a consequence, this engine has a finite octane requirement.

Prechamber Stratified Charge Engines

A number of designs achieve charge stratification through division of the combustion region into two adjacent chambers. The emissions reduction potential for two types of dual-chamber engines has been demonstrated. First, in a design traditionally called the "pre-chamber engine," a small auxiliary or ignition chamber equipped with a spark plug communicates with the much larger main combustion chamber located in the space above the piston (Figure 5). The prechamber typically contains 5-15% of the total combustion volume. In operation of this type of engine, the prechamber is supplied with a small quantity of fuel-rich ignitable fuel-air mixture while a very lean and normally unignitable mixture is supplied to the main chamber above the piston. Expansion of high temperature flame products from the prechamber leads to ignition and burning of the lean main chamber fuel-air charge.

The prechamber stratified charge engine has existed in various forms for many years. Early work by Ricardo (11) indicated that the engine could perform very efficiently within a limited range of carefully controlled operating conditions. Both fuel-injected and carbureted prechamber engines have been built. A fuel-injected design initially conceived by Brodersen (12) was the subject of extensive study at the University of Rochester for nearly a decade (13,14). Unfortunately, the University of Rochester work was undertaken prior to widespread recognition of the automobile emissions problem; and, as a consequence, emissions characteristics of the Brodersen engine were not determined. Another prechamber engine receiving attention in the early 1960's is that conceived by R. M. Heintz (15). The objectives of this design were reduced HC emissions, increased fuel economy, and more flexible fuel requirements.

Initial experiments with a prechamber engine design called "the torch ignition engine" were reported in the U.S.S.R. by Nilov (16) and later by Kerimov and Mekhtier (17). This designation refers to the torchlike jet of hot combustion gases issuing from the precombustion chamber upon ignition. In the Russian designs, the orifice between prechamber and main chamber is sized to produce a high velocity jet of combustion gases. In a recent publication (18), Varshaoski et al. have presented emissions data obtained with a torch engine system. These data show significant pollutant reductions relative to conventional engines; however, their interpretation in terms of requirements based on the Federal emissions test procedure is not clear.

A carbureted three-valve prechamber engine, the Honda Compound Vortex-Controlled Combustion (CVCC) system, has received considerable recent publicity as a potential low emissions power plant (19). This system is illustrated schematically in Figure 6. Honda's current design employs a conventional engine block and piston assembly. Only the cylinder head and fuel inlet system differ from current automotive practice. Each cylinder is equipped with a small precombustion chamber communicating by means of an orifice with the main combustion chamber situated above the piston. A small inlet valve is located in each prechamber. Larger inlet and exhaust valves typical of conventional automotive practice are located in the main combustion chamber. Proper proportioning of fuel-air mixture between prechamber and main chamber is achieved by a combination of throttle control and appropriate inlet valve timing. Inlet ports and valves are oriented to provide specific levels of air swirl and turbulence in the combustion chamber. In this way, a relatively slow and uniform burning process giving rise to elevated combustion temperatures late in the expansion stroke and during the exhaust process is achieved. High temperatures in this part of the engine cycle are necessary to promote complete oxidation of HC and CO. It should be noted that these elevated temperatures are necessarily obtained at the expense of a fuel economy penalty.

Results of emissions tests with the Honda engine have been very promising. The emissions levels shown in Table IV for a number of lightweight Honda Civic vehicles are typical and demonstrate that the Honda engine can meet statutory 1975-1976 HC and CO standards and can approach the statutory 1976 NO_x standard (10). Of particular importance, durability of this system appears excellent as evidenced by the high mileage emissions levels reported in Table IV. The noted deterioration of emissions after 30,000-50,000 miles of engine operation was slight and apparently insignificant.

Recently, the EPA has tested a larger vehicle converted to the Honda system (20). This vehicle, a 1973 Chevrolet Impala with a 350-CID V-8 engine, was equipped with cylinder heads and induction system of Honda manufacture. Test results are presented in Table V for low vehicle mileage. The vehicle met the present 1976 interim Federal emissions standards though NO_x levels were substantially higher than for the much lighter weight Honda Civic vehicles.

Fuel economy data indicate that efficiency of the Honda engine, when operated at low emissions levels, is somewhat poorer than that typical of well-designed conventional engines operated without emissions controls. However, EPA data for the Chevrolet Impala conversion show that efficiency of the CVCC engine meeting 1975-1976 interim standards was comparable to or slightly better than that of 1973 production engines of similar size operating in vehicles of comparable weight. It has been stated by automobile manufacturers that use of exhaust oxidation catalysts beginning in 1975 will result in improved fuel economy relative to 1973 production vehicles. In this event fuel economy of catalyst-equipped conventional engines should be at least as good as that of the CVCC system.

The apparent effect of vehicle size (more precisely the ratio of vehicle weight to engine cubic inch displacement) on NO_x emissions from the Honda engine conversions demonstrates the generally expected response of NO_x emissions to increased specific power demand from this type of engine. For a given engine cubic inch displacement, maximum power output can be achieved only by enriching the overall fuel-air mixture ratio to nearly stoichiometric proportions and at the same time advancing ignition timing to the MBT point. Both factors give rise to increased NO_x emissions. This behavior is evidenced by Table VI, which presents steady state emissions data for the Honda conversion of the Chevrolet Impala (20). At light loads, NO_x emissions are below or roughly comparable to emissions from a conventionally powered 1973 Impala. This stock vehicle employs EGR to meet the 1973 NO_x standard. It is noted in Table VI that for the heaviest load condition reported, the 60-mph cruise, NO_x emissions from the Honda conversion approached twice the level of emissions from the stock vehicles. This points to the fact that in sizing engines for a specific vehicle application, the decreased air utilization (and hence specific power output) of the pre-chamber engine when operated under low emissions conditions must be taken into consideration.

Divided-Chamber Staged Combustion Engine

Dual-chamber engines of another type, often called "divided-chamber" or "large-volume prechamber" engines, employ a two-stage combustion process. Here initial rich mixture combustion and heat release (first stage of combustion) are followed by rapid dilution of combustion products with relatively low temperature air (second stage of combustion). In terms of the concepts previously developed, this process is initiated in the vicinity of Point A of Figure 2. Subsequent mixing of combustion products with air is represented by a transition from Point A to Point B. The object of this engine design is to effect the transition from Point A to Point B with sufficient speed that time is not available for formation of significant quantities of NO. During the second low temperature stage of combustion (Point B), oxidation of HC and CO goes to completion.

An experimental divided-chamber engine design that has been built and tested is represented schematically in Figure 7 (21,22). A dividing orifice (3) separates the primary combustion chamber (1) from

the secondary combustion chamber (2), which includes the cylinder volume above the piston top. A fuel injector (4) supplies fuel to the primary chamber only. Injection timing is arranged such that fuel continuously mixes with air entering the primary chamber during the compression stroke. At the end of compression, as the piston nears its top center position, the primary chamber contains an ignitable fuel-air mixture while the secondary chamber adjacent to the piston top contains only air. Following ignition of the primary chamber mixture by a spark plug (6) located near the dividing orifice, high temperature rich mixture combustion products expand rapidly into and mix with the relatively cool air contained in the secondary chamber. The resulting dilution of combustion products with attendant temperature reduction rapidly suppresses formation of NO. At the same time, the presence of excess air in the secondary chamber tends to promote complete oxidation of HC and CO.

Results of limited research conducted both by university and industrial laboratories indicate that NO_x reductions of as much as 80-95% relative to conventional engines are possible with the divided-chamber staged combustion process. Typical experimentally determined NO_x emissions levels are presented in Figure 8 (23). Here NO_x emissions for two different divided-chamber configurations are compared with typical emissions levels for conventional uncontrolled automobile engines. The volume ratio, β , appearing as a parameter in Figure 8, represents the fraction of total combustion volume contained in the primary chamber. For β values approaching 0.5 or lower, NO_x emissions reach extremely low levels. However, maximum power output capability for a given engine size decreases with decreasing β values. Optimum primary chamber volume must ultimately represent a compromise between low emissions levels and desired maximum power output.

HC and particularly CO emissions from the divided-chamber engine are substantially lower than conventional engine levels. However, further detailed work with combustion chamber geometries and fuel injection systems will be necessary to fully evaluate the potential for reduction of these emissions. Table VII presents results of tests cited by the National Academy of Sciences (10).

Emissions from the divided-chamber engine are compared with those from a laboratory PROCO stratified charge engine, the comparison being made at equal levels of NO_x emissions. NO_x emissions were controlled to specific levels by addition of EGR to the PROCO engine and by adjustment of operating parameters for the divided-chamber engine. These data indicate that the divided-chamber engine is capable of achieving very low NO_x emissions with relatively low HC and CO emissions.

As shown by Table VII, fuel economy of the divided-chamber staged combustion engine is comparable to that of conventional piston engines without emissions controls. When compared with conventional piston engines controlled to equivalent low NO_x emissions levels, the divided-chamber engine is superior in terms of fuel economy.

The Diesel Engine

The diesel engine can be viewed as a highly developed form of stratified charge engine. Combustion is initiated by compression ignition of a small quantity of fuel-air mixture formed just after the beginning of fuel injection. Subsequently, injected fuel is burned in

a heterogeneous diffusion flame. Overall fuel-air ratios in diesel engine operation are usually extremely fuel lean. However, major combustion reactions occur locally in combustion chamber regions containing fuel-air mixtures in the vicinity of stoichiometric proportions.

The conventional diesel engine is characterized by low levels of CO and light HC emissions, a result of lean mixture operation. On a unit power output basis, NO_x emissions from diesel engines are typically lower than those of uncontrolled gasoline engines, a combined result of diffusion combustion and, in an approximate sense, low mean combustion temperatures. Work devoted to mathematical simulation of diesel combustion has shown that NO formation occurs primarily in combustion products formed early in the combustion process, with the later portions of diffusion-controlled combustion contributing substantially less (24).

Table VIII presents emissions levels for three diesel-powered passenger cars as reported by the EPA (25). These vehicles, a Mercedes 220D, Opel Rekord 2100D, and Peugeot 504D, were powered by 4-cylinder engines ranging in size from 126-134 CID with power ratings ranging from 65-68 bhp. Two of the diesel-powered vehicles were capable of meeting the 1975 statutory emissions standards. NO_x emissions were in excess of the original Federal 1976 standards but were well within present interim standards.

The preceding data do not include information on particulate and odorant emissions, both of which could be important problems with widespread diesel engine use in automobiles. Complete assessment of the environmental potential for the diesel engine would have to include consideration of these factors as well as emission of polynuclear aromatic hydrocarbons. All are the subject of ongoing research.

Fuel economy data referred to both 1972 and 1975 Federal test procedures are presented in Table VIII. As expected, diesel engine fuel economies are excellent when compared with gasoline engine values. However, a more accurate appraisal would probably require comparison at equal vehicle performance levels. Power-to-weight ratios and, hence, acceleration times and top speeds for the diesel vehicles cited above are inferior to values expected in typical gasoline-powered vehicles.

Gas Turbine, Stirling Cycle, and Rankine Cycle Engines

Gas turbine, Stirling cycle, and Rankine engines all employ steady flow or continuous combustion processes operated with fuel-lean overall mixture ratios. In a strict sense, the gas turbine is an internal combustion engine since high temperature combustion products serve as the cycle working fluid. Rankine and Stirling engines are external combustion devices with heat exchanged between high temperature combustion gases and the enclosed cycle working fluid.

In contrast to the situation with conventional spark ignition piston engines, the major obstacles related to use of continuous combustion power plants are in the areas of manufacturing costs, durability, vehicle performance, and fuel economy. The problem of exhaust emissions, which involves primarily the combustion process, has been less significant than the foregoing items.

As a consequence of lean combustion, these continuous combustion power plants are characterized by low HC and CO emissions. Several investigators have reported data indicating that existing combustion systems are capable of approaching or meeting statutory 1975 and 1976 vehicle emissions standards for HC and CO (26,27).

For a given power output, NO_x emissions appear to be lower than those of conventional uncontrolled gasoline engines. However, it has been shown that existing combustors probably will not meet the statutory 1976 NO_x standard when installed in motor vehicles (26).

The formation of NO_x in continuous-flow combustors has been found to result from the presence of high temperature zones with local fuel-air ratios in the vicinity of stoichiometric conditions. Approaches suggested for minimizing NO_x formation have involved reduction of these localized peak temperatures through such techniques as radiation cooling, water injection, and primary zone air injection. Other approaches include lean mixture primary zone combustion such that local maximum temperatures fall below levels required for significant NO formation. Laboratory gas turbine combustors employing several of these approaches have demonstrated the potential for meeting the 1976 standards (28). With a laboratory Stirling engine combustor, Philips has measured simulated Federal vehicle test procedure emissions levels well below 1976 statutory levels (29).

Conclusion

As an alternative to the conventional internal combustion engine equipped with exhaust treatment devices, modified combustion engines can, in principle, yield large reductions in vehicle exhaust emissions. Such modifications include stratified charge engines of both open and dual chamber design. On an experimental basis, prototype stratified charge engines have achieved low exhaust emissions with fuel economy superior to that of conventional engines controlled to similar emissions levels.

The diesel engine is capable of achieving low levels of light HC, CO, and NO_x emissions with excellent fuel economy. Potential problems associated with widespread diesel use in light-duty vehicles are initial cost, large engine size and weight for a given power output, the possibility of excessive particulate and odorant emissions, and excessive engine noise.

Several power plants based on continuous combustion processes have the potential for very low exhaust emissions. These include the gas turbine, the Rankine engine, and the Stirling engine. However, at the present time major problems in the areas of manufacturing costs, reliability, durability, vehicle performance, and fuel economy must be overcome. As a consequence, these systems must be viewed as relatively long range alternatives to the piston engine.

References

1. Beckman, E. W., Fagley, W. S., and Sarto, J. O., Society of Automotive Engineers Transactions, Vol. 75 (1967).
2. Cantwell, E. N., and Pahnke, A. J., Society of Automotive Engineers Transactions, Vol. 74 (1966).

3. Bartholomew, E., Society of Automotive Engineers, Paper 660109 (1966).
4. Campion, R. M., et al, Society of Automotive Engineers, Publication SP-370 (1972).
5. Kopa, R. D., Society of Automotive Engineers, Paper 660114 (1966).
6. Newhall, H. K., and Shahed, S. M., Thirteenth Symposium (International) on Combustion, p. 365, The Combustion Institute (1971).
7. Longwell, J. P., and Weiss, M. A., Ind. Eng. Chem., 47, pp. 1634-1643 (1955).
8. Bishop, I. N., and Simko, A., Society of Automotive Engineers, Paper 680041 (1968).
9. Mitchell, E., Cobb, J. M., and Frost, R. A., Society of Automotive Engineers, Paper 680042 (1968).
10. "Automotive Spark Ignition Engine Emission Control Systems to Meet Requirements of the 1970 Clean Air Amendments," report of the Emission Control Systems Panel to the Committee on Motor Vehicle Emissions, National Academy of Sciences, May 1973.
11. Ricardo, H. R., SAE Journal, Vol. 10, pp. 305-336 (1922).
12. U.S. Patent No. 2,615,437 and No. 2,690,741, "Method of Operating Internal Combustion Engines," Neil O. Broderson, Rochester, New York.
13. Conta, L. D., and Pandeli, D., American Society of Mechanical Engineers, Paper 59-SA-25 (1959).
14. Conta, L. D., and Pandeli, D., American Society of Mechanical Engineers, Paper 60-WA-314 (1960).
15. U.S. Patent No. 2,884,913, "Internal Combustion Engine," R. M. Heintz.
16. Nilov, N. A., Automobilnaya Promyshlennost No. 8 (1958).
17. Kerimov, N. A., and Metentiev, R. I., Automobilnoya Promyshlennost No. 1, pp. 8-11 (1967).
18. Varshaoski, I. L., Konev, B. F., and Klatskin, V. B., Automobilnaya Promyshlennost No. 4 (1970).
19. "An Evaluation of Three Honda Compound Vortex Controlled Combustion (CVCC) Powered Vehicles, Report 73-11 issued by Test and Evaluation Branch, Environmental Protection Agency, December 1972.
20. "An Evaluation of a 350-CID Compound Vortex Controlled Combustion (CVCC) Powered Chevrolet Impala," Report 74-13 DWP issued by Test and Evaluation Branch, Environmental Protection Agency, October 1973.
21. Newhall, H. K., and El-Messiri, I. A., Combustion and Flame, 14, pp. 155-158 (1970).

22. Newhall, H. K., and El-Messiri, I. A., SAE Trans. 78, Paper 700491 (1970).
23. El-Messiri, I. A., and Newhall, H. K., Proc. Intersociety Energy Conversion Engineering Conference, p. 63 (1971).
24. Shahed, S. M., and Chiu, W. S., Society of Automotive Engineers, Paper 730083, January 1973.
25. "Exhaust Emissions from Three Diesel-Powered Passenger Cars," Report 73-19 AW issued by Test and Evaluation Branch, Environmental Protection Agency, March 1973.
26. Wade, W. R., and Cornelius, W., General Motors Research Laboratories Symposium on Emissions from Continuous Combustion Systems, pp. 375-457, Plenum Press, New York (1972).
27. Brogan, J. J., and Thur, E. M., Intersociety Energy Conversion Engineering Conference Proceedings, pp. 806-824 (1972).
28. White, D. J., Roberts, P. B., and Compton, W. A., Intersociety Energy Conversion Engineering Conference Proceedings, pp. 845-851 (1972).
29. Postma, N. D., VanGiessel, R., and Reinink, F., Society of Automotive Engineers, Paper 730648 (1973).

:ljr

Table I
Federal Exhaust Emissions Standards
Emissions, Grams/Mile¹

	1975			1976			1977 Statutory
	Statutory	Interim		Statutory	Interim		
		U.S.	California		U.S.	California	
HC	0.41	1.5	0.9	0.41	0.41	0.41	0.41
CO	3.4	15	9.0	3.4	3.4	3.4	3.4
NO _x	3.0	3.1	2.0	0.4	2.0	2.0	0.4

¹As measured using 1975 CVS C-H procedure.

Table II
 Average Emissions from Military Jeep Vehicles
 with Stratified Engine Conversions (Reference 10)

Engine	Miles	Emissions, g/Mile ²			CVS Fuel Economy, mpg
		HC	CO	NOx	
L-141 Ford ¹ PROCO	Low	0.37	0.93	0.33	18.5-23
	17,123	0.64	0.46	0.38	
L-141 Texaco ¹ TCCS	Low	0.37	0.23	0.31	16-22
	10,000	0.77	1.90	0.38	

¹Engines equipped with oxidation catalysts and exhaust gas recirculation.

²1975 CVS C-H test procedure.

Table III

Average Low Mileage Emissions Levels -
Ford PROCO Conversions (Reference 10)

	Emissions, ² g/Mile			CVS Fuel Economy, mpg	Inertia Weight, lb
	HC	CO	NOx		
PROCO 141-CID ¹ Capri Vehicles	0.12 0.13 0.11	0.46 0.18 0.27	0.32 0.33 0.32	20.4 25.1 22.3	2500
PROCO 351-CID ¹ Torino Vehicle	0.30	0.37	0.37	14.4	4500
PROCO 351-CID ¹ Montego Vehicles	0.36 0.36	0.13 1.08	0.63 0.39	- 12.8	- -

¹All vehicles employed noble metal exhaust oxidation catalysts and exhaust gas recirculation.

²1975 CVS C-H test procedure.

Table IV
Honda Compound Vortex-Controlled Combustion-
Powered Vehicle¹ Emissions (Reference 19)

	Emissions, ² g/Mile			Fuel Economy, mpg	
	HC	CO	NOx	1975 FTP	1972 FTP
Low Mileage Car ³ No. 3652	0.18	2.12	0.89	22.1	21.0
50,000-Mile Car ⁴ No. 2034	0.24	1.75	0.65	21.3	19.8

¹Honda Civic vehicles.

²1975 CVS C-H procedure with 2000-lb inertia weight.

³Average of five tests.

⁴Average of four tests.

Table V

Emissions from Honda Compound
 Vortex-Controlled Combustion
 Conversion of 350-CID
Chevrolet Impala (Reference 20)

Test	Emissions, ¹ g/Mile			Fuel Economy, mpg
	HC	CO	NO _x	
1	0.27	2.88	1.72	10.5
2 ²	0.23	5.01	1.95	11.2
3 ³	0.80	2.64	1.51	10.8
4	0.32	2.79	1.68	10.2

¹1975 CVS C-H procedure, 5000-lb inertia weight.

²Carburetor float valve malfunctioning.

³Engine stalled on hot start cycle.

Table VI

Steady State Emissions from Honda Compound
Vortex-Controlled Combustion Conversion of
350-CID Chevrolet Impala (Reference 20)

Vehicle Speed, mph	Emissions, g/Mile					
	HC		CO		NO _x	
	350 CVCC	350 Stock	350 CVCC	350 Stock	350 CVCC	350 Stock
15	0.15	0.60	3.30	7.26	0.37	0.52
30	0.00	1.22	0.65	9.98	0.53	0.37
45	0.00	0.51	0.19	4.71	1.00	0.93
60	0.01	0.32	0.53	2.48	3.00	1.78

Table VII

Single-Cylinder Divided Combustion Chamber
Engine Emissions Tests (Reference 10)

Engine	NOx Reduction Method	Emissions, g/ihp-hr			Fuel Economy, Lb/ihp-hr
		NOx	HC	CO	
PROCO Divided Chamber	EGR	1.0	3.0	13.0	0.377
	None	1.0	0.4	2.5	0.378
PROCO Divided Chamber	EGR	0.5	4.0	14.0	0.383
	None	0.5	0.75	3.3	0.377

Table VIII
Automotive Diesel Engine Emissions
(Reference 25)

Vehicle	Emissions, g/Mile				Inertia Weight, Lb	Fuel Economy, mpg	
	HC (Cold Bag)	HC (Hot FID)	CO	NOx		1975 FTP	1972 FTP
Mercedes 220DD	0.17	0.34	1.42	1.43	3500	23.6	23.3
Mercedes 220D (Modified)	0.13	0.23	1.08	1.48	3500	24.6	23.6
Opel Rekord 2100D	0.16	0.40	1.16	1.34	3000	23.8	23.2
Peugeot 504D	1.30	3.53	3.34	1.04	3000	25.2	24.2

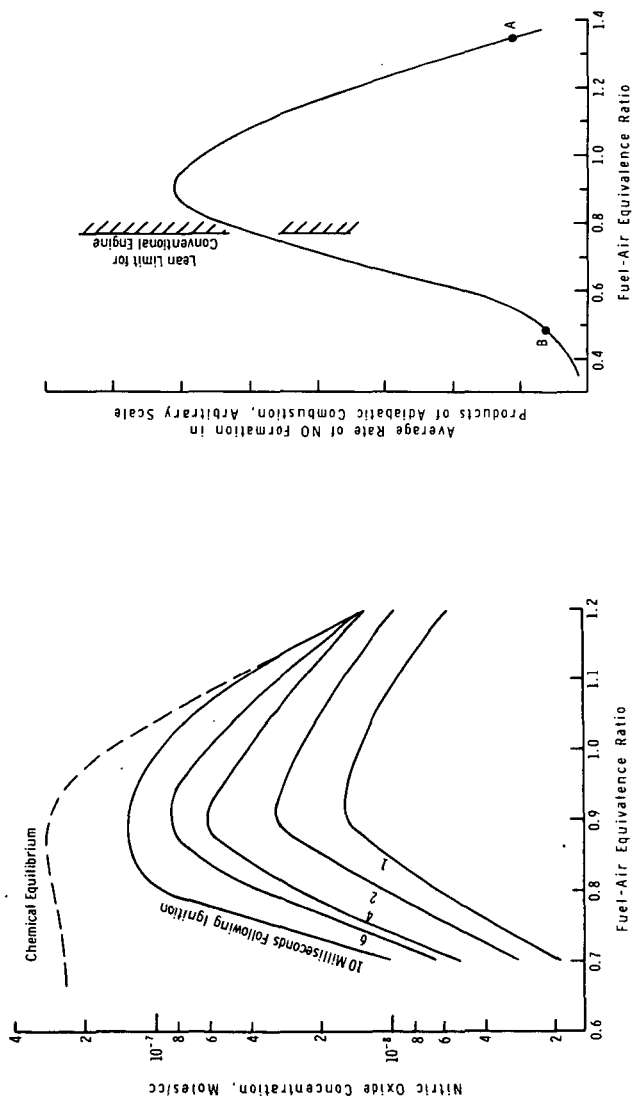


Figure 2: Influence of Fuel-Air Ratio on Rate of Nitric Oxide Formation

Figure 1: Rate of Nitric Oxide Formation in Engine Combustion Gases (Reference 6)

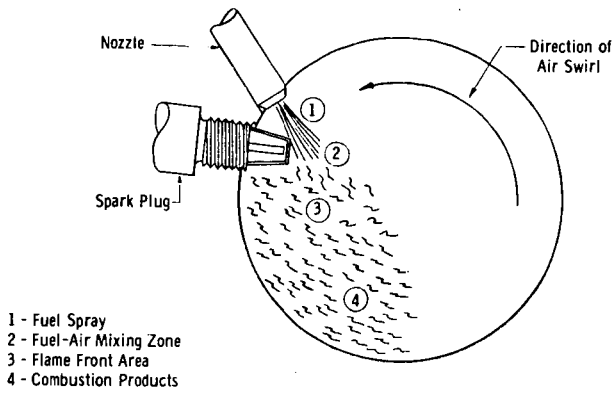


Figure 3: Texaco-Controlled Combustion System (TCCS)

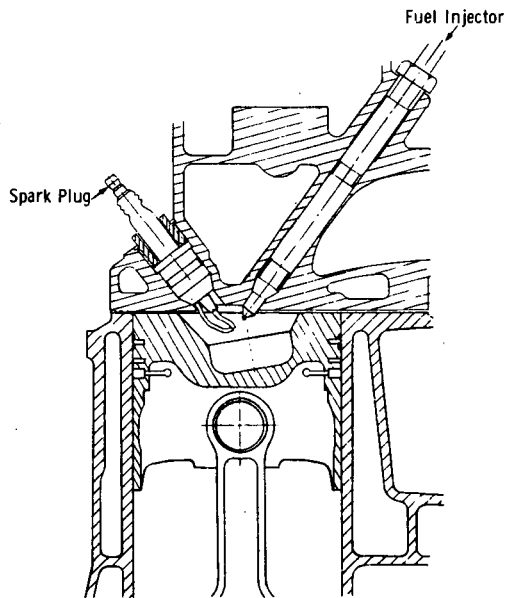


Figure 4: Ford-Programmed Combustion (PROCO) System

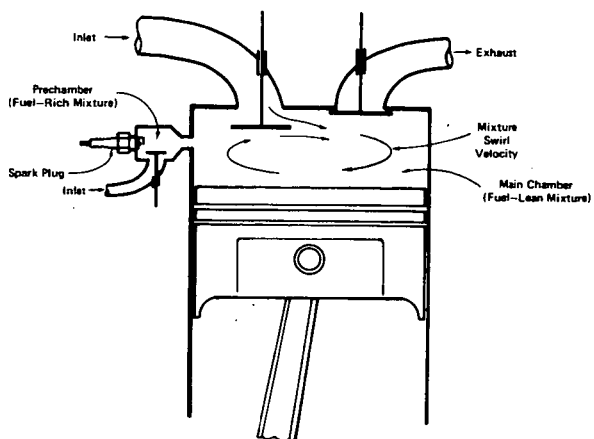


Figure 5: Schematic Representation of Prechamber Stratified Charge Engine

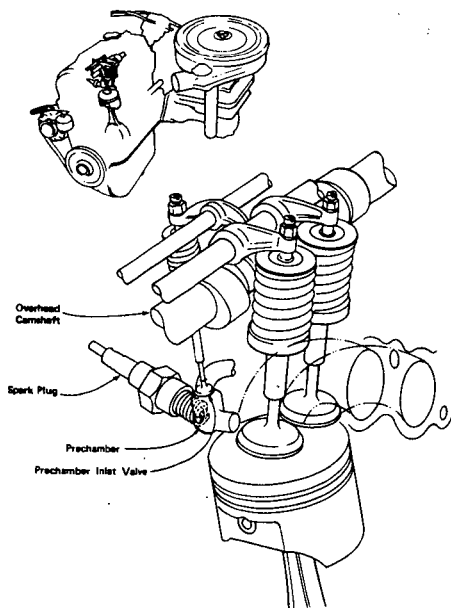


Figure 6: Honda CVCC Engine (Reference 19)

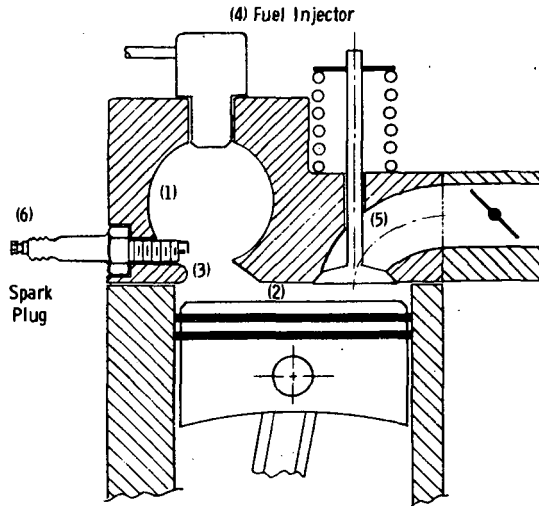


Figure 7: Schematic Representation of Divided Chamber Engine (Reference 21)

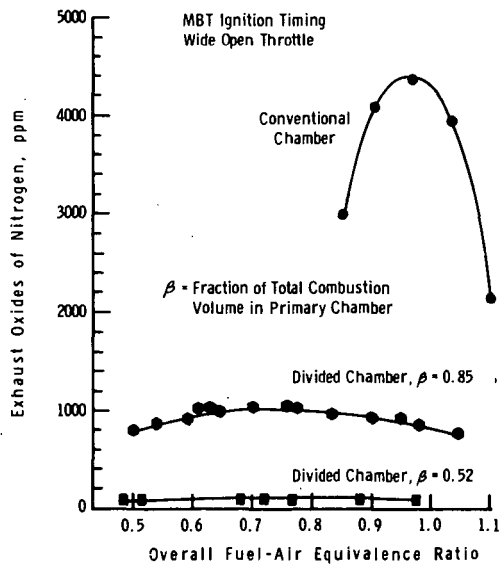


Figure 8: Comparison of Conventional and Divided Combustion Chamber NO_x Emissions (Reference 23)

TWO CURRENT APPROACHES TO AUTOMOTIVE EMISSION CONTROL. I. N. Bishop and J. H. Jones, Ford Motor Company, Dearborn, Michigan 48121

With the ever tightening requirements for automotive emission control, as especially regards the oxides of nitrogen, and the more recent increased need for improved fuel economy, two unique variants of the spark ignited internal combustion engine have been investigated for their potential in meeting these most important objectives. These engines are:

•Fast Burn - A homogeneous charge mixture cycle engine which utilizes maximum charge dilution for NO_x control while maintaining the combustion rate and thus the engine efficiency (fuel economy) through an increased level of chamber turbulence.

•PROCO (programmed Combustion) - A direct cylinder, fuel injected, stratified charge engine which utilizes the rich/lean combustion stratification scheme for both NO_x control and improved fuel economy.

The investigations of these alternate power systems have included math modeling for prediction of NO_x levels, basic engine configuration and operating parameter studies conducted on an engine dynamometer, vehicle evaluations of low mileage emission control capabilities, fuel economy, performance and driveability and system durability when subjected to 25,000 miles of the EPA mileage accumulation schedule. The results of these investigations have led to the conclusion that low NO_x levels can be achieved with good driveability and a definite improvement in fuel economy over conventional engine designs when calibrated to the same emission levels. However, the hydrocarbon and carbon monoxide levels are extremely high and were not able to be contained even with double the nominal catalyst volume.

Authors - Edward N. Cantwell, Jr.

Emmett S. Jacobs

Title: Alternate Automotive Emission Control Systems

ABSTRACT

Automotive emission control systems have been developed to meet current and future exhaust emission standards with optimum fuel economy.

The 1973-1974 U. S. vehicle emission standards were easily met with full size 1970 model sedans which were modified by changing combustion chamber, piston head, spark and valve timing, carburetion, and increasing the engine compression ratio. The acceleration performance and city/suburban fuel economy were improved over that of unmodified 1970 cars and were markedly better than comparable 1974 model vehicles.

A 1971, 1.6 liter Pinto was equipped with the Du Pont Total Emission Control System (TECS) and driven 100,000 miles on leaded gasoline. It easily met interim Federal emission standards in effect for California for 1975. This emission control system used exhaust manifold thermal reactors, exhaust gas recirculation (EGR), and carburetor and spark timing modifications to control gaseous emissions. In road tests the Pinto low emission car gave 6 percent better fuel economy than comparable 1973 models which met less stringent emission standards. This low emission vehicle was equipped with a muffler lead trap which reduced the total lead emissions by 84% without deterioration in efficiency over 100,000 miles. This emission control system has been used on standard sized vehicles equipped with V-8 engines with similar results.

Both large and small vehicles have been equipped with catalytic exhaust emission control systems. The fuel economy of these vehicles designed to meet a range of emission standards have been determined. Potential advantages and disadvantages of the various systems with respect to fuel consumption are discussed.

Automotive Engines for the 1980's

Robert W. Richardson

Eaton Corporation, Southfield, Michigan

The reciprocating piston engine has dominated the automotive scene for more than 60 years and until very recently, at least to most realists, seemed unlikely to ever be displaced. Although the piston engine has served its users well for many years and is likely to continue to do so for some time to come, it does have a number of shortcomings which are becoming more serious as ever greater numbers come into use and as we become enlightened on social values. It is a major contributor to air and noise pollution. It is also relatively inefficient and has a narrow fuel tolerance consuming large amounts of highly refined petroleum.

The early phases of an expected long-term energy crisis are now upon us. The era of abundant low cost energy is over. Much higher prices are certain and rationing likely cannot be avoided. The need to greatly increase efficiency rather than trade off efficiency for emission control is therefore becoming more obvious. Before the end of this century (which is closer than the end of World War II) petroleum must likely be replaced as the dominant fuel for mobile powerplants.

Although much progress has been made in reducing automotive emissions, it has been achieved at the price of increased fuel consumption. Much further reductions in emissions are needed to meet the requirements of the Clean Air Act of 1970. Growing, but of somewhat lesser importance is the issue of noise pollution.

Wankel, Stirling, turbine, stratified charge and diesel engines are the most serious contenders to replace or supplement today's piston engines. Electric vehicles are not considered serious contenders because of grossly inadequate technology and steam engines have too low an efficiency.

In addition to the three social parameters discussed previously, there are seven other major engine selection parameters - flexibility (torque-speed characteristics and driveability), smoothness, cost, weight, size, maintenance requirements and durability. Figure 1 lists these parameters in order of importance for passenger cars as of 1973. Arrows show the importance of noise and especially, fuel consumption rising to late 1970's (and perhaps Mid-1970's) values. The five contenders are compared on these ten parameters with the 4-cycle gasoline piston engine.

The Wankel, despite much recent fanfare, has little to offer in the three important social areas and uses substantially more fuel. It

is also a more costly and less flexible engine and has poorer durability characteristics.

The Wankel is smaller and lighter, but nowhere near as much as often claimed. These advantages are not readily convertible into major reductions in vehicle size and weight. Design studies indicate that several of the most compact cars using transverse piston engines would have to increase in length if a Wankel engine were substituted.

The turbine engine is quieter and can have very low emission but has higher fuel consumption. It is lighter, smoother and more flexible, should require less maintenance, but is costly and its durability has not been proven (automotive application). The turbine requires considerable additional development before it could enter volume production.

The Stirling engine has the lowest fuel consumption, lowest emissions, and the lowest noise of any known engine. It is potentially capable of burning any fuel since it is an external combustion engine. It is becoming increasingly apparent that we must supplement or begin to replace petroleum consuming mobile powerplants within the next 10 to 20 years. The Stirling engine also has flexibility, smoothness, maintenance and durability advantages, but tends to be somewhat bulky and costly.

The Stirling engine is in an early state of development. Introduction in high volume production is not likely until at least the early to Mid-1980's.

Stratified charge engines could be introduced relatively quickly into production as it is a variation of today's piston engine. The stratified charge engine provides a better trade off between fuel consumption and exhaust emissions; the engine appears to be capable of meeting the interim 1975 and 1976 emissions standards while equalling or bettering today's engines' fuel economy.

Stratified charge engines have a disadvantage in that their specific power output is somewhat less than conventional engines, resulting in lower performance cars or an increase in engine size. Ultimately this disadvantage may be overcome by turbocharging but at least the first generation of stratified charge engines are not likely to use turbochargers.

Diesel engines have low fuel consumption and low emissions of controlled pollutants but high emission of smoke, odor and noise. They require less maintenance and have a long life but are at a disadvantage in all other characteristics.

On balance therefore, the stratified charge reciprocating engine appears to be the leading near-term challenger and the Stirling engine, the leading long-term contender.

Figure 2 is a composite chart showing our estimated range of probable market penetration of each engine type through 1985. The lower dark shaded band is for the Wankel. The maximum probable is about 13% by 1980 and 23% by 1985. The minimum probable rises to 3% in the late 1970's gradually fading away in the early-1980's. Second, for the turbine and Stirling engines - penetration again, from none up to 8%. The balance of the market, the reciprocating piston engine is obtained by subtracting the sum of turbine and Wankel minimum and maximum penetrations from 100. It would have a market share of at least 69% and could conceivably take the whole market in 1985. The maximum piston engine market share in 1980 is 97% due to the forecast minimum Wankel penetration. The number of catalyst-controlled reciprocating engines will be substantially lower than shown if the 1975 standards are liberalized. The picture for 1976 and beyond is still very unsettled.

The catalyst curve shows an early decline as the stratified charge engine comes into use. The stratified charge engine may indeed prove sufficiently attractive to not only take over this whole reciprocating engine segment, at least 69% of the total, but to even recapture the small segment lost to the Wankel in the mid- and late-1970's. By 1985 the stratified charge engine could be the only engine in production.

In conclusion:

1. Reciprocating piston engines will remain dominant well into the 1980's.
2. Vehicle and engine manufacturers continue to approach change with caution and will follow conservative introduction and commercialization strategies.
3. Economics will continue to be the dominant influencing factor.
4. But social requirements, especially fuel consumption, will become more significant in influencing change to different engines.

The overall conclusion, therefore, is that there still is considerable uncertainty as to the choice and rate of commercialization of specific new engines, but no revolutions are likely in the near future.

This summary is based on a complete report by the same title published by the Eaton Corporation.

Major inputs for the report were obtained from over 60 in-depth interviews worldwide. These included car and truck manufacturers; heavy duty and small engine producers; developers of new engines; materials, parts, fuels and lubricants suppliers; machine tool builders; government agencies; trade associations; independent research institutes and consultants. These inputs were combined with business, technical and historical analyses and an evaluation of the social, political and economic forces that cause change.

Primary emphasis was placed on the Wankel engine and on those factors which will have the greatest bearing on its (degree and rate of) commercialization. Priority was placed on passenger car application followed closely by heavy duty markets with a relatively modest effort in the small engine area.

Relative Importance of Selection Parameter Passenger Cars

Compared with 4-Cycle
Spark Ignition Piston Engine

	Wankel	Turbine	Stirling	Stratified Charge	Diesel
Flexibility	-	+	+	0	-
Smoothness	+	++	++	0	-
Emissions	0	+	++	+	+
Cost	-	-	-	?	-
Noise	0	+	++	0	-
Weight	+	+	0	-	-
Size	+	0	-	-	-
Maintenance	0	+	+	0	+
Fuel Consumption	-	-	++	+	++
Durability	-	?	+	0	+

Advantage (+) or Disadvantage (-) *Two-Shaft Regenerative 1900 F Turbine Inlet Temperature

FIGURE 1

Range of Expected Market Penetration

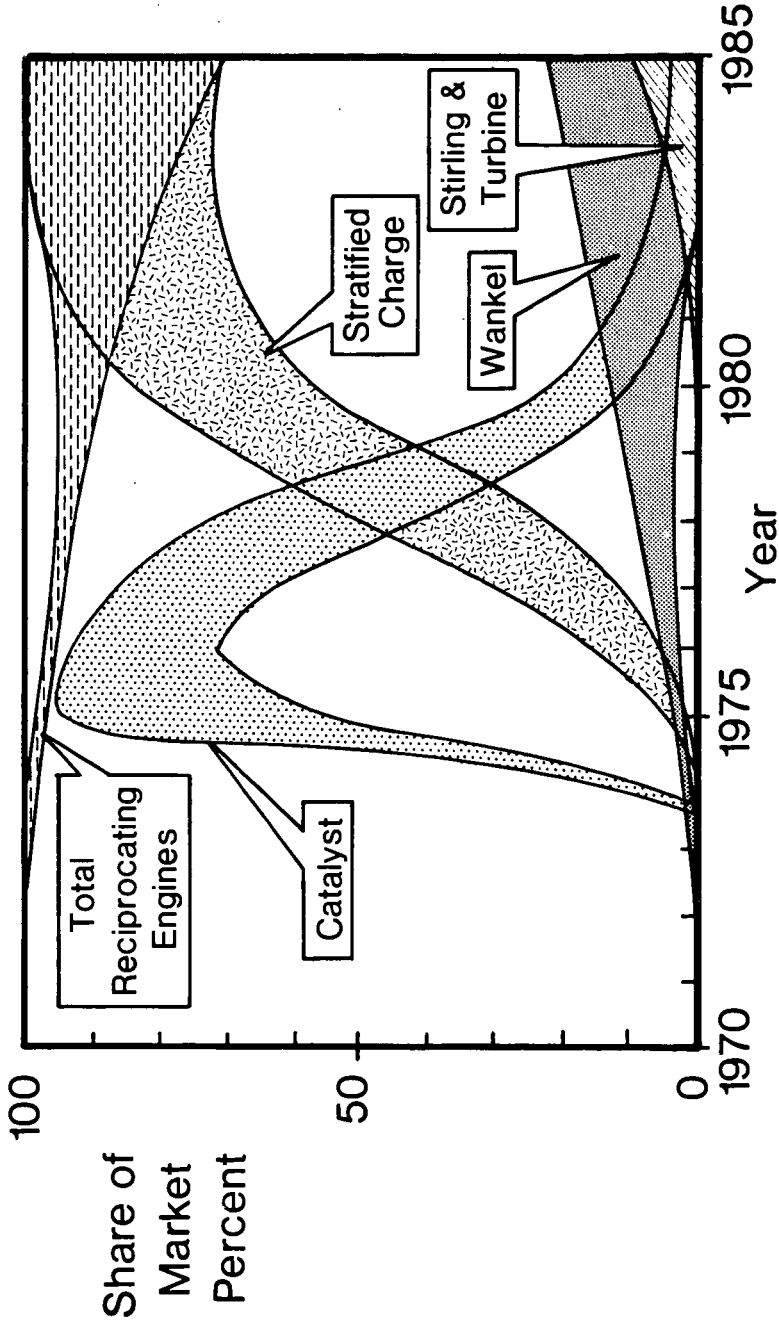


FIGURE 2

The Application of the High Speed Diesel Engine
as a Light Duty Power Plant in Europe

C.J. Hind

Perkins Engines Company, Peterborough, England

The fact that the diesel engine has been considered and used as a saloon car power unit for some 40 years may come as a surprise to some people. They may admit that this is so but will come back with the reply that it has not made very much progress through the years. The diesel engine succeeded in getting a name very early on, and quite rightly so in some cases, as a dour thumping engine that plods on for ever, and not so flatteringly as a smelly, noisy, and rather smoky power unit. Very few of us would disagree with this description up to say 30 years ago, but great strides have been made since the mid-forties which have elevated the small diesel engine into a much more acceptable automotive power unit. The days when only an enthusiast or an eccentric would drive a diesel powered car are now passing and the wisdom and foresight of those early engineers is now bearing fruit. The design and combustion features of the diesel engine are showing to be more compatible with the strict legislative demands that are being thrust upon us and more people are now looking for a vehicle with good reliability, long life and maximum fuel economy. The words "fuel resources and energy crisis" are becoming commonplace these days and so it is worth remembering that the great redeeming feature of the diesel engine is its excellent fuel economy and low running costs.

But when did it all begin and why?

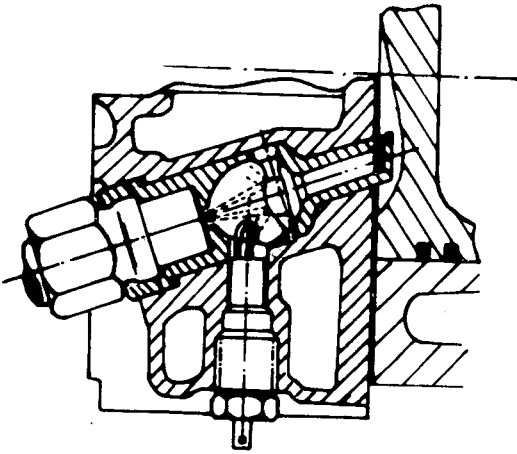
The beginning in Europe.

The early 1930's really saw the first production high speed diesel engines, and these required a whole new philosophy to be applied. The first diesel engines had been very heavy and bulky industrial and marine units with a maximum speed of around 1000 RPM, which made them unsuitable for vehicle applications.

Eventually the fuel economy shown by these engines, along with the attractive low fuel costs, made their progression into the commercial vehicle market a natural move. The rated speeds were raised to around 2000 RPM, although some of them remained below 2000 RPM, and in fact Gardner engines to this day still keep their rated speed in that same speed range.

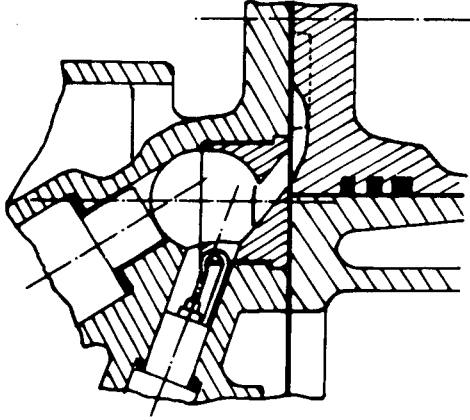
The rapid development of these engines from the mid-1920's to the mid-1930's was very impressive and the commercial vehicle operators attracted by the lower operating costs very soon saw the advantages of the diesel engine vehicle and helped this market to rapidly expand. Various companies, mainly in Great Britain and Germany, were developing these engines, whilst most of the French engines were being built under licence, excluding Peugeot who had extended their very successful petrol engine experience into the diesel engine field in 1928. Those early marine and industrial engines were made even more bulky by the fact that an air compressor was required to help atomise the fuel and provide the necessary air movement for good mixing. With the advent of the Bosch fuel injection equipment in Germany and later when C.A. Vandervell took up the manufacture of Bosch equipment in England, real strides were taken in the development process.

The high speed diesel engine, with rated speeds of 3000 RPM plus came to be used in the light truck market by two different roads. The company who manufactured both trucks and diesel engines saw the high speed engine as a natural extension of his engines in his trucks. The other approach was being made by the



MERCEDES - BENZ

FIG. 1.



RICARDO COMET

FIG. 2.

diesel engine manufacturer who offered to replace an existing gasoline engine in another company's truck. In the former case a vast amount of experience had been gained in the designing of the diesel engines for the bigger commercial vehicles and from this a large amount of knowledge was drawn which assisted in the development of the smaller units. In many cases the smaller engine was a scaled down version of its bigger brother, and the basic design and combustion principles were very similar.

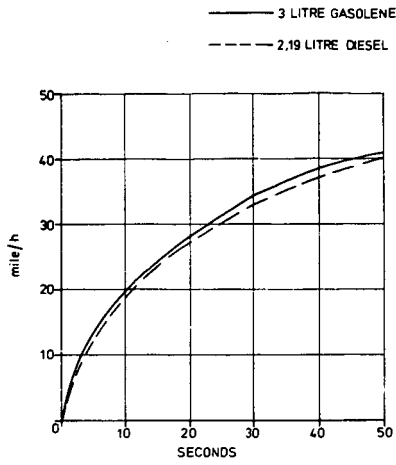
In the latter cases where an existing gasoline engine was being replaced by a diesel engine, a whole new design philosophy had to be applied, because interchangeability was a key factor and the diesel engine had to fit into the space vacated by the gasoline engine. As the transmission of the trucks was again designed for the displaced gasoline engine, this meant that the equivalent diesel engine had to have a similar speed and torque range. All this was a considerable break away from the traditional diesel requirement, and a large amount of design and development work was required.

It was realised early on in the development of the high speed diesel engine that cylinder pressures and engine breathing were going to be prime reliability and performance parameters.

The adoption of an indirect chamber engine allowed the intake port to be concerned only with inducing as high a mass of air as possible, and the swirl properties required for efficient combustion were provided by the air movement into and out of the chamber. Many designs of chambers were evolved during this time, each with its own theory and optimistic efficiency put forward by its inventor. One of the earliest and most successful designs was the Benz, later Mercedes Benz of course, pre-chamber or pepper pot design. This type of chamber has certainly stood the test of time as it is still widely used today and in many sizes of engines. This chamber was first used in the bigger design of engine, as was the well-known Ricardo Comet combustion chamber, which again underwent a smooth transition into the high speed engine, where it is still very widely used. See Fig. 1 and 2.

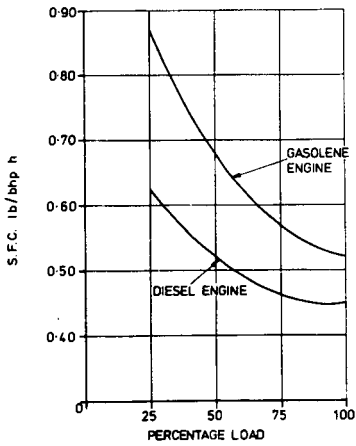
My own Company, Perkins Engines Company, was formed in 1932 specifically to manufacture high speed diesel engines for the lighter class of vehicle. As previously mentioned, interchangeability with the gasoline engine wherever possible was the primary aim. Fig. 3 shows comparative acceleration data from a road test of 4.2 GVW ton truck when fitted with its original 3 litre, six cylinder gasoline engine, and a 2.19 litre, four cylinder diesel engine. Both trucks had the standard gasoline transmission. The similarity between the two curves was very encouraging at the time, especially when the fuel consumption of 15 mpg for the gasoline engine and 25 mpg for the diesel was also considered. The rated speed of 3000 RPM was the same for both types of engine, and it was said that the diesel engine had run smoothly at 4000 RPM. It should be added that the engine was run ungoverned. The savings due to the substantially better fuel economy of the diesel engine were even more enhanced when one considers that gasoline in Great Britain in 1933 cost the equivalent of 17 cents per gallon, whereas the diesel fuel cost only 5 cents per gallon. The main reason for the difference was because the gasoline fuel tax was some eight times higher than that on the diesel fuel. In France diesel oil cost about half of the gasoline price, and in Germany an even greater differential of approx. 70% was seen.

Fig. 4 shows a comparative set of running costs that were issued in 1933 by the Commercial Motor. The considerably lower fuel costs are an obvious point, but the lower maintenance costs, even though the diesel engine was a new type of power unit, shows that one of the other virtues of the diesel engine, was born in those early development days. The diesel engine had a 20% lower maintenance cost than the gasoline engine.



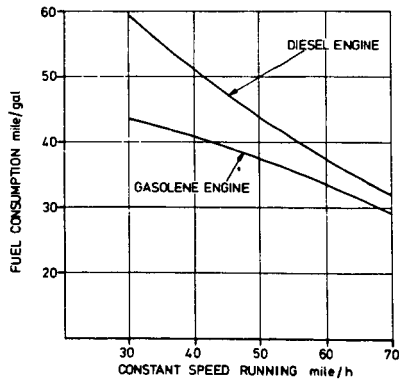
4.2 G.V.W. VEHICLE ACCELERATION
WHEN FITTED WITH A GASOLENE AND
DIESEL ENGINE

Fig. 3



CONSTANT SPEED FUEL CONSUMPTIONS
OF SAME CAPACITY ENGINES IN DIESEL
AND GASOLENE FORM

Fig. 6



CONSTANT ROAD SPEED FUEL CONSUMPTION

Fig. 7

FIG. 4. RUNNING COSTS (PENCE PER MILE) IN 1933 IN GREAT BRITAIN.

	<u>Petrol Engined Vehicles</u>			
	<u>2 Ton</u>	<u>3 Ton</u>	<u>4 Ton</u>	<u>5 Ton</u>
Fuel	1.33	1.80	2.10	2.63
Lubricants	0.06	0.07	0.09	0.09
Tyres	0.28	0.35	0.44	0.49
Maintenance	1.23	1.42	1.57	1.70
Depreciation	0.54	0.66	0.93	1.05
Total :	<u>3.44</u>	<u>4.33</u>	<u>5.13</u>	<u>5.96</u>

	<u>Diesel Engined Vehicles</u>		
	<u>3 Ton</u>	<u>4 Ton</u>	<u>5 Ton</u>
Fuel	0.38	0.44	0.55
Lubricants	0.12	0.16	0.16
Tyres	0.56	0.74	0.84
Maintenance	1.15	1.26	1.35
Depreciation	0.80	1.10	1.27
Total :	<u>3.01</u>	<u>3.70</u>	<u>4.17</u>

FIG. 5. CHANGES IN THE VEHICLE ROAD TAX IN GREAT BRITAIN IN 1934

<u>Weight Unladen</u>	<u>Gasolene</u>		<u>Diesel</u>		<u>Diesel</u>
	<u>Pneumatic Tyres</u>		<u>Pneumatic Tyres</u>		<u>Solid Tyres</u> *
	<u>1933</u>	<u>From 1.1.34</u>	<u>1933</u>	<u>From 1.1.34</u>	<u>From 1 Jan '34</u>
Under 12 cwt.	£10	£10	£10	£35	£46
12 cwt - 1 ton	£15	£15	£15	£35	£46
1 - 1½ ton	£20	£20	£20	£35	£46
1½ - 2 ton	£25	£25	£25	£35	£46
2 - 2½ ton	£28	£30	£28	£35	£46

- * For gasolene engined vehicles with solid tyres the road tax remained unchanged at the same rate as the present pneumatic tyre tax.

This Utopia for the diesel engine vehicle could not last, and in Great Britain in 1934, they were penalised against the equivalent gasoline engine by a higher road tax. See Fig. 5. The new tax could be offset to some extent by the conversion from solid tyres to pneumatic tyres, and thus a saving of £11 per annum was possible. So this showed that technology was not altogether being retarded by the new laws.

One novel fact that was put forward was that the increased motor taxes could lead to more deaths. The reasoning behind this statement being that more people would now go back to horse driven carts, and these beasts attracted flies which killed more people by infection than did the motor vehicle by road accidents at that time.

Further pressure was applied to the diesel engine in 1935 when the British Government realised that there was a danger to its gasoline revenue, and so they increased the tax on the diesel fuel and made it equal to that on the gasoline.

A number of statements made at the time make interesting reading such as the Minister's statement that "The oil engine can do as much work on 1 gallon of fuel as the petrol can do on 1½ gallons", and the pro-diesel faction who "believe that the oiler will continue to live and flourish but it must not be stunted in its youth", and the increase of tax even pleased some people as it would "encourage the steam vehicle trade". Times don't change that much do they?

This increase of tax was a considerable blow to all concerned in the diesel market, but work continued as the better fuel economy of the diesel was still worthwhile, but it now became even more essential that the first cost should be maintained as low as possible. This meant that the production principles and techniques that applied to the gasoline engine manufacturing industry, had also to be applied to the diesel engine wherever possible. This was especially essential for the smaller diesel engine, as it took that much longer to offset the first costs with the lower fuel consumption, simply because the total quantity of fuel consumed was small. The manufacturer who made both gasoline and diesel engines had an advantage in that he had many components at hand which he could design into both engines and maximise on rationalisation between the two types of engines.

The fuel injection equipment was, and still is, an expensive component in relation to the total engine first costs of a small diesel engine. This was, therefore, one of the main factors why the engine first costs were so high, and this coupled with customer inexperience of this type of equipment was a holding factor in the possibly even more rapid development of the smaller engine. Due to the commendable reliability of these first fuel pumps it was not long before most operators' doubts were dispelled and it soon became obvious that the reliability of the fuel pump was considerably better than that of the electric ignition equipment fitted to the gasoline engine. Consequently, the lower maintenance and down time costs were soon seen as a further bonus to the diesel engine vehicle operator.

The first diesel powered saloon cars.

It was obvious that the excellent fuel economy of the diesel engine would also prove attractive to the private motorists, and so the early 1930's saw parallel tests being run in both trucks and passenger cars.

The need for comparative size, weight, power and engine speed between the diesel engine and the gasoline engine became even more important when installation into a passenger car was considered. Further factors had also now to be considered such as noise, vibration and smell.

The first production diesel engined car was the Mercedes Benz "260D" which was powered by a four cylinder 2.6 litre engine which gave 45 HP at 3000 RPM. The car was normally fitted with a 2.3 litre gasoline engine. This diesel engine, the OM138, was a descendant of the pre-chamber truck engine and proved to be the very successful forerunner of a whole range of Mercedes diesel engines designed to suit the passenger car. The fuel consumption of 30 mpg and a maximum speed of 60 mph was very commendable, especially when the size and weight of the vehicle, which was really only a small transition from the light commercial vehicle, was considered. This car gave excellent service to many people, but of course the war years prevented any further development on these lines, and it was not until 1949 that a new model, the 170D, was seen.

The passenger car application was also being looked at in England in the early 1930's with an eye to Diesel conversion. In 1933, a 2.9 litre Perkins engine was installed in a gasoline production car and a creditable running cost of $\frac{1}{3}$ cent per mile was seen with equivalent performance to that given by the displaced gasoline engine.

Various capacity diesel engines were tested and one of the bigger conversions was a 3.8 litre Gardner engine rated at 83 BHP at 3200 RPM which replaced a 3.5 litre gasoline engine. This saloon car had a top speed of 83 mph and an overall fuel consumption of 44 mpg, which was considerably better than the 16 - 18 mpg achieved with the gasoline engine. A point of note was also that the conversion only added 100 lbs. to total vehicle weight.

The excellent fuel economy and reliability of these cars attracted people who had to cover very long distances, but even greater benefits were to be seen by the operators of stop start vehicles such as small delivery vans and taxis.

Further impetus to the development of the diesel engine was given by the political climate in Europe during the mid and late 1930's. Independence from imported fuels was aimed at, and so a variety of home produced fuels from coal and gas fuel were tested. As it was simpler to convert a diesel engine to operate on a variety of fuels rather than a petrol engine, it was generally the former which was the basic engine used for the development work.

The Second Era.

In 1949, Daimler-Benz produced the 170 Series of saloon cars. This model was the forerunner of a whole new series of passenger cars produced by this company, and has seen gasoline and diesel engines installed in parallel up to the present time.

The 1.76 litre diesel engine (OM 636) embodied much of the experience gained from the earlier 2.6 litre engine, and this enabled the smaller engine to have a rated speed of 3200 rpm and an output of 21.6 bhp/litre. The popularity of this vehicle is shown by the fact that 27,000 170D's were sold in the three years from 1949 to 1952. The first cost of the diesel engined car was only \$185 more than the equivalent petrol model, and with a fuel consumption of 40 - 45 mpg, it took very little time before the diesel car was making a considerable saving.

This engine was developed further and in 1953 the 180D was introduced with the four cylinder engine now rated at 43 bhp at 3500 rpm, 24.4 bhp/litre, and a capability of 3800 rpm. These engines had a stroke/bore ratio of 1.33, but when a new 2 litre engine was introduced in 1959, it had a reduced ratio of 0.96, which allowed a higher operating speed of 4350 rpm and a specific output of 27.5 bhp/litre.

The European Continental countries still gave an extra boost to the development of the diesel engine in the early fifties by keeping the cost of diesel fuel well below the gasoline costs, whilst in Great Britain the difference in 1954 was only a little over 2.5 cents. There was also very little difference in fuel costs in the U.S.A. at this time and, so again, the incentive was low.

Various European Continental manufacturers now began producing diesel powered cars, such as Fiat in Italy and Borgward Hansa in Germany and eventually in 1954 the Standard Motor Company Limited began producing a saloon model in England. The essential point on first costs was pointedly shown by an automotive magazine at the time which stated that 61,200 miles was needed to be covered by this car before the high price differential of \$640 was offset. This mileage was required on the basis of the diesel engine car giving 40 mpg as against 23 mpg of its equivalent gasoline engine.

The top speeds of the diesel car were generally some 10 - 20 mph lower than the gasoline, but even more frustrating was the poor acceleration. This generally was due to the prime essential of interchangeability. The specific output HP/litre of the diesel engine has always been lower than the gasoline and, as the engine bulk dimensions had to remain essentially the same for both engines, this meant that the diesel had a 10 - 15% lower power output, and a maximum engine speed between 1000 - 1500 rpm lower than the gasoline. In many cases the transmission ratios were not changed and so the vehicle performance suffered again from this. Sometimes an overdrive ratio was fitted which enabled a higher top speed, but the poor acceleration was generally seen as a big disadvantage to the average motorist.

The driver who covered very long distances and required a reasonable cruising speed with good reliability, found the diesel car to his liking.

An even more beneficial application was in the vehicle that used a stop start and low load factor type of operation.

The diesel engine has nominally a constant volumetric efficiency and compression ratio through the load range at a given speed, whereas the gasoline engine has to contend with falling values at part load due to the throttling of the air flow at these conditions. This difference is shown in the better part load economy of the diesel engine and so the stop start or part load applications show the diesel engine to considerable advantage.

Fig. 6 shows how the specific fuel consumption curves of the same capacity engine when tested in diesel and gasoline forms diverge at the part load condition. This feature when transferred to actual road running results shows that the light load running gives approximately three times the fuel saving seen at the high load factor running. See Fig. 7.

Various types of vehicles saw the economy of the diesel engine in this way in the mid 1950's, and the engine was used in applications varying from taxis to delivery vans and road sweepers.

The rapid increase in the use of the diesel engine for taxi applications was most spectacular in Great Britain. Fig. 8 shows how the first taxi was

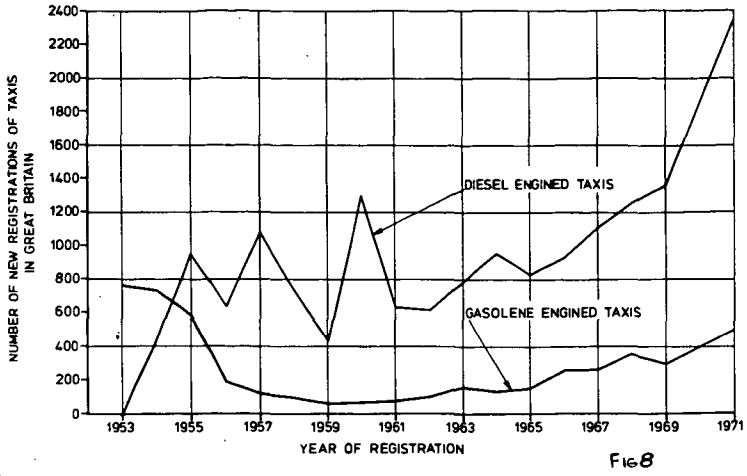


FIG 8

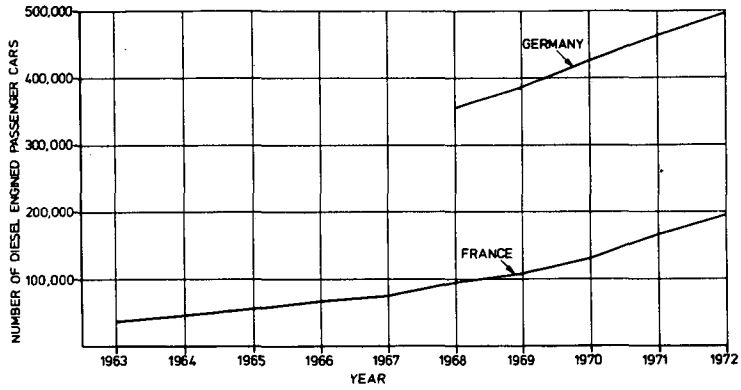


FIG 9

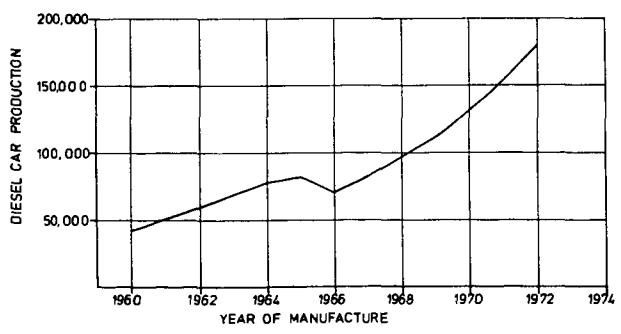


FIG 10

registered in 1953 and within 2 years the number of new registrations had overtaken that of the gasoline engine taxis. The late 1950's saw an erratic trend, possibly due to the economic climate at that time, but since 1961 the increase has shown a positive upwards swing. The rising trend of the gasoline taxi since 1961 is due to the number of smaller companies and individuals who are using their private cars in this market.

Fig. 9 shows how the German diesel passenger car market has always been the largest in the world, with an impressive figure of 0.5 million diesel cars being used in 1972. It is estimated that 45,000 taxis will be registered in Germany during 1972/73, and 80% of these will be diesel powered. This shows that the vast majority of diesel engine cars are being run by companies and the public for their private use and overall fuel consumption and reliability must be priority features as they are in this market in any country. The position in France since 1963 is also shown on Fig. 9, and although the actual numbers involved are much smaller, the trend shown from 1969 - 1972 is parallel to the German experience.

The owner of a motor car who travels above the average annual mileage, say 25,000 miles or more, will see the benefit of running a diesel car, and the auto-routes seen across the European Continent are ideal roads for this type of driving, as are the American freeways.

In Great Britain we do not have the road system, or even possibly the square mileage of country, to see the same usage of diesel engine cars as on the European Continent, and consequently the majority of these vehicles are used as taxis. As the fuel savings are so much greater at these part load running conditions, the mileage necessary to offset the higher first costs is much less. A typical difference in the fuel consumption for a London taxi cab type of duty would be 20 mpg for the gasoline engine taxi and 35 mpg for its diesel engine equivalent.

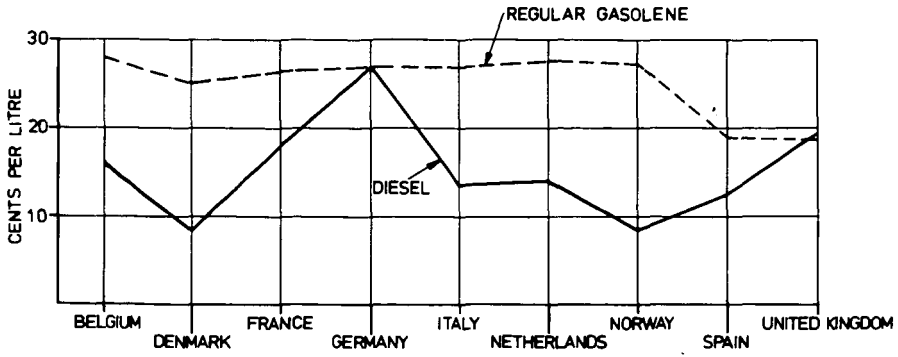
The 12cwt - 1 ton light van market is a very high quantity market, but as yet the diesel engine has made very few inroads. This again is essentially because of first costs, although to some extent the performance penalty is still felt in this low weight vehicle.

The 1 - 1½ ton vehicle market is also a very lucrative market, and the diesel engine vehicle is showing a steady rise here.

The light truck applications used by local Authorities for road cleaning, refuse disposal and other city work, see the advantages of the diesel in these applications. The part load economy again shows its benefit in these trucks, and the higher first costs can be offset in about 3 years. The reliability of these engines giving less 'down-time' and 'call out' problems is a further added bonus. These trucks give about 10 years' service before a major overhaul is necessary.

If we look at the production rate of the diesel engine car in Europe over the last 15 years, we see that there has been a positive increasing rate - See Fig. 10. The graph does not include conversions but only production line cars.

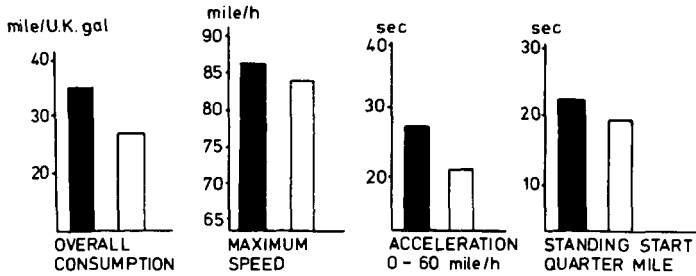
This trend proved attractive to more gasoline engine car manufacturers and today we have three major manufacturers who produced a total of 180,000 diesel engine saloon cars in 1972. Between them, these manufacturers - Mercedes Benz, Peugeot and Opel, produce a wide range of diesel engine vehicles ranging from a small saloon to an 8 seater limousine.



RETAIL PRICE OF DIESEL AND GASOLENE FIG.11

FIG 13

■ TURBOCHARGED DIESEL ENGINES
 □ GASOLENE ENGINES



All the vehicles have four cylinder engines, even the biggest which has a 2.4 litre engine, and the highest rated speed is now a creditable 5350 rpm seen from the Peugeot cm³ engine.

Whilst the diesel engine has been making considerable strides in its development with an eye on the saloon car market, the gasolene engine has, of course, equally been intent on further development and, consequently, it would be true to say that the performance gap has not decreased. The performance of the gasolene engined car has improved substantially since the end of the 2nd World War, and so in a direct comparison the gasolene car is still superior in acceleration and maximum speeds. But we must not let this overshadow the developments that have been seen in the diesel engine, where a 50% increase in rated speed has been achieved and specific outputs have nearly doubled. Without a doubt, the saloon car market has provided the stimulus for this development, and many people believe that the potential world market for the diesel engined car and light truck has yet to be exploited.

Today's gasolene engined car has on average still a 10 seconds advantage on a 0 - 60 mph acceleration test, and a top speed some 15 - 20 mph faster, but in these days of increasing legislation to reduce speed limits, the diesel car performance giving 75 - 85 mph is more than adequate.

We still have the old problem of first costs and the basic price differential varies from £250 to £750, but equally so we also still have the considerably better fuel consumption from the diesel car. Such adjectives as "astonishing", "tremendous" and "dramatic" are frequently used when people compare the fuel consumptions of these cars and, in general, they give 60 - 70% miles more per gallon than their gasolene engined counterparts.

We have seen how economy has always been a paramount factor in the sales of diesel cars, and this was undoubtedly helped by the beneficial differential in fuel costs seen in most European countries. It is possibly a demonstration of the insight and gratitude of the politician to see from Fig. 11 that Germany, who for so long has been the leader in the diesel car market, has now, along with the United Kingdom, the dubious honour of having no or even an adverse cost differential when compared with current gasolene prices. Extra strength is really given to the case for the diesel engine by this fact, as the fuel economy is still being seen as a worthwhile factor in purely mpg terms.

THE FUTURE:

If we now look into the future, how do we see the diesel engined saloon car in the light of legislative and fuel resource pressures.

The use of the I.D.I. combustion principle for the small diesel engine began, as I said before, at the very beginning of the development era of the diesel engine. Some people might call it foresight, fortuitous or just luck, that this type of engine is now proving to be a much better emission controlled engine than either the D.I. diesel engine or the gasolene engine. But really the fact that they were chosen because they had lower cylinder pressures, along with better breathing, is the reason why this combustion principle is now showing to advantage in these days of low NO and noise. Lowering the rates of pressure rise and peak cycle temperatures by retarding the injection is a well known principle and in the I.D.I. engine this also has the added benefit of reducing the exhaust smoke. This later timing also reduces the combustion noise levels and so we gradually have a situation where the previous disadvantages of the diesel engine are also being reduced. Taking the old problem of installation. If we can sufficiently decrease the rate of cylinder

pressure rise and hence the combustion noise, at both high and low speeds, it may be possible to reduce the bulk and weight of the diesel engine and so reduce the installation problems, and at the same time reduce the first cost differential.

This principle has of course to be investigated in considerable detail and analysis, or the situation will arise where the reduction in engine bulk will allow more noise to be released.

By extensive analysis of the cylinder block loading and vibration it may be possible to design a block which can distribute the loading more effectively and so reduce the noise generating sources along with a reduction in engine bulk.

The diesel knock becomes more obtrusive in the car application at the lower engine speeds, and means of reducing ignition delay periods and smoothing out the rates of cylinder pressure rise seen at part load conditions will have to be found before the average motorist will be satisfied. His previous experience of such sounds with his gasoline engine car has usually given him visions of failing bearings and pistons, and possible some re-education is needed to convince him that the diesel engine is designed to withstand these loads.

The U.S. legislation on gaseous emissions has caused enormous headaches for all engine manufacturers all over the world.

The manufacturers of the gasoline engine have been the hardest hit, but after all it was them who created the problem in the first place and are now experiencing the greatest difficulty in meeting the stringent requirements.

Many estimates and gloomy predictions have been made on the reduced power, increased fuel consumption, and increased first costs of the gasoline engine car that can meet the 1975/1976 and subsequent years' legislation. The Honda CVCC, and various rotary engine design concepts have been developed so as to meet the legislation, whilst the standard reciprocating gasoline engine has had to introduce many external innovations. The I.D.I. diesel engine has many of the required design and combustion features already built into it and any further modifications will generally come about by engine internal modifications. This means that the offending pollutants are not generated in the first place, and so the need for expensive corrective action is not required.

The number of engine modifications required by the diesel engine are relatively small if the 1975/76 Federal limits are to be met, and it is generally true to say that the stricter the limits the more able the diesel engine is to meet them. A very small power and SFC penalty is expected from the diesel engine if it has to meet the projected 1975 California legislation, and with only marginal increased cost. Very few figures are released by the gasoline engine manufacturer on the effects of tidying up his emissions problem, but considerable power derates, increases of vehicle weight, increases of first costs, and most critical of all increased fuel consumption, are all factors which will generally apply.

The lower specific output of the diesel engine has to be increased if it is to effectively compete on a performance basis with the gasoline engine saloon. This increase can come about by turbocharging and along with it, further improvements in fuel economy. The turbocharger will obviously increase the first costs, but these will be more than offset by the very

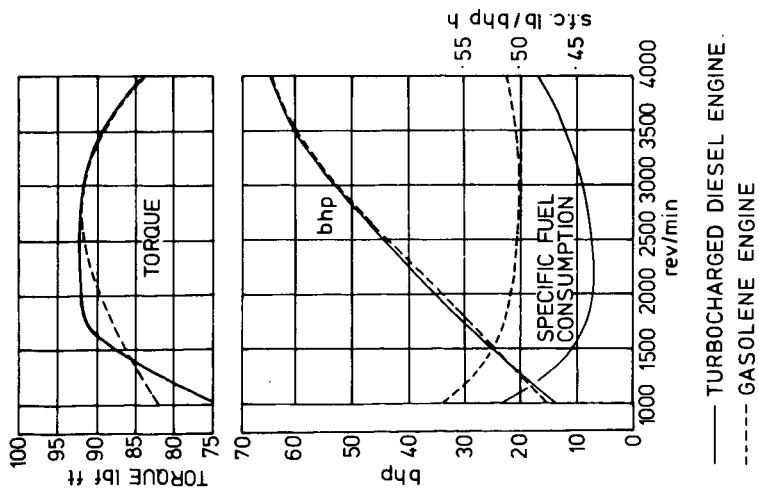
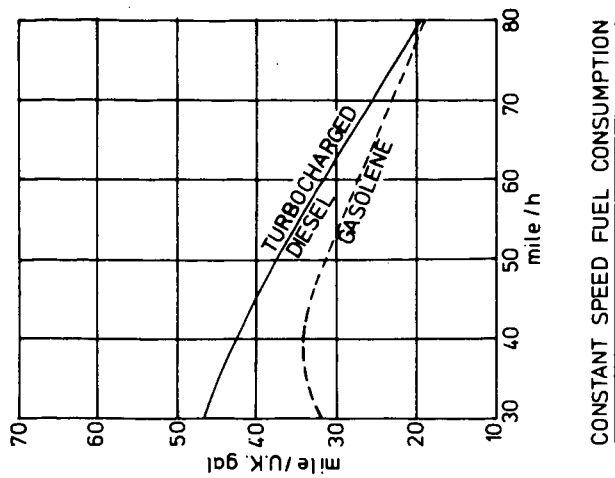


FIG. 12

— TURBOCHARGED DIESEL ENGINE.
 - - - GASOLINE ENGINE



CONSTANT SPEED FUEL CONSUMPTION

FIG. 14

expensive catalytic converters required by the gasoline engine.

Fig. 12 shows a test bed comparison between a 4-cylinder 108 cu. in. turbocharged diesel engine and a 104 cu. in. gasoline engine. The gasoline engine was in standard, non-de-toxed condition. Since 4000 rev/min was the maximum speed of the diesel, the gasoline curve was also discontinued at this speed although not reaching a maximum until 4800 rev/min. The superior fuel consumption of the diesel is clearly shown.

Each engine was installed in a UK Ford passenger car and comparative road test data obtained. Histograms of fuel consumption, maximum speed and acceleration are shown in Fig. 13. The standing start acceleration of the diesel powered vehicle was slightly inferior to the gasoline car, due mainly to the higher rotating inertia of the diesel engine and heavier installed weight. Top gear acceleration above 40 mph was, however, better with the diesel engine, as was the top speed. Fuel consumption was considerably better with the diesel, particular at lower speeds. Fig. 14 shows the steady speed fuel consumption at various speeds.

So the turbocharger will give improved performance and fuel economy to the diesel engine vehicle, whilst its gasoline counterpart is subjected to reduced performance and economy.

Two more fundamental yet substantial changes may be required to the diesel saloon philosophy, which affect both engine and car manufacturer, if this type of vehicle is to be fully accepted.

First, engines of six cylinder configuration may be required, one manufacturer has split the difference and is working on a five cylinder engine, but if powers over 120 BHP are required then a turbocharged six cylinder will be the answer.

Second, the transmission should be designed for the diesel engine and, if the engine is turbocharged, then a torque converter should be matched to its torque curve.

I therefore foresee the role of the small high speed diesel engine increasing in the light duty market, and this market potential should provide a real stimulus to the diesel engine manufacturer to further improve his product and prove that the image of the diesel engine car is due for a well deserved brush-up.

The vehicle manufacturer has to accept that the transmission has to be developed around the diesel engine, and if a concerted effort was made by all parties concerned, the late 1970s and into the 1980s could see improvements in both environmental conditions and a substantial reduction in the rate of exhaustion of our valuable fuel resources.

CURRENT LIMITS FOR LIGHT DUTY DIESEL ENGINES:

1. Power - This is dependent of speed (rev/min) and brake mean effective pressure (b.m.e.p.).
2. Speed - For the size of engine considered, the limiting factor is usually mean piston speed. Problems arise if diesel engines are operated for sustained periods at piston speeds over 2500 ft/min. Some gasoline engines operate at up to 3500 ft/min. Fig. 15 shows the permissible stroke dimension for various maximum engine speeds.

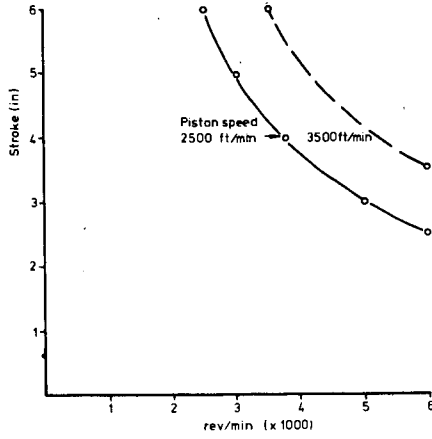


FIG. 15

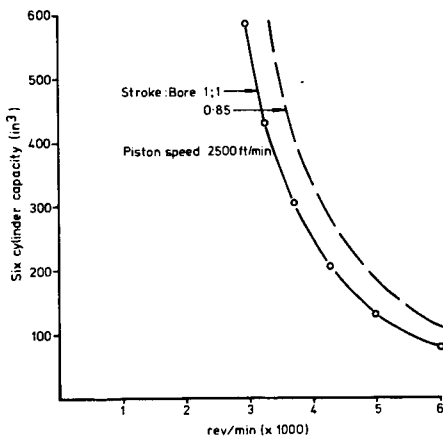


FIG. 16

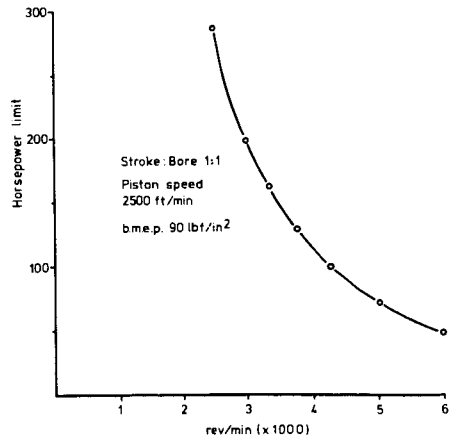


FIG. 17

3. Stroke to Bore Ratio - For indirect injection diesels, a stroke/bore ratio of between 1.0 and 0.85 is possible. This therefore sets a limit on cylinder capacity for a given rev/min. and piston speed. Fig. 16 shows the permissible maximum speed of various capacity six cylinder engines.
4. B.M.E.P. - Normally aspirated diesel engines should produce 90 lbf/in² b.m.e.p. at maximum speed. Using this value, Fig. 17 shows the horsepower limit at various rated speeds for the six cylinder engine.
5. Supercharging - More power can be obtained by turbocharging, but limited by the temperature of pistons, rings, cylinder head face and valves, and cylinder pressure. By turbocharging, an increase in power of 30% may be expected.
6. Engine bulk - Diesel engines tend to be longer than gasoline engines due to water passages between bores, more robust crankshaft and bearings and heavy duty timing drive.

Siamesed cylinders may be used for light duty applications, but problems due to cylinder distortion are likely.

The height is usually greater than for an equivalent gasoline engine, due to longer stroke and thicker head. Carburetors, however, frequently add to the height of gasoline engines. Oil pans tend to be deep to hold a larger volume of oil.

There is little difference in engine width, particularly in-line engines.

The bulk of a diesel is likely to be up to 50% greater for a given cylinder capacity.

7. Engine weight - Where cast iron is used for the blocks and heads of both diesel and gasoline engines, the diesels are usually heavier. This can amount to 100% more for equal power, normally aspirated.

Fig. 18 shows a comparison between a light commercial vehicle diesel engine and a typical compact car gasoline engine.

FIG. 18.

ENGINE COMPARISONMAIN DIMENSIONS.

	Diesel Engine	Six Cylinder Gasolene Chrysler 225 ins ³ "RG" Inclined 30° from Vert.
	inches	inches
Cylinder block length	27.6	26.1
Length engine from rear face cylinder block to front of fan	36.6	31.0
Height of water pump	8.2	6.7
Depth of sump	10.6	8.6
Height above crankshaft	18.4	18.3
Overall height	29.0	26.9
Width L.H. Looking from drivers seat	10.7	9.0
Width R.H. Looking from drivers seat	12.5	13.8
Overall width	23.2	22.7
Engine weight (lbs.) (dry)	708	475
	Flywheel plus backplate. Starter plus alternator plus fan.	Alternator plus air cleaner only. 555 lbs. if to equivalent specification

SULFUR PROBLEMS IN THE DIRECT CATALYTIC PRODUCTION
OF METHANE FROM COAL-STEAM REACTIONS

J. L. Cox, L. J. Sealock, Jr. and F. C. Hoodmaker

Mineral Engineering Department
University of Wyoming
Laramie, Wyoming 82071

The use of a multiple catalyst system consisting of potassium carbonate and a commercial nickel methanation catalyst for the direct production of methane from coal-steam reactions has been described in earlier papers (1,2). This system combines the beneficial catalytic effects of these catalysts to produce in a single-step conversion a product gas consisting primarily of methane and carbon dioxide with lesser amounts of carbon monoxide and hydrogen and has a CO₂-free heating value of about 850 Btu per SCF. Two of the apparent problems inherent with such a system are catalyst recovery and the loss of catalyst activity over prolonged periods of time at the conversion temperatures ($\geq 1200^{\circ}\text{F}$) in the presence of the various reactants produced from the coal gasification. In conjunction with the latter problem, this paper addresses the influence of sulfur compounds produced during gasification upon catalyst life and activity. This situation is compared and contrasted to the catalyst performance in the catalytic methanation of synthesis gas.

EXPERIMENTAL

Experimental Systems

The coal gasification was carried out in 1" o.d., batch-charge reactor which was constructed of 316 stainless steel. A schematic is shown in Figure 1.

The methanation studies with synthesis gas were performed in a 1/2" o.d. adiabatic flow reactor. It too was constructed of 316 stainless steel. Its schematic is shown in Figure 2.

Feed Materials

A subbituminous coal from Glenrock, Wyo., and Consol lignite from Stanton, N. Dak., both ground to 60-100 mesh were used in this investigation. Tables I and II contain the proximate and ultimate analyses of these materials. Although it was intended to use only anhydrous potassium carbonate (K₂CO₃) as the alkali catalyst x-ray studies indicated that it had taken up water to form some K₂CO₃ · 3/2 H₂O. The methanation catalyst, which contains approximately 35% nickel, was purchased from Harshaw Chemical Company. Additional chemicals and reagents that were used in conjunction with this investigation are commercially available or readily prepared by routine procedures.

Gas Analyses

The product gas volume was measured with a calibrated wet test meter, while the composition was periodically monitored with a gas chromatograph equipped with two thermal conductivity detectors. A Porapak Q column with helium carrier gas was used in conjunction with one detector while a molecular sieve column with argon carrier was used with the other. A total analysis required about 15 minutes. Data reduction was facilitated with an Auto Lab System IV digital integrator equipped with a calculation module.

Sulfur Analyses

The total sulfur and sulfate sulfur in the nickel methanation catalyst were determined by ASTM Method E39. The sulfide sulfur was calculated as the difference

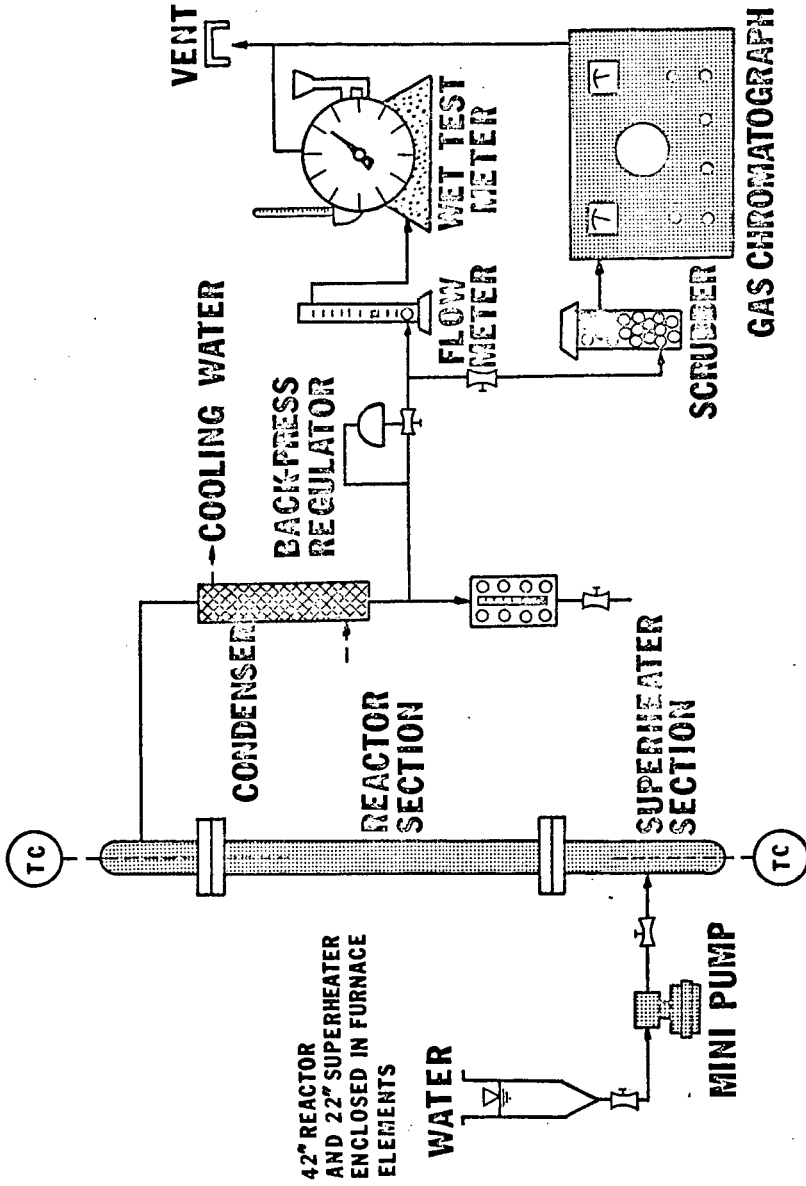


FIGURE 1. SCHEMATIC FLOW DIAGRAM ONE INCH REACTOR

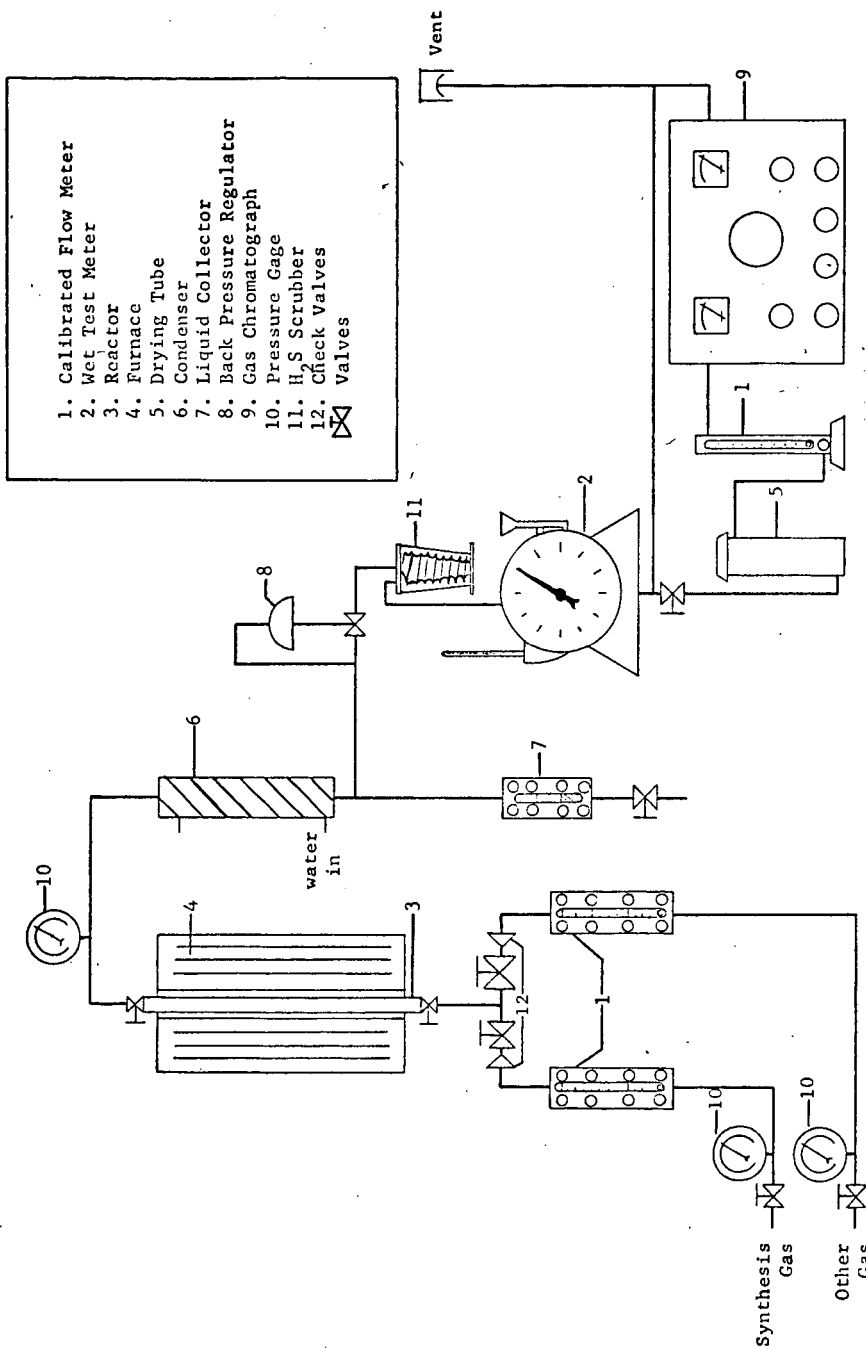


FIGURE 2 SCHEMATIC FLOW DIAGRAM 1/2" FLOW REACTOR

between the total sulfur and sulfate sulfur. A LECO sulfur analyzer was used to determine total sulfur in the coal and ash as well as in the nickel methanation catalyst. In addition some sulfur determinations employed the ASTM method D1757.

X-Ray Diffraction

Coal, ash and catalysts were examined with a General Electric XRD-5 diffractometer. Copper radiation at 35-50 kvp and 16 ma was used for the analyses. Scanning was started at an angle 2θ of $4-6^\circ$ and continued through 70° . The patterns were recorded on a strip chart. Interplanar spacings were determined from $\text{CuK}\alpha$ ($\lambda=1.5418 \text{ \AA}$) tables, whereas compound identifications employed the ASTM x-ray powder diffraction file.

Methodology

The coal gasification experiments were conducted by dry mixing the coal, catalysts and other additives and charging them to the reactor. Generally the runs employed 100g of coal, 20g K_2CO_3 and 100g of nickel methanation catalyst. The reactor temperature was brought to an operating value of about 650°C in less than two hours. A predetermined operating pressure was employed. These conditions were maintained throughout the remainder of the run. The total run time was about seven and half hours. During the run the gaseous product was monitored every half-hour and the results presented as time rated averages.

Methanation investigations with the half-inch adiabatic flow reactor employed rather standard operating procedures. A catalyst bed one inch in length was charged to the reactor. The temperature was monitored by a thermocouple positioned in the catalyst bed while means for varying the temperature, pressure, space velocity and gas composition were provided by external control. The product gas composition was periodically monitored with a gas chromatograph set-up similar to the one described above under Gas Analyses.

Table I. Analysis of Glenrock Coal (wt.%)

	As Received	Moisture Free
Proximate Analysis		
Moisture	12.2	--
Volatile Matter	39.6	45.1
Fixed Carbon	36.1	41.1
Ash	12.1	13.8
Heating Value (Btu/lb)	9140	10410
Ultimate Analysis		
Hydrogen	5.1	4.3
Carbon	52.7	60.0
Nitrogen	0.6	0.7
Oxygen	28.6	20.2
Sulfur	0.8	1.0
Ash	12.1	13.8

Table II. Analysis of Consolidation Lignite (wt.%)

	As Received	Moisture Free
Proximate Analysis		
Moisture	25.1	--
Volatile Matter	31.8	42.5
Fixed Carbon	38.3	51.1
Ash	4.8	6.4
Heating Value (Btu/lb)	9800	10720

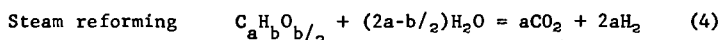
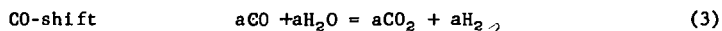
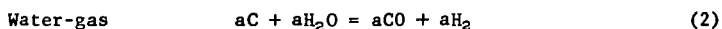
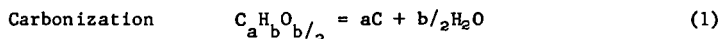
Ultimate Analysis	As Received	Moisture Free
Hydrogen	6.4	4.8
Carbon	50.3	67.2
Nitrogen	0.6	0.8
Oxygen	37.5	20.3
Sulfur	0.4	0.5
Ash	4.8	6.4

RESULTS AND DISCUSSION

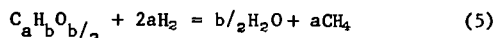
Multiple Catalyst Single Step Conversion

In the direct production of hydrocarbons from coal-steam reactions catalysts are employed to increase reaction rates and lower conversion temperatures. Lower temperatures result in a more favorable equilibrium. Consequently, more methane is realized in the product gas. By employing this method 850 Btu/SCF gas has been produced by the single step conversion (2).

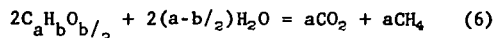
In view of the complexity of the coal it is not surprising that a good mechanistic description of gasification has not been forwarded. Nevertheless, from several hundred experimental runs with this system, the following empirical description of the conversion has evolved. The overall objective is to increase the atomic H/C ratio and at the same time eliminate the oxygen from the hydrogen deficient coal. This in turn calls for a source of hydrogen which can be obtained from water as a coupled reactant. Hydrogen production may be ascribed to carbonization followed and accompanied by the water-gas, CO-shift and steam reforming reactions as illustrated by Eqs. 1, 2, 3 and 4.



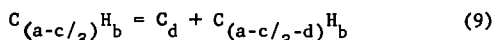
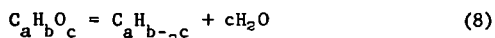
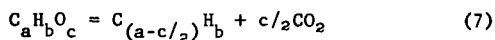
The major product component of SNG can be arrived at by reacting the hydrogen produced from the preceding reactions with the initial feed material as shown in Eq. 5.

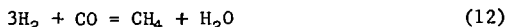
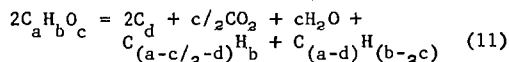
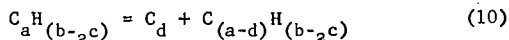


Combining Eqs. 4 and 5 give Eq. 6, which is a simplified form of the overall conversion reaction where the small amounts of nitrogen and sulfur in the feed material have not been accounted for.



Reactions also of importance in describing the direct conversion of coal are devolatilization and methanation. The devolatilization reactions can be viewed as Eqs. 7-10 or Eq. 11 overall, whereas the methanation reaction is demonstrated by Eq. 12.





Although the extent of the catalysts' role in the above reactions is not known from a mechanistic point of view, the influence of the alkali carbonate and nickel methanation catalyst has been amply demonstrated (2). The alkali catalyzes the coal-steam and devolatilization reactions for the production of intermediate reactants while the nickel catalyzes the conversion of these intermediates on to final products.

There has been some criticism of the thermodynamics concerning the feasibility of the direct production of SNG from coal-steam reactions by a single-step conversion. However, independent calculations by Edmiston (3) and Higgins (4) have shown that the overall conversion (Eq. 6) has a favorable standard free energy change in the vicinity of 900°K. Furthermore, the National Research Council (5) has taken the position that the reaction is thermodynamically feasible. These conclusions indicate that previous thermodynamic analyses have been based on β -graphite, which does not provide a good approximation of the coal's carbon for thermodynamic considerations. Consequently, erroneous conclusions are likely to arise therefrom.

The enthalpy of Eq. 6 has been calculated (4,6) from heats of combustion and amounts to about 10 kcal/mole. This value will vary somewhat with the rank of the coal. In spite of its endothermic nature, the single-step conversion is believed to be considerably more thermally efficient than the more conventional multiple-step processes for the production of SNG from coal.

Sulfur in the Multiple Catalyst Single-Step Conversion

In previous discussions of the process concept no mention of the influence of the coal's sulfur on the conversion was made. The sulfur contained in the coal is of particular concern in a multiple catalyst single-step conversion since its derived intermediates often function as catalyst poisons (7).

During the gasification of coal under reducing conditions the organic and pyritic sulfur of the coal are converted to gaseous sulfur compounds in their most reduced state. The extent of the coal's sulfur conversion is strongly dependent upon the gasification temperature (8). Although the type of reduced sulfur gases produced have not been extensively investigated and correlated with gasification conditions, H_2S , CS_2 and COS seem to be the predominate forms. These compounds are known to act as catalyst poisons in catalytic methanators even when present in small concentrations. Although the extent of sulfur poisoning of the nickel methanation catalyst used in the single-step conversion is more difficult to predict in view of the multitude of competing equilibria here too sulfur poisoning is anticipated to be a problem.

Table III contains some sulfur material balances that were undertaken to determine the extent of sulfur buildup on the nickel catalyst in the integrated system. Representative runs for both Glenrock coal and Consol lignite are included. These runs were completely integrated using the coal or lignite dry mixed with potassium carbonate and the nickel methanation catalyst. An examination of the data demonstrates that some of the sulfur is lost to the system, some remains in the ash and some is deposited upon the nickel methanation catalyst.

It is noted that there is considerable variance in the distribution of the coal's sulfur in the grouped runs. This apparently is attributed to the sensitivity toward experimental conditions and difficulty in obtaining a homogeneous reaction mixture of the 60-100 mesh coal and alkali carbonate with the 1/8" nickel catalysts.

The sulfur loss to the system is the computed difference between total sulfur in reactants charged and that found in the nickel catalyst and ash. In addition to

Table III Sulfur Material Balances

Run No.	Coal ^a	% Coal Conv.	MSCF Gas/Ton (CO ₂ -free)	Btu/SCF (CO ₂ -free)	Ni catalyst	% Original Coal Ash	Sulfur In System Loss
714 ^b	L	52	10.7	860	51.1	43.0	5.9
722 ^b	L	48	9.4	780	63.6	33.5	2.9
724 ^b	L	51	8.6	800	40.5	53.1	6.4
651 ^b	G	62	9.7	820	40.7	50.8	8.5
652 ^b	G	61	10.6	840	28.7	64.8	6.5
687 ^b	G	59	8.9	780	44.2	48.3	7.5
734 ^c	G	59	10.8	770	88.5	9.7	1.8
737 ^c	G	61	15.4	580	87.4	11.6	1.0
738 ^c	G	66	10.8	780	89.8	9.5	0.7

^a L, Consol lignite; G, Glenrock coal. ^b Runs all at 32 psia. ^c Runs all at 112 psia.

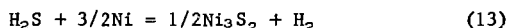
Table IV Sulfur Scavenger Runs

Run No.	% Coal Conv.	Scavenger, g/g coal	MSCF Gas/Ton (CO ₂ -free)	Btu/SCF (CO ₂ -free)	Ni Catalyst	% Original Coal Ash	Sulfur In System Loss
750	68	Fe ₂ O ₃ , 0.017	11.9	740	20.9	81.0	-1.9
752	58	Fe ₂ O ₃ , 0.017	9.0	880	7.9	92.9	-0.1
756	66	Fe ₂ O ₃ , 0.032	9.4	970	6.2	92.4	1.4
763	70	Fe ₂ O ₃ , 0.024	10.3	900	14.3	85.1	0.6
764	66	Fe ₂ O ₃ , 0.042	10.8	910	7.1	92.6	0.3
761	68	Fe ₂ O ₃ , 0.048	9.2	900	7.0	94.9	-1.9
765	64	Fe ₂ O ₃ , 0.063	10.0	920	20.4	77.3	2.3
753	73	ZnO, 0.021	7.7	890	6.3	98.4	-4.7
755	72	ZnO, 0.042	8.6	940	9.3	91.9	-1.2
757	68	PbO, 0.010	10.2	960	3.2	98.6	-1.8

sulfur escaping in the product gas, metallic sulfides were formed on the walls of the stainless steel reactor.

Runs 734, 737 and 738 were at 112 psia while the rest of the tabulated runs were at 32 psia. Although the per cent coal conversion was essentially the same for both low and high pressure runs, a significant difference in the original sulfur was observed. The elevated pressure increased the distribution of the coal's amount of sulfur deposited on the nickel catalyst and decreased the amount in the ash and that lost to the system. Experimentally there was essentially no difference in the sulfur distribution of the low pressure results for Consol lignite and Glenrock coal.

Roughly between 30 and 60% of the coal's sulfur was deposited on the nickel catalyst in the low pressure runs. In some of the runs the form of nickel sulfide was identified by x-ray diffraction to be Ni_3S_2 , presumably formed by the following reaction.



The presence of the sulfide instead of the sulfate is in agreement with the reducing atmosphere within the system. This has been supported by qualitative analysis performed on the catalyst. In view of the large amounts of nickel catalysts employed in the experiments, no decrease in its activity was observed for the batch charge runs.

The nature of sulfur compounds in the ash containing alkali carbonate was not determined by x-ray diffraction. There was no evidence to support sulfate formations by the alkali carbonate. Some wet analytical results have indicated that in the neighborhood of 70% of the sulfur remaining in the Glenrock ash under these conversion conditions is in the sulfate form. This represents a considerable increase in this form since the Glenrock coal initially contained only about 0.05% sulfate. Of the remaining 0.75% sulfur in this coal, 0.3% is organic and 0.5% pyritic. Although there have been no intensive attempts to identify the sulfate compounds in the Glenrock ash, the coal is known to contain considerable amounts of Ca, Mg, Fe and Al, all of which could potentially form sulfates.

By employing an average value of 45% of the coal's sulfur combining with the nickel catalyst in the above low pressure runs, one can estimate the amount of coal required to completely sulfide the methanation catalyst (35% Ni) by using Eq. 13. This value is 35.4g coal per g nickel catalyst or 54.9 lb catalyst per ton of coal. In view of the price of nickel methanation catalysts and provided the data extrapolation is valid, such a high catalyst usage would be economically infeasible without some means of catalyst regeneration. In view of this situation, some preliminary efforts have been directed at this problem.

Tentative Solutions to Sulfur Problems

Four general approaches to coping with catalyst poisoning in the multiple catalyst direct conversion process have been considered. These include:

1. Employing sulfur scavengers in the system
2. Devising some means of catalyst regeneration
3. Searching for active, more sulfur resistant catalysts and
4. Sulfur removal from coal prior to gasification.

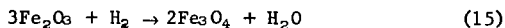
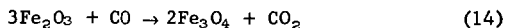
Sulfur Scavengers.-Although several techniques for the clean up of sour gas are commercially available, the direct use of sulfur scavengers in a coal gasifier has received considerably less attention. The approach in the direct conversion process was to mix inorganic materials with the catalysts and coal so that they could compete with the nickel catalyst for the gaseous compounds produced during the gasification. These sulfur scavengers were selected on the basis of their thermodynamic suitability for sulfide formation and relative cost.

Sulfur scavenger results with Fe_2O_3 , ZnO and PbO are contained in Table IV. The powdered inorganic scavengers were dry mixed with the coal. The variance in the results of the sulfur retained in the ash is analogous to the results with no scavengers present. Here again this is attributed to the sensitivity to experimental conditions and difficulty in obtaining homogeneous samples. Nevertheless, when these scavenging results are compared to the non-scavenging results it is clear that the scavengers have played a definite role. Only 6-20% of the coal's original sulfur was deposited on the nickel catalyst in the iron scavenger runs and 3-10% for PbO and ZnO scavenger runs. These values may be compared to 30-60% of the coal's sulfur reacting with the nickel catalyst in the absence of the scavengers. Based on this data, the use of scavengers could provide as much as an order of magnitude improvement in the nickel catalyst life.

The tabulated sulfur scavenger results with Fe_2O_3 indicated that the method of contacting the scavenger and coal is more important than its concentration over the investigated concentration range. Although the ZnO and PbO were not investigated as extensively as the Fe_2O_3 scavenger, they appear to function as well, if not better, than the hematite. Although the first three tabulated iron runs (750, 752, 756) were at 112 psia, the sulfur scavenging results were essentially the same as later runs with iron at 32 psia.

Some of the ash samples from the sulfur scavenger runs were examined by x-ray diffraction. The only sulfide definitely identified was ZnS in the case of the zinc scavenger runs. The failure to observe the metallic sulfides in the iron runs may have been due to insufficient concentrations or formation of amorphous compounds.

It is interesting to note that the ash from the iron scavenger experiments failed to show the presence of hematite (Fe_2O_3) but the reduced form, magnetite (Fe_3O_4) was observed. This is not surprising in view of the reducing atmosphere present in the system. The reduction is probably due to a combination of the following reactions.



Another effect of such reactions is to increase the CO_2 -free heating value of the product gas, since the low heating value constituents H_2 and CO are removed by these redox reactions. This is in agreement with the observed heating values for the scavenger runs being somewhat higher than the non-scavenger runs.

Catalyst Regeneration.—For the sake of completeness, it is informative to examine the $\text{Ni-H}_2\text{S}$ equilibrium. Under conversion conditions in the integrated system, the nickel sulfide formation (Ni_3S_2) according to Eq. 13 is predicted from the phase diagram (9). The equilibrium temperature dependence of this reaction has been investigated by Kirkpatrick (10) and Badger (11). Figure 3 is an extrapolation of this data. Clearly, if the $\text{H}_2\text{S}/\text{H}_2$ ratio at any designated temperature should exceed the equilibrium value at that temperature, then Ni_3S_2 would form according to Eq. 13. On the other hand, if the $\text{H}_2\text{S}/\text{H}_2$ ratio should fall below the equilibrium value at a given temperature sulfur would be removed from the nickel catalyst. Furthermore, it is apparent that as the temperature is increased a larger concentration of H_2S can be tolerated without Ni_3S_2 formation.

This information suggests an approach to catalyst regeneration, namely the use of essentially sulfur-free hydrogen or synthesis gas at elevated temperatures to remove sulfur from the nickel catalyst according to Eq. 13. This approach has been employed for sulfur removal from a sulfided form of the nickel methanation catalyst. The experiment was carried out in the previously described 1/2" adiabatic flow reactor using a sulfur-free synthesis gas composed of 28.4% CO , 71.3% H_2 and 0.3% CO_2 . Regeneration conditions were 690°C, 117 psia and 10,500 hr^{-1} space velocity. The results are tabulated in Table V. Although the run continued over a 17-hour period, the most rapid improvement in the catalyst activity was in the first

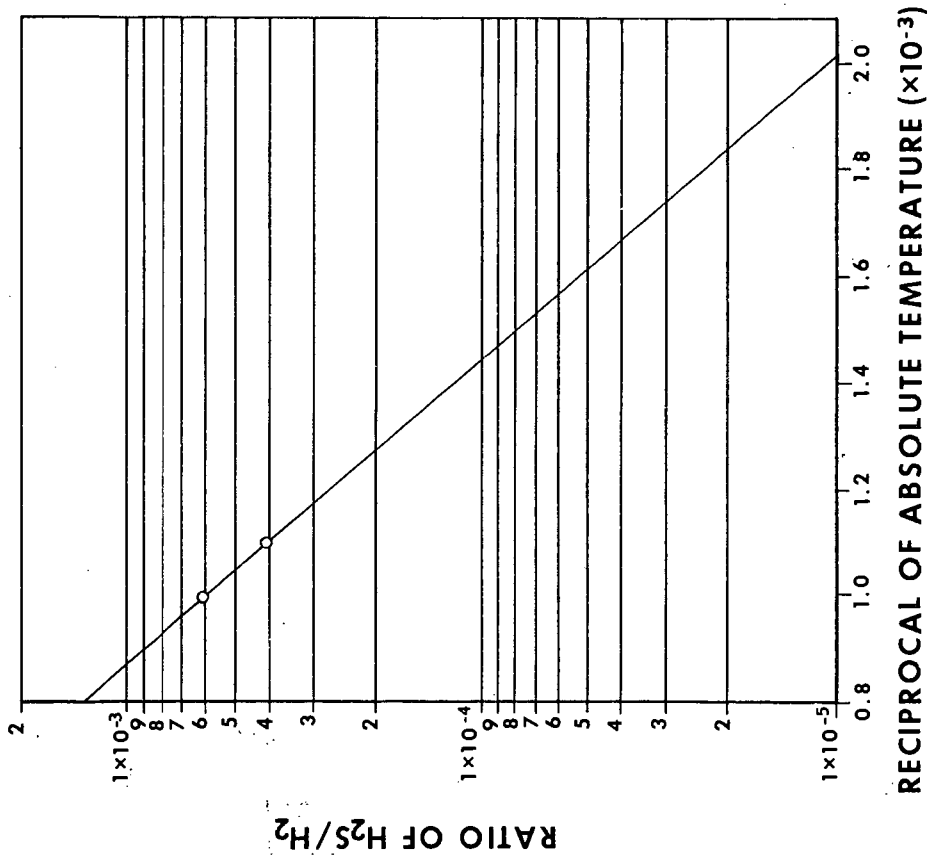


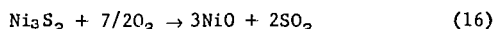
FIGURE 3 THE Ni-H₂S EQUILIBRIUM. $1/2 \text{Ni}_3\text{S}_2 + \text{H}_2 = 3/2 \text{Ni} + \text{H}_2\text{S}$

Table V. Catalyst Regeneration Data

	Initial Catalyst	Final Catalyst
Total Sulfur (wt. %)	9.4	0.4
Sulfide Sulfur	7.4	0.3
Sulfate Sulfur	2.0	0.1
Regeneration Conditions		
Pressure (psia)	117	117
Temperature (°C)	690	695
Space velocity (hr ⁻¹)	12,000	10,500
Product Gas Composition (mole %)		
H ₂	68	54
CO	26	13
CH ₄	4	26
CO ₂	1	6

5 hours where the methane in the product increased from 4% to about 18%. During this time there was a detectable odor of H_2S in the product gas. Even though a significant improvement in the methanability of the sulfur poisoned nickel catalyst was achieved by the regeneration, it was still found to be less active than the non-sulfided catalyst since the product composition from the latter at $H_2/CO = 2.86$, $667^\circ C$, 120 psia and $213,000 \text{ hr}^{-1}$ space velocity was 41.2% H_2 , 2.4% CO , 49.0% CH_4 and 7.2% CO_2 . Aside from the Ni_3S_2 formation, additional deactivations of the catalyst are implicated. This would appear to be caused either during the sulfiding of the catalyst with H_2S or during its regeneration with sulfur-free synthesis gas.

Two additional, less successful means of sulfur removal were briefly considered. One method was to use air or oxygen to oxidize the sulfur to SO_2 according to the following reaction.



This approach suffered the competing reaction for nickel sulfate formation. Consequently, about half of the sulfur was expelled as SO_2 while the remainder was retained by the catalyst as nickel sulfate. The other approach was the use of aqueous solutions of acids for sulfur removal as H_2S . Although, the sulfur was readily liberated, the acidic solutions badly degraded the catalysts' physical structure. Some success in sulfur removal was realized by employing dilute aqueous solutions of hydrogen peroxide to liberate the sulfide as SO_2 . No activity tests have been made to date in these latter two instances.

Alternate Catalysts.—Since nickel methanation catalysts are susceptible to deactivation in the presence of small concentrations of sulfur gases produced during coal gasification, alternate catalyst possibilities have been considered. Alternatives that have been suggested are either active more sulfur resistant catalysts or active sulfided catalysts.

In view of the generally favorable thermodynamics of metallic sulfide formation from metallic catalysts it would appear that the search for active sulfided forms of catalysts would be the most profitable. Furthermore, there are a number of different sulfided catalysts that are currently used for hydrotreating in the hydrocarbon processing industry that show hydrogenation activity. In this regard a completely sulfided form of the nickel methanation catalyst used in the single-step conversion process was prepared and tested for its methanation activity in the $1/2''$ adiabatic flow reactor. A comparison between the activity of this sulfided catalyst (14.2% S) and its nonsulfided (0.06% S) form are presented in Figure 4. It is apparent that the sulfided form of the catalyst shows considerable methanation activity although it is still inferior to the nonsulfided catalyst. The thermal conversion is an order of magnitude less than that for the sulfided catalyst. In view of these results it would appear that further investigations of sulfided catalysts for high temperature methanation are warranted. In this respect a number of sulfided catalysts of various transition metals are commercially available.

A Prior Sulfur Removal.—The removal of a portion of the coal's sulfur prior to its utilization would reduce the extent of catalyst sulfidation. Prior sulfur removal schemes have recently been reported (12,13,14) and this appears to be an area in which considerable future research will be directed. Although these prior sulfur removal techniques are not particularly economically attractive that does not preclude significant breakthroughs in the area with intensified research. In regard to the single-step conversion, a prior sulfur removal would conceivably be combined with one or more of the preceding remedies to help alleviate the sulfur poisoning problem.

CONCLUSIONS

A qualitative description of the chemical processes involved in the single-step catalytic production of high Btu gas from coal-steam reactions has been presented. The role of the catalysts in the conversion and thermodynamic justifications were also presented. Using this direct approach for the production of SNG from coal, several

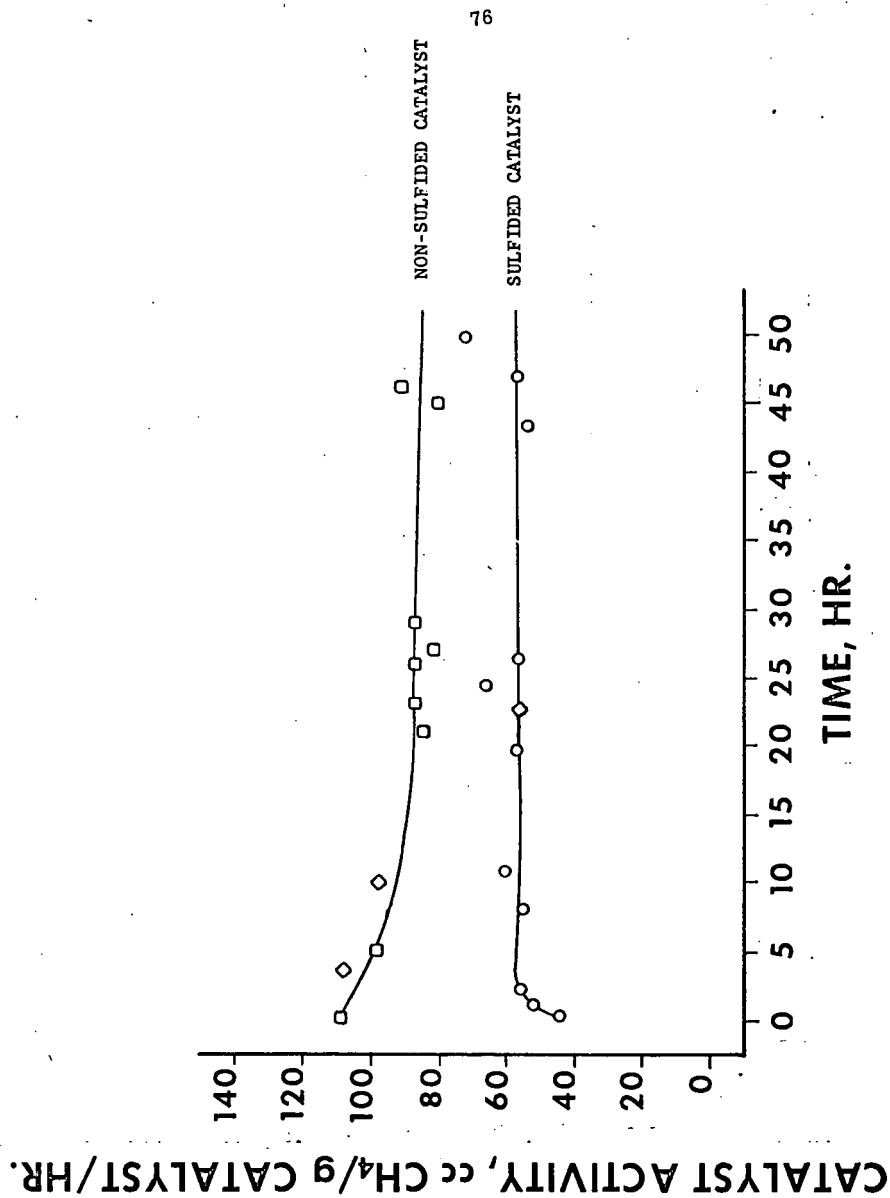


FIGURE 4. COMPARATIVE CATALYST ACTIVITY $3H_2/1CO$ at 25 psia, 675°C and 1000 hr^{-1} space velocity.

processing steps could potentially be eliminated and the thermal efficiency of the overall conversion increased. However, problematic areas concerning the poisoning of nickel catalysts used in the single-step conversion remain unanswered.

Although several approaches to coping with catalyst poisoning by sulfur compounds in the direct conversion process have been presented, no clear cut solution to date is indicated. Instead, a proper combination of the use of sulfur scavengers, catalyst regeneration, more sulfur resistant catalysts and a prior sulfur removal could be the final solution. Although, the experimental results of using sulfur scavengers, catalyst regeneration and sulfided catalysts have been encouraging, neither of these methods have proven to date to be completely satisfactory. Nevertheless, the potential reward to be derived from the direct single-step production of SNG from coal is of such magnitude that continued efforts in this area are necessary.

ACKNOWLEDGEMENTS

The work reported here has been sponsored by the United States Department of Interior, Office of Coal Research and is presented with their permission. The technical assistance and unwavering enthusiasm provided by R. W. Hoffman is greatly appreciated.

REFERENCES

1. Hoffman, E. J., J. L. Cox, R. W. Hoffman, J. A. Roberts and W. G. Willson, Preprints, Division of Fuel Chem., 16 (2), 64-67(1972).
2. Willson, W. G., L. J. Sealock, Jr., F. C. Hoodmaker, R. W. Hoffman, D. L. Stinson and J. L. Cox, "Advances in Chemistry Ser.; Coal Gasification", in press.
3. Edmiston, C., Personal Communication, Chemistry Dept., University of Wyoming, Laramie, Wyo., 1972.
4. Higgins, G. H., "A New Concept for In Situ Coal Gasification", UC RL-51217, Lawrence Livermore Laboratory, University of California, April 17, 1972, 17 pp.
5. R&D Report No. 74-Interim Report No. 1, "Evaluation of Coal-Gasification Technology Part I", Prepared for OCR by National Research Council, 1973, p. 44.
6. Cox, J. L., W. G. Willson and E. J. Hoffman, "Conversion of Organic Waste to Fuel Gas", J. of Environ. Eng. Div., ASCE, in press.
7. Anderson, R. B., "Catalysis; Catalysts for the Fischer-Tropsch Synthesis", Vol. IV, Reinhold Pub. Corp., New York, P. H. Emmett, ed., 1956, p. 242-9; Maxted, E. B. "Advances in Catalysis; The Poisoning of Metallic Catalysts", Vol. III, Academic Press Inc., 1951, p. 129-78.
8. Vestal, M. L. and W. H. Johnston, Preprints, Div. of Fuel Chemistry, 14 (1), 1-11 (1970).
9. Nickless, G., "Inorganic Sulfur Chemistry", Elsevier, New York, 1968, p. 719.
10. Kirkpatrick, W. J., "Advances in Catalysis and Related Subjects; Nickel Sulfide Catalysts", Vol. III, Academic Press Inc., ed. W. G. Frankenburg et al., 1951, p. 330-2.
11. Badger, E. H. M., R. H. Griffith and W. B. S. Newling, Proc. Roy Soc. (London) 197A, 18A(1949).
12. Meyers, R. A., J. W. Hammersma, J. S. Land and M. L. Kruff, Science, 177 (4055), 1187-8(1972).

13. Perry, H. and J. H. Field, Eng. Dig. (Toronto), 14 (4), 49-51(1968).
14. Messman, H. C., Chem. Tech., Feb. 1971, pp. 114-6.

CONVERSION OF SOLID FUELS TO LOW BTU GAS

Thomas E. Ban

McDowell-Wellman Engineering Company
Cleveland, Ohio 44110

BACKGROUND AND INTRODUCTION

More than 11,000 gas producers were in operation during 1926, gasifying about 15 million tons of coal per year into low BTU gas. This fuel served both industrial and town requirements with approximately 50 percent utilized by the steel industry alone. In special cases the producer gas was cleaned by methods commonly used for purifying coke oven gas and water gas. The industrial success of making a clean, desulfurized manufactured gas from coal was apparent.

The current energy and environmental crises should not seem possible to those unfamiliar with the further history of coal gasification. However, this reveals that the 11,000 gas producers operating in 1926 decreased to about 4,000 in 1948, gasifying only 4 million tons of coal per year and the process extended to the cleaner fuels, anthracite and coke⁽¹⁾. Today, in the United States only a few bituminous coal gas producers exist and these have been placed in mothballed and perhaps standby positions.

The decline of manufactured gas production has been attributed to a number of factors, most prominent of which was the advent of low cost and versatile hydrocarbon fuels; fuel oil and natural gas as developed from domestic reserves and new pipeline transportation systems.

It is reasonable to claim that America became complacent over cheap natural hydrocarbons and did not pay great heed to those concerned with the eventual depletion of these fuels. Only token efforts of research and national interest were applied to the objectives of meeting fuel requirements and standards that could be expected for the 1970's and 1980's. During the 1950's and 1960's only a small number of new young technologists could be convinced of the challenges offered by the mineral industry fields. Only a small portion of these were inclined to have interest in smelly coal gas developments, an area which then had signs of becoming obsolete. In view of the foregoing, it appears as if the present day coal-to-gas technologists will have to "play catch-up."

FIXED BED GASIFICATION

The production of low BTU gas from coal is a broad topic of coal gasification which ranges from the long established coke oven practices to the more sophisticated high pressure fluo-solid reactions of coal, oxygen enriched air, and water. A general classification of coal gasification processes has been qualified by Von Fredersdorff and Elliot and their listing has been expanded with further items as presented in Table 1⁽²⁾. The subject of this presentation will largely concern production of low BTU gas from coal by classical and improved technologies listed as the initial

items in the outline of Table 1. This involves fixed bed gasification of coal autothermally converted by a countercurrent air-stream draft in an atmospheric producer disposing of dry granular ash.

A generalized version of this gasification process is illustrated in Figure 1 which shows reaction zones in a section of a producer and the corresponding temperature-composition gradients when a solid fuel is converted into low BTU producer gas. Sized and selected qualities of coal are charged and distributed to the top of a cylindrical shaft and descend countercurrently to a forced air-steam blast. The fixed bed designation refers to fixation of the top and bottom surfaces of the bed with respect to space while the continuously applied charge moves downward and converts into gas and ash. The forced draft enters through the grates and exchanges heat with ash prior to combustion within the narrow peak temperature oxidation zone. Herein oxygen combines with carbon to form CO_2 causing the greatest evolution of heat in the process and control is exercised to prevent excessive ash fusion by appropriate steam additions. Preheated steam and CO_2 from the oxidation zone cause endothermal reactions in the reduction zones which give rise to production of the main fuels of producer gas, carbon monoxide, and hydrogen.

Hot reduced gases from the reduction zones provide heat for pyrolysis reactions and drying-preheating within the topmost zone of the charge. Pyrolysis largely involves thermal cracking of the volatile hydrocarbonaceous matter of coal and tars. Large molecular weight compounds are thermally degraded into lighter, smaller, and more volatile constituents as a wide range of compounds comprising soot, tars, light oils, tar acids, and noncondensable gases. The degradation brings about production of methane, hydrogen, water, carbon, and carbon oxides.

The coexistence of all cited reactions of Figure 1 within specific zones is governed by reactivities of the fuel and chemical equilibria limitations. The distinct zones illustrated in Figure 1 are shown only for purposes of simple isolation. For instance, the reversal of CO_2 reduction of the Boudouard reaction can cause carbon deposition in the upper cooler zones of pyrolysis. Also, possibilities can exist for the methanation reaction of carbon and carbon monoxide reacting with hydrogen to a very limited extent. During gasification organic and pyritic sulfur of coal is largely converted to gaseous forms such as H_2S , CS_2 , COS , and various light mercaptans. These are brought about by oxidation-reduction reactions and direct reactions with labile sulfur from the pyrolysis of pyrite. Sulfides of coal ash are oxidized by the initial air-steam draft and the sulfur oxides originating in this zone and the oxidation zone are subsequently reduced in the reduction zones to high portions of hydrogen sulfide.

Evolution of tars, condensable oils, and carbonaceous soot within the pyrolysis zone contributes to problems of bed permeability and depositions within the off-gas ducts. Use of the producer gas in a hot raw state (1100-1500 °F) has necessitated measures for coping with duct and burner problems. Condensables and other particulates can be removed, however, by cooling, condensation, scrubbing, and precipitation. These provide cold clean gas and necessitate disposition plans for the oily and aqueous by-products. Clean

producer gas can be further purified by removal of gaseous sulfur compounds through use of a number of removal and recovery schemes, new and old, some of which are listed in Table 2.

Thermal efficiencies of gas production systems are defined as the percentage of heat from the solid fuel which reports in the sensible and latent heat of the gas. Hence hot raw gas producers show efficiencies of about 90 percent and cold clean gas producers using bituminous coal have efficiencies of about 70 percent which increase to about 85 percent with coke and anthracite.

GAS PRODUCERS

A wide variety of gas producer designs were constructed during the early 1900's based largely on the original concepts of Bischof, Ebelman, Ekman, and Siemens. Since the initial inventions about 150 different organizations manufactured gas producers⁽³⁾. Some specific designs available as early as 1907 are listed as follows:

Amsler	Siemens
Swindell	Wellman
Smythe	Fraser-Talbot
Taylor	Morgan
Wood	Loomis
American Furnace	Wile

These producers operated under forced draft. During the same time period there were about an equal number of designs which functioned under induced draft. Through evolution of design and market acceptance only a few producer gas units survived into the 1920's, 1930's, and 1940's. Some prominent units were the Morgan, the Wellman-Hughes, the Wood, the Semet-Solvay-Koller, the Koppers-Kerpely, and the Wellman-Galusha. The latter is the only producer to survive into the 1950's-1970's with some current applications involving production of special high CO gases for chemical purposes. Features of some of the producers are illustrated in Figures 4, 5, and 6 which are described as follows:

1. Figure 2 - Wellman-Hughes Gas Producer (4)

This was a refractory-lined and water sealed unit with rotating shell and oscillating agitator for gasifying bituminous coal.

2. Figure 3 - Koppers-Kerpely Gas Producer (5)

This unit had refractory and water cooled walls which were stationary components and it used a rotary water sealed ash removal system. This producer was largely used for gasifying coke.

3. Figure 4 - Wellman-Galusha Gas Producer (3)

This unit is designed for gasifying all forms of solid fuels including bituminous coal, anthracite, coke, and charcoal. The producer consists of a choke filled hopper, stationary water cooled walls which provide humidity for the blast, rotary grates, and a rotary agitator used for inducing controlled perme-

ability to troublesome burdens such as swelling varieties of coals. A battery of 14 Wellman-Galusha producers constructed in a gas plant is shown in Figure 5.

Producer gas was widely developed for open hearth type furnace applications which benefited from hot raw gas and preheated air from regenerative sections. The open hearth steelmaking and glassmaking furnaces are typical in this respect, commonly using hot raw producer gas generated from a battery of producers. After cooling and cleaning systems were developed, producer gas was extended into applications for smaller industrial furnaces and gas engines. Cleaned and purified producer gas was applied as a fuel blend for town gas plants and chemical-metallurgical industries used producer gas for synthesis and reduction applications.

FUELS

Production of low BTU gas from anthracite and coke does not necessitate extensive cleaning because there are no significant pyrolysis reactions. As a result, these fuels have extensive acceptance for production of producer gas because of the lower capital and conversion cost factors inherent with low volatile fuels.

Gas-solid reactions in producers are dependent on uniform charge permeability. For this reason closely sized fuels have been preferred and in some cases they have been required. Producers using bituminous coals usually use nut and egg sizes and those using anthracite and coke have generally used buckwheat and rice sized charge.

Both swelling and nonswelling qualities of bituminous coal have been successfully gasified in commercial applications and specially designed mechanical agitators have been used for maintaining bed permeability with troublesome burdens. Various types of agitators have been designed to allow producers to cope with coals having high free-swelling indices and unusual softening-agglomerating characteristics. These coals are prevalent in the eastern and midwestern coal regions of the United States.

The composition of producer gas is dependent on the quality of volatile matter in the fuel, the reactivity of the fuel, and to a certain extent, the ash fusion characteristics which influence the requirement of steam. Table 3 provides general data on composition of various manufactured gases including low BTU producer gas made from four different types of fuel.

COSTS

Costs for production of producer gas have been presented by several articles based on factual records and projections^(1,6,7). Specific costs obviously depend on items such as objectives, rates, quality of operations, and quality of raw materials, all of which are subject to change with time. Table 4 presents conversion costs of coal as derived from different producer gas plants operating at different periods of time producing hot raw low BTU gas. It is noteworthy that a span of 17 years did not indicate a marked change of costs. However, unless there is a marked improvement of technologies, it can be expected that the escalation of labor rates,

fuel rates, and environmental requirements will cause future costs to increase. For instance, the data of the 1965 report indicated that the 43¢ per million BTU for hot raw gas would increase to about 55¢ for cold clean gas and this study (1965) did not account for removing sulfur to the levels now expected to be necessary for 1974.

PRESSURE APPLICATIONS

The incentive for production of hydrocarbons and high BTU gas from coal justified development of the oxygen blown pressure producer designed to operate under about ten to twenty atmospheres of pressure. The Lurgi high pressure gas producer was developed in Germany in the 1930's to utilize the noncaking brown coals. A number of similar applications have been extended since this early development. McDowell-Wellman Engineering Company constructed the retort and mechanical components of the high pressure pilot plant gas producer for the U. S. Bureau of Mines which was specifically designed for gasification of the swelling type coals of the United States. The Lurgi unit also has been tested for this purpose. Diagrams of these two types of producers are shown in Figures 6 and 7(8,9).

ASPECTS OF FUTURE COMMERCIALIZATION

Production of clean, low cost, low BTU producer gas for future industrial purposes will depend on achieving a number of process improvements. This is especially important if the gas is to be made from a wide variety of fuels with varying values. Some aspects of gas production which require attention or improvement are cited as follows:

1. Fuel Sizes

The gasification system should be developed to accept a wide variety and range of fuel sizes rather than the more costly specific coarse size fraction.

2. Fuel Qualities

The machinery and processing systems should be improved for broadly accepting (a) weak structured coals which tend to degrade during gasification and (b) the severe high swelling fuels which tend to strongly agglomerate during gasification.

3. By-product Utilization

Utilization of all by-product liquids including tars, oils and aqueous liquors along with solid wastes will become of increasing importance for all gasification processes and proper approaches should be developed for recycling the by-products to the processing system or isolation and upgrading of by-products for market purposes.

4. Environmental Requirements

It can be expected that environmental require-

ments for more complete control will continue to increase and extensive processing provisions will be required for (a) production of high purity products from the processing system and (b) design of appropriate safeguards from accidental or designed venting of gases and liquids from the system.

5. Unit Capacities

Increasing costs of labor for operations and maintenance and increasing costs for materials of construction and improvement of thermal efficiencies will direct processing systems to high unit capacities and capabilities of treating high tonnages with single or small multiples of large machines rather than the large numbers of small machines.

6. Usage

Use of clean low BTU gas in large quantities for boiler fuel and large industrial furnace applications will require renewed attention to aspects of gasification which combine large capacity units with high availability factors and wide turndown capabilities.

PROCESS DEVELOPMENTS

The six cited items which deserve improvement for growth of the producer gas industry indicate merit to the design of larger diameter units as well as design of systems for charge preparation and recycle of by-products. Expansion of the peak 10-ft. diameter design for atmospheric producers will bring increasing attention to factors such as (1) charge preparation for uniformity of burden column permeability, (2) uniformities and control of ash removal, (3) control of the specific reaction zone levels, and (4) control of bed agitation for mechanically inducing bed permeability. The current and future designs can markedly benefit from charge preparation schemes of "beneficiation charge" that would integrate precarbonizing-agglomerating and recycling with fixed bed gas production. Research and pilot plant work in this area appear to be justified. Such schemes might parallel the successful evolution of the iron blast furnace smelting practices which evolved with the largest units in the following approximate order of peak blast furnace capacities.

<u>Era</u>	<u>T/D of Iron</u>
1940's	1,500
1950's	3,000
1960's	6,000
1970's	10,000

History reveals that these increases were attained by developments of both charge preparation and furnace enlargement.

Charge preparation for modern blast furnace practices include (1) production of strong durable sized coke from coal and (2) production of strong durable sized ore agglomerates from a blend of ores, fluxes, and plant recycles such as dusts and sludges. Iron ore agglomerates are produced as close sized structures of sinter or pellets prepared largely by continuous traveling grates. These machines are of a Dwight-Lloyd type and have enormous unit capacities. Individual machines of a modern plant have sinter production capacities which exceed 12,000 T/D of beneficiated charge for blast furnaces. An artist's diagram of a sinter plant is shown in Figure 8.

The sintering process involves preparation and conversion as a continuous series of operations⁽¹⁰⁾. The initial preparation consists of proportioning and blending of fine ores and fluxes with about 5 percent coke breeze and moisture to form a nodular textured burden. This is continuously charged to the sintering machine as a thin bed supported on the moving grates. Some of the larger Dwight-Lloyd machines have a grate hearth area of about 15 feet wide and 350 feet long. The raw material is flame ignited after charging to the grates and an induced draft performs combustion, calcination, partial fusion, and cooling to form a coherent cellular structured sinter cake. This is subsequently crushed and graded into an appropriate size for the blast furnace and the fines are recirculated.

The traveling grate process for beneficiating or converting coal for gas production is a subject of current patents and research at the Dwight-Lloyd Research Laboratories of McDowell-Wellman Engineering Company. A general concept involves preparation of a thin bed comprised of nodulized coal and recycle materials followed by traveling grate processing of high temperature pyrolysis-gasification which evolves low BTU gas, liquids and agglomerated residue of coke-char composition suitable for final gasification. Figure 9 illustrates two simplified species of the Dwight-Lloyd traveling grate processes for converting coal. One of these involves combustion of oil or gas for sustaining operations and the other involves combustion of fixed carbon. As the charge enters the pyrolysis or carbonizing zone it becomes intercepted by hot gases which cause coking and gasification of the thin bed. Cooling and condensation is effected by both the lower incremental layers of charge and the heat sink. These enable coal gases to be recycled to the cooling zone which in turn provides preheated media for carbonizing.

Tests which simulate the time - temperature - draft flow conditions of the aforementioned traveling grate processes have been performed with a wide variety of fuels ranging from lignites to highly coking coals. Agglomeration and permeability characteristics of the bed for such tests were controlled by use of recycle materials. In cases of treating coals by the pelletizing process, the recycle materials can comprise portions of the green pellet as well as portions of the bed to maintain consistent bed permeability for uniform processing operations.

Table 5 presents resume data on conversion of a strongly caking coal into gases, liquids and pelletized coke using combinations of the pelletizing process and the traveling grate carbonizing processes illustrated in Figure 9. A graphical portrayal of the thermal history of the bed within the traveling grate pelletizing-carbonizing

process for both species is shown in Figures 10 and 11. The data show both processes to be capable of converting coal into durable pellet coke for final gasification in fixed bed gas producers.

A liquid sealed circular Dwight-Lloyd machine is involved in this development and Figure 12 illustrates a rendition of this unit. Current designs on the order of 3,000 square feet and greater have the potential of converting more than 1,000,000 T/Yr of coal into hardened coke-like masses with about 50 percent of the fuel evolved into gaseous and liquid fractions. These can be recycled or combined with producer gas made from a final stage of gas production using either an enlarged shaft furnace or traveling grate. Gas desulfurization can be applied to the recycle stream to assist desulfurization of the char or it can be applied to the final vented or combined gas streams.

Charge preparation schemes such as the traveling grate - pre-coking processes can be integrated with an upgraded and enlarged version of fixed bed gas producers to meet the challenges of making clean, low cost, low BTU gas from coal. Approaches such as this could welcome offgrade coals back into our energy picture.

ACKNOWLEDGEMENTS

Appreciation is expressed to McDowell-Wellman Engineering Company for support of this work. Special acknowledgement is also made to personnel of the Dwight-Lloyd Research Laboratories of McDowell-Wellman for their efforts on development of the pellet conversion process.

REFERENCES

1. Foster, J. F. and Lund, R. J., "Economics of Fuel Gas From Coal," McGraw-Hill Book Co., New York, 1950, pp 23-25.
2. Lowry, H. H., "Chemistry of Coal Utilization," Supplementary Volume, John Wiley & Sons, New York, 1963, pp 947-963.
3. Hamilton, G. M., "Gasification of Solid Fuels in the Wellman-Galusha Gas Producer," presentation to AIME, St. Louis, February 1961.
4. Wellman-Seaver-Morgan Co., "The Open Hearth," U. P. C. Book Co., New York, 1920, pp 209-251.
5. Wilson, P. J. and Wells, J. H., "Coal, Coke, and Coal Chemicals," McGraw-Hill Book Co., New York, 1950, pp 6-39.
6. Bituminous Coal Research, Inc., "Gas Generator Research and Development Survey and Evaluation, Report L-156 to the Office of Coal Research," U. S. Department of the Interior, Washington, D. C., 1965
7. Schwalbe, S. G., "Economic Problems in Use of Alternate Fuels," Glass Industry, Vol. 29, March 1948, pp 137-140.
8. Lewis, P. S., Liberatore, A. J., McGee, J. P., "Strongly Coking Coal Gasified in a Stirring-Bed Producer," USBM, R.I. 6721, 1971.
9. Hartman, W. V., "Coal to Gas via the Lurgi Route," Proceedings, Second Energy Resource Conference, University of Kentucky, October 24, 1972, pp 40-43.
10. Ban, T. E., Czako, C. A., Thompson, C. D., Violetta, D. C., "The Continuous Sintering Process - Research and Applications, Agglomeration," Intersciences, New York, 1962, pp 511-536.

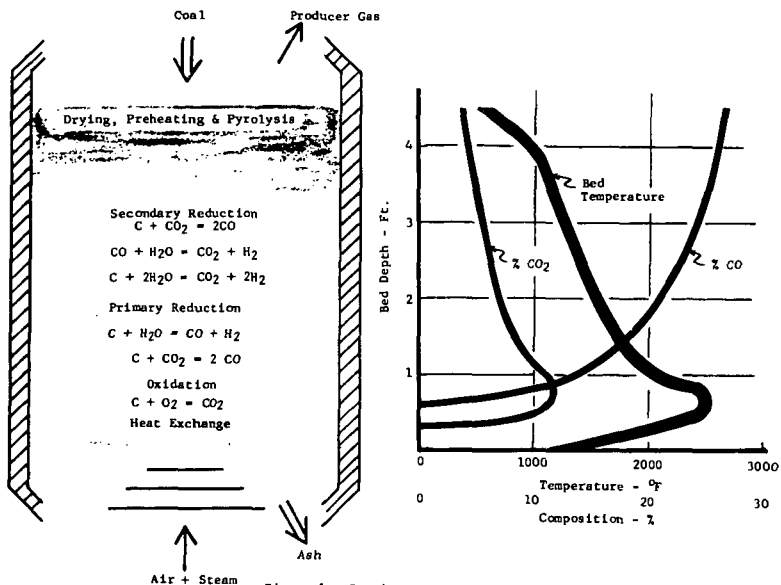


Figure 1 - Section and Gradients for Fixed Bed Gas Production

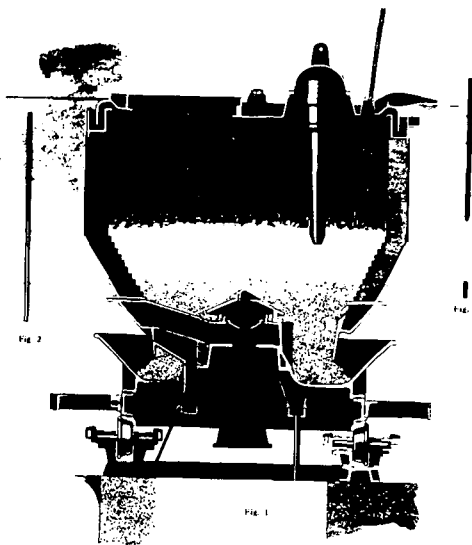


Figure 2 - Wellman-Hughes Gas Producer

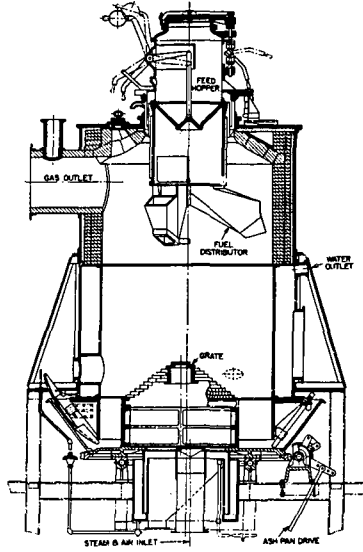


Figure 3 - Koppers-Keperley Gas Producer

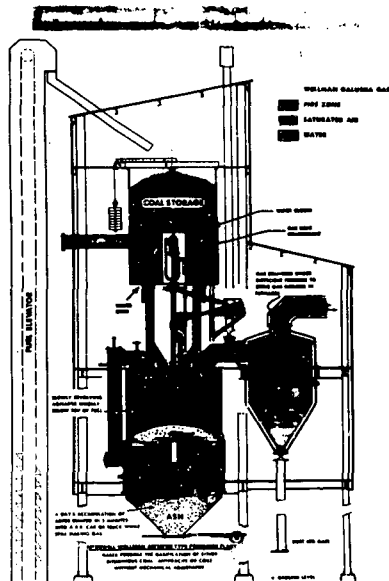


Figure 4 - Wellmann-Galusha Gas Producer

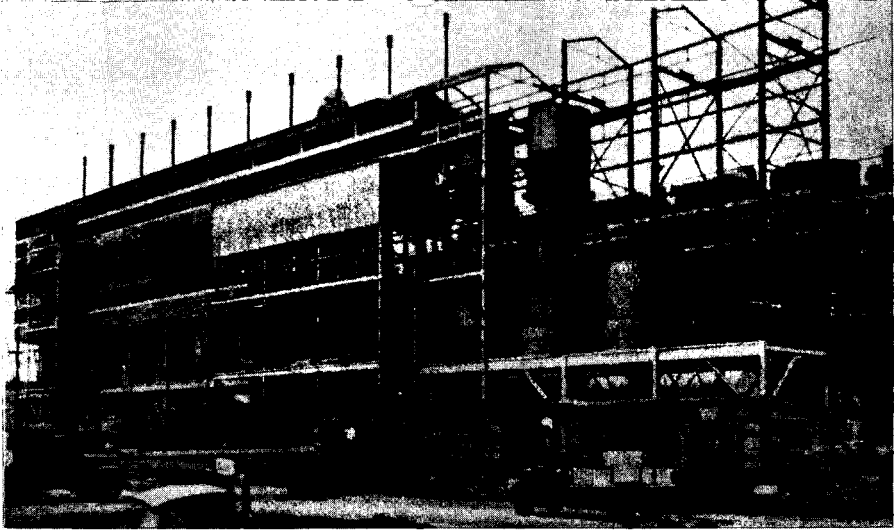


Figure 5 - A Battery of Fourteen Producers
Within a Wellman-Galusha Gas Plant

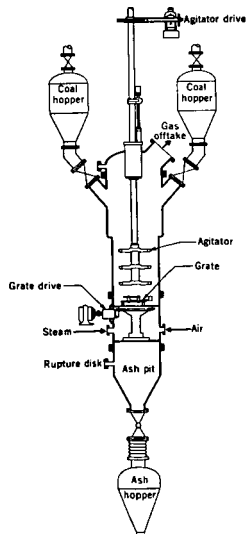


Figure 6 - USRM Pilot Plant Pressure Producer
Constructed by McDowell-Wellman
Engineering Company

91

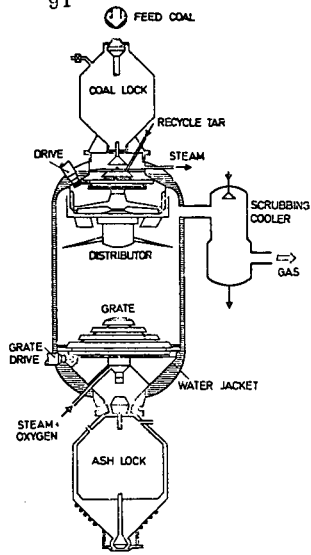


Figure 7 - Large Pressure Producer of Lurgi Minerva-Loechnik GmbH

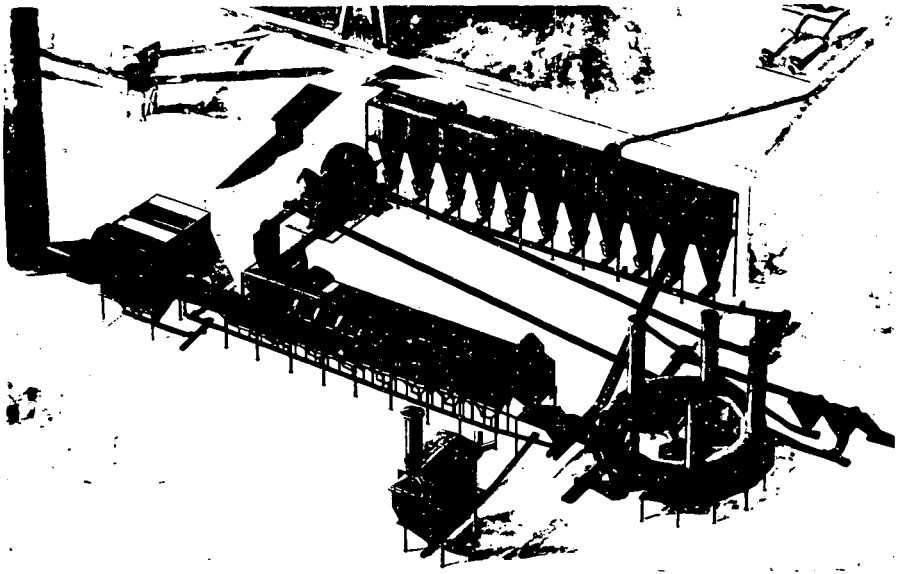


Figure 8 - Iron Ore Sintering Plant

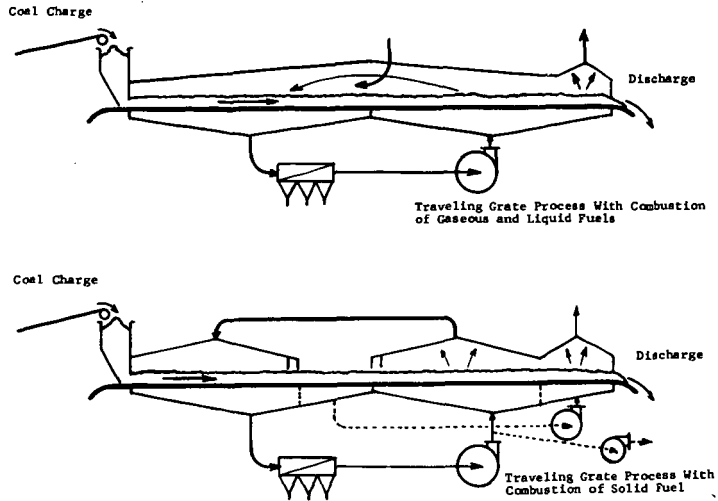


Figure 9 - Dwight-Lloyd Traveling Grate Processing Systems for Carbonizing-Gasifying Coal

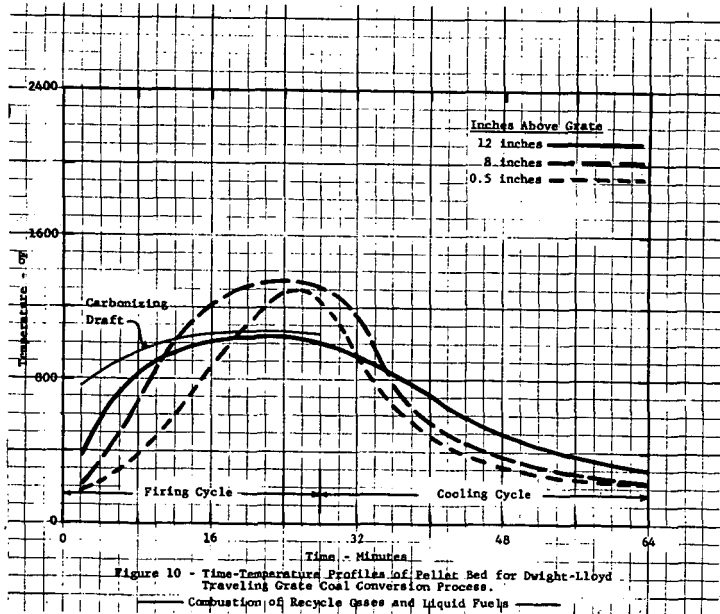


Figure 10 - Time-Temperature Profiles of Pellet Bed for Dwight-Lloyd Traveling Grate Coal Conversion Process.

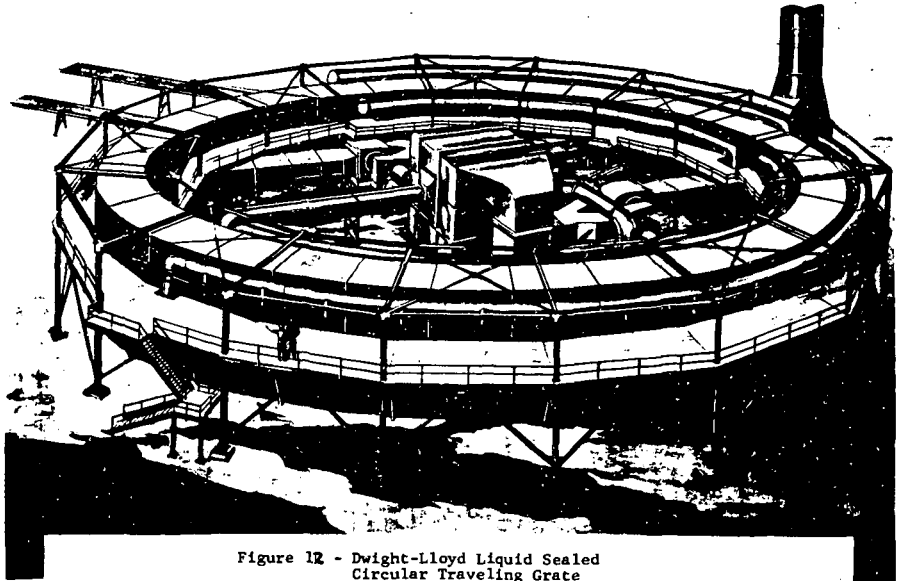
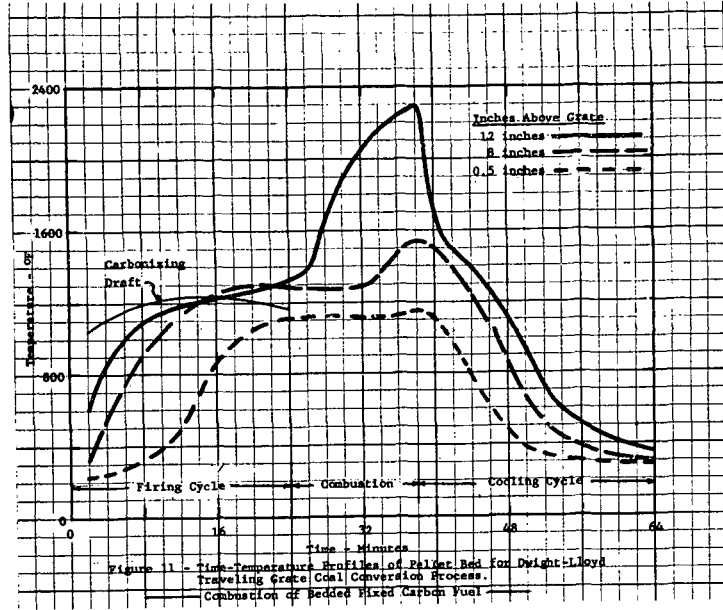


Figure 12 - Dwight-Lloyd Liquid Sealed Circular Traveling Grate

Table 1

CLASSIFICATION OF GASIFICATION PROCESSES

- I. Method of Supplying Heat
 - A. Internal (direct)
 - 1. Autothermic
 - 2. Cyclic
 - 3. Fluids or solids
 - B. External (indirect)
 - 1. Transferred through walls
- II. Method of Reacting
 - A. Fixed bed
 - B. Fluidized bed
 - C. Suspension or entrainment
- III. Flow of Reactants
 - A. Countercurrent
 - B. Concurrent
- IV. Gasification Media
 - A. Air with steam
 - B. Oxygen with steam
 - C. Enriched air with steam
 - D. Hydrogen
 - E. Spent air with generated gases
- V. Ash Disposition
 - A. Dry and granular
 - B. Liquid as slag
- VI. Conditions of Reaction
 - A. Atmospheric pressures
 - B. Elevated pressures

Table 2
SOME SULFUR REMOVAL SYSTEMS
FOR
PURIFYING LOW BTU GAS

<u>Process System</u>	<u>Principal Reagent</u>
Iron box	Ferric oxide and hydroxide
Vacuum carbonate	Sodium carbonate
Ferrox	Ferric hydroxide
Amine absorption	Mono and diethanolamine
Thylox	Sodium thioarsenate
Hot potassium carbonate	Potassium carbonate
Appleby-Frodingham	Ferric oxide
Stredford	Sodium ammonium vanadate

Table 3 - Comparison of Various Typical Gases

Analysis	Water Gas (Coke)		Carburetted Water Gas		Coke Oven Gas		Typical Wellman-Galusha Producer Gas (under full load operating conditions)			
	Gas	(Coke)	Water Gas	Gas	Oven Gas	Gas	Bituminous	Anthracite	Charcoal	Coke
Carbon Monoxide	37.0		32.0		6.3		28.6	27.1	29.5	29.0
Hydrogen	47.3		34.0		46.5		15.0	16.6	12.0	10.0
Methane	1.3		15.5		32.1		2.7*	0.5*	0.5*	0.7*
Ethane										
Propane										
Butane										
Ethylene				4.7	3.5					
Benzene				2.3	0.5					
Carbon Dioxide	5.4		4.3		2.2		3.4	5.0	3.0	3.5
Oxygen	0.7		0.7		0.8		0.0	0.0	0.0	0.0
Nitrogen	8.3		6.5		8.1		50.3	50.8	55.0	56.8
Common Properties:										
B.T.U. (a) Gross	286		532		572		168.13	146.2	139.0	132.9
(b) Net	262		492		512		157.90	137.4	132.5	127.2
Ratio of Net to Gross B.T.U.	.916		.925		.895		.939	.940	.953	.957
Approximate Flame Temp. °F	3670		3700		3610		3200	3100	3080	3020
Cu. Ft. Dry Air per Cu. Ft. Gas	2.10		4.51		4.99		1.30	1.09	1.04	1.00
B.T.U./Cu. Ft. Quantitative Mix										
(a) Gross	92.3		96.6		95.5		73.1	70.0	68.1	66.4
(b) Net	84.5		89.3		88.6		68.7	65.7	65.0	63.6
Cu. Ft. Combustion Products per Cu. Ft. Gas	2.71		5.24		5.78		2.105	1.89	1.85	1.82
B.T.U. per Cu. Ft. Combustion Products										
(a) Gross	105.5		101.5		99.0		80.0	77.4	75.1	73.0
(b) Net	96.7		93.9		88.6		75.2	72.7	71.6	69.9
Specific Gravity	0.57		0.67		0.44		0.84	0.85	0.88	0.90

*Methane content increases with percent volatile content

Table 4

**GAS PRODUCER OPERATING COSTS
FOR
PRODUCTION OF HOT RAW GAS***

	<u>1948 Data</u> <u>\$/NT Converted Coal</u>	<u>1965 Data</u> <u>\$/NT Converted Coal</u>
Operating labor & supv.	\$.77	\$.61
Electrical energy	.07	.18
Steam charges	.42	
Water	.02	.29
Maintenance	.31	.29
Capital charges	<u>.72</u>	<u>.85</u>
Cost per ton of coal	\$2.39	\$2.22
Producer gas heat costs based on coal at 8\$/T	56¢/MMBTU	43¢/MMBTU

(1,6,7)

* Data from different sources for plants using 10-ft. producers.

TABLE 5

RAW MATERIAL AND PELLET COKE PROPERTIES
(Traveling Grate Process for Conversion of Coal)

<u>Proximate Analysis</u> (dry basis)	<u>Coal</u>	<u>Pellet Coke</u>	<u>Pellet Coke</u>
		<u>Gas Combustion</u>	<u>Carbon Combustion</u>
Volatile matter	34.5%	6.5%	4.8%
Fixed carbon	52.1%	68.7%	67.0%
Ash	13.4%	24.8%	28.2%
Free swelling index	6	0	0
<u>Cold Strength</u>			
Point contact			
Crush load	50 lb	100 lb	150 lb
<u>Coke Tumble Test</u>			
1 lb, 200 rev. 25 rpm, % + $\frac{1}{2}$ " ret.	33.0%	71.0%	80.0%
<u>Size Analyses</u> (feed and product)			
<u>Ground coal</u>			
-20M +100M	13.5%	-	-
-100M +200M	31.5%	-	-
-200M	55.0%	-	-
<u>Fired pellets</u>			
-1" +3/4"	-	3.6%	5.4%
-3/4" +1/4"	-	92.3%	91.1%
-1/4" +0	-	4.1%	3.5%

Effect of Manganese Additives on NO-Emissions from a
Small Laboratory Oil Burner

Elmar R. Altwicker, Ira S. Brodsky, and Thomas T. Shen

Rensselaer Polytechnic Institute, Troy, N. Y. and New York State
Department of Environmental Conservation, Albany, N. Y.

Introduction Many techniques for emission reduction from oil fired installations can be cited. These include⁽¹⁾ 1) operating procedures; 2) fuel selection; 3) design and installation; 4) combustion modifications; 5) new combustion procedures; 6) additives. Although additives are in use to some extent, there is little evidence of reliable performance for the lowering of pollutant emissions.

There is even less information on or understanding of the effect of oil additives on levels of NO_x-emissions from oil diffusion flames. Such understanding is of interest since small installations that burn #2 distillate fuel oil form a large group of sources in urban areas which emit near ground level. Control techniques other than burner modifications, new furnace and burner design, or additives are unlikely to be of commercial importance for these sources. We have previously reported on combustion studies which utilized a small-scale atomizing burner and distillate fuel oil, and some indications of the effect of metallic and nonmetallic additives on nitric oxide emissions, which were marginal^(2,3). The results of extensive evaluations of several chemical compounds and commercial formulations have been published and it was concluded that none of the compounds investigated showed an effect on the nitric oxide level⁽⁴⁾. A detailed review on available data has recently appeared⁽⁵⁾.

The reactions whereby an additive might lower NO_x-levels observed in the stack gases are unknown but could be basically of three types: 1) the additive interferes with reactions leading to NO-formation; 2) the additive catalyzes NO-decomposition; 3) the additive affects only NO_x-formation from fuel nitrogen.

Experimental Since small burners were not available commercially, it was necessary to construct a burner that met the requirements for our laboratory investigations, i.e. low total oil and air flow, in order to facilitate the frequent switch between oil flow for baseline data and oil flow for additive studies. The final assembly of the burner system is shown in Figure 1. Details of second experimental burner are shown in Figure 2.

The operating conditions of the burner system for each test were kept constant. Fuel flow rate was adjusted to 3.0 ± 0.1 grams per minute; combustion air flow was 37.7 liters per minute (5.1 liters per minute of this was primary air flow); a slight excess of air was used corresponding to $\phi = 0.96$, based on an ultimate analysis of the fuel. The burner was stabilized for 30 minutes or longer before sampling commenced.

The effectiveness of fuel additives was determined by measuring CO₂, SO₂, NO_x and flame temperature. These measurements were compared at 30 minute intervals with and without additive treatment of fuel oil. This simple process of switching the fuel line back and forth from two fuel reservoirs prevented possible effects from burner instability and therefore permitted accurate quantitative assessment of any change as a result of the additive. NO was measured by chemiluminescence.

All additives tested under this study were either oil-soluble liquids or oil/benzene-soluble powders. The additives were selected on the basis of previous studies^(2,3). The maximum dosage of liquid additives was 1% and was reduced successively until no significant effect was observed. The liquid additives were used as supplied by the manufacturer. The actual metal content was determined by atomic absorption spectroscopy and ranged from 10-45 mmoles Mn per kg oil.

Results The decrease in the NO_x -emissions has been expressed in terms of an emission ratio, defined as: NO_x -emission in the presence of additives/ NO_x -emission under baseline conditions. Plots of this ratio vs. the $(\text{Mn})^{1/2}$ are linear (Figure 3). The results appear to be independent of the system used.

The difference in the slopes of the MnN- and MMTC-plots in Figure 3 suggests the operation of a ligand effect. The manganous acetylacetonate results (not plotted, since only two data points were obtained) would tend to support this conclusion. This observation makes any explanation of the effect based only on the metal highly speculative.

Flame temperature and NO-profiles were measured in order to obtain some insight into additive function. Examples of the isopleths that resulted are shown in Figures 4 and 5. (These data were obtained with the burner of Figure 2.) As indicated sampling was done at four levels above the origin of the flame and at nine points across the flame (in two directions). The isolines were drawn by linear interpolation of the actual measurements between any two sampling points. It would appear that the additive substantially decreases the rate of NO-formation.

A series of experiments were conducted by changing the oxygen index (vol % $\text{O}_2/\text{O}_2 + \text{N}_2$) in the presence of 1% manganese naphthenate (12.4 mmoles Mn/Kg oil). The data have been compared in Table 1. Of particular interest is the relative constancy of the NO_x -emission ratio (both as observed and as corrected to 12.7% CO_2) which indicates that although the NO-concentration in the stack gases increases over three-fold when the index changes from 0.21 to 0.27, the percentage reduction effected by the additive remains about the same.

Discussion The nitric oxide levels presumably are controlled by the time-temperature history of the gases in the furnace^(6,7). The following sequence is usually considered for NO-formation



For a steady state concentration of N-atoms the rate of NO-formation is given by

$$\frac{d \text{NO}}{dt} = \frac{2 k_1 (\text{O}) (\text{N}_2) \left[1 - (\text{NO})^2 / K (\text{N}_2) (\text{O}_2) \right]}{1 + k_{-1} (\text{NO}) / k_2 (\text{O}_2)}$$

If one assumes that step 1 is rate controlling and k_{-1} is small this expression simplifies to

$$\frac{d \text{NO}}{dt} = k_1 (\text{N}_2) (\text{O}) = k_1 K (\text{N}_2) (\text{O}_2)^{1/2}$$

where

$$K = \frac{(\text{O})}{(\text{O}_2)^{1/2}}$$

One possible function of the additive may be competition for O-atoms in the post-flame zone via equation 3



Since the reduction in NO-concentration showed a square root dependence on the Mn-concentration, the rate equation may be modified as follows

$$\begin{aligned} \frac{d \text{NO}}{dt} &= k_1 K (N_2) (O_2)^{\frac{1}{2}} - k_3 (\text{Mn})^{\frac{1}{2}} (O) \\ &= K (O_2)^{\frac{1}{2}} (k_1 (N_2) - k_3 (\text{Mn})^{\frac{1}{2}}) \end{aligned} \quad (4)$$

which would predict that as $K (O_2)^{\frac{1}{2}}$ increases with increasing temperature - and assuming N_2 and $\text{Mn}^{\frac{1}{2}}$ to be constants - that the $(k_1 - k_3)$ -term controls the difference that is actually measured.

In the simplest case integration of 4 would yield

$$\left[(\text{NO})_0 - (\text{NO}) \right]_A = K (O_2)^{\frac{1}{2}} (k_1 (N_2) - k_3 (\text{Mn})^{\frac{1}{2}}) t$$

where $(\text{NO})_0$ = NO-concentrations measured in the absence of additive, where $(\text{NO})_0 = 0 = (\text{Mn})$

$\left[(\text{NO})_0 - (\text{NO}) \right]_A$ = NO-concentration measured in the presence of additive

t = residence time in the flame at a temperature where above mechanism would predominate

References

1. R. A. Beals, MASS-APCA Semi-Annual Technical Conference, Edison, New Jersey, May 12, 1972; p. 48.
2. E. R. Altwicker, P. E. Fredette and T. T. Shen, 64th Annual APCA-meeting, Atlantic City, New Jersey, June 1971, Paper #71-14.
3. T. Shen and E. R. Altwicker, Paper presented at 4th Annual NOFI-meeting, Philadelphia, Pennsylvania, October 1971.
4. G. B. Martin, D. W. Pershing and E. E. Berkau, Effects of Fuel Additives on Air Pollutant Emissions from Distillate-Oil Fired Furnaces, OAP Publication #AP-87, June 1971.
5. H. Shaw, Transactions of the ASME, Journal of Engineering for Power, Paper #73-GT-S, pp. 1-8 (1973).
6. P. J. Marteney, Combustion Science and Technology 1, 461 (1970).
7. F. A. Bagwell et al., J. Air Poll. Control Assoc. 21, 702 (1971).
8. E. R. Altwicker and T. Shen, Combustion Science and Technology (1974), in press.

FIGURE 2
Experimental Burner

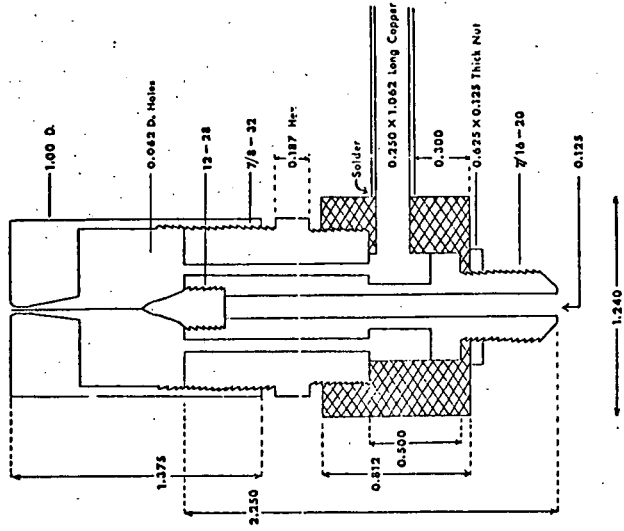


FIGURE 1
Schematic Burner System

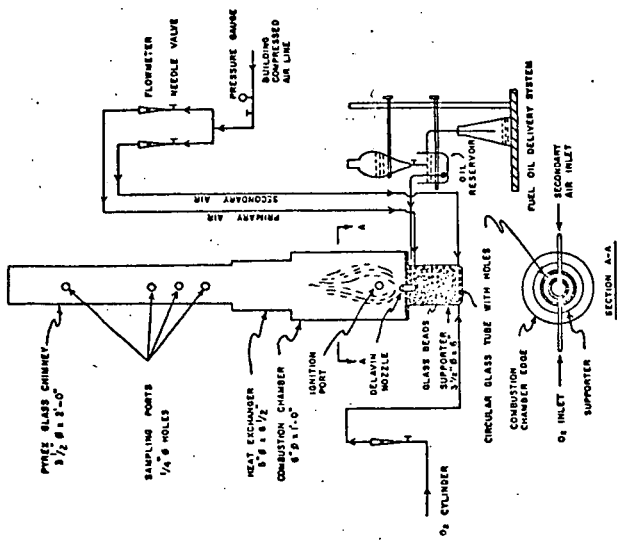


FIGURE 4
NO ISOPLETH (ppm), BASELINE

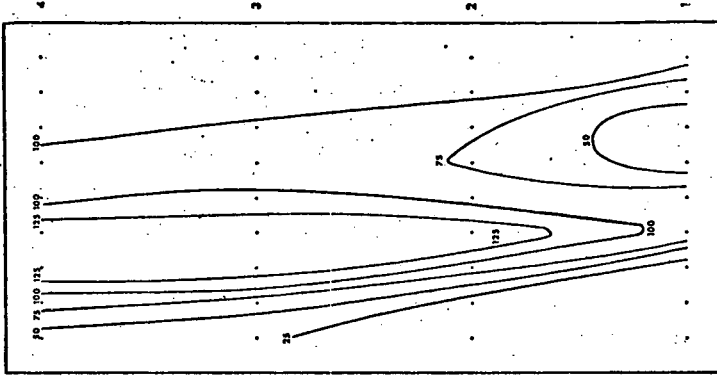


FIGURE 3
Reduction of Flue NO by Min

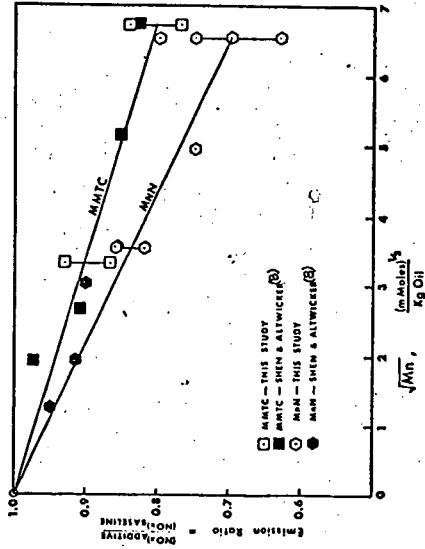


FIGURE 5

NO ISOPLETH (ppm), 0.25% M.M.T.C.

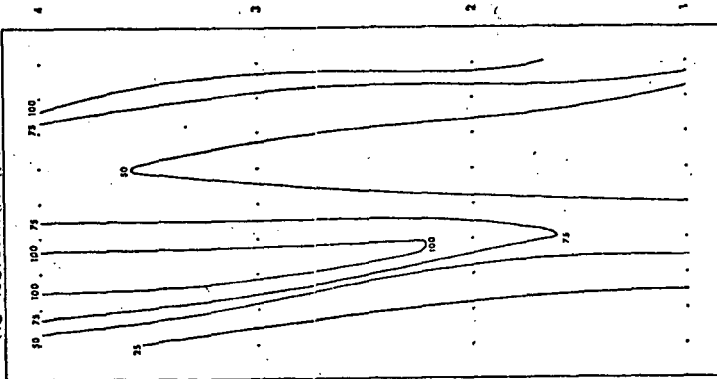


Table 1. - Effect of 1% Manganese Naphthenate at Varying Oxygen Indices

Component	Oxygen Index		
	0.21	0.23	0.25
Baseline (no additive)			
NO _x , Ppm	116 ± 7	180 ± 10	285 ± 20
CO ₂ , %	12.7 ± 0.2	13.7 ± 0.2	14.2 ± 0.3
Max. Flame Temp. °C	1280 ± 30	1410 ± 30	1490 ± 30
1% Manganese Naphthenate			
NO _x , ppm	96 ± 6	146 ± 10	236 ± 15
CO ₂ , %	12.8 ± 0.2	13.9 ± 0.2	14.3 ± 0.3
Max. Flame Temp. °C	1340 ± 30	1440 ± 30	1540 ± 30
NO _x Emission Ratio	0.827	0.812	0.828
NO _x Emission Ratio (Corrected to 12.7% CO ₂)	0.827	0.803	0.821
Flame Temp. Ratio	1.03	1.02	1.03

Figure 1
SCHEMATIC BURNER SYSTEM

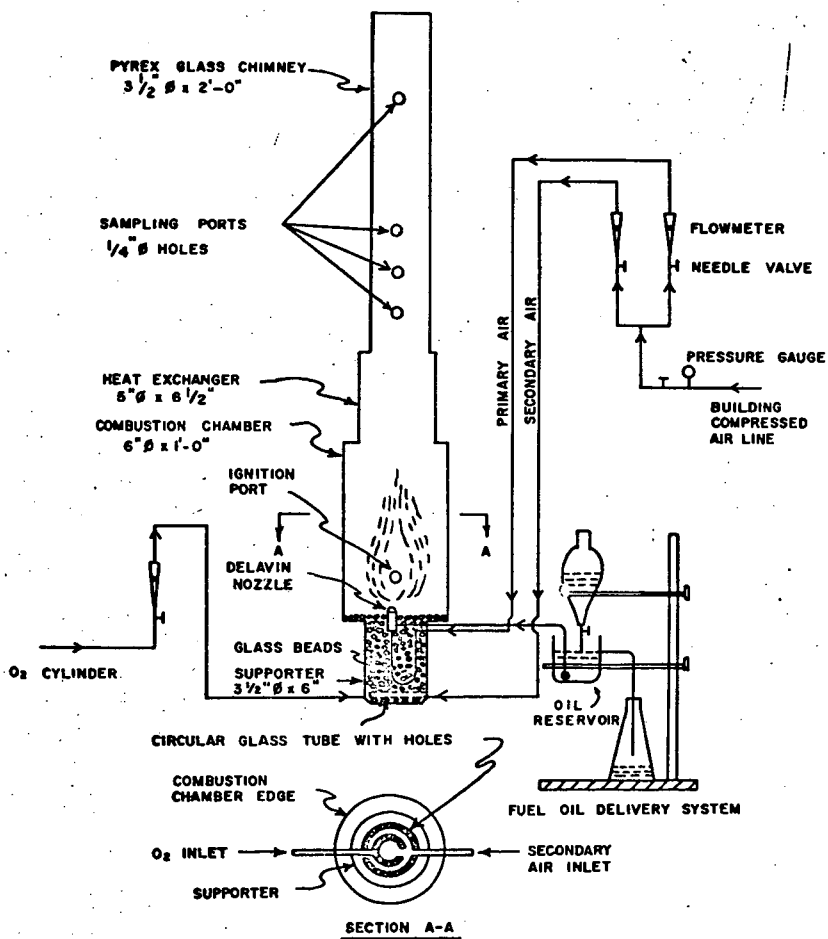


FIGURE 2
Experimental Burner

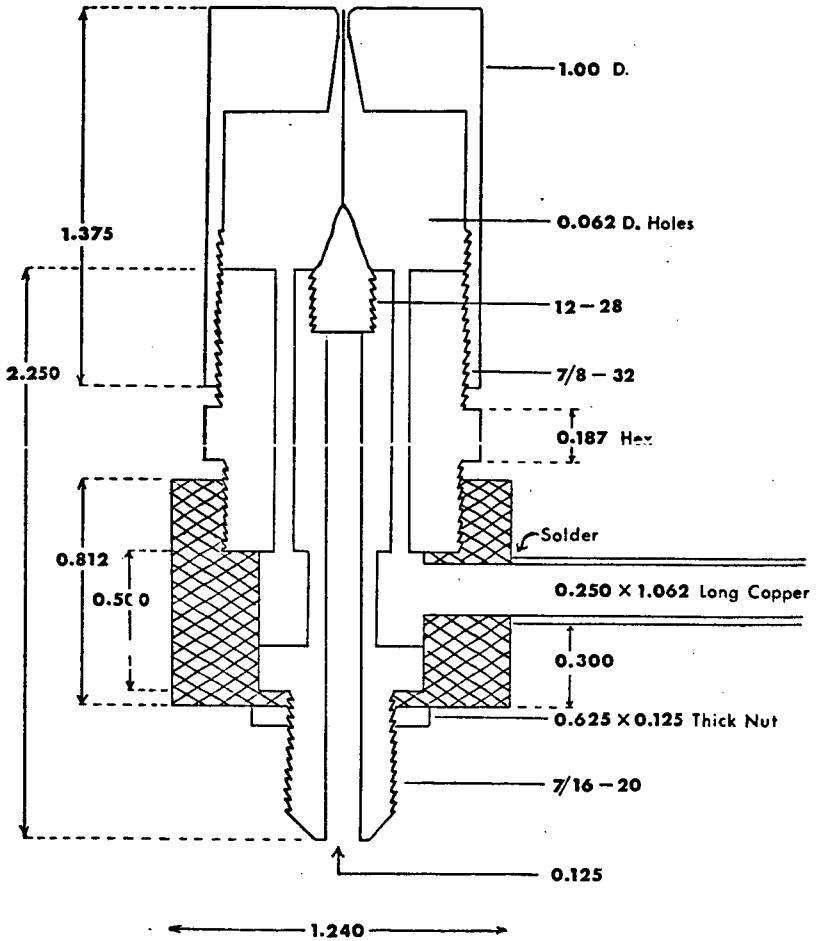


FIGURE 3
Reduction of Flue NO by Mn

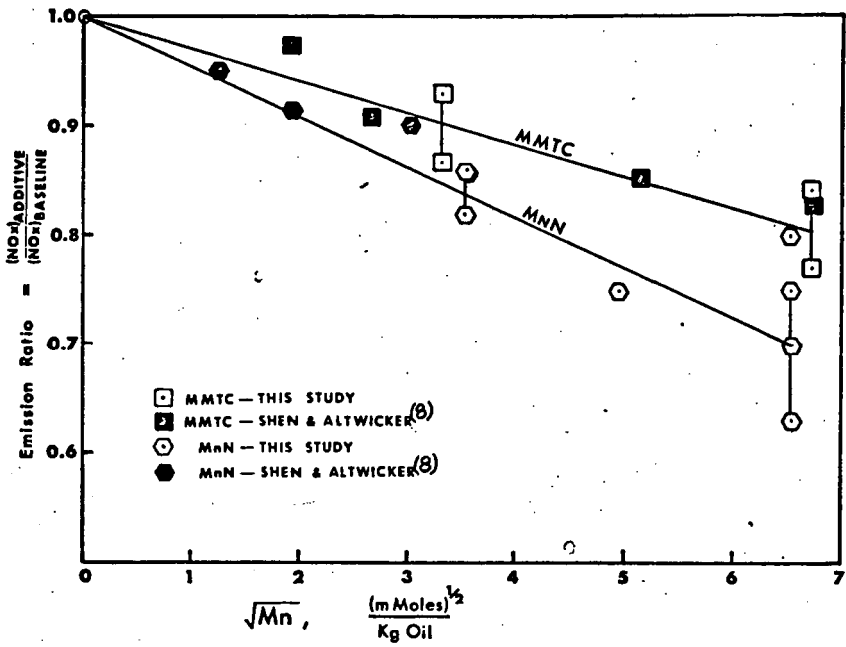


FIGURE 4

NO ISOPLETH (ppm), BASELINE

DIRECTION



RUN
81 b

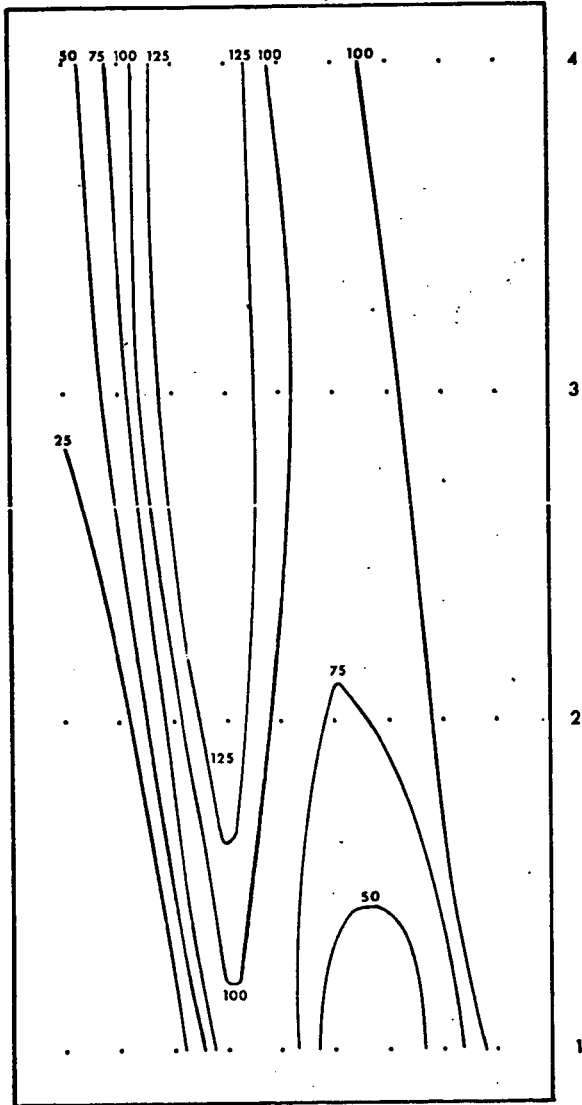


FIGURE 5

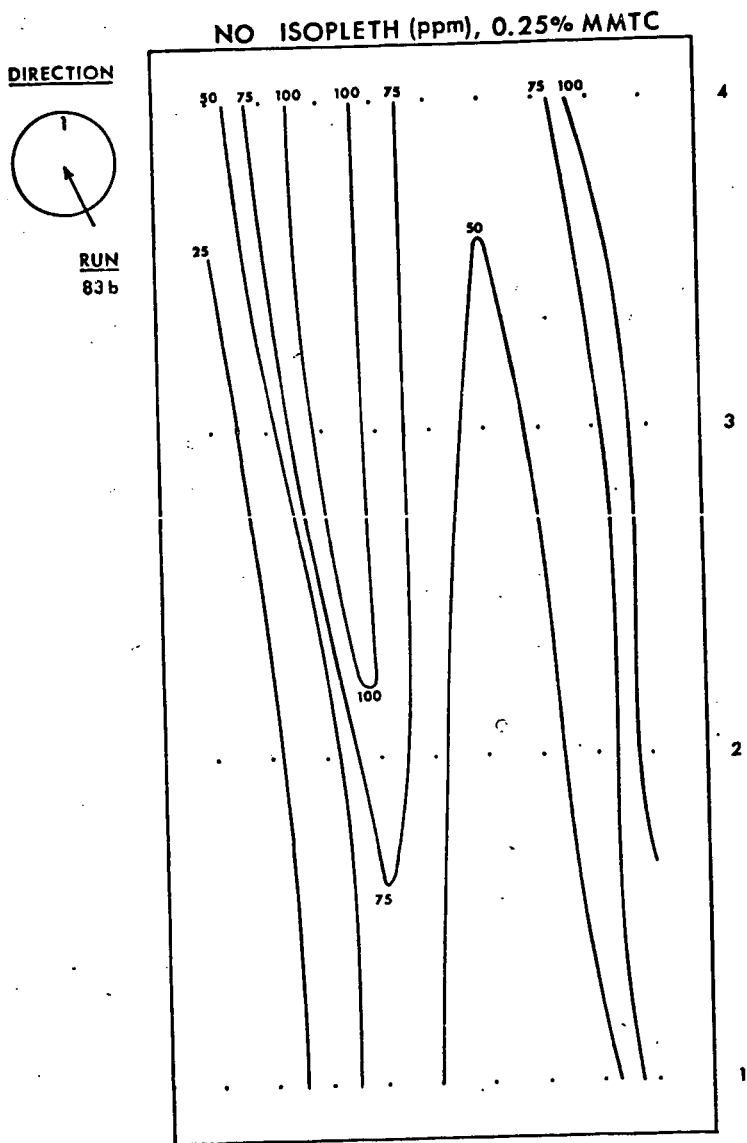


Table 1 - Effect of 1% Manganese Naphthenate at Varying Oxygen Indices

Component	Oxygen Index		
	<u>0.21</u>	<u>0.23</u>	<u>0.27</u>
Baseline (no additive)			
NO _x , ppm	116 ± 7	180 ± 10	285 ± 20
CO ₂ , %	12.7 ± 0.2	13.7 ± 0.2	14.2 ± 0.3
Max. Flame Temp. °C	1280 ± 30	1410 ± 30	1540 ± 30
1% Manganese Naphthenate			
NO _x , ppm	96 ± 6	146 ± 10	236 ± 15
CO ₂ , %	12.8 ± 0.2	13.9 ± 0.2	14.3 ± 0.3
Max. Flame Temp. °C	1340 ± 30	1440 ± 30	1540 ± 30
NO _x -Emission Ratio	0.827	0.812	0.828
NO _x -Emission Ratio (corrected to 12.7% CO ₂)	0.827	0.803	0.821
Flame Temp. Ratio	1.03	1.02	1.03

EFFECT OF ADDITIVES UPON THE GASIFICATION OF COAL IN THE SYNTHANE GASIFIER

Albert J. Forney, W. P. Haynes, S. J. Gasior, and R. F. Kenny

Bureau of Mines, U.S. Department of the Interior, Pittsburgh, Pa.

Introduction

The Synthane process (1)¹, developed by the Bureau of Mines of the U.S. Department of the Interior, is a coal-gasification process in which caking coal is successively decaked and gasified in two individual fluidized beds. The decaked coal is fed from the pretreater directly into the gasifier. Based upon this technique, the Lummus Co. designed a 75-ton-per-day prototype plant, which is presently being built by the Rust Engineering Co. near the Bureau's laboratories at Bruceton, Pa., in South Park Township. In a continuing effort to improve the gasification process, tests are being performed in the original 4-inch-diameter gasifier located at the Pittsburgh Energy Research Center at Bruceton, Pa. Results from the latest gasification tests performed with additives are discussed in this report.

Additives Used

Table 1 shows the analysis of the compounds used as additives in the Bruceton gasifier. The additives were mixed with coal and the mixture then fed to the pretreater-gasifier. Table 2 lists typical gasification tests showing data in which following graphs are based. Lignites and subbituminous coal tests are included for comparison purposes but are not shown in the graphs.

Effect on Carbon Conversion

Figure 1 shows results of tests where we operated with and without additives² showing carbon conversion vs bed temperatures. We used 2%, 5%, and 10% limestone (dolomitic limestone), 2% and 5% hydrated lime, 2% quicklime, and 5% lignite ash. Results show an average increase of about 10% in carbon conversion for the parameter for additive tests above the parameter shown for nonadditive tests.

Effect on Steam Decomposition

Figure 2 shows the effect of the same additives on the steam decomposition. The steam decomposition was increased 5% to 10% above the parameter for nonadditive tests. The highest increases were with CaO and hydrated lime.

Effect on H₂ + CO + CH₄ Yields

As would be expected because of the increased carbon conversion, the yields of H₂ + CO + CH₄ increased about 1 to 2 scf/lb coal (MAF basis) using the additives as shown in figure 3. Again the use of hydrated lime shows the greatest increase.

Effect on Sulfur in the Char

As shown in figure 4, some additives increase the sulfur in the char. What we were interested in especially was a reduction. Agricultural limestone (showing sulfur in char of 0.4% and 0.6%) showed the greatest decrease in the sulfur. Hydrated lime and CaO showed that their use would increase the sulfur in the char. This is an undesirable effect because a low-sulfur char is needed to raise steam needed for the plant, and the stack gas effluent must meet EPA standards. The line shown in this figure is the average for the nonadditive tests.

¹ Underlined numbers in parentheses refer to list of references at end of this paper.

² All tests using additives were made with Illinois No. 6 coal. All nonadditive tests discussed in figures 1 to 5 were made with Illinois No. 6 coal.

Effect on Slag³ Formed in the Gasifier

In Figure 5 the amount of slag (cinder) formed in the gasifier is shown as a function of the maximum temperature in the gasifier. The majority of the tests with the additives show no slag formation. This is an important point since if the slagging temperature can be raised, the gasifier could be operated at a higher temperature, thus achieving a higher throughput in the gasifier. This result has been noted in the literature (2) as has other effects of these additives as discussed in this paper (3, 4).

Effect of Additives on the Water Effluent From the Gasifier

The effect of additives on water effluents resulting from gasification of various coals is shown in Table 3, which shows analyses of water effluents from Illinois No. 6 coal, Wyoming subbituminous, Illinois char, North Dakota lignite, Western Kentucky, and Pittsburgh seam coal. Coke-plant effluent was shown for comparison since it has been successfully treated for over 10 years by Bethlehem Steel Co. at Bethlehem, Pa. (5). Since the coke-plant effluent can be treated, we know the gasifier plant effluent can be also. As shown in the table, compared with Illinois No. 6 coal test without additives, the additive caused higher quantities of phenol, ammonia, and COD (chemical oxygen demand). Reasons for such increases are not known at this time.

Effect of Additives on the Gas Made in the Gasifier

Table 4 shows the effect of CaO and dolomitic limestone on components in the gasifier gas. The largest increase is in the BTX (Benzene-Toluene-Xylene) fraction. Reasons for these changes are not known.

We plan also to examine the tars to see if there is a difference in tar quality with additive tests, but such results are not yet known.

Conclusions

Additives such as limestone, hydrated lime, and quicklime all have a positive effect on the gasification rate. Limestone, in addition, raises the sintering temperatures and may lower the sulfur contained in the char from the gasifier. More tests are needed to establish the effect on the water and gas from the gasifier. We also plan to perform tests using ashes and chars from various coals as additives. When we have enough data to assess the advantages of the additives, cost studies will be made to determine economic feasibility.

³ This material called "slag" is more like a cinder in that it is not a hard slag.

TABLE 1. - Additives used in the Synthane Gasifier

<u>Material</u>	<u>Analysis, wt-pct</u>				
	<u>CaCO₃</u>		<u>Mg CO₃</u>		
Limestone (Dolomitic)	54		44		
Ca(OH) ₂ Hydrated or Slaked Lime.....	<u>CaO</u> 72. (min.)		<u>MgO</u> 0.05		<u>H₂O</u> 23
CaO Quicklime.....	97				
Lignite Ash.....	<u>SiO₂</u> 12.3	<u>Al₂O₃</u> 11.5	<u>Fe₂O₃</u> 12.5	<u>TiO₂</u> 0.3	<u>P₂O₅</u> 0.6
	<u>CaO</u> 23.0	<u>MgO</u> 8.9	<u>Na₂O</u> 3.8	<u>K₂O</u> 0.4	<u>SO₃</u> 25.4

TABLE 2. - Typical data from coal gasification tests

Test ^{1/}	11	3	48	83	37	46	W-2	L-7
	Ill.	Ill.	Ill.	Ill.	Ill.	Ill.	Sub-	
Coal Type.....	#6	#6	#6	#6	#6	#6	bit.	Lignite
Additive.....	None	None	5% Lime- stone	5% Lime- stone	2% Lime- stone	5% Hydr. lime	None	None
Coal Feed								
lb/hr.....	18.9	20.4	18.7	25.9	20.7	19.0	38.0	32.4
lb/hr-ft ²	221	239	219	304	242	223	446	379
lb/hr-ft ³	40	43	40	55	44	40	81	69
Steam Rate								
lb/lb coal.....	1.06	0.87	1.25	0.97	0.98	1.08	0.55	0.77
Oxygen Rate								
lb/lb coal.....	0.30	0.27	0.33	0.25	0.35	0.41	0.14	0.13
Carbon Conversion, %.	68	65	68	60	93	81	68	75
Steam Conversion.....	15	25	15	20	36	30	18	51
$\frac{SCF H_2 + CO + CH_4}{lb Coal, MAF}$	13.3	13.9	12.8	12.1	20.4	16.7	12.7	18.2
$\frac{SCF CH_4}{lb Coal, MAF}$	3.6	3.9	3.6	3.4	4.5	4.2	3.4	4.2
Max. Temp., ° C.....	970	960	958	965	1020	1040	925	880
Av. Temp., ° C.....	928	947	920	900	951	919	867	855
Sulfur in coal, %....	3.4	3.4	3.3	3.3	3.2	3.4	0.6	1.3
Sulfur in char, %....	0.8	1.2	0.4	0.9	1.3	1.7	0.2	1.6
Slag, % of coal feed.	3.0	0.6	0.9	0.0	6.0	2.6	2.7	1.0

^{1/} All coals are ground to 20 x 0 mesh, about 30% through 200 mesh.

TABLE 3. - Byproduct water analysis¹ from Synthane gasification of various coals

	Coke plant	Illinois No. 6	Ill. #6 w/5%		Ill. #6 w/20%		Ill. char	N. Dak. lignite	W. Ky.	Pgh. Seam	Wyoming sub-bit
			lime-stone	lime-stone	lime-stone	lime-stone					
pH.....	9	8.6	8.4	9.2	7.9	9.2	8.9	9.3	8.7		
Suspended solids	50	600	136	92	24	64	55	23	140		
Phenol.....	2,000	2,600	3,500	4,950	200	6,600	3,700	1,700	6,000		
COD.....	7,000	15,000	22,000	22,134	1,700	38,000	19,000	19,000	43,000		
Thiocyanate.....	1,000	152	196	102	21	22	200	188	23		
Cyanide.....	100	0.6	0.8	0.5	0.1	0.1	0.5	0.6	0.2		
NH ₃	5,000	2,8,100	15,100	10,400	2,500	7,200	10,000	11,000	9,520		
Chloride.....		500	435		31						
Carbonate.....		3 6,000									
Bicarbonate.....		311,000									
Total Sulfur....		4 1,400									

¹ Mg/liter (except pH)² 85% free NH₃³ Not from same analysis⁴ S⁼ = 400SO₂⁼ = 300SO₄⁼ = 1,400S₂O₃⁼ = 1,000

Table 4. - Components in gasifier gas¹

Ill. No. 6	Ill. #6 w/5% lime- stone	Ill. #6		Ill. #6 w/2% CaO	Ill. char	Wyoming sub-bit	W. Ky.	N. Dak. lignite	Pgh. Seam
		w/5% CaO	w/2% CaO						
9,800	3,600	7,480	8,100	186	2,480	2,530	1,750	860	
150	70	10	330	2	32	119	65	11	
31	134	40	260	0.4	10	5	25	55	
10	50	6	37	0.4	--	--	--	7	
10	11	5	37	0.5	--	--	11	6	
340	1,890	510	2,790	10	434	100	1,727	1,050	
94	230	85	720	3	59	22	167	185	
24	36	20	160	2	27	4	73	27	
10	20	9	---	1	6	2	10	10	
10	--	5	---	--	--	--	--	--	
60	125	50	330	0.1	0.4	33	10	8	

¹PPM by volume.

References

1. Forney, A. J., and McGee, J. P. "The Synthane Process--Research Results and Prototype Plant Design." Proceedings of Fourth Synthetic Pipeline Gas Symposium, American Gas Association, Oct.30-31, 1972, pp. 51-69.
2. Moraikib, M., and Franke, F. H. "Carbon Gasification by the High Temperature Winkler Process." Chem. Ing. Tech. 42, No. 12, 834-36 (1970).
3. Franke, F. H., and Meraikib, M. "Catalytic Influence of Alkalis on Carbon Gasification Reaction." Carbon 8, 423-433 (1970).
4. Haynes, W. P., Gasior, S. J., and Forney, A. J. "Catalysis of Coal Gasification at Elevated Pressure." 165 National Meeting ACS, Dallas, Texas, Sept. 8-12, 1973, v. 18, No. 2, pp. 1-28.
5. Kostenbader, P. D., and Flechsteiner, J. W. "Biological Oxidation of Coke Plant Weak Ammonia Liquor." Journ. of Water Pol. Control Federation, Chicago, Ill., Sept. 22-27, 1968.

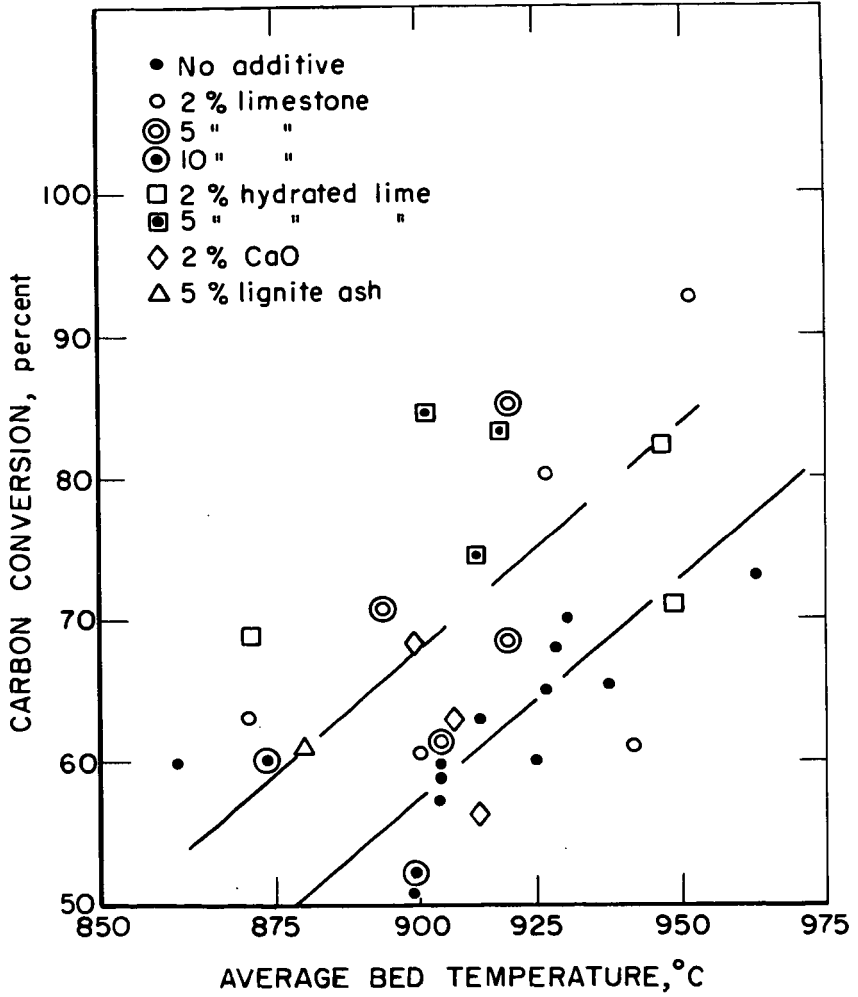


Figure 1. Effect of Additives on Carbon Conversion

L-13391

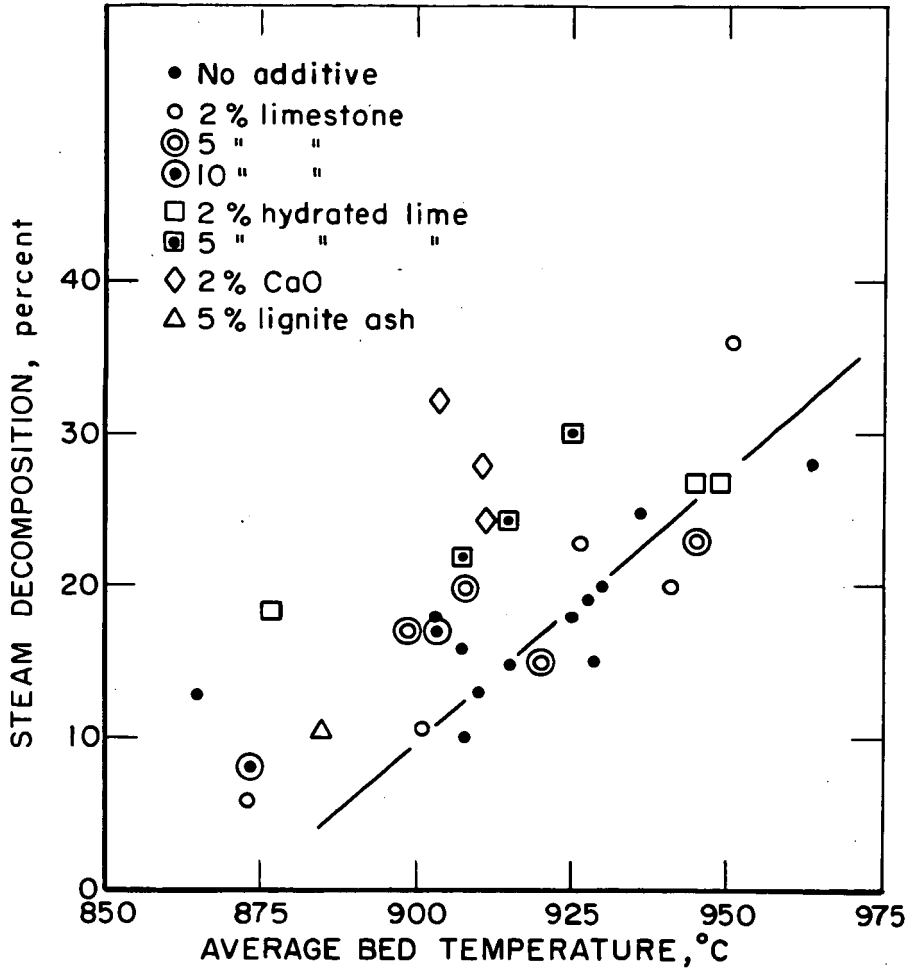
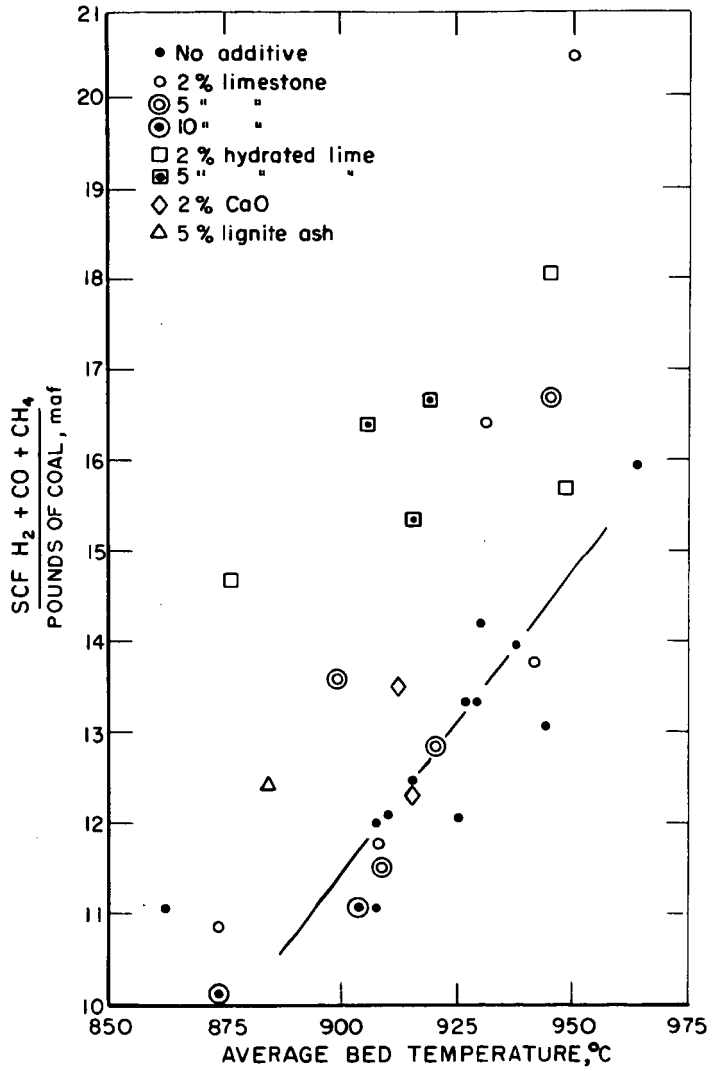


Figure 2. Effect of Additives on Steam Decomposition

L-13390

Figure 3. Effect of Additives on H₂ + CO + CH₄ Yields

L-13389

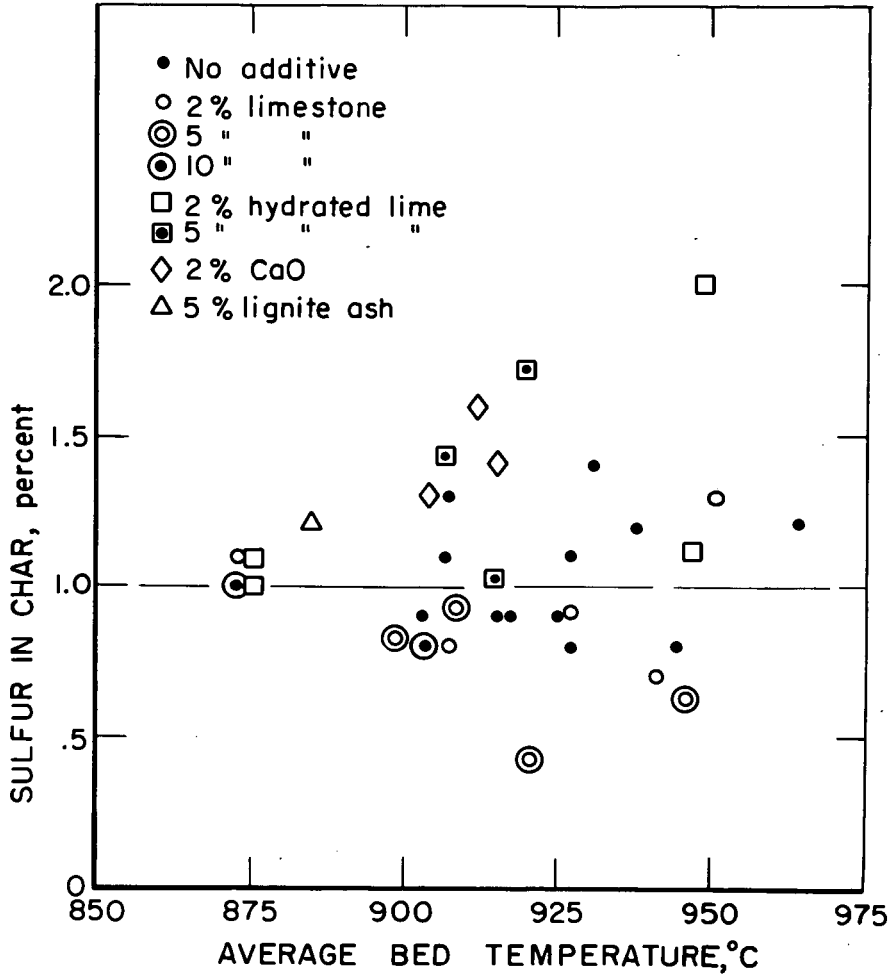
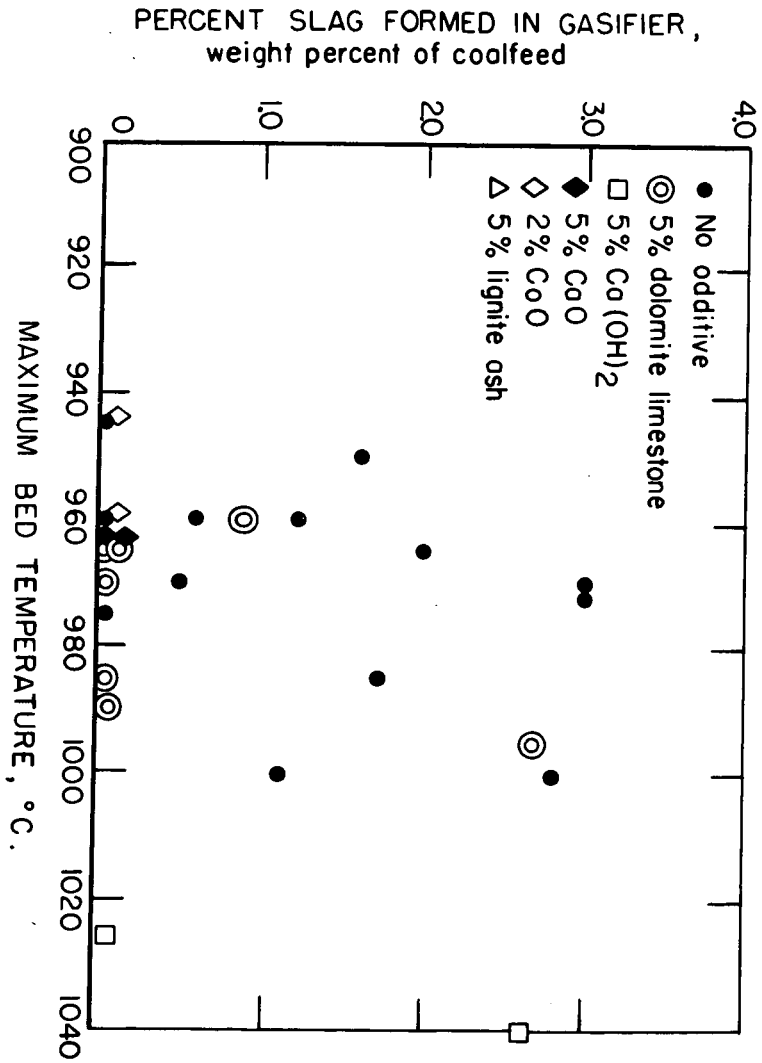


Figure 4. Effect of Additives on Sulfur in Char

L-13392



THERMAL RADIATION PROPERTIES OF CERIA-THORIA MANTLE FABRIC

D. M. Mason

Institute of Gas Technology
Chicago, Illinois 60616Introduction

Gas lighting has been based on the Welsbach mantle since its introduction in the 1890's, and little new scientific information on its operation or on that of other forms of flame-heated thermal light radiators has appeared since 1918. However, during the last 20 years new burner technology has emerged: porous plate and surface combustion burners for production of infrared radiation are particularly noteworthy. In many applications where radiant heating is effective there is an accompanying need for lighting. Potential applications include patios, restaurants, stadiums, warehouses, and foundaries. At the time this work was undertaken it appeared that development of combination lighting and heating devices could fill a real need. The investigation reported here was undertaken to obtain information that would allow us to design, or at least guide the development of, new light and heat radiating devices.

Previous Studies of Emittance of Ceria-Thoria

Rubens investigated the Welsbach mantle, composed of thoria and ceria (1). He found that the mantle, when hot, had a high emittance in the blue region of the visible spectrum. By optical pyrometry in this wavelength region, with corrections obtained from reflectance measurements, he estimated its temperature to be about 1550°C. He found the high efficiency of the 99% thoria, 1% ceria mixture to be due to two causes: first, to the low emittance of the thoria, particularly in the near infrared, by virtue of which it attains a high temperature in the flame; second, to a high emittance in the visible region imparted by the presence of ceria. He showed that thoria alone has too little emittance in the visible range to give much light, while ceria, in amounts greater than about 1%, increased the emittance in the near infrared, lowering the temperature and the emission in the visible range. This is because blackbody radiation at the relevant temperatures occurs mainly in the near infrared, and secondly because in the visible range the intensity of blackbody radiation varies by a much higher power of the absolute temperature than does the total radiation.

Ives, Kingsbury, and Karrer in 1918 published an extensive investigation of mantle materials (2). Alumina, beryllia, magnesia, silica, and zirconia were investigated as base materials in comparison with thoria. Uranium, manganese, nickel, lanthanum, praseodymium, neodymium, and erbium were investigated as colorants, but none of these were superior to cerium. Temperatures of mantles prepared from the various base materials were determined by measurements with thermocouples of different wire sizes, so that results could be extrapolated to zero wire diameter. The spectral emittance of the oxides were also measured. These measurements confirmed the theory that thoria has less total emittance in the infrared than other refractory

oxides, although it is not lowest in the 1 to 5 μ m region. Magnesia was next best. Ives *et al.* concluded that if higher temperatures should become feasible, then wavelengths beyond 5 μ m would have relatively less effect on the radiation and magnesia would become as good as, or better than, thoria.

In agreement with Rubens' observations, the emittance of thoria was found to increase as the concentration of ceria was increased. The increase was uniform and gradual in the infrared, while in the visible, and particularly in the blue, the increase was very abrupt. As pointed out by Rubens, the ordinary mantle with approximately 1% of ceria is practically black (emits and absorbs like a blackbody) in the blue end of the spectrum when it is hot. This behavior, in contrast to the whiteness of the cold mantle, is ascribed to the occurrence of an absorption-emission band of the ceria in the near ultraviolet, which broadens into the visible at elevated temperatures. The yellow color of the ordinary mantle that is observed as the mantle cools after the fuel is turned off is caused by this absorption band.

Ives *et al.* also found that the effect of the ceria on visible radiation was highly dependent on the oxidizing-reducing conditions (2). When the flame is adjusted so that the mantle is in the reducing part of the flame, the emittance became much less selective; that is, emittance in the blue decreased and emittance elsewhere increased. Mantle fabric heated in the reducing part of the flame and cooled without access to air came out dark gray, but if reheated in an oxidizing flame, regained its ordinary color. Similar results were obtained when the mantle was heated in hydrogen or in a cathode discharge tube.

Ritzow and other investigators made emittance measurements on bulk ceria-thoria and found higher emittance in the near infrared than Ives or Rubens obtained on mantles (3). (The consolidated state of the material and the greater thickness of the section probably caused the increase in emittance from <0.02 to about 0.20.) With bulk material Ritzow found a decrease in emittance with the addition of ceria, then an increase with addition of greater amounts (4). Liebman made measurements on pure thoria in the visible (5). Similar measurements in the infrared were made at the National Bureau of Standards over the range 1200° to 1600°K.

The emittance of a material is related to its intrinsic absorption coefficient. The coefficient of thorium oxide was determined at room temperature in the visible by Weinrich (6), from measurements on fused thoria. He showed that the color of thoria changes from red to colorless when it is heated in a vacuum at 1000°C and can be changed back to red by reheating it in air at the same temperature. A change in absorption spectrum accompanies the treatments. A different spectrum again is obtained after heating the thoria to 1800°C under vacuum. He attributed these effects to changes in oxygen content and defect structure. A small but measurable change in weight was observed with the 1800°C treatment but not with the 1000°C treatment.

Alumina is the only oxide whose intrinsic absorption coefficient, from 0.5 to $6\mu\text{m}$, has been determined at elevated temperatures (7). According to these measurements temperature has a much greater effect on the absorption coefficient at shorter wavelengths (1 to $3\mu\text{m}$) than at longer wavelengths. Emittance determinations at the National Bureau of Standards confirm this observation not only for alumina but also for thoria, magnesia, and zirconia (8).

Theory of Radiation Characteristics of Translucent Materials

Thermal emission is usually thought of as a surface effect. This is a good approximation for metals, where absorption and emission occur within 1 wavelength of the surface. However, with dielectrics - which, when not too thick, are usually transparent or translucent - not only the surface but also the volume of the material is involved. Because radiation is emitted from and penetrates into the bulk of the material, it is necessary to consider transmission and scattering of the radiation as well as surface absorption and emission.

Development of Kubelka-Munk Equations

One method of treating this problem is by the Kubelka-Munk theory, which was first developed for media under conditions where emission need not be considered. In this form, the theory has been applied to many problems, such as the transmission of light through fog, reflection and transmission of light by opal glass, and reflection by paint, paper, and plastics. The theory was extended by Hamaker to include emission from the medium (9).

According to this theory, we consider a slab or sheet of an isotropic nonhomogeneous (light-scattering) dielectric. Its lateral extent is large compared with the distance required for opacity, and its thickness and other conditions, including external illumination (if any), are taken to be uniform from point to point in the lateral plane. Radiation in the material is diffuse; that is, it occurs in every direction, although not necessarily uniformly so. We consider the radiation to be composed of two parts, one traveling inward from one face of the slab and the other outward. These fluxes are labeled I and J as indicated by the arrows in Figure 1. It is understood that I is composed of the hemisphere of flux having an inward (positive x) component of direction, and similarly J is composed of the hemisphere of flux having an outward (negative x) component of direction. This reduces the problem to one dimension.

On passing through an infinitesimal layer dx , a fraction $KIdx$ of the flux I will be absorbed and a fraction $SIdx$ will be lost by scattering in a backward direction. On the other hand, a quantity $SJdx$ will be added by scattering from the flux J . Sideward scattering is disregarded with the assumption that any sideward loss of radiant energy is compensated by an equal contribution from the neighboring parts of the layer. In addition, by Kirchhoff's law, this layer, dx , will contribute by radiating the amount $KEdx$, where E designates the blackbody radiation at the temperature and wavelength in question.

By adding these quantities we obtain -

$$\frac{dI}{dx} = -(K + S) I + SJ + KE \quad 1)$$

$$\frac{dJ}{dx} = (K + S) J - SI - KE \quad 2)$$

With the assumption that the temperature in the slab is uniform, the equations have been integrated to obtain the general solution:

$$I = A(1 - \beta) e^{\sigma x} + B(1 + \beta) e^{-\sigma x} + E \quad 3)$$

$$J = A(1 + \beta) e^{\sigma x} + B(1 - \beta) e^{-\sigma x} + E \quad 4)$$

where A and B are constants dependent on the boundary conditions and

$$\sigma = [K(K + 2S)]^{1/2} \quad 5)$$

$$\beta = [K/(K + 2S)]^{1/2} \quad 6)$$

Both σ and β are taken to be the positive roots.

If the continuous medium has a refractive index different from 1, then surface or specular reflectance has to be considered. For the present we confine the treatment to a body of particles suspended in air, so that only a diffuse boundary is present and surface reflectance can be neglected. With this restriction, equations for the boundary conditions have been derived from the general solution as follows:

With no radiation incident on either side, the emittance ϵ for a slab of thickness D is -

$$\epsilon = \frac{J_0}{E} = \frac{I_D}{E} = \frac{2\beta [(1+\beta) e^{\sigma D} + (1-\beta) e^{-\sigma D} - 2]}{(1+\beta)^2 e^{\sigma D} - (1-\beta)^2 e^{-\sigma D}} \quad 7)$$

If the slab is thick enough to be opaque, this reduces to -

$$\epsilon = \frac{J_0}{E} = \frac{I_D}{E} = \frac{2\beta}{1+\beta} \quad 8)$$

Also, it can be shown that

$$K/S = \frac{(1-R_\infty)^2}{2R_\infty} \quad 9)$$

where R_∞ is the diffuse reflectance of the opaque slab.

With diffuse incident radiation I_0 , the radiation from the slab on the transmission side is -

$$I_D = \frac{I_0(4\beta) + E(2\beta) [(1+\beta) e^{\sigma D} + (1-\beta) e^{-\sigma D} - 2]}{(1+\beta)^2 e^{\sigma D} - (1-\beta)^2 e^{-\sigma D}} \quad 10)$$

On the reflection side the radiation, including that emitted, is -

$$J_o = \frac{I_o (1-\beta^2) (e^{\sigma D} - e^{-\sigma D}) + E(2\beta) [(1+\beta)e^{\sigma D} + (1-\beta)e^{-\sigma D} - 2]}{(1+\beta)^2 e^{\sigma D} - (1-\beta)^2 e^{-\sigma D}} \quad 11)$$

The last two equations apply to a translucent emitter in a burner in which the emitter receives radiation I_o from some other emitter.

If the slab has an underlayer of reflectivity r at $x = D$, then -

$$J_o = \frac{I_o [1-\beta^2 - r(1-\beta)^2] [e^{\sigma D} - e^{-\sigma D}] + E(2\beta) [(1+\beta-r(1-\beta))e^{\sigma D} + (1-\beta-r(1+\beta))e^{-\sigma D}]}{(1+\beta)^2 - r(1-\beta^2) e^{\sigma D} - (1-\beta)^2 - r(1-\beta^2) e^{-\sigma D}} \quad 12)$$

When $I_o = 0$ this reduces to -

$$\epsilon = \frac{J_o}{E} = \frac{(2\beta) [(1+\beta-r(1-\beta))e^{\sigma D} + (1-\beta-r(1+\beta))e^{-\sigma D}]}{[(1+\beta)^2 - r(1-\beta^2)]e^{\sigma D} - [(1-\beta)^2 - r(1-\beta^2)]e^{-\sigma D}} \quad 13)$$

This case occurs in some of our emittance and reflectance determinations.

For a consolidated material the dielectric is the continuous phase and specular reflection must be taken into account. In the differential equations we must replace E by $n^2 E$, but to avoid confusion, we will indicate the (internal) absorption coefficient by K' rather than K . The relation between the two coefficients will be discussed later. Let ρ_i be the internal diffuse (hemispherical illumination-hemispherical collection) reflectance and ρ_e the external diffuse reflectance at the surface of the slab. According to Klein, the expressions for diffuse reflectance R (including both surface and internal reflection), transmittance T , and emittance ϵ , with hyperbolic functions substituted for exponentials, are (10) -

$$R = \frac{[(1-\rho_i)^2 - \beta^2(1-\rho_i-2\rho_e)(1+\rho_i)] \sinh \sigma D + 2\beta(\rho_e + \rho_i)(1-\rho_i) \cosh \sigma D}{[\beta^2(1+\rho_i)^2 + (1-\rho_i)^2] \sinh \sigma D + 2\beta(1-\rho_i^2) \cosh \sigma D} \quad 14)$$

$$T = \frac{2\beta(1-\rho_e)(1-\rho_i)}{[\beta^2(1+\rho_i)^2 + (1-\rho_i)^2] \sinh \sigma D + 2\beta(1-\rho_i^2) \cosh \sigma D} \quad 15)$$

$$\epsilon = \frac{2\beta(1-\rho_e)[\beta(1+\rho_i) \sinh \sigma D + (1-\rho_i)(\cosh \sigma D - 1)]}{[\beta^2(1+\rho_i)^2 + (1-\rho_i)^2] \sinh \sigma D + 2\beta(1-\rho_i^2) \cosh \sigma D} \quad 16)$$

If the slab is thick enough to be opaque, the expression for emittance reduces to -

$$\epsilon = \frac{2\beta(1-\rho_e)}{1 + \beta - \rho_i(1-\beta)} = \frac{2n^2\beta(1-\rho_i)}{1 + \beta - \rho_i(1-\beta)} \quad 17)$$

The latter form is a consequence of the equilibrium relationship

$$1 - \rho_e = n^2(1 - \rho_i) \quad (18)$$

The hemispherical external reflectance for a plane surface with diffuse illumination can be calculated from the refractive index. This is most easily done by means of Walsh's equation, which he obtained by integration of the Fresnel equations for oblique incidence (11, 12). Corresponding values of ρ_i can then be obtained by Equation 18. It does not appear that ρ_i or ρ_e for a plane surface is greatly different from that for a surface with shallow roughness, especially in the visible and near infrared region where dielectrics are only weakly absorbing (13). Furthermore, it turns out that the expression for emittance of opaque dielectric bodies is quite insensitive to the value of ρ_i , as shown by Richmond and also confirmed experimentally (11).

The foregoing expressions have all been derived for total hemispherical flux. Measurements, however, are usually directional, at least in part. Thus, reflectance measurements discussed later in this report are either with directional illumination and hemispherical illumination and directional viewing. Directional emittance is the complement of these. The data from such measurements are customarily treated with the Kubelka-Munk theory as if they were hemispherical rather than directional. Our data also have been treated in this way.

Relations Between K-M and Intrinsic Absorption Coefficients

Now let us consider the relationship between the different absorption coefficients: K for dispersed material, K' for consolidated material, and α the intrinsic coefficient, which is the one measured on clear material with corrections to exclude the effect of surface reflectance. To obtain a common basis we express all coefficients in units of sq cm/g instead of cm^{-1} ; x then is the g/sq cm. Consider a single particle in the case of the dispersed material. (A fiber disposed crosswise to the flux can be treated similarly.) Here we limit ourselves to particles and wavelengths such that absorbcency is low and the differential form of expression is accurate enough that bulk optical properties still apply. From Mie scattering calculations it appears that for thoria, with a refractive index of about 2, the limit for this is a diameter of one-third the wavelength (14). We envisage a hemispherical beam, I , incident on the particle. A fraction ρ_e of the beam I is reflected from the particle. The remainder traverses the particle with an average path length l_1 , then is partly transmitted and partly internally reflected. The fluxes and absorptions of this and succeeding traverses are as follows:

	<u>In Transit</u>	<u>Absorbed</u>	<u>Reflected</u>
1st Traverse	$I(1 - \rho_e)$	$I(1 - \rho_e) l_1 d\alpha$	$I(1 - \rho_e) \rho_i$
2nd Traverse	$I(1 - \rho_e) \rho_i$	$I(1 - \rho_e) \rho_i l_2 d\alpha$	$I(1 - \rho_e) \rho_i^2$
3rd Traverse	$I(1 - \rho_e) \rho_i^2$	$I(1 - \rho_e) \rho_i^2 l_3 d\alpha$	$I(1 - \rho_e) \rho_i^3$

and so on, where d is density, so that ld has the dimensions of x . If $l_1 = l_2 = l_3 = l_n$, then the total absorption by the particles is -

$$\frac{I(1-\rho_e) ld\alpha}{1-\rho_i} = In^2ld\alpha \quad (19)$$

A similar expression in which I is replaced by E is obtained when we consider emission.

We wish to sum the absorption over all particles encountered by the hemispherical beam, I , in traversing the differential, dx . In addition to the assumption made above as to the equality of path lengths of the reflections inside the particle, we also assume that refraction at the surface of the particles does not affect the ratio of average path length to the amount of material. One method of visualizing this question is to consider the division of bulk material into space-filling cells such as cubes and octahedrons followed by separation of the cells. We are assuming that the average path length after separation is the same as before separation. This is perhaps not true when the particles have forms such as spheres or cylinders (except at their midsections). We think it is more likely to be true when the particle surface is highly irregular. Later in this paper we show that mantle fibers are very irregular in cross section.

In addition, note that the number of particles encountered by a directional beam varies with the angle that it makes with the x -direction. Note also that we must average the path according to the intensity of the beam components in the different directions. We obtain an average path length, $d\bar{l} = Ldx$, where L is the dimensionless ratio of average path length to dx . This gives us $IKdx = In^2L\alpha dx$ or $K = n^2L\alpha$. Kubelka has shown that, if the radiation is perfectly diffuse (has the same intensity in all directions), then $L = 2$ (15).

In the case of consolidated material the similar relationship is $K' = L\alpha$. In this case too, the components of the beam traveling at an angle to x have a longer path than those traveling along x , and again $L = 2$ for perfectly diffuse radiation.

Another effect needs consideration. As pointed out by Klein, the path of part of the radiation entering and leaving the element, dx , in a given direction may actually be a circuitous one, longer than would be expected according to the geometry (10). No data on the magnitude of this effect have come to our notice in the literature. If we ignore this effect and take $L = 2$, we have -

$$K' \text{ (absorption coefficient for consolidated material)} = 2\alpha \quad (20)$$

$$K \text{ (absorption coefficient for dispersed material)} = 2n^2\alpha \quad (21)$$

$$K = n^2K'$$

Refractive Index

The refractive index thus enters calculations of emittance. Furthermore, the refractive index is the physical constant, which, along with microstructure, controls scattering. Thus the variation of the refractive index with temperature is a matter of some importance. Ramaseshan *et al.* have reviewed the relevant theory and data in the visible region (16). It appears that variation of the refractive index of metal oxides in the visible is quite small, amounting to no more than 0.02/1000°C for magnesium oxide. Less data available on its variation in the infrared. Results of one study (again on magnesium oxide) show very little variation at 12.5 μ m when the temperature increases from 8.5° to 950°K; however, when the temperature increases to 1950°K, the refractive index increases from about 0.87 to about 0.94 (17). Thus it seems likely that the temperature dispersion of the refractive index of thoria and other oxides should increase with wavelength but not to more than about 10%/1000°C at 12 μ m.

The small variation of the refractive index with temperature indicates that scattering coefficients ordinarily should not vary appreciably with temperature. However, the broadening of the ceria absorption band in the visible with temperature rise will be accompanied by an increase in the refractive index in the neighboring higher wavelength range.

Procedures for Measurement of Radiation Properties

Materials

Mantles used in this study were of single-stitch weave, obtained from the Welsbach Corporation. Mantles of normal ceria content were from commercial production; those with no ceria and nominally 3 times the normal amount of ceria were supplied on special request. Chemical analyses of the mantle fabrics (excluding the neck portion) are shown in Table 1.

Table 1. CHEMICAL ANALYSIS OF MANTLE FABRIC SAMPLES

	Zero Ceria	Normal Ceria	Thrice Normal Ceria
	wt %		
Al ₂ O ₃	0.25	0.32	0.25
BeO	0.09	0.09	0.11
CeO ₂	0.00	0.61	3.26
MgO	0.05	0.11	0.11
SiO ₂	0.60	0.29	0.61

Determination of Kubelka-Munk (K-M) Coefficient at Room Temperature

These measurements were made at the IIT Research Institute (IITRI). A General Electric Co. spectrophotometer equipped with a diffuse reflectance attachment was used for wavelengths from 0.38 to 0.7 μ m. Measurements were extended to 2.4 μ m with a laboratory-constructed instrument consisting of an integrating sphere attached to a Perkin-Elmer single-beam monochromator with a lead sulfide detector.

To prepare the fabric the collodion coating of the hard mantles was burned off, the top of the mantle cut off, and the remaining fabric cut lengthwise into two equal parts. We flattened the fabric by placing it on a flat stainless steel screen and by impinging the air-natural gas flame of a hand torch on it. The pieces of fabric were then cut to size and weighed.

To determine the Kubelka-Munk coefficients, one reflectance spectrum (R_{∞}) is obtained with a sample thick enough to be opaque, and another, R_0 , is obtained with a thinner sample backed by a black cavity. The latter sample must be thin enough to show a substantial difference from R_{∞} . On the other hand, several layers of mantle fabric had to be used to reduce the area of holes and increase the uniformity of effective thickness. Five layers of the single-stitch mantle fabric gave satisfactory results. Change in orientation of the layers to one another did not affect the results. Use of four layers gave reasonably close agreement, which indicated that five layers were enough to obtain uniformity of thickness.

The values of SX were obtained from the two reflectance values by means of a Kubelka-Munk chart (18). Values of K/S were obtained from a chart or table of K/S against R_{∞} that had been calculated by means of Equation 9.

Emittance Determinations

Normal emittance measurements were made at IITRI with an apparatus in which the sample and a silicon carbide plate (used as a standard) are mounted side by side in a tube furnace and continuously moved back and forth along the length of the furnace (19) (Figure 2). For readings, a cooled shield is inserted at the center of the furnace as close to the traversing sample as possible. The radiation emitted is dispersed and measured by a Perkin-Elmer spectrophotometer with sodium chloride optics. Mantle fabric for these determinations was prepared by the method described above. The pads of fabric were mounted on the vertical-facing alumina tray of the apparatus by clamps of rhodium sheet placed along the sides and bottom of the sample and cemented to the tray.

Cooling of the sample as it comes before the cooled shield was investigated as a source of error. It was feared that the mantle fabric would cool much faster than the standard because of its unconsolidated nature and resulting inaccessibility of heat stored in adjacent layers.

Rate-of-cooling data were obtained by stopping the sample or standard in front of the port for about 10 seconds while the emission was being recorded. The rate of signal decrease in percent of the initial signal per second is shown in Figure 3 plotted against wavelength.

At each wavelength the emitted radiation to which the signal is directly proportional is considered to be the product of the emittance and the radiative power of a blackbody. The emittance remains substantially constant as the sample or standard cools during the 10-second period since only a small temperature change occurs. The rate of signal decrease can then be expressed as -

$$\frac{1}{S_{\lambda}} \frac{dS_{\lambda}}{dt} = \frac{1}{E_{\lambda}} \frac{dE_{\lambda}}{dT} \frac{dT}{dt} \quad 23)$$

where dS/dt is the experimental rate of decrease, E_λ is the radiative power of a blackbody at wavelength λ , T is temperature, and t is time. Values of $\frac{dE_\lambda}{E_\lambda dT}$ have been calculated from the Planck equation and plotted in Figure 3

with dT/dt evaluated to make the curve pass through the experimental point for the silicon carbide at $2\mu\text{m}$. The experimental points for the silicon carbide standard follow the theoretical curve satisfactorily. The mantle fabric, on the other hand, shows a greater rate of signal decrease at the longer wavelengths and a slower rate at the short wavelengths. However, at wavelengths above $1\mu\text{m}$ indicated rates of cooling of sample and standard are of about the same magnitude. The actual cooling period was less than 2.5 seconds, which was the time of traversal of the 1-1/4-in. sample width. Error from this period of cooling did not appear to be serious, except at wavelengths below $2\mu\text{m}$.

The effect of sample-to-port distance was also investigated. As this distance increases, more radiation from the furnace wall can strike the front surface of the sample and be reflected into the measurement beam. The amount of radiation reflected from the sample is greater than that from the standard because the mantle fabric has greater reflectance than the standard. Also, more of the radiation, which strikes sample and standard at a high angle of incidence, is reflected specularly by the standard than by the sample; the specular component is not included in the beam collected by the monochromator. Measurements were made at several different wavelengths with sample-to-port distance varied from 1/16 to 1/4 in. Emittance values increased at the rate of 0.05 per 1/16 in. and 2 to 4 m, and a slightly higher rate at higher wavelengths. Because of unevenness of the sample surface and variation in the sample mounting and tracking, it was not possible to reduce the estimated sample-to-port distance below about 1/16 in. Thus there is an uncertainty of about 0.05 in emittance values. We think the observed values are likely to be too high rather than too low, except at wavelengths from 1 to $2\mu\text{m}$ where error from cooling may have more effect.

Emittance measurements were made on 12-layer samples of mantle fabric backed by the alumina sample tray, and on 4-layer samples backed by silicon carbide of known emittance.

In treatment of the data, the 12-layer samples were assumed to be thick enough to be opaque; this may not be strictly true, but the situation is helped by the fact that the emittance of the alumina tray is low (similar to that of thoria) in the low-wavelength region where the mantle fabric is most translucent. Absorption and scattering coefficients were calculated by application of Equations 8 and 12.

Reflectance Measurements

Some reflectance measurements were also obtained at the National Bureau of Standards. Two instruments were used. In one a laser is used as a source of radiation (20). Illumination is at 12 degrees from the normal; an integrating sphere is used to collect the reflected radiation. Measurements could be made at temperatures from ambient to about 1900°C in vacuum, or to about 1400°C in air, but only at wavelengths of 0.6328 and $1.15\mu\text{m}$. In this instrument, at least for measurements at elevated temperature, the sample is required to be in the form of a consolidated disk of 1/2-in. diameter.

We prepared samples for measurement on this instrument by grinding the mantle fabric for about 15 minutes on a motorized mortar and pestle; pressing the powder, lubricated with a few drops of a 2.5% aqueous solution of polyvinyl alcohol, in a die at about 12,000 psi; and sintering. The time of sintering was 2 hours, and the atmosphere was air. The temperature of sintering was adjusted to obtain about the same density on each sample: 1270°-1290°C for the sample with no ceria, 1230°-1260°C for the sample with normal ceria, and 1180°-1200°C for the sample with thrice-normal ceria. Densities obtained were 5.10, 5.05, and 5.29 g/cu cm.

The other instrument used at NBS was a Cary-White Model-90 recording spectrophotometer with a diffuse reflectance attachment that operates over the spectral range 2.5 to 22.2 μ m and at temperatures from 20° to 1000°C (21). The specimen in the form of powder is irradiated hemispherically and viewed at a direction of 20° from the normal to the sample surface. Temperature of the sample is monitored by a thermocouple probe. Powder for these determinations was prepared by grinding the fabric for 15 minutes under water in a motorized mortar and pestle.

Results of Experimental Measurements

Refractive Index

A specimen of fused thoria made by the Norton Company was obtained from W. E. Danforth of the Bartol Research Foundation; a prism was cut from it and polished at the IIT Research Institute. The refractive index was determined at Eastman Kodak Company at room temperature by the minimum deviation method. Kodak estimated the accuracy to be $\pm 5 \times 10^{-3}$. The results are shown in Table 2.

Table 2. REFRACTIVE INDEX OF THORIA

<u>Wavelength, μm</u>	<u>Refractive Index</u>	<u>Wavelength, μm</u>	<u>Refractive Index</u>
0.405	2.1485	3	2.0415
0.436	2.1354	4	2.0214
0.486	2.1200	5	1.9952
0.546	2.1076	6	1.9657
0.593	2.1010	7	1.9254
0.656	2.0930	8	1.8744
1	2.0698	9	1.8148
2	2.0554		

Microstructure of Mantle Materials

The microstructure of filaments of a single-stitch mantle mounted in an epoxy resin is shown in the photomicrograph in Figure 4. This is a cross section of filaments of two adjacent threads crossing at a small angle. The streaks in the photomicrograph are diffuse light reflected from filaments buried in the resin. The diameter of the filaments is about 10 μ m; the extreme irregularity and hollows of the cross section probably greatly increase the scattering at wavelengths below about 6 μ m.

The weight of the mantle fabric was 0.011 g/sq cm. Holes in the fabric amount to about one-half of the area, so that the actual thickness of the threads of a single layer of mantle fabric varies from about 0.02 to about 0.04 g/sq cm where the threads cross.

A photograph of an experimental Thermacomb mantle (from the 3M Company) is shown in Figure 5. The material is an open three-dimensional network composed of straight members 1 to 3 mm long joined to form irregular polygons. In the form shown it serves as a mantle; in flat sheets it could serve as the radiator of a porous plate burner.

The connecting members of this material are triangular and hollow in cross section, with an effective thickness several times the thickness of a thread of an ordinary mantle. This is a probable explanation for the lower ceria content (about 0.2%) reported to be optimum for light emission in this mantle (22), compared with about 1% in ordinary mantles.

Absorption and Scattering Coefficients

Absorption and scattering coefficients obtained from the reflectance measurements at room temperature over the wavelength range 0.4 to 2.4 μ m are shown in Figure 6 and 7. Each point represents the average results for two or three samples.

The general trend of absorption coefficients is as expected; however, there is no consistent trend with ceria content except at wavelengths below 0.42 μ m, where the effect of the ceria absorption band predominates. Both absorption and scattering coefficients are less accurate at the higher wavelengths where the reflectance is above 90% and where there is less difference between the two reflectance readings. The scattering coefficients for the different ceria contents are very nearly the same, and the differences do not appear to be significant. The increase in scattering coefficients with wavelength in the range from 0.8 to 2.4 μ m is unexpected.

Emittance values obtained on the mantle fabric with three different levels of ceria content are shown in Table 3. Results agree well, with no significant difference among the three samples at wavelengths from 1 to 6 μ m. We attribute differences at higher wavelengths to experimental error.

Table 3. INFRARED EMITTANCE OF MANTLE FABRIC AT 1200° C

Wavelength, μ m	Thoria Having				
	No Ce	3X Normal Ce	Normal Ce		SiC*
	12 Layer	12 Layer	12 Layer	4 Layer	
	Emittance				
1	0.09	0.09	0.10	0.26	0.74
1.5	0.11	--	0.115	0.31	0.85
2	0.12	0.14	0.14	0.34	0.92
3	0.13	0.15	0.14	0.32	0.90
4	0.14	0.15	0.15	0.32	0.88
4.5	--	--	0.17	0.32	0.875
5	0.17	0.17	0.19	0.32	0.87
6	0.20	0.21	0.225	0.335	0.87
7	0.22	0.24	0.28	0.36	0.865
8	0.28	0.32	0.355	0.45	0.87
9	0.41	0.44	0.51	0.615	0.84

* Reference values, determined against a blackbody.

An emittance spectrum (Table 3) from four layers of mantle fabric backed by a silicon carbide plate was obtained from a sample of fabric having normal ceria content. Absorption and scattering coefficients at wavelengths from 2 to 8 μ m were calculated from the spectra of the two (12-layer and 4-layer) samples.

Scattering coefficients ranged from 40 to 55 sq cm/g (average 50) and had no significant trend with wavelength. As noted previously, we do not expect the scattering coefficient to vary with temperature. When the possibilities of error in the emittance determinations are considered, this value is in remarkable agreement with the coefficients determined at room temperature.

The absorption coefficient spectrum from these emittance determinations is shown in Figure 8, together with the visible-near infrared spectrum obtained on the same kind of mantle fabric at room temperature. In the near infrared where the curves overlap, the high-temperature absorption coefficient is greater than the low-temperature coefficient by a factor of about 2, which we consider a reasonable value. However, it should be noted that the calculated absorption coefficient has a high rate of change with change in emittance. With the scattering coefficient assumed to be constant, an increase from 0.14 to 0.19 in emittance is equivalent to a doubling of the absorption coefficient by a factor of 2.6. These factors correspond to the estimated maximum error of the emittance determination.

A comparison of our K's with those calculated from Weinrich's intrinsic absorption coefficients provides us with a test of our theoretical relationship. Values were obtained at 0.4 and 0.66 μ m according to the formula $K = \frac{2n^2}{d} \alpha$ as follows:

Wavelength, μ m	Intrinsic Absorption Coefficient, cm ⁻¹	Refractive Index	K-M Absorption Coefficient, sq cm/g	
			Calculated	Observed
0.4	8	2.15	7.4	4.8
0.66	3	2.09	2.6	1.3

The density of thoria was taken as 10.0 g/cu cm. Values of the intrinsic absorption coefficient were those for the red material, heated at 1000°C in air. Values for material heated at 1000°C in vacuum are lower and would give closer agreement. We are uncertain as to the exact oxidation state of the mantle fabric, which had been heated in an oxidizing flame. The agreement shown appears reasonable in consideration of the assumptions made in the theory and of the experimental accuracy.

Reflectance Measurements at National Bureau of Standards

Results of reflectance determinations made at NBS in the infrared on powder samples are shown in Figure 9 in the form of emittance spectra. The emittance here is a directional one, at a 20 degree angle from the normal. This is calculated, according to Kirchhoff's law, as the complement $(1-R)$ of the reflectance determined with hemispherical illumination and 20 degree viewing. Reflectance was determined both at 20° and 1000°C on mantle material with normal ceria content, and at 1000°C on mantle material with zero ceria and with thrice-normal ceria. We attribute the anomalous peaks in the 20°C spectrum in the wavelength range 2.5 to 8 μ m to adsorbed water and other adsorbed impurities. These should not be present in the 1000°C spectra. The origin of the small peaks still present in the 1000°C spectra is not known. The emittance from 2.5 to 5 μ m is much lower than values obtained at 1200°C on consolidated material (8), which indicates the effect of scattering by the powder.

Reflectance spectra were also obtained at NBS on powder samples of different thicknesses, backed by a black diffusing paint surface, in an attempt to determine absorption and scattering coefficients. The temperature was raised to 250°C to decrease the amount and effect of adsorbed material. A higher temperature would have endangered the paint backing. However, effects of adsorption were still quite appreciable, and results were not consistent enough to obtain coefficients. It appears that measurements at elevated temperature on mantle fabric (rather than on powder) would give us a better chance of obtaining the coefficients. The lesser scattering power of the fabric would give lower reflectance and a slower rate of change of K/S with reflectance.

Reflectance values, R, from the NBS laser instrument and values of K's/S calculated by means of Equation 17 are shown in Table 4. [Values of ρ_e were obtained from the Walsh equation with room-temperature values of the refractive index (11).] Measurements were made at 20°C, near 1000°C, and near 1200°C. A second measurement at 20°C, after the high-temperature measurements, indicates the effect of changes in the material such as further sintering or change in oxygen content. Standard deviations of the reflectance measurements ranged from 0.001 to 0.004.

These measurements do not show the substantial drop in K'/S in going from 0.6328 to 1.15 μ m that was found in K/S in the ITRI measurements on mantle fabric (Figure 6). This may be caused by a large change in the scattering coefficient of the consolidated and sintered material with change in wavelength. No data are available on this point. However, variation of K'/S with temperature should not be affected. This allows us to calculate absorption coefficients for mantle fabric at elevated temperature at these two wavelengths. We assume that the scattering coefficient of the sintered sample is constant with temperature and thus that the change in absorption coefficient with temperature, determined on the sintered material, also applies to mantle fabric. Absorption coefficients at 1200°C and at 0.6328 and 1.15 μ m have been calculated for mantle fabric of normal ceria content using these assumptions. The values, as shown in Figure 8, line up well with the infrared values at 1200°C obtained from emittance determinations.

Table 4. RADIATION PROPERTIES OF SINTERED MANTLE MATERIAL

Temp, °C	No Ceria			Normal Ceria			Thrice Normal Ceria				
	R	K'/S	Relative Temp, °C K'/S	R	K'/S	Relative Temp, °C K'/S	R	K'/S	Relative Temp, °C K'/S		
	At 0.6328 μ m										
20	0.712	0.0046	1.00	20	0.768	0.0025	1.00	20	0.738	0.0035	1.00
990	0.697	0.0053	1.14	985	0.724	0.0041	1.61	955	0.637	0.0094	2.69
1230	0.668	0.0071	1.54	1220	0.661	0.0076	3.00	1190	0.511	0.0292	8.32
20*	0.728	0.0039	--	20	0.781	0.0022	--	20	0.742	0.0034	--
	At 1.15 μ m										
20	0.691	0.0059	1.00	20	0.744	0.0034	1.00	20	0.741	0.0036	1.00
1110	0.663	0.0077	1.30	985	0.694	0.0058	1.68	1015	0.669	0.0073	2.05
1235	0.629	0.0106	1.79	1220	0.664	0.0076	2.22	1210	0.610	0.0126	3.54
20	0.689	0.0061	--	20	0.756	0.0030	--	20	0.736	0.0037	--

* Measurement repeated after high-temperature measurements.

The temperature coefficients increase with increasing ceria content at both 0.6328 μ m and 1.15 μ m. The great increase with ceria content at 0.6328 μ m can be attributed to the effect of the ceria absorption band.

Discussion

A graph of the emittance function (Equation 7) for dispersed material is shown in Figure 10 for a wide range of thickness and for several decades of the scattering and absorption coefficients. Several observations are worth noting. First, it is apparent that the effect of absorptivity can, under some conditions, be interchanged with the effect of thickness. Thus, when the section is thin enough (how thin depends on both coefficients), the emittance is simply the product of the thickness and the absorption coefficient. The ceria content of mantle material has a large effect on its absorption coefficient in the visible part of the spectrum. It should not be surprising, then, that the optimum ceria content should depend on the effective thickness of the mantle.

The scattering coefficient also can have important effects. For example, we can show that for optically opaque specimens, those so thick that additional thickness does not change the emittance, the emittance depends solely on the ratio of the absorption coefficient to the scattering coefficient. Although the absorption coefficient depends mainly on the chemical composition and crystal structure of the material at the atomic level, the scattering coefficient depends on the microstructure, particularly on the presence and number of boundaries in the material where a change in the refractive index occurs. For particles dispersed in an otherwise homogeneous medium, the scattering coefficient depends mainly on the size, shape, and refractive index of the particles relative to the medium. For consolidated ceramic materials, it depends mainly on the number, size, shape, and relative index of the particles of different phases, including pores, in the material. In anisotropic crystalline materials, crystallite boundaries also contribute to scattering. In some cases, variation of the microstructure within the mechanical requirements provides another means of obtaining desired properties of radiators.

Now let us consider the position of the mantle in this picture. The weight of a single layer of the single-stitch mantles used in our investigation was 0.011 g/sq cm. We see the emission from two layers of fabric when we look at the center portion of an ordinary cylindrical upright mantle. The actual thickness in the path of a ray may vary from zero to perhaps 0.08 g/sq cm for a ray through crossed threads in both layers. From Figure 10, we see that at this thickness the emittance is equal, with little deviation, to the product of the absorption coefficient and average thickness, for absorption coefficients up to about 2 sq cm/g. Emittance of two layers of mantle fabric at several different wavelengths in the infrared have been calculated from the absorption coefficients of Figure 8 and are shown in Figure 10. These emittance values are compared below with those from Ives and coworkers (2) and from Rubens (23). With consideration of the possible differences in mantle composition and weight, good agreement is shown at wavelengths below 8 μ m.

Wavelength, μm	This Work	Emittance	
		Ives et al. (2)	Rubens (23)
2	0.011	0.01-0.02	0.007
3	0.011	0.01-0.02	0.0088
5	0.026	0.03	0.014
8	0.11	0.3	0.211

We do not know how to account for the apparently low emittance values we found at wavelengths of $8\mu\text{m}$ and above. Alternatively, at wavelengths from about 0.6 to about $6\mu\text{m}$ the absorption coefficient can apparently be calculated from an emittance spectrum, such as that of Rubens or Ives et al., by use of an average fabric weight. At shorter wavelengths the absorption coefficient can still be estimated by application of the known scattering coefficient (Equation 7) and an estimated effective thickness. At longer wavelengths the same method could be used, but the scattering coefficient is not known here.

ACKNOWLEDGMENTS

This work was sponsored by the American Gas Association. The author is grateful to it for permission to publish this paper.

Also we wish to thank Mr. O. H. Olson of IIT Research Institute for advice and for supervision of measurements made there; similarly, we wish to thank Mr. J. C. Richmond and Dr. V. Wiedner of the National Bureau of Standards for their contributions.

Literature Cited

1. Rubens, H., "Emittance and Temperature of Welsbach Mantles With Different Ceria Contents," Ann. Phys. **18**, 725 (1905).
2. Ives, H. E., Kingsbury, E. J., and Karrer, K., "A Physical Study of the Welsbach Mantle," J. Franklin Inst. **186**, 401-38, 585-625 (1918).
3. Rutgers, G. A. W., "Temperature Radiation of Solids," in Flugge, S., Ed., Handbuch Der Phys. Vol. **24**, 168. Berlin: Springer, 1958.
4. Ritzow, G., "The Heat Radiation of Glowing Oxides and Oxide Mixtures in the Infrared Region," Ann. Phys. **19**, 769-99 (1930).
5. Liebman, G., "The Temperature Radiation of Colorless Oxides in the Visible," Z. Physik **63**, 404-36 (1930).
6. Weinrich, O. A., and Danforth, W. E., "Optical Properties of Crystalline Thoria," Phys. Rev. **88**, 953-54 (1952).
7. Gryvnak, D. A. and Burch, D. E., "Optical and Infrared Properties of Al_2O_3 at Elevated Temperatures," J. Opt. Soc. Amer. **55**, 625 (1965).
8. Clark, H. E. and Moore, D. G., "A Rotating Cylinder Method for Measuring Normal Spectral Emittance of Ceramic Oxide Specimens From 1200° to 1600°K ," J. Res. NBS **70A**, 393-415 (1966).

9. Hamaker, H. C., "Radiation and Heat Conduction in Light-Scattering Material," Philips Res. Rep. 2, 55-67 (1947).
10. Klein, J. D., "Radiation Heat Transfer Through Scattering and Absorbing Nonisothermal Layers," in Katzoff, S., Ed., Symposium on Thermal Radiation of Solids, NASA SP-55, 73-81. Washington, D.C.: Govt. Print. Office, 1965.
11. Richmond, J. C., "Effect of Surface Roughness on Emittance of Nonmetals," J. Opt. Soc. Amer. 56, 253-54 (1966).
12. Richmond, J. C., "Relation of Emittance to Other Optical Properties," J. Res. NBS 67C, 217-26 (1963).
13. Giovanelli, R. G., "A Note on the Coefficient of Reflection for Internally Diffuse Light," Opt. Acta 3, 127-30 (1956).
14. Plass, G. N., "Mie Scattering and Absorption Cross Sections for Aluminum Oxide and Magnesium Oxide," Appl. Opt. 3, 867-72 (1964).
15. Kubelka, P., "New Contributions to the Optics of Intensely Light-Scattering Materials. Part 1," J. Opt. Soc. Amer. 38, 448-57 (1948).
16. Ramaseshan, S., Vedam, K. and Krishnan, R. S., "Thermo-Optic Behavior," in Krishnan, R. S., Ed., Progress in Crystal Physics, Vol. 1, 139-67. Madras, India: S. Viswanathan, 1958.
17. Jasperse, J. R. et al., "Temperature Dependence of Infrared Dispersion in Ionic Crystals LiF and MgO," Phys. Rev. 146, 526-42 (1966).
18. American Society for Testing and Materials, "Standard Method of Test for Reflectivity and Coefficient of Scatter of White Porcelain Enamels," ASTM Designation: C347-57, in 1966 Book of ASTM Standards, Part 13, 312-15. Philadelphia, 1966.
19. Olson, O. H. and Katz, S., "Emissivity, Absorptivity, and High-Temperature Measurements at Armour Research Foundation," in Claus, F. J., Ed., Surface Effects of Spacecraft Materials, 164-81. New York: John Wiley, 1960.
20. Kneissl, G. J. and Richmond, J. C., "A Laser-Source Integrating Sphere Reflectometer," U.S. NBS Tech. Note 439 (1968). February.
21. White, J. V., "New Method of Measuring Diffuse Reflectance in the Infrared," J. Opt. Soc. Amer. 54, 1332-37 (1964).
22. Stack, T. N. and Manske, W. J., "Development of the Thermocomb Gas Light Mantle." Paper presented at the American Gas Association Research and Utilization Conference, Cleveland, June 2-4, 1964. Cat No. M31460.
23. Rubens, H., "Concerning the Emittance Spectrum of Welsbach Burners," Ann. Phys. 18, 725-38 (1905).

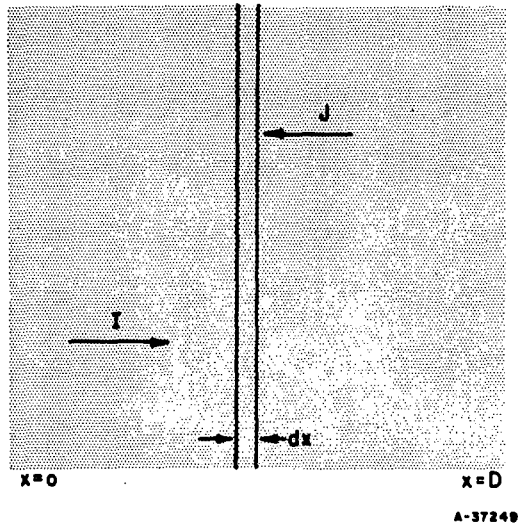


Figure 1. RADIANT FLUX OF UNIFORM ONE-DIMENSIONAL SLAB

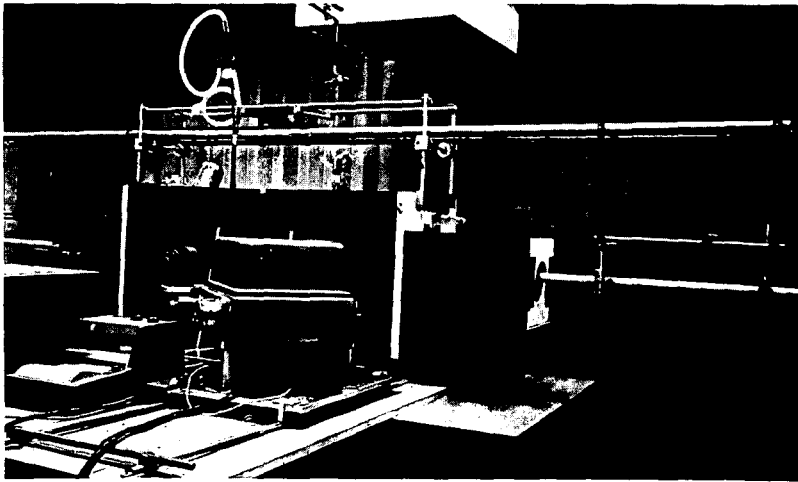


Figure 3. EMITTANCE MEASUREMENT APPARATUS

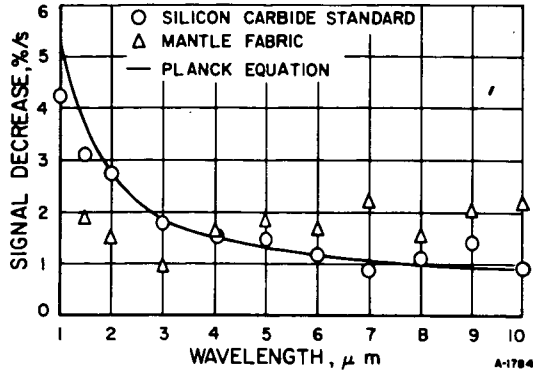


Figure 3. EFFECT OF SAMPLE COOLING

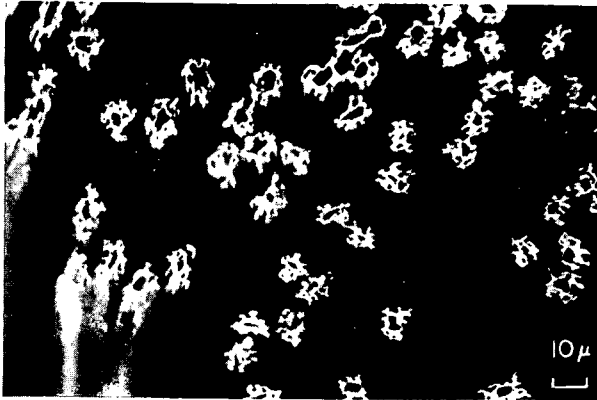


Figure 4. PHOTOMICROGRAPH OF CROSS SECTION OF SINGLE-STITCH MANTLE FABRIC

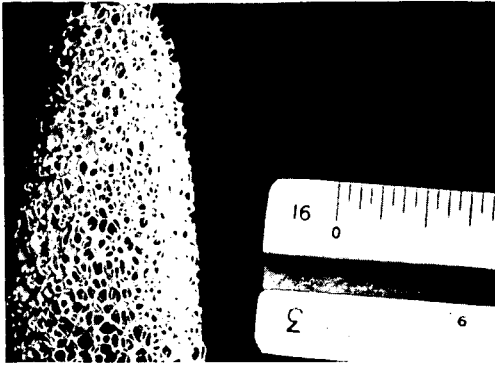


Figure 5. EXPERIMENTAL THERMACOMB MANTLE

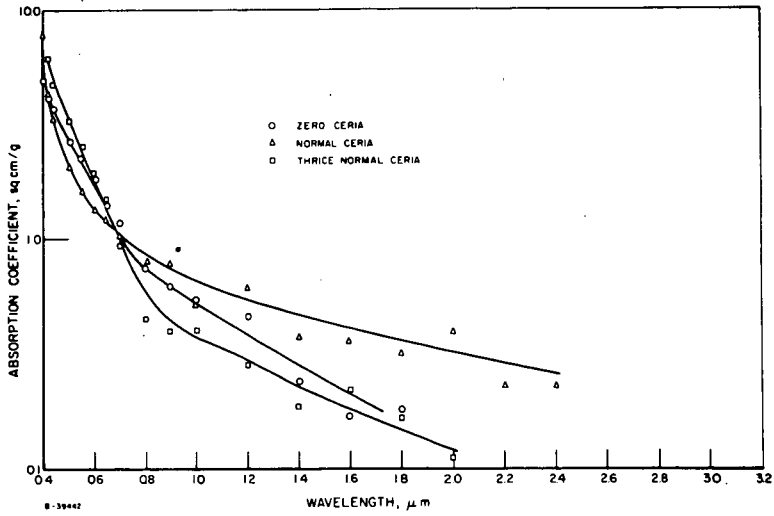


Figure 6. ABSORPTION COEFFICIENT OF MANTLE FABRIC AT ROOM TEMPERATURE

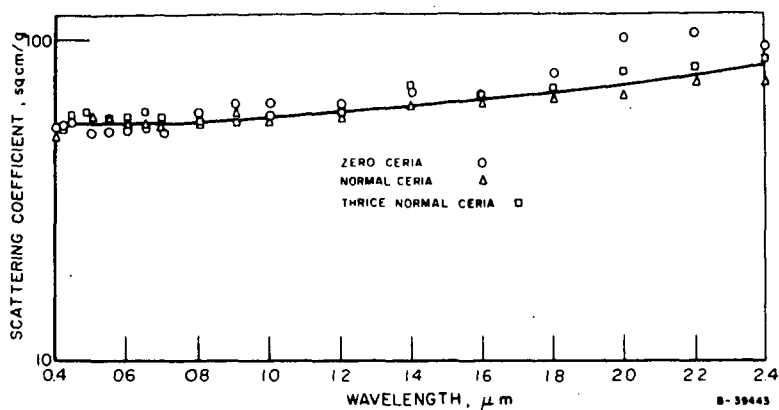


Figure 7. SCATTERING COEFFICIENT OF MANTLE FABRIC AT ROOM TEMPERATURE

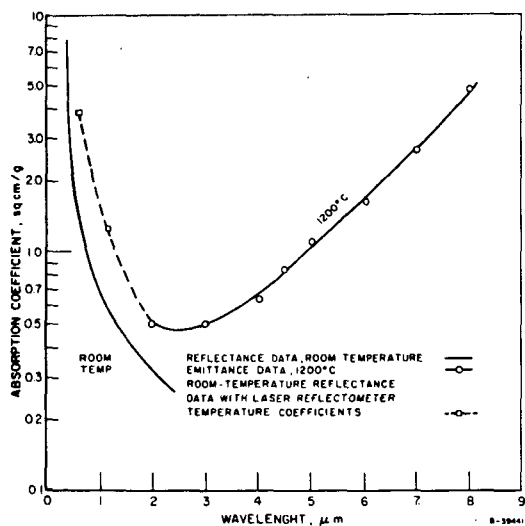


Figure 8. ABSORPTION COEFFICIENT OF MANTLE FABRIC WITH NORMAL CERIA CONTENT

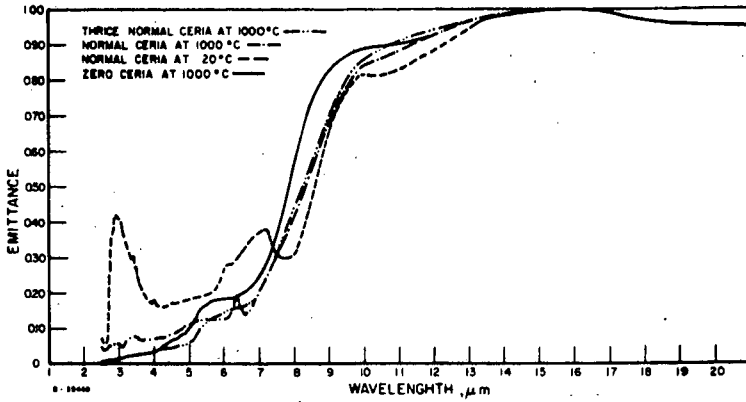


Figure 9. EMITTANCE OF GROUND MANTLE
(Obtained by Reflectance Measurement)

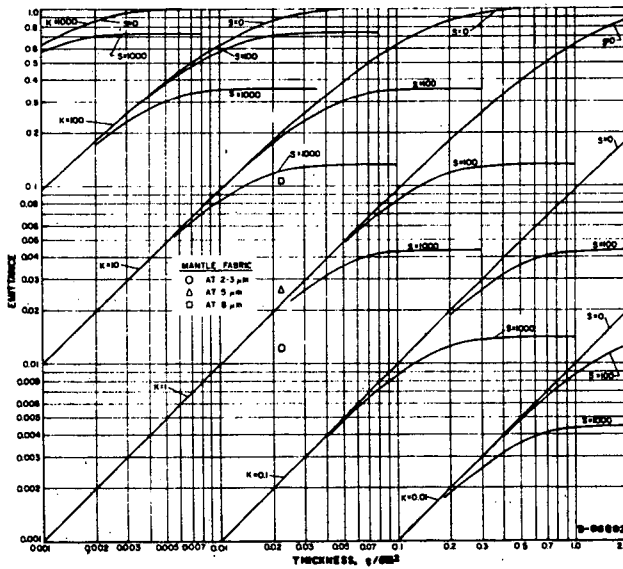


Figure 10. EFFECT OF THICKNESS; ABSORPTION COEFFICIENT, K;
AND SCATTERING COEFFICIENT, S, ON EMITTANCE
OF A DISPERSED DIELECTRIC

HYDROGENATION OF CARBON DIOXIDE OVER A
SUPPORTED RUTHENIUM CATALYST

by

Frank L. Kester*

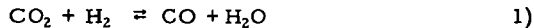
Hamilton Standard
Division of United Aircraft Corporation
Windsor Locks, Connecticut 06096

INTRODUCTION

The ever increasing demand for natural gas as a fuel and raw material has stimulated renewed efforts to find other ways of producing methane. With more and more evidence of an "energy crisis" upon us, alternative approaches such as catalytically synthesizing methane from hydrogen and carbon dioxide meet with more promise of development.

A fairly complete summary of the research on carbon dioxide methanation has been given by Emmett (5), and details of the carbon monoxide-hydrogen reactions by Kirk and Othmer (10). Recent studies on the reaction between hydrogen and carbon dioxide over a supported nickel catalyst have been conducted by Binder and White (1) and by Dew *et al.* (3). Hydrogenation of carbon monoxide over a nickel catalyst has also been investigated (6). A few years ago, Karn and his associates (9) studied ruthenium as a possible methanation catalyst. In a recent experiment, Lunde and Kester (13) studied the reaction rates of methane production from hydrogen and carbon dioxide. The work described here is an extension of this effort, and presents the kinetics and possible mechanisms for the reaction between hydrogen and carbon dioxide.

It is believed by many workers (5) that carbon monoxide is a critical intermediate in carbon dioxide methanation. The following reactions summarize the overall reduction process.



Because the equilibrium for Equation 1 is somewhat unfavorable at the reaction temperatures (200^o-400^o C), it can be argued that this reaction path is somewhat unlikely. A way out of this difficulty is to require that at these temperatures the methanation of carbon monoxide (Reaction 2) proceeds much faster than carbon monoxide production (Reaction 1). Reaction 2 could be in equilibrium. If carbon monoxide were rapidly consumed as it formed, no carbon monoxide would be observed in the reactor exit stream. This was the case with the data treated here (13). However, in his work with a ruthenium catalyst, Karn (9) did observe 1.5-2% carbon monoxide in the exit stream. The reason for his observation

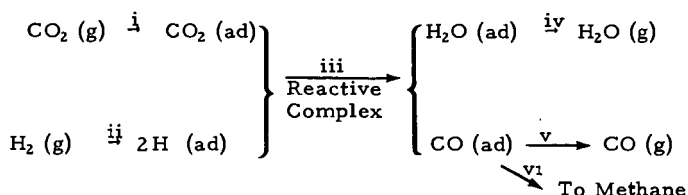
* Present address: Institute of Gas Technology, 3424 S. State Street, Chicago, Illinois 60616

is not clear. It is possible that because of the extended operation (80 days) the catalyst may have become deactivated for the reaction converting carbon monoxide to methane.

REACTION MECHANISMS

Mechanism I

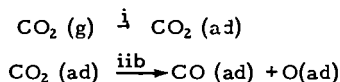
The reaction mechanism outlined here follows the work of Oki and Mezaki (14, 15) for the water-gas-shift reaction over iron oxide.



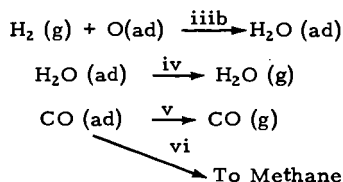
The absorbed carbon monoxide is ultimately reduced to methane by some reaction path not examined here. For the rate model developed in the next section, the reaction of 2H(ad) and CO(ad) (step iii) is assumed to offer the controlling resistance. The other reactions are assumed to be in equilibrium.

Mechanism II

An alternative mechanism, first suggested by Doehlemann (4) in 1938 and subsequently by Kul'kova and his coworkers (11, 12), has been described by Wagner (17). The catalyst was also iron oxide; however, the reaction temperatures were much higher (870°-1122°C) than in Oki and Mezaki's work (400°-450°C) and higher than in these data (207°-371°C) on ruthenium. This mechanism is included because it displays the observed dependence on both hydrogen and carbon dioxide, each to the first power (Table 2); it does not contain the hydrogen adsorption constant in its expression (which was found to be very small or zero); and it does not require the presence of three active sites indicated in Mechanism I (which may be somewhat improbable). The alternative mechanism (17) is -



Adsorbed oxygen atoms react with molecular hydrogen in a single step:



This mechanism assumes that step iiib is rate-controlling and that the other steps are in equilibrium. *

RATE EQUATIONS

The model follows Hougen and Watson (7, 8) and employs a Langmuir-Hinshelwood rate model for Mechanism I. The modifications necessary for Mechanism II are given in the footnote below.

Assuming reaction step iii, Mechanism I, as rate-controlling, and with i, ii, iv, v, and vi in equilibrium, the following rate expression can be written:

$$r = k_F \theta_H^2 \theta_{CO_2} \quad 3)$$

where r is the forward reaction rate, k_F is the forward reaction rate coefficient, and θ_i represents the fraction of catalyst surface coverage of the i^{th} species.

The surface concentrations in equilibrium with the gaseous reactants or products can be represented by -

$$\theta_H^2 = K_{H_2} P_{H_2} \theta_V^2 \quad 4)$$

$$\theta_{CO_2} = K_{CO_2} P_{CO_2} \theta_V \quad 5)$$

$$\theta_{H_2O} = K_{H_2O} P_{H_2O} \theta_V \quad 6)$$

$$\theta_{CO} = K_{CO} P_{CO} \theta_V \quad 7)$$

where θ_V is the fraction of vacant catalyst surface, P_i is the equilibrium partial pressure, and K_i is the equilibrium absorption constant of the i^{th} species.

Inserting relationships 4 and 5 into Equation 3 gives -

$$r = k \theta_V^3 P_{H_2} P_{CO_2} \quad 8)$$

where

$$k = k_F K_{H_2} K_{CO_2} \quad 9)$$

The total fraction surface coverage is equal to the sum of all occupied and unoccupied sites, which equals unity -

* Mechanism II would modify the rate expression by reducing the exponent in the denominator of Equation 14 (presented later) to one and also eliminate $P_{H_2}^{1/2} K_{H_2}^{1/2}$ from the denominator of this expression.

$$1 = \theta_V + \theta_H + \theta_{CO_2} + \theta_{CO} + \theta_{H_2O} \quad 10)$$

On inserting Equations 4, 5, 6, and 7 into Equation 10, one obtains -

$$1 = \theta_V + P_{H_2}^{1/2} K_{H_2}^{1/2} \theta_V + P_{CO_2} K_{CO_2} \theta_V + P_{CO} K_{CO} \theta_V + P_{H_2O} K_{H_2O} \theta_V \quad 11)$$

which, on solving for θ_V^3 , yields -

$$\theta_V^3 = 1/[1 + P_{H_2}^{1/2} K_{H_2}^{1/2} + P_{CO_2} K_{CO_2} + P_{CO} K_{CO} + P_{H_2O} K_{H_2O}]^3 \quad 12)$$

Given the Arrhenius relationship

$$k = A e^{-Ea/RT} \quad 13)$$

and upon inserting Equations 12 and 13 into Equation 8, the final relationship obtained for correlation with the experimental data is -

$$r = A e^{-Ea/RT} \frac{P_{H_2} P_{CO_2}}{[1 + P_{H_2}^{1/2} K_{H_2}^{1/2} + P_{CO_2} K_{CO_2} + P_{CO} K_{CO} + P_{H_2O} K_{H_2O}]^3} \quad 14)$$

where*

$$r = \text{reaction rate} = - \frac{dP_{CO_2}}{dt}$$

A = pre-exponential factor

Ea = activation energy, cal/mole

R = 1.987 cal/deg-mole

T = degrees Kelvin

To evaluate this equation and to determine unknown constants, Equation 14 was rearranged as follows -

$$Y \equiv \ln \frac{r}{P_{H_2} P_{CO_2}} \quad 15)$$

* Other constants are the same as defined earlier.

where --

$$Y \equiv \ln A - \frac{Ea}{R} \left(\frac{1}{T} \right) \quad (16)$$

After Y has been evaluated, the rate expression is then of the form $Y = mX + b$, so that a plot of Y versus $1/T$ for several runs forms a line with a slope $-Ea/R$ and a $1/T = 0$ intercept of $\ln k$. If the correlation is good, the plot will show minimum scatter and good linearity when a proper form the rate equation has been chosen or a proper value of an adsorption coefficient has been obtained. A least squares calculation of a number of data points will give σ , the standard deviation.

The 62 data points shown in Table 1 contained experimental information on space velocity, average methane partial pressure (P_{CH_4}), average water vapor partial pressure (P_{H_2O}), and reactor temperature $^{\circ}K(T)$. The equilibrium carbon monoxide partial pressure, P_{CO} , was obtained from --

$$P_{CO} = \frac{P_{CH_4} P_{H_2O}}{P_{H_2}^3 K_2} \quad (17)$$

using average experimental partial pressures and K_2 , the equilibrium constant for Reaction 2. The value K_2 was calculated as equal to $\exp(1/1.987)(0.00266T + 23095. T^{-1} - 17688. T^{-2} + 17.600 - 6.744 \ln T)$ from data contained in Reference 16.

The experimental reaction rate, r , was calculated as --

$$r = S_v (P_{CO_2 in} - P_{CO_2 out}) \quad (18)$$

where --

S_v is the experimental space velocity,

$P_{CO_2 in}$ is the partial pressure of CO_2 at the reactor inlet, and

$P_{CO_2 out}$ is the partial pressure of CO_2 at the reactor outlet.

DISCUSSION

Determination of Form of Rate Equations

The minimum least squares standard deviation, σ , was taken as a quantitative measure of a fit of the data when correlating various forms of the driving force portion of the rate equation. Adsorption coefficients are treated below. The rate data treated are summarized in Table 1.

Since some of the data were collected at moderate to high conversions, an initial screening was conducted on all runs to determine if any were close to the thermodynamic limit. Two runs were found to be closer than 5% (Runs 533 and 534 in Ref. 13) of the thermodynamic limit and were not included in the final treatment. This means that any influence by the reverse reaction, Equation 1, on the rate data was no greater than 5% and for most runs was much less than 1%.

If one assumed that the adsorption of hydrogen is rate-controlling (reaction path i), then σ is found to be equal to 0.3305 (Table 2); if the adsorption of carbon dioxide is assumed to be controlling (reaction path ii), σ is 0.4688. It appears that assuming hydrogen to be in equilibrium is consistent with Bond (2), who has summarized the activation energies and pre-exponential factors for hydrogen reactions on various transition metals. Bond indicates an activation energy for hydrogen adsorption generally around 5 kcal and never greater than 10.6 kcal. It appears that a lower activation energy than was observed for these data (18.33 kcal) is necessary for the adsorption of hydrogen onto active metal sites to be controlling. Bond also tabulates pre-exponential factors that would indicate reaction rates much faster than observed for these data.

Secondly, the adsorption of carbon dioxide was not considered to be rate-controlling, as the resulting rate equation would not reflect the preferred dependence on the rate on P_{H_2} to the first power (Table 2). Oki and Mezaki (14) also considered the possibility of only one adsorbed hydrogen atom reacting with one adsorbed carbon dioxide molecule. This would reflect a dependence of P_{H_2} to the one-half power with P_{CO_2} to the first power in the rate equation. This relationship, when correlated with the data, yields an unsatisfactorily high standard deviation of 0.3165.

The most significant improvement and the best correlation of the data with the driving force expression were obtained with a dependence of $P_{H_2}P_{CO_2}$ (both to the first power) giving a σ of 0.2113. This expression suggests a rate-controlling reaction of two adsorbed hydrogen atoms with one adsorbed carbon dioxide molecule (Mechanism I) or the reaction of gaseous hydrogen with an adsorbed oxygen atom (Mechanism II).

Determination of Adsorption Coefficients

With this form of the rate expression, further least squares calculations were performed to evaluate the various adsorption constants. A constant such as K_{CO_2} would be systematically varied on a trial-and-error basis until a minimum was obtained in the σ versus K_{CO_2} curve (Figure 1). The other adsorption constants were also evaluated in this manner. The minimum values for the adsorption constants are given in Table 3. Minimum values were obtained for all reaction gases except hydrogen. The σ versus K_{H_2} curve (not shown) was quite broad and shallow in the region of K_{H_2} below 10^{-3} atm⁻¹. Apparently these experimental data are not of sufficient quality to obtain a precise value of K_{H_2} , which is therefore reported to be less than 10^{-3} atm⁻¹ for this temperature range. No temperature dependence of the adsorption constants was included in the evaluation.

Table 2. FIT OF RATE EQUATION TO EXPERIMENT DATA

<u>Form of Rate Equation*</u>	<u>Least Squares Standard Deviation, σ</u>
Driving Force Evaluation	
P_{H_2}	0.3305
P_{CO_2}	0.4688
$P_{H_2}^{1/2}$	0.3708
$P_{H_2}^{1/2} P_{CO_2}$	0.3165
$P_{H_2} P_{CO_2}$	0.2113
Adsorption Coefficient Evaluation	
$\frac{P_{H_2} P_{CO_2}}{[1 + K_{CO_2} P_{CO_2}]}$	0.1818
$\frac{P_{H_2} P_{CO_2}}{[1 + K_{CO} P_{CO_2}]^2}$	0.1795
$\frac{P_{H_2} P_{CO_2}}{[1 + K_{CO_2} P_{CO_2}]^3}$	0.1294
$\frac{P_{H_2} P_{CO_2}}{[1 + K_{CO_2} P_{CO_2} + K_{CO} P_{CO}]^3}$	0.1157
$\frac{P_{H_2} P_{CO_2}}{[1 + K_{CO_2} P_{CO_2} + K_{CO} P_{CO} + K_{H_2O} P_{H_2O}]^3}$	0.1144
$\frac{P_{H_2} P_{CO_2}}{[1 + K_{CO_2} P_{CO_2} + K_{CO} P_{CO}]}$	0.1680
$\frac{P_{H_2} P_{CO_2}}{[1 + K_{CO_2} P_{CO_2} + K_{CO} P_{CO} + K_{H_2O} P_{H_2O}]}$	0.1650

* Driving force and adsorption terms only

Table 3. EVALUATION OF ADSORPTION CONSTANTS FOR 1/2% RUTHENIUM ON ALUMINA*

<u>Adsorption Constant</u>	<u>Experimental Value, atm⁻¹</u>
MECHANISM I	
K_{CO_2}	0.760
K_{H_2}	$< 10^{-3}$
K_{CO}	475
K_{H_2O}	0.160
MECHANISM II	
K_{CO_2}	2.62
K_{H_2}	$< 10^{-3}$
K_{CO}	1490
K_{H_2O}	0.491

* Determined by the least squares trial-error fit of the 62 data points over a temperature range of 207°-358°C. These are average constants for this temperature range.

For Mechanism I, the various adsorption constants included in Equation 15, the least squares calculation for the 62 data points, gave a correlation of $\sigma = 0.9144$. The resulting curve is shown in Figure 2. The activation energy was found to be 18.33 kcal/mole, and the pre-exponential factor was $3.524 \times 10^{10} \text{ atm}^{-1} \text{ hr}^{-1}$.

For Mechanism II, the values were slightly different, with $A = 1.037 \times 10^{10} \text{ atm}^{-1} \text{ hr}^{-1}$, and $E_a = 17.90 \text{ kcal/mole}$.

CONCLUSION

Literature data on the rates of carbon dioxide methanation collected over a 1/2% ruthenium-on-alumina catalyst at 1 atmosphere and temperatures from 207° to 371°C have been interpreted to proceed stepwise first to carbon monoxide and ultimately to methane. Correlation of the data yielded a dependence on P_{H_2} and P_{CO_2} , both to the first power. Two possible mechanisms consistent with previous literature studies have been suggested and discussed. Rate constants, activation energies, and adsorption constants were determined.

LITERATURE CITED

1. Binder, G. G. and White, R. R., "Synthesis of Methane from Carbon Dioxide and Hydrogen," Chem. Eng. Progr. **46**, 563-574 (1950) November.
2. Bond, G. C., Catalysis by Metals. New York: Academic Press, 1962.
3. Dew, J. N., White, R. R. and Sliepceвич, C. M., "Hydrogenation of Carbon Dioxide on Nickel-Kieselguhr Catalyst," Ind. Eng. Chem. **47**, 140-146 (1955) January.
4. Doehlemann E., "The Mechanism of the Water-Gas Reaction on an Iron Catalyst," Z. Elektrochem. **44**, 178-83 (1938)[Chem. Abstr. **32**, 4060 (1938)].
5. Emmett, P. H., Ed., Catalysis, Vol. **4**, 299-303. New York: Reinhold, 1951.
6. Gilkeson, M. M., White, R. R. and Sliepceвич, C. M., "Synthesis of Methane by Hydrogenation of Carbon Monoxide in a Tubular Reactor," Ind. Eng. Chem. **45**, 460-467 (1953) February.
7. Hougen, O. A. and Watson, K. M., "Solid Catalysts and Reaction Rates. General Principles." Ind. Eng. Chem. **35**, 529-541 (1943) May.
8. Hougen, O. A. and Watson, K. M., "Kinetics," in Chemical Process Principles. New York: John Wiley, 1947.
9. Karn, F. S., Shultz, J. F. and Anderson, R. B., "Hydrogenation of Carbon Monoxide and Carbon Dioxide on Supported Ruthenium Catalysts at Moderate Pressures," I & EC Product Res. Develop. **3**, 265-269 (1965) December.
10. Kirk, R. E. and Othmer, D. F., "Carbon Monoxide-Hydrogen Reactions," in Encyclopedia of Chemical Technology, 2nd Ed., Vol. **4**, 446-489. New York: Interscience Publishers, 1963.
11. Kul'kova, N. V. and Temkin, M. I., "Kinetics of the Reaction of Conversion of Carbon Monoxide by Water Vapor," Zh. Fiz. Khim. **23**, 695-713 (1949)[Chem. Abstr. **43**, 7308 (1949)].
12. Kul'kova, N. V., Kuznets, Z. D. and Temkin, M. I., "The Exchange of Oxygen Isotopes Between Carbon Monoxide and Carbon Dioxide on an Iron Oxide Catalyst," Dokl. Akad. Nauk SSSR **90**, 1067-70 (1953) [Chem. Abstr. **49**, 8684 (1955)].
13. Lunde, P. J. and Kester, F. L., "Rates of Methane Formation from Carbon Dioxide and Hydrogen Over a Ruthenium Catalyst," J. Catal. **30**, 423-429 (1973) September.
14. Oki, S. and Mezaki, R., "Identification of Rate-Controlling Steps for the Water-Gas Shift Reaction Over an Iron Oxide Catalyst," J. Phys. Chem. **77**, 447-452 (1973) February 15.
15. Oki, S. and Mezaki, R. "Mechanistic Structure of the Water-Gas Shift Reaction in the Vicinity of Chemical Equilibrium," J. Phys. Chem. **77**, 1601-1605 (1973) June 15.
16. Wagman, D. D. et al., "Heats, Free Energies, and Equilibrium Constants of Some Reactions Involving O₂, H₂, H₂O, C, CO, CO₂, and CH₄." RP 1634, J. Res. Nat. Bur. Stand. **34**, 143-161 (1945).
17. Wagner, C., "Adsorbed Atomic Species as Intermediates in Heterogeneous Catalysis," in D. D. Eley, et al., Eds., Advances in Catalysis and Related Subjects, Vol. **21**, 323-81. New York: Academic Press, 1970.

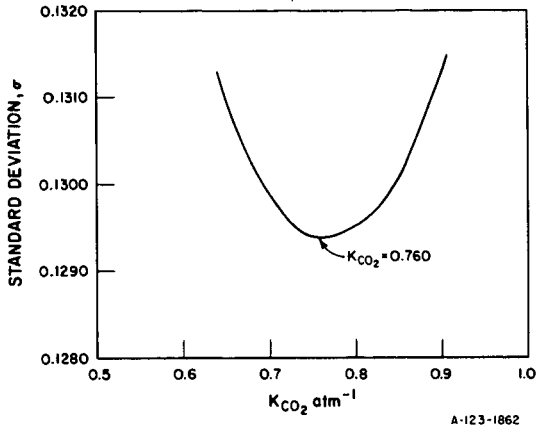


Figure 1. DETERMINATION OF CO_2 ADSORPTION CONSTANT USING EQUATION 15, MECHANISM I

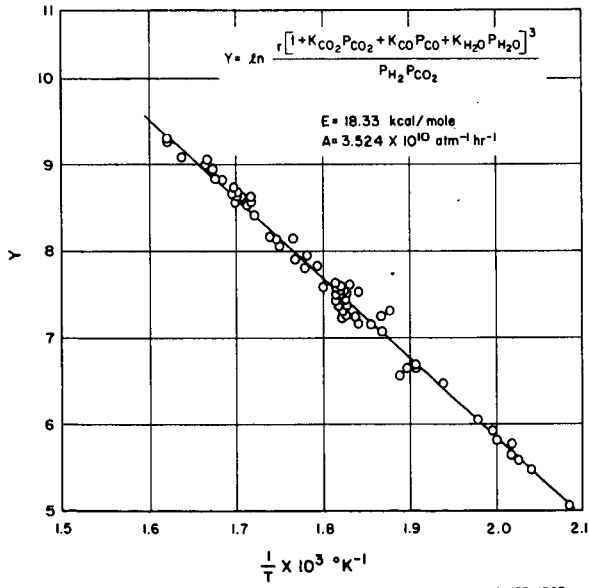


Figure 2. ACTIVATION-ENERGY PLOT OF 62 DATA POINTS

Active Sites for Coal Hydrogenation

Kanjiro Matsuura, David M. Bodily and Wendell H. Wiser

Mining, Metallurgical and Fuels Engineering
University of Utah
Salt Lake City, Utah 84112

INTRODUCTION

The development of new catalyst systems and the understanding of reaction mechanisms are of utmost importance in the development of processes for converting coal to liquid and/or gaseous products. Mills (1) has recently reviewed some new catalytic concepts for the hydrogenation of coal. Among the affective catalysts are certain molten metal halides such as $ZnCl_2$ and $SnCl_4 \cdot 2H_2O$. In amounts comparable to the reactant they show hydrocracking activity for coal and polynuclear hydrocarbons (2). Although many workers have reported the use of molten salts as hydrocracking catalysts, little work has been done on the mechanism of the reactions. It is well known that these metal halides are Lewis acid type catalysts and have fairly good catalytic activity for most Friedel-Crafts reactions. Zielke et al (2) suggested that the active catalyst for the hydrocracking of polynuclear hydrocarbons may be the acid produced by the interaction of zinc chloride with water. On the other hand, when molten halides are used for coal hydrogenation, it has been suggested that they are easily decomposed in feedstocks which contain sufficient sulfur and are not the true catalysts. They are generally supposed to be partially converted to other forms such as the sulfide or oxide during the hydrocracking reaction (3).

In a previous report (4), we presented some unusual results on the dehydrogenation of 2-pentanol over several molten halide catalysts impregnated on coal. The halides, which were first heat-treated up to 400°C in a flow of N_2 , gave a high selectivity for the conversion of 2-pentanol to 2-pentanone due to the dehydrogenation reaction. It was concluded that the acidity of the halides in the solid form was very low after the heat-treatment. Thus, the role of Lewis acidity in catalysis by metal halides appears to be still open to controversy, especially when the halides are impregnated on coal.

The object of this work is to obtain a basic understanding of the catalytic behavior of molten metal halides before and after their impregnation on coal. This would give us a means of elucidating the catalytic action of the halides in the coal hydrogenation reaction.

EXPERIMENTAL

Reagent grade $ZnCl_2$, $SnCl_4 \cdot 2H_2O$ and $FeCl_3 \cdot 6H_2O$ were used without purification. The halides were impregnated on Hiawatha, Utah coal (45% V.M., d.a.f. basis) from aqueous solution. In some cases, activated charcoal (AC) was used as a catalyst support for impregnation. Pretreatment was carried out overnight in a N_2 stream.

The total acidity was determined by back titration of n-butyl amine with hydrochloric acid. Basicity was also determined by back titration of benzoic acid with sodium hydroxide.

The conversion reaction of 2-pentanol was carried out continuously over fixed-bed catalysts under atmospheric pressure. The product was sampled periodically using a dry ice-methanol trap, and analyzed on a 5-ft Carbowax 20M gas chromatographic column with a flame ionization detector. The selectivity to 2-pentanone was determined as the moles of 2-pentanone produced per mole of 2-pentanol re-

acted, multiplied by 100.

Hydrogen adsorption measurements were made on one gram samples with a standard BET system. Hydrogen was introduced into the system at the initial pressure of 180-505 torr and the decrease in the pressure was recorded as a function of time.

The surface area was determined from carbon dioxide adsorption at 298°K. The Dubinin-Polanyi equation was used to calculate surface areas as described by Marsh and Sigmieniewska (5). The molecular area of carbon dioxide at 298°K was taken as 25.3 Å² (6). Nitrogen adsorption at -195°C was also carried out to obtain micro-pore surface areas.

RESULTS AND DISCUSSION

The effect of heat treatment on acidity and basicity is shown in Table I.

Table I. Surface Acidity and Basicity

Sample	Preheating temp., °C	Acidity mmol/g	Basicity mmol/g
23.1% ZnCl ₂ /coal	130	0.73	0
"	200	0.40	0
"	300	0.07	0
"	400	0.05	0
23.1% SnCl ₂ /coal	400	0.08	0

The acidity of ZnCl₂ on coal substantially decreased with the increase of preheating temperature from 130 to 400°C. The amount of basic sites was zero in all cases, irrespective of pretreatment. The acidity is nearly completely lost by pretreatment at the 400°C. Since the metal halides melt below some pretreatment temperatures, significant portions of the salt may have vaporized in the N₂ stream.

The loss of acidity on pretreatment is supported by the dehydrogenation/dehydration reaction of 2-pentanol. It is well known that relatively weak acids catalyze the dehydration of some alcohols. Accordingly, if almost all of the halides are left unchanged as acidic catalysts during the preheating process, the main products with this reaction would be olefins from dehydration rather than ketones from dehydrogenation. Table II shows the results of the activity of various molten metal halides supported on activated charcoal and coal. Activated charcoal was selected as a support because its surface acidity is too weak to catalyze the reaction under the experimental conditions. The three zinc halides and tin chloride showed conversions of 84.0 - 95.7% when supported on activated charcoal. The selectivity to 2-pentanone by dehydrogenation was about 30 to 49% for these samples. On the other hand, when the halides were impregnated on coal, they showed much higher selectivity to ketones. For FeCl₃, both conversion and selectivity were very low. As is generally expected, ZnO²⁺ which is believed to be a good catalyst for hydrogenation reactions, gave 100% selectivity with a low conversion, while NiSO₄, a strong acid, showed zero selectivity to ketone.

The results of the 2-pentanol conversion reaction together with those of the acidic and basic properties indicate that there is an interaction of the molten halides with the coal, resulting in the formation of a new effective sites for the

Table II. Catalytic Conversion of 2-Pentanol

Catalyst	Pretreatment temp., °C	Reaction temp., °C	Total conv. mol %	Selectivity to 2-pentanone mol %
ZnCl ₂ on AC	404	404	95.7	31.2
ZnBr ₂ on AC	404	404	85.2	35.3
ZnI ₂ on AC	410	410	84.0	48.7
SnCl ₂ on AC	300	300	84.5	30.2
ZnCl ₂ on coal	455	405	61.9	73.5
SnCl ₂ on coal	393	387	78.2	70.4
FeCl ₃ on coal	395	395	47.8	0
ZnCl ₂ on SiO ₂	466	369	99.0	0
NiSO ₄	404	301	99.0	0
SiO ₂	404	302	19.7	0
AC	355	307	0	0
coal	404	406	5	0

dehydrogenation of the alcohol. Among the most active molten halides are ZnCl₂ and SnCl₂, which have been reported to have a strong activity for the hydrogenation of coal at short reaction times (7). Ferric chloride is a less active catalyst for hydrogenation and shows no selectivity to ketone. This indicates that the hydrogenation activity is not always dependent upon the Lewis acidity of the catalyst as proposed by Zielke et al (2). Ferric chloride is a much stronger Lewis acid than ZnCl₂ and tin chloride (8). It retains more of its acidic properties when impregnated on coal and heated, but is less effective as a hydrogenation catalyst. The possibility of basic sites being important must be rejected based on results shown in Table I.

Adsorption of H₂ on ZnCl₂, SnCl₂ and FeCl₃ impregnated on coal was measured at 200 to 415°C. Figure 1 shows typical results for hydrogen adsorption at 415°C and 505 torr. Although the slow adsorption process was detectable for several days with all samples, rapid initial adsorption was observed only with active hydrogenation catalysts. In some cases, the volume of hydrogen adsorbed amounts to 10-15 ml/g after 5 min. Original coal and FeCl₃ impregnated coal did not show any rapid adsorption under the experimental conditions. This may be important from the view point of active sites for hydrogenation. It was attempted to separate experimentally the fast and slow adsorption, as was done by Dent and Kokes (9). This work indicated that almost all of the chemisorbed hydrogen was not easily removed by degassing. The fast and slow chemisorption with the ZnCl₂ impregnated sample could not be separated. Hydrogen adsorption was markedly affected by pretreatment at 300-400°C.

It has been widely recognized that the determination of the surface areas of various coals is not straightforward. Recently, Marsh and Siemieniowska (5) proposed the use of Dubinin-Polanyi equation to calculate surface areas. The surface areas of various kinds of coals can be calculated using the equation from CO₂ adsorption data at 298°K in a conventional vacuum apparatus (6). Figure 2 shows some typical Dubinin-Polanyi plots for CO₂ adsorption at 298°K on several molten halides impregnated on coal. Excellent linear plots were obtained in all cases. Surface area results are summarized in Table III. When original coal, without any impregnation, was heat-treated in a stream of N₂ at 200° to 400°C, the surface area substantially increased to 415.8 m²/g. Once ZnCl₂ was impregnated on the coal, the surface area increased sharply with the heat temperature. Similar increases in

Table III. Surface Areas of Coal and Halide-impregnated Coals

Sample	Pretreatment temp., °C	Surface area, m ² /g	
		CO ₂ adsorption at 22°C	N ₂ adsorption at -195°C
Coal	200	170.6	1.3
	300	195.2	
	400	415.8	25.5
	1,000	109.2	25.5
ZnCl ₂ on coal (23.1%)	200	108.4	
	300	332.9	77.4
	400	581.3	432.1
SnCl ₂ on coal (23.1%)	400	557.1	317.1
FeCl ₃ on coal (23.1%)	400	471.6	206.5
ZnCl ₂ on AC	400		487.4
AC			711.5

surface area were observed with SnCl₂, but they were relatively smaller for FeCl₃. This trend of increases in surface area is in good agreement with measurements of N₂ adsorption at -195°C. This result shows that the heating of coal on which active halide hydrogenation catalysts are impregnated to 400°C, yields a much higher micropore surface area of ~ 580 m²/g. Micropores which are inaccessible for low-temperature adsorption in coals become accessible for impregnated coals. Less active FeCl₃ does not give such a sharp increase in surface area.

The nature of the active sites is as yet uncertain. A surface compound formed between the metal halide and the coal during heat treatment is thought to be responsible for the experimental observations. Lewis acidity may be important in forming this compound but is not the only requirement and does not play a role once the compound is formed. The hydrogen chemisorption properties indicate that these sites are also important in coal hydrogenation.

REFERENCES

- 1) Mills, G. A., *Ind. Eng. Chem.*, **61**, 6 (1969).
- 2) Zielke, C. W., Struck, R. T., Evans, J. M., Costanza, C. P., and Gorin, E., *Ind. Eng. Chem., Process Des. Develop.*, **5**, 151, 158 (1966).
- 3) Weller, S., "Catalysis", P. H. Emmett, ed., Chap. 7, Reinhold, New York, 1956.
- 4) Matsuura, K., Bodily, D. M., and Wiser, W. H., *Preprints Fuel Chem. Div., Am. Chem. Soc.*, **18**, No. 3, 227 (1973).
- 5) Marsh, M., and Siemieniowska, T., *Fuel*, **44**, 355 (1965).
- 6) Walker, P. L., Jr. and Patel, R. L., *Fuel*, **49**, 91 (1970).
- 7) Wood, R. E., and Hill, G. R., *Preprints Fuel Chem. Div., Am. Chem. Soc.*, **17**, No. 1, 28 (1972).

- 8) Cook, C., Can. J. Chem., 41, 522 (1963).
- 9) Dent, A. L., and Kokes, R. J., J. Phys. Chem., 73, 3772 (1969).

This research was sponsored by the Office of Coal Research on Contract No. 14-32-0001-1200.

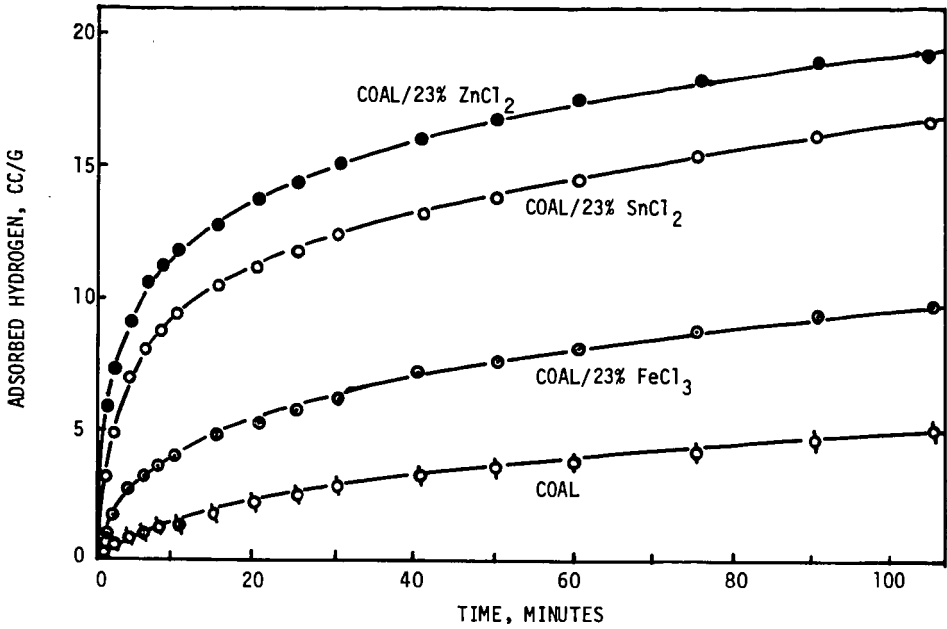
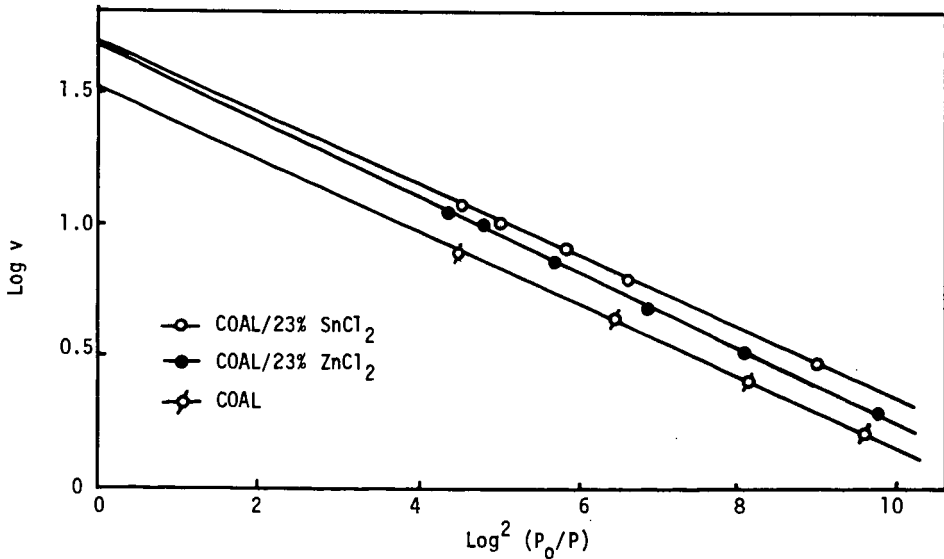


FIGURE 1. HYDROGEN ADSORPTION AT 415°C AND 505 TORR

FIGURE 2. DUBININ-POLANYI PLOTS FOR CO₂ ADSORPTION AT 298°K

Dehydrogenation of Coal by Metal Salt Catalysts

David M. Bodily, Sheldon H. D. Lee and Wendell H. Wiser

Mining, Metallurgical and Fuels Engineering
University of Utah
Salt Lake City, Utah 84112

INTRODUCTION

Coal is dehydrogenated below 400°C by a number of catalysts. Mazumdar et al¹⁻⁴ obtained up to 50% removal of hydrogen with sulfur, iodine and benzoquinone as catalysts. Reggel et al⁵⁻⁷ used palladium catalyst supported on CaCO₃ and phenanthridine solvent to dehydrogenate coals. The hydrogen is reported to originate primarily from the hydroaromatic portions of the coal. Mazumdar et al⁸ reported on the pyrolysis at 600°C of coal dehydrogenated by sulfur. The coals show an increased yield of char and a corresponding decrease in tar yields. Untreated coals show a dependence of tar yield on the fraction of hydroaromatic structures in the coals. The decreased tar yields in dehydrogenated coals was attributed to the destruction of hydroaromatic units during dehydrogenation. Other processes are probably involved, although the hydroaromatic groups may be the major source of hydrogen.

Zinc halides and stannous chloride are known to be effective coal hydrogenation catalysts. Their capacity to rapidly hydrogenate coal has stimulated the study of the mechanism of catalytic hydrogenation and of the properties of coal impregnated with metal salts. A previous report¹⁰ presented some pyrolysis results. Coals impregnated with zinc halides and stannous chloride were found to yield less hydrocarbon gases and tar during low-temperature pyrolysis. The possibility that the suppression of tar evolution was caused by destruction of hydroaromatic groups lead to the present study of the dehydrogenation of coal by zinc chloride.

EXPERIMENTAL

Hiawatha, Utah coal was impregnated with zinc chloride as previously described¹⁰. The analysis of Hiawatha coal is shown in Table I.

Table I. Analysis of Hiawatha Coal

% Ash	4.1	% C	79.5
% V. M.	43.1	% H	5.2
% F. C.	52.8	% N	1.6
Heating value	14,100 Btu/lb.	% S	0.6
		% O	13.4
		% O (difference)	13.1

Six gram samples were heated at 5°C/min under a nitrogen flow. Evolved gases were sampled at 50°C intervals and analyzed by gas chromatography. Hydrogen was determined using argon carrier gas, a molecular sieve column and a thermal conductivity detector operating at 25°C and low bridge currents. Hydrocarbon gases were removed prior to analysis with a liquid nitrogen trap. This method does not give quantitative yields of hydrogen but only relative yields.

Coal and impregnated coal samples were dehydrogenated by palladium after the method of Reggel et al⁵⁻⁷. One quarter gram of coal, 0.3 grams of catalyst (1% Pd) and 3.5 grams of phenanthridine were refluxed at 345°C for 12 hours. The

volume of evolved gas was measured and the gases analyzed to determine the yield of hydrogen.

RESULTS AND DISCUSSION

The weight loss and hydrogen evolution during pyrolysis of coal and coal impregnated with 12% by weight $ZnCl_2$, are shown in Figure 1. The coal shows hydrogen evolution occurring above 300°C, with a maximum at about 600°C. In the presence of $ZnCl_2$, the initial hydrogen evolution is shifted to 200°C and two maxima appear. Significant amounts of molecular hydrogen are evolved below 400°C while the evolution of hydrogen at higher temperatures is unaffected. The impregnated coal also shows a decrease in weight loss above 400°C compared to the unimpregnated coal.

Results from the catalytic dehydrogenation with Pd are shown in Table II.

Table II. Dehydrogenation with Palladium Catalyst

Sample	H_2 evolved ml/gm ² coal at STP	% H_2 evolved
Hiawatha coal	311	44.0
12% $ZnCl_2$ /H coal	356	50.4
12% $ZnCl_2$ /H coal (without Pd catalyst)	243	34.4
200°C Residue from pyrolysis of 12% $ZnCl_2$ /H coal	353	50.0
400°C Residue from pyrolysis of H coal	140	--
400°C Residue from pyrolysis of 12% $ZnCl_2$ /coal	281	--

Hiawatha coal shows dehydrogenation to the extent of 311 cc/g, corresponding to 44.0% of the original hydrogen. When impregnated with 12% $ZnCl_2$, the coal shows additional dehydrogenation, while the impregnated coal shows significant dehydrogenation under the experimental conditions without Pd present. An impregnated coal heated to 200°C and then cooled prior to dehydrogenation shows no difference from an unheated sample. This is to be expected since pyrolysis results show no affect below 200°C. An impregnated coal heated to 400°C prior to dehydrogenation shows less hydrogen evolution than an unheated sample, but significantly more than an unimpregnated coal heated under the same conditions.

Palladium is thought to be a specific catalyst for the dehydration of hydroaromatic groups. The hydroaromatic groups in coal are evolved as tar or otherwise destroyed during the early stages of pyrolysis. The coal sample heated to 400°C shows only about 45% as much hydrogen available for removal by Pd as compared to an unheated coal. When hydroaromatic structures in coal are removed prior to heating, the yield of tar is decreased. These experiments indicate that $ZnCl_2$ has the property of dehydrogenating coal below 400°C. The catalytic dehydrogenation experiments with Pd indicate that some of the hydrogen comes from hydroaromatic groups in the coal. An impregnated sample heated to 400°C is altered in such a way that tar yields at temperatures above 400°C are reduced, but the sample still contains nearly all the hydrogen that can be removed with Pd catalyst. The same behavior on pyrolysis is noted with coals impregnated with $ZnBr_2$, ZnI_2 and $SnCl_2 \cdot 2H_2O$, all of which show catalytic hydrogenation ability. A comparison of

metal chlorides and metal sulfates, indicates little dehydrogenation activity by the sulfates although some sulfates are reported to be good coal hydrogenation catalysts in longer-residence-time reactors.

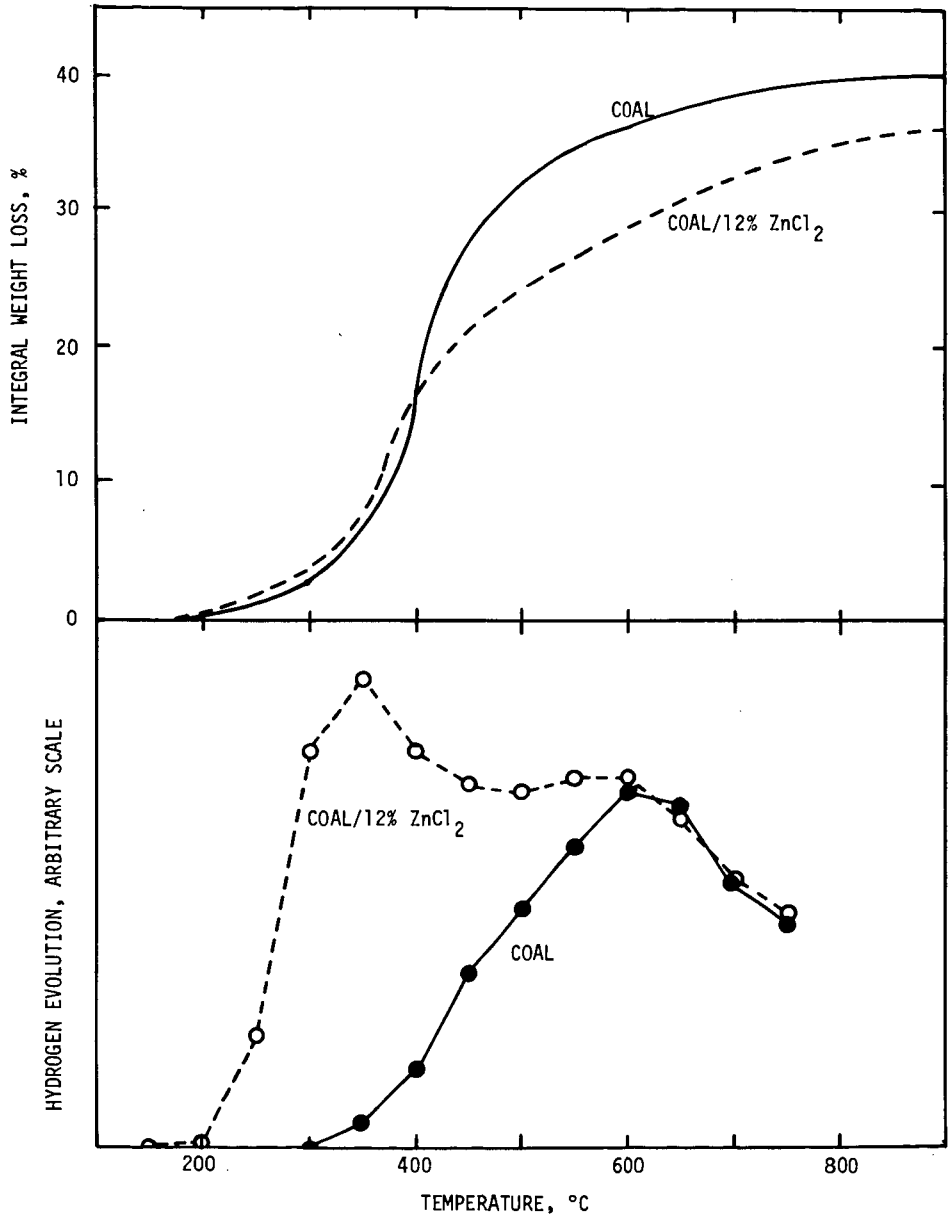
The mechanism of catalytic dehydrogenation of coal by $ZnCl_2$ is not clear. The mechanism is different than in the case of dehydrogenation with sulfur since molecular hydrogen is produced. No solvent is required for dehydrogenation with $ZnCl_2$. Zinc chloride is altered when impregnated on coal surfaces and heated. The nature of the compound formed between coal and $ZnCl_2$ and the mechanism of reaction are being studied.

REFERENCES

1. Mazumdar, B. K., Choudhury, S. S., Chakrabartty, S. K., and Lahiri, A., J. Sci. Ind. Res., 17B, 509 (1958).
2. Mazumdar, B. K., Choudhury, S. S., and Lahiri, A., Fuel, 39, 179 (1960).
3. Mazumdar, B. K., Bhattacharyya, A. C., Ganguly, S., and Lahiri, A., Fuel, 41, 105 (1962).
4. Mazumdar, B. K., Chakrabartty, S. K., De, N. G., Ganguly, S., and Lahiri, A., Fuel, 41, 121 (1962).
5. Reggel, L., Wender, I., and Raymond, R., Fuel, 47, 373 (1968).
6. Reggel, L., Wender, I., and Raymond, R., Fuel, 50, 152 (1971).
7. Reggel, L., Wender, I., and Raymond, R., Fuel, 52, 162 (1973).
8. Mazumdar, B. K., Chakrabartty, S. K., and Lahiri, A., Fuel, 3B, 112 (1959).
9. Wood, R. E., Anderson, L. L., and Hill, G. R., Colorado School Mines Quart., 65, 201 (1970).
10. Bodily, D. M., Lee, H., and Hill, G. R., Fuel Chem. Division Preprints, Am. Chem. Soc., 16, 124 (1972).
11. Matsuura, K., Bodily, D. M., and Wiser, W. H., to be presented at the 167th National Meeting, Am. Chem. Soc., Los Angeles, April 1974.

This research was sponsored by the Office of Coal Research on Contract No. 14-32-0001-1200.

FIGURE 1. WEIGHT LOSS AND HYDROGEN EVOLUTION DURING PYROLYSIS OF HIAWATHA COAL AND HIAWATHA COAL IMPREGNATED WITH 12% $ZnCl_2$.



REMOVAL OF SULFUR FROM COAL
BY TREATMENT WITH HYDROGEN

J. H. Gary, R. M. Baldwin, C. Y. Bao, R. L. Bain,
M. S. Kirchner, and J. O. Golden

Chemical and Petroleum-Refining Engineering Dept.
Colorado School of Mines
Golden, Colorado 80401

This study was performed with the financial support of the Office of Coal Research (Contract No. 14-32-0001-1225), United States Department of the Interior; the State of Colorado; and the Office of Research Services, Colorado School of Mines.

ABSTRACT

The Colorado School of Mines is performing a research contract under the sponsorship of the Office of Coal Research, the State of Colorado, and the Office of Research Services of the Colorado School of Mines to determine the importance of operating variables and raw material properties upon coal desulfurization via the solvent refining process.

The solvent refining process is being studied in bench scale, high-pressure, high-temperature, rocking-bomb autoclave batch reactors. The liquid product from the reactor is vacuum distilled to give a solvent refined coal and the refined coal product is analyzed for sulfate, pyritic, and total sulfur content, with organic sulfur content being determined by difference. Initially five variables were studied; temperature, partial pressure of hydrogen, solvent-to-coal ratio, solvent type, and reaction time. The reaction time was determined to be statistically unimportant; and anthracene was shown to be the better solvent. Further experimental work has been completed to investigate the three remaining operating variables. Statistical analysis of experimental data is now being performed to investigate the non-linearity of sulfur removal from coal as influenced by the operating variables.

ACKNOWLEDGMENTS

The authors gratefully acknowledge the assistance of the following students in conducting a portion of this investigation: Mr. Steve Barker, Mr. Jeff Handwerk, Mr. Russ Lambert, Miss Dana Light, Mr. Richard Long, Miss Carol Payne, Miss Leonila Quintanilla, and Mr. S. Rao. Dr. Dean Dickerhoof, of the Colorado School of Mines Chemistry Department, has contributed many valuable suggestions concerning the chemical analysis of the various forms of sulfur. Professor William Astle, of the Colorado School of Mines Mathematics Department, contributed significantly to the statistical analysis of the experimental data. The personnel of the Pittsburgh and Midway Coal Mining Company (Merriam, Kansas) were very helpful in discussing several aspects of the coal desulfurization problem. In particular, Mr. W. C. Bull, Dr. C. H. Wright, and Mr. R. E. Perrussel, offered a number of valuable suggestions regarding the total experimental program.

The authors also gratefully acknowledge the financial support of the following agencies in conducting this investigation:

- 1) The Office of Coal Research, United States Department of the Interior
- 2) The State of Colorado
- 3) The Office of Research Services, Colorado School of Mines.

BACKGROUND

The Colorado School of Mines is currently engaged in a three year, three-phase research program to study coal desulfurization via the solvent refining process. The importance of operating variables and raw material properties is being investigated to ascertain their influence on the degree of desulfurization.

Bench-scale, high-pressure, high-temperature rocking bomb autoclave batch reactors are being used to study the solvent refining process. Coal of a specific size fraction (-28 mesh) is mixed with an organic solvent and charged to the reaction bomb. The coal-solvent slurry is agitated and brought to reaction temperature under a hydrogen blanket. After a 15 minute time interval at the reaction conditions, the bomb is pulled and the reaction quenched by rapid cooling. The liquid product (including undissolved ash) is then charged to a distillation flask and vacuum distilled to recover the solvent and a solid coal product, at a maximum temperature of 300°C and an ultimate absolute pressure of 3 mm of mercury. The refined coal product is analyzed for sulfate, pyritic and total sulfur content, with organic sulfur content being determined by the difference between total sulfur and inorganic (sulfate + pyritic) sulfur content. Recovered solvent is analyzed for total sulfur content by induction furnace techniques and for hydrogen content by infra-red spectroscopy.

Phase I (first year effort) studied, in a statistically designed experiment, the importance of five operating variables. These variables were studied at two levels, as listed below:

- 1) Temperature: 325, 400°C
- 2) Partial pressure of hydrogen (at reaction conditions):
600, 1200 psig
- 3) Solvent to coal ratio: 2/1, 3.5/1
- 4) Solvent type: Anthracene, tetralin
- 5) Reaction time: 7.5 minutes, 15 minutes

The results of the factorial analysis for significance showed temperature, pressure and solvent-to-coal ratio to be significant at the 90% confidence level. Anthracene oil was also shown to be a clearly superior solvent by the Phase I significance tests.

The operating variables chosen as significant from the Phase I experimental investigation are being further examined in Phase II (second year) of the research program. Phase II is examining the non-linearity of the removal of sulfur from coal via the solvent refining process as influenced by the operating variables.

The conditions chosen from the Phase I study for the Phase II study were as follows:

- 1) Temperature: 375, 400, 425°C
- 2) Partial pressure of hydrogen (at reaction conditions):
1000, 1500, 2000 psig
- 3) Solvent-to-coal ratio: 2/1, 3/1, 4/1

Anthracene oil, the better Phase I solvent, was chosen for use in the Phase II experimental program. The operating variables have been studied at three levels in a full-factorial, triply-replicated experimental design to gather the data necessary to perform the significance tests and construct a mathematical model for desulfurization of coal via the solvent refining process. Initial data reduction and significance testing of the variables has allowed significant linear and quadratic effects of the operating variables and interactions (through second order) to be identified in each of the four data sets (total sulfur, sulfate sulfur, pyritic sulfur, organic sulfur) for one bituminous and one sub-bituminous coal. The main effects and interactions will be used as independent variables in a mathematical model for the desulfurization of coal via the solvent refining technique.

LITERATURE SURVEYSolvent Refining Process

The Pott-Broche (1) process was developed in Germany for use in obtaining an ash-free product that could be readily hydrogenated to a liquid hydrocarbon. Ground coal was mixed with a middle oil in a 1:2 ratio and heated to 400-420°C at 100 atmospheres. The solution was filtered to remove ash and the solvent was recovered by vacuum distillation. Kloepper et al. (2) have carried out extensive research on the solvent refining process. The ash content of a raw coal was reduced from 12% to 0.2%, with a concurrent reduction in total sulfur content from 1.4% to 0.5%. The Pittsburgh and Midway Coal Mining Company (3,4,5,6) developed a solvent refining process that used an internally generated solvent and hydrogen to dissolve the coal and produce a low-ash, low-sulfur coal. Cudmore and Guyot (7) studied the solvent extraction of coal under a hydrogen blanket using anthracene oil as a solvent. The total sulfur content of a raw coal was reduced from 1.1% to 0.4% in a batch autoclave. Gary et al. (8) have studied the solvent refining process in batch autoclaves, using anthracene oil as the solvent, with the distribution of all sulfur types (total, organic, pyritic, sulfate) in the refined coal product being investigated.

Kirchner (9) studied solvent type, solvent-to-coal ratio and coal rank in a statistically designed set of experiments to determine the effects of these three variables on the removal of total sulfur, organic sulfur, and inorganic sulfur (sulfate and pyritic) from four raw coals. The analysis of the data showed both solvent type and coal rank to be statistically significant at the 0.95 confidence level for the removal of sulfur from coal.

Ferrall (10) also studied the desulfurization of coal in anthracene under a hydrogen blanket and found that pressure and temperature were significant variables in the process, but that reaction times in excess of 15 minutes were not statistically significant.

Desulfurization by Other Methods

The Atlantic Richfield Company (11) was granted a patent for a process which simultaneously desulfurizes and deashes coal. Total sulfur content was reduced by 54% and ash content by 27% by simply treating the coal in a batch reactor for one hour with water at 650°F and a pressure of 2350 psig. Flotation methods have been examined and developed by Miller and Baker (12), Galiguzov (13), Leonard and Cockrell (14) and Terchik (15). Deurbrouck (16) made an extensive computer study of the removal of pyritic sulfur by flotation. A carbonization process was used by Van Hoëssle and Quadri (17) to produce a smokeless fuel from sub-bituminous coal

and resulted in a 95% reduction of pyritic sulfur and 60-70% reduction on both organic and sulfate sulfur. Alkali metal hydroxides have been used by Murphy and Messman (18) in a patented process that reduces the total sulfur content of coal by 35-50%. A process has been patented by Lefrancois, Barclay and Van Hook (19), in which sulfur is leached from coal with a sodium carbonate melt. Nagy and Ezz (20) studied the thermal desulfurization of ultra-high sulfur-petroleum coke, while Sinha and Walker (21,22) carried out extensive research on the desulfurization of coals and chars using various gaseous atmospheres at temperatures ranging from 350 to 600°C.

Pyritic Sulfur Removal

Given and Jones (23) have found that some of the pyritic sulfur released is fixed in the organic matter of coal and contributes to the higher organic sulfur content of the treated coal. This observation agreed with results reported by Smith (24). Hydrogen contacting was used by McKinley and Henke (25) in a patented process achieving a 53% sulfur removal on a coal with high pyritic sulfur content. Blum and Cindea (26) optimized an air-stream fluidized process and reported removal of up to 90-95% of the pyritic sulfur. Abel et al. (27) used a centrifugal-electrostatic method with stage grinding and removed 50-70% of pyritic sulfur and 30-40% total sulfur. Nearly 90% of the pyritic sulfur was removed from a Pittsburgh seam roof coal with this technique. Meyers et al. (28) achieved a 40-70% sulfur reduction on coal by treatment with a ferric ion solution. The pyritic sulfur in the coal matrix was oxidized and elemental sulfur and iron sulfate were recovered. A subsequent patent was issued to Meyers (29). Further work on the Meyers process has been done by Hamersma et al. (30).

Organic Sulfur Removal

A U.S. patent was granted to Mayland (31) for a pebble heated gasification unit. Mayland observed that a major portion of the organic sulfur in the coal was converted to H₂S during the process. Mukai and his co-workers (32) reported that they removed 100% of the organic sulfur from a bituminous coal by treating at room temperature with a 3% solution of hydrogen peroxide. Meyers, Laud, and Flegal (33) investigated several coals, and found that leaching with a weak organic acid would remove 45-80% of the organic sulfur. Phenyl-nitrate was the most efficient solvent tested for organic sulfur removal and a patent was later issued to Meyers (34). Organic sulfur removal from coal has also been investigated by Kawinskii (35).

Catalyst Application

Winkler (36) found that an activated iron powder catalyst used on finely ground bituminous coal in a hot, highly aromatic oil can

reduce the coal's total sulfur content by 56%. A French patent was granted to Fohlen (37), who lists catalysts capable of splitting organic sulfur linkages prior to desulfurization. These catalysts include the oxides and salts of calcium, magnesium, lead, copper, zinc, and molybdenum. Manmohan and Goswami (38) found that sodium chloride gave 80% total sulfur removal during carbonization. Depolymerization catalysts for coal have been studied by Ouchi, Imuta, and Yamashita (39).

Kinetic Considerations

The kinetic studies of the dissolution of bituminous coal in tetralin by Hill (40) have shown that the ΔH (heat of activation) and ΔS (entropy of activation) can be determined from the temperature dependence of the rate. Kloepper et al. (2) concluded the transfer of hydrogen from the solvent phase was the most important mechanism of free radical termination for the dissolved coal. Formation of low molecular weight compounds during the dissolution of coal at high temperatures was favored by using a solvent which transfers hydrogen or by having available a highly active hydrogen atmosphere during the reaction. The amount of coal in solution increased markedly with an increase in the partial pressure of hydrogen in a batch autoclave system. Charlot (41) observed the dissolution process had an average activation energy of 7 kcal/mole.

Non-isothermal reaction kinetics have been used in the study of coal gasification and desulfurization by Juntgen et al. (42), and Vestal and Johnson (43). Hill (40) studied the dissolution of coal in tetralin solvent, and proposed a multiple reaction scheme that involves a series of first order reactions and increasingly active intermediates as chemical bonds are broken at high temperatures.

Effect of Hydrogen

Blackwood and McCarthy (44) considered the reaction of coal and hydrogen to be a two-stage process, with the first step being very rapid hydrogenation of the oxygen-containing functional groups of the coal, followed by a slow reaction between the hydrogen and residual char. The hydrogen in the process served two purposes: to saturate the solvent used, and to form H_2S with sulfur compounds present. Curran et al. (45) found that very little hydrogen transfer was necessary to dissolve the first 50% of the coal but the amount of hydrogen required increased by a factor of seven for the next 50% of the coal. They proposed the dissolution was a pseudo-first order reaction.

Cudmore and Guyot (7), in their study of the dissolution of coal in anthracene oil, noted the overall heat of combustion of the products exceeds the heat of combustion of the reactants. Kloepper et al. (2) also found the solvent refined coal to have a heating value 20% higher than that of the parent coal. Kloepper

et al. (2) attributed this effect to the loss of oxygen and sulfur atoms from the coal matrix during the treatment, which left polynuclear aromatic products in the solvent-refined coal product. These compounds have very high resonance energies, and therefore a high heat of combustion. This conclusion is supported by Cudmore and Guyot (7), who observed an enrichment in polycyclic aromatic compounds in their solvent refined product and a corresponding increase in the heating value of the treated coal.

Hydrogenation of coal in tetralin solvent has been studied by Potzieter (46), and Liebeberg and Potzieter (47). Kirk and Seitzer (48) studied the hydrogenation process at 750-840°F and 2500 psig, with a liquid product resulting.

Choice of Organic Solvent

Orechkin (49) found the presence of hydrogen in the reaction atmosphere is not always required for an effective extraction. Solvents of sufficiently high hydrogen content may effectively dissolve the coal; however, the average molecular weight of the product is high due to the fact that hydrogen required to reduce the coal to low molecular weight compounds is supplied entirely by the solvent and this quantity is limited by the solvent characteristics, especially the degree of unsaturation.

STATISTICAL THEORY

The goal of the Phase II experimental investigation was to examine the non-linearity of coal desulfurization via the solvent refining process, as a function of the operating variables found to be important in the Phase I experimental program. Phase I investigated five operating variables at two levels, and a full factorial experimental design was completed to allow all main effects and interactions to be statistically examined for importance. Four coals were studied, two bituminous and two sub-bituminous with sulfur contents ranging from 0.76% to 4.20%. Variables and levels studied were as follows:

- 1) Temperature: 325, 400°C
- 2) Partial pressure of hydrogen: 600, 1200 psi
- 3) Solvent-to-coal ratio: 3/1, 4.5/1
- 4) Solvent type: Anthracene, tetralin
- 5) Time (at reaction temperature): 7.5, 15 minutes

The statistical reduction of the Phase I data was accomplished by Yates' technique, and the sum of the four and five-factor interactions was lumped to give an estimate of the error mean square. "F" tests were then performed on the mean squares for the main effects and interactions (through order 3), and the following results were obtained:

I. Variables Very Highly Significant (99% confidence level)

- A. Bituminous
 1. Solvent type
 2. Temperature
- B. Sub-bituminous
 1. Solvent type
 2. Temperature

II. Variable Highly Significant (95% confidence level)

- A. Bituminous
 1. Solvent type
 2. Temperature
- B. Sub-bituminous
 1. Solvent type
 2. Temperature
 3. Solvent type/temperature interaction

III. Variables Significant (90% confidence level)

- A. Bituminous
 - 1. Solvent type
 - 2. Temperature
 - 3. Solvent type/temperature interaction
- B. Sub-bituminous
 - 1. Solvent type
 - 2. Temperature
 - 3. Solvent type/temperature interaction
 - 4. Solvent-to-coal ratio
 - 5. Pressure

Accordingly, the solvent type for the Phase II study was fixed as anthracene oil (the better Phase I solvent) and the variables temperature, pressure and solvent-to-coal ratio were chosen for further investigation in the non-linearity studies of Phase II.

The Phase II non-linearity studies consisted of two major parts, the first being a re-examination of the significance of the three process variables chosen for study, and the second being mathematical modeling of the process based on the results of the Phase II significance tests. A full-factorial, triply-replicated experimental design of the three variables at three levels allowed all the necessary data to be gathered for the significance testing and mathematical modeling. The design was applied to one bituminous and one sub-bituminous coal. Variables and levels chosen were as follows:

- 1) Temperature: 375, 400, 425°C
- 2) Partial pressure of hydrogen (at reaction temperature): 1000, 1500, 2000 psi
- 3) Solvent-to-coal ratio: 2/1, 3/1, 4/1

The data from the Phase II experimental design were initially reduced by hypothesis testing, and outliers were identified and rejected from the data field. An analysis of variance on the experimental design was then performed by means of constructing comparisons from a table of orthogonal polynomials. A Fortran computer program allowed the data and the orthogonal polynomials to be manipulated, and the sum of squares of each main effect and interaction (through second order) to be calculated. An estimate of the mean square error was then obtained from the sum of squares within treatments, and "F" tests allowed the significance levels for the main effects and interactions to be identified for each data set. Data sets collected from the Phase II study were as follows:

- A. Bituminous Coal
1. Sulfate sulfur
 2. Pyritic sulfur
 3. Organic sulfur
 4. Total sulfur
- B. Sub-bituminous Coal
1. Sulfate sulfur
 2. Pyritic sulfur
 3. Organic sulfur
 4. Total sulfur

Mathematical modeling of the solvent refining process will next be attempted using the main effects and interactions found to be important in the significance tests as the independent variables for the model. The Omnitab computing programs will be used to fit the data by means of multiple linear regression, and models and terms will be accepted or rejected based on the significance of the regression coefficients and the goodness of fit as indicated by the multiple correlation coefficient. Models of the following form will be investigated:

$$Y_1 = \alpha_1 + \beta_1 X_1^{m_1} + \gamma_1 X_2^{m_2} + \dots + \zeta_1 X_n^{m_n}$$

where Y_1 = sulfur removal, %, dependent variable

$\alpha_1, \beta_1, \gamma_1, \dots, \zeta_1$ = regression coefficients

X_1, X_2, \dots, X_n = independent variables and interactions from significant tests

m_1, m_2, \dots, m_n = exponents of the effects and interactions

Equipment

Four major equipment systems were employed in the study, the reactor system, the off-gas scrubber system, the solvent recovery system, and the LECO total sulfur analysis system. A brief description of the components of each system is given below.

Three reactor systems were used in the study, all of the batch autoclave generic type. For each reactor system, a gas delivery system, a reaction vessel, and a shaking assembly existed as a functional part of the experimental complex. The reaction vessels were manufactured by the American Instrument Company (Aminco) of Silver Spring, Maryland, and were from the 4 3/8 inch series. The reaction vessels had inside depths of 10 inches, inside diameters of 3 5/16 inches and approximate weights of 50 pounds. The vessels had a working pressure rating of 5,050 psi at 100°F and had effective volumes of approximately 1410 milliliters.

Three shaking assemblies were employed in the reactor complex. Two of the assemblies were standard Aminco 4 3/8 inch series assemblies while the other was manufactured by High Pressure Equipment Company, Inc. The shaking assembly from HIP Company of Erie, Pennsylvania, consisted of a 6,000 watt, 208-volt heating jacket mounted on a rocker assembly. The heating jacket was rocked by means of a 1/3 hp, 220 volt electric motor actuating an eccentric lever drive connected to the heating jacket. The Aminco shaking assemblies consisted of 3000 watt, 208-volt heating jackets mounted on rocker assemblies. The rockers for the Aminco shaking assemblies were actuated by 1/3 hp, 110 volt motors driving eccentric levers connected to the heating jackets. The low voltage heating jackets had the capacity to heat from room temperature to 400°C in approximately 1 1/2 hours while the high voltage HIP heating jacket could heat from room temperature to 400°C in about 2 1/4 hours. All shaking assemblies were equipped with 0 to 3000 psi pressure gauges; and 30,000 psi valves and fittings from the Aminco line were used to regulate the inlet and exit of the reaction gases from the reaction vessels. Tubing used on the shaking assemblies was 304 stainless steel, 1/4 inch o.d., and rated for operation at 100,000 psi at 100°F.

In the 6000-watt system the temperature was controlled by a Leeds and Northrup, Series 60 controller, with a Model 11906 SCR final control element. Temperature response of the reaction vessel was recorded on a Leeds and Northrup Speedomax H continuous recorder. In the 3000-watt systems, Leeds and Northrup Electromax III controllers, with Model 11906 SCR final control elements were used for temperature control. Temperatures were recorded on a Honeywell Elektronik III two-channel continuous recorder.

All shaking assemblies were connected to purging-charging gas delivery systems. Each of these systems consisted of a nitrogen cylinder, a hydrogen gas cylinder, pressure regulators for each cylinder and Aminco stainless steel tubing and fittings similar to those used on the shaking assemblies.

A diagram of the off-gas collection system is given in Figure 1. A 0-3000 psig Duragauge pressure gauge was used to measure pressure. Reaction vessel temperature was measured by a Foxboro Dynalog 6-point circular recorder with a range of 0 to 400°C. Thermocouples used as temperature sensors were iron-constantan. The collection vessel was a 250-ml Erlenmeyer flask agitated by means of a magnetic stirrer. Gas volume was measured using water displacement in a 250-ml graduated buret.

The solvent recovery system used is shown in Figure 2. The distillation vessel was a 500-ml Hempel flask. The vessel was heated using a 330 watt, 115 volt heating mantle controlled with a Powerstat, a 110-volt and 7 1/2 amp variable transformer. Two 1000-ml flasks were used to trap the reclaimed solvent. A condenser was used to prevent any low boiling solvent fractions from

FIGURE 1
SCRUBBER COLLECTING SET-UP

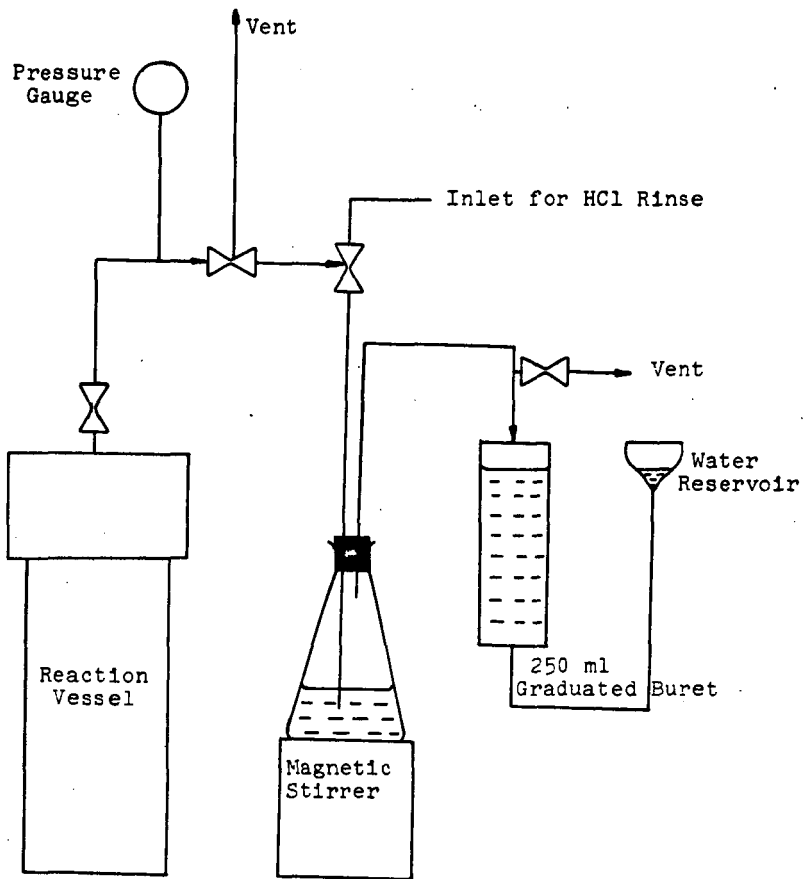
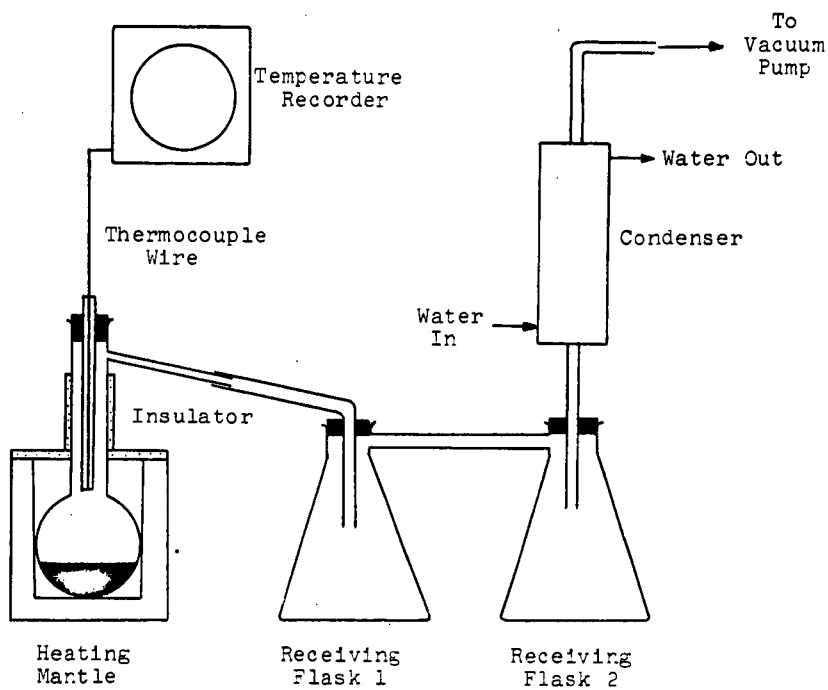


FIGURE 2
SOLVENT RECOVERY SYSTEM



leaving the distillation system and entering the vacuum pump. The vacuum for the system was supplied by a Cenco Mega-Vac pump driven by a 1/4 hp, 110 volt electric motor. The vacuum on the system was measured with a 0 to 30 in. Hg Duragauge vacuum gauge. The temperature of the distillation flask was continuously monitored by a Foxboro Dynalog 6-point circular chart recorder. Iron-constantan type thermocouples were used for the input to the recorder.

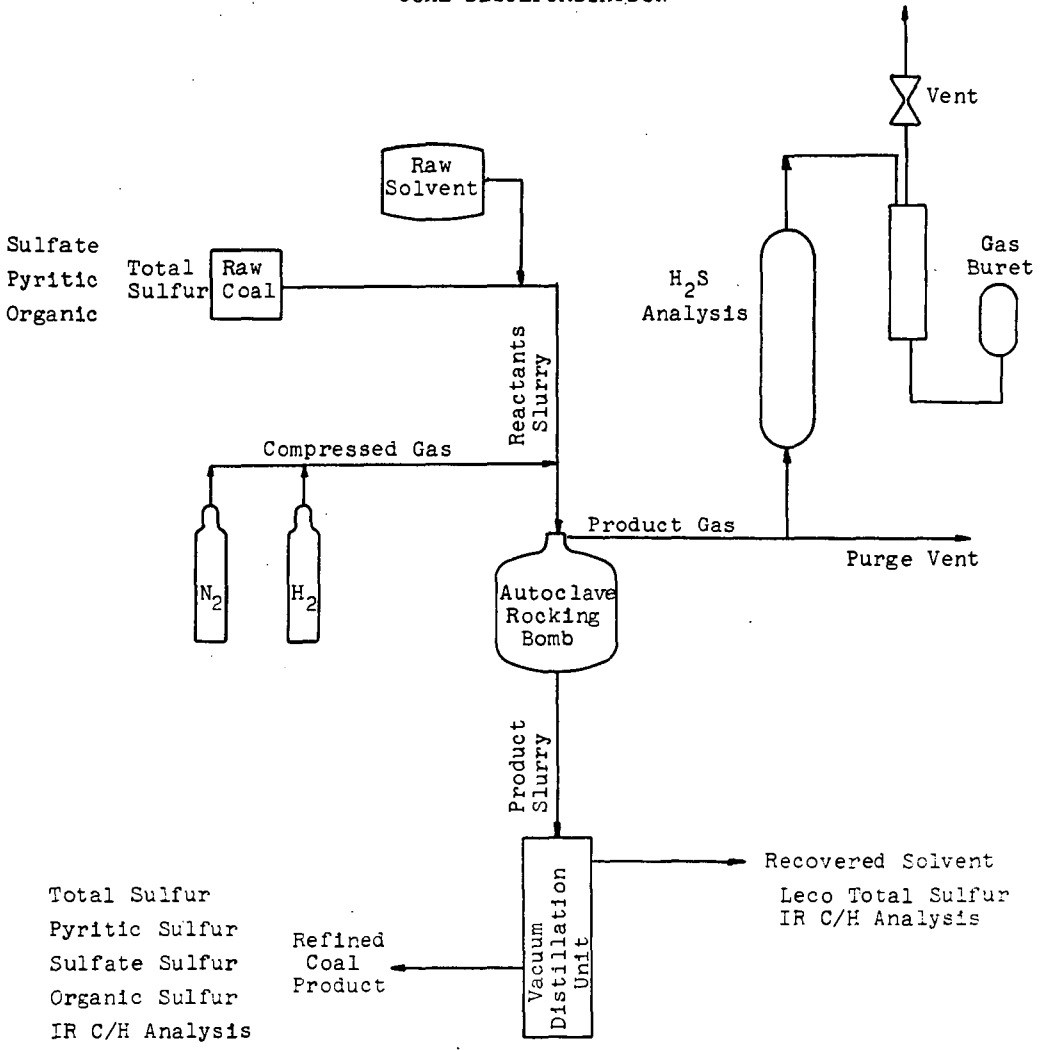
The Leco total sulfur analysis system consisted of three components, a gas purification train, an induction furnace, and a semi-automatic titrator unit. The gas purifying train contained an acid tower, a dry reagent tower, and a rotameter and was used to measure and scrub any residual sulfur from the entering oxygen. The induction furnace was a Leco model 521, equipped with the "L" modification on the combustion chamber. A special feature of the "L" modification is the inclusion of a high temperature igniter in the combustion chamber. The exhaust gases from the induction furnace combustion chamber were sent through an electrically heated glass delivery tube and into the Leco semi-automatic titrator model 518. The semi-automatic titrator used an idiometric reaction with a color change endpoint to analyze the combustion gases. The titrator proved to be a rapid and reliable method for analyzing the solvent for total sulfur.

Experimental Procedure

An overall view of the experimental procedure, including stages at which sulfur analyses are performed, is given by Figure 3. The experimental procedure can be divided into four major areas of discussion: sulfur analysis, desulfurization procedure, off-gas collection, and solvent recovery. The desulfurization procedure is given below.

- a) Fifty grams of raw dried coal, -28 mesh, and the appropriate amount of solvent (100, 150, or 200 grams of anthracene oil) are weighed, mixed, and placed in the reaction vessel.
- b) The reaction vessel is sealed and connected into the heating-rocking assembly.
- c) The reaction vessel is purged with nitrogen by pressurizing the system to 200 psig and venting to atmospheric pressure three consecutive times. After purging, the system is pressurized with hydrogen; the initial pressure is predetermined and is a function of run temperature, run pressure, compressibility factors, and initial temperature. At this time initial pressure and temperature are recorded, and the system is checked for leaks.

FIGURE 3
 SOLVENT REFINING PROCESS FLOWSHEET
 COAL DESULFURIZATION



- d) The temperature recorder, control system, rocker assembly, and the reactor heaters are switched on and heating begins. When the system reaches the desired maximum temperature, the pressure of the reaction vessel is recorded. The reactor is held at the maximum temperature for 15 minutes; at this time the system temperature and pressure are again recorded.
- e) The reaction vessel, still pressurized, is removed from the heating-rocking system and cooled by forced convection.

The off-gas collection step is given by the following procedure:

- a) The pressurized reaction vessel is connected to the scrubber system (see Figure 1).
- b) Reaction vessel temperature and pressure, ambient temperature, and barometric pressure are recorded. Four gas samples are bubbled through the scrubber solution, an ammonical zinc sulfate solution. The volume of gas is determined by water displacement.
- c) The reaction vessel is vented and disconnected from the scrubber system.

A diagram of the solvent recovery system is given by Figure 2. The solvent recovery technique utilized vacuum distillation to separate the anthracene oil from the solvent refined coal product.

- a) The product-solvent slurry is removed from the reaction vessel, placed in a 500-ml Hempel distillation flask, and weighed.
- b) The flask is placed in the heating mantle, and connected to the vacuum system.
- c) The heating mantle is turned on and the system is heated.
- d) At approximately 150°C the vacuum pump is turned on and a vacuum is slowly drawn.
- e) The distillation is completed at approximately 300°C and 3 mm Hg pressure.
- f) The solvent recovered in the receiving flasks is removed for weighing.
- g) The solvent refined coal product is taken from the flask, weighed, crushed, and placed in a sealed sample bottle for further use.

The following analysis techniques were used for sulfur determination:

- I. Total sulfur - Eschka method ASTM D 271 - 68
- II. Inorganic sulfur
 - A. Pyritic - ASTM D 2492 - 68
 - B. Sulfate - ASTM D 2492 - 68
- III. Organic - Difference (I - II)
- IV. H₂S - An adaptation of ASTM D 2385 - 66 as developed by Pittsburgh and Midway Coal Mining Co., Merriam, Kansas
- V. Solvent sulfur content - LECO method ASTM D 1552 - 64.

RESULTS

A Fortran-IV computer program has been written to perform the analysis of variance (ANOVA) calculations described in the statistical analysis section. Table I presents the results from the ANOVA study performed on the Phase II experimental results.

For both the bituminous and sub-bituminous coal, the pyritic sulfur analysis and the sulfate sulfur analysis showed none of the effects studied to be significant. This result indicates that within the limits of variation of the three variables, temperature, pressure, and solvent to coal ratio, no trend in sulfate sulfur or pyritic sulfur removal could be statistically determined as a function of these operating variables. The results do not indicate that there was no removal of pyritic or sulfate sulfur. For example, initial calculations for the bituminous coal show maximum pyritic sulfur removal to be approximately 70 percent.

The ANOVA calculations for total sulfur removal in the bituminous coal showed the following effects to be significant at a 90% confidence level: the linear temperature effect; the linear temperature, quadratic pressure interaction effect; and the linear temperature, quadratic pressure, and linear solvent-to-coal ratio interaction. These interactions were also shown to be significant for the ANOVA calculations for the bituminous coal organic sulfur removal. Since no effects were significant for the pyritic and sulfate sulfur; and the organic sulfur removal is determined by the difference in total sulfur removal and pyritic plus sulfate sulfur removal, the covariance between the total sulfur removal and organic sulfur removal is statistically correct and expected.

The ANOVA calculations for the total sulfur removal in the sub-bituminous coal showed the following effects to be significant at a 90% confidence level: the linear temperature, quadratic pressure interaction; and the linear temperature, quadratic pressure, and linear solvent-to-coal ratio interaction. For the organic sulfur removal only the linear temperature, quadratic pressure interaction was shown to be significant. These results are also statistically expected.

Further results will be presented after the mathematic modeling work is completed.

TABLE I

Phase II Results - Effects Significant in ANOVA Calculations

where: T = Temperature
 P = Pressure
 S = Solvent to Coal Ratio
 L = Linear Effect of Variable
 Q = Quadratic Effect of Variable

Sulfur Type	Effect	Significant @		
		90% F(90%)=2.805 1,54	95% F(95%)=4.026 1,54	99% F(99%)=7.148 1,54
Bituminous Coal				
Total Sulfur	T_L	Yes	No	No
	$T_L P_Q$	Yes	Yes	No
	$T_L P_Q S_L$	Yes	No	No
Sulfate Sulfur	None			
Pyritic Sulfur	None			
Organic Sulfur	T_L	Yes	No	No
	$T_L P_Q$	Yes	Yes	No
	$T_L P_Q S_L$	Yes	No	No
Sub-Bituminous Coal				
Total Sulfur	$T_L P_Q$	Yes	Yes	Yes
	$T_L P_Q S_L$	Yes	No	No
Sulfate	None			
Pyritic	None			
Organic	$T_L P_Q$	Yes	No	No

REFERENCES CITED

1. Lowry, H. H., and Rose, H. J., Pott-Broche coal extraction process and plant of Ruhrol G.M.B.H., Bottrop-Welheim, Germany: U.S. Bureau of Mines I.C. 7420, 1947.
2. Kloepper, D. L., Rogers, T. F., Wright, C. H., and Bull, W. C., Solvent processing of coal to produce a deashed product: U.S. Department of Interior, Office of Coal Research, Research and Development Report no. 9, 1965.
3. Pittsburgh and Midway Coal Mining Co., Economic evaluation of a process to produce ashless, low-sulfur fuel from coal: U.S. Dept. of Interior, Office of Coal Research, R. and D. report no. 53, Interim report no. 1, 1970.
4. _____ Development of a process for producing an ashless, low-sulfur fuel from coal - Design of pilot plant: U.S. Dept. of Interior, Office of Coal Research, R. and D. report no. 53, Interim report no. 2, 1971.
5. _____ Development of a process for producing an ashless, low-sulfur fuel from coal - Volume I - Engineering Studies, Part II, C.O.G. Refinery Economic Evaluation, Phase I: U.S. Dept. of Interior, Office of Coal Research, R. and D. report no. 53, Interim report no. 3, 1971.
6. Pittsburgh and Midway Coal Mining Co., Development of a process for producing an ashless, low-sulfur fuel from coal - Volume I - Engineering Studies, Part 3, C.O.G. Refinery Economic Evaluation - Phase II: U.S. Dept. of Interior, Office of Coal Research, R. and D. report no. 53, Interim report no. 4, 1972.
7. Cudmore, J. F., and Guyot, R. E., Solvent extraction of coal, batch autoclave studies: Australian Coal Industry Research Laboratories, Ltd., P.R. 67-6, 1967.
8. Gary, J. H., Baldwin, R. M., Eao, C. Y., Kirchner, M. S., Golden, J. O., Removal of sulfur from coal by treatment with hydrogen - Phase I: The effect of operating variables and raw material properties: Office of Coal Research, R. and D. report no. 77, Interim report no. 1, 1973.
9. Kirchner, M. S., The effects of solvent to coal ratio solvent type, and coal rank on coal desulfurization by hydrogen treatment: Unpublished M.S. Thesis, Arthur Lakes Library, Colorado School of Mines, Golden, Colorado, 1973.
10. Ferrall, J. F., Desulfurization by hydrogenation of coal in solution: Unpublished M.S. Thesis, Arthur Lakes Library, Colorado School of Mines, Golden, Colorado, 1972.

11. Rieve, R. W., Coal upgrading: U.S. Patent 3,660,054, 1972.
12. Miller, K. J., and Baker, A. F., Removal of pyrite from coal by froth flotation: U.S. Natl. Tech. Inform. Serv., P. B. rep. no. 208015, 1972.
13. Galiguzov, N. S., Laws governing the behavior of coal pyrite in flotation and practical directions for desulfurization of coal by flotation: Obogashch. Britket. Uglei, no. 17, 59-68, 1961.
14. Leonard, J. W., and Cockrell, C. F., Pyritic sulfur removal from coal: Mining Congr. J., v. 56, no. 12, 65-70, 1970.
15. Terchik, A. A., Sulfur reduction through improved coal washing practices: Mining Congr. J., v. 57, no. 7, 48-55, 1971.
16. Deurbrouck, A. W., Sulfur reduction potential of the coals of the United States: Bureau of Mines Report of Investigation no. 7633, 1972.
17. Van Hoessle, H. H., and Quadri, S. A. A., Upgrading and desulfurization of West Pakistan coals: Pakistan Jour. Science Ind. Res., no. 5, 119-123, 1962.
18. Murphy, R. M., and Messman, H. C., Desulfurization of carbonaceous materials: U.S. Patent 3,387,941, 1968.
19. Lefrancois, P. A., Barclay, K. M., and Van Hook, J. P., Recovery of sulfur values from sulfur-bearing carbonaceous materials: U.S. Patent 3,567,377, 1971.
20. Nagy, E. K., and Ezz, A. F., Thermal desulfurization of ultra-high-sulfur petroleum coke: Fuel, v. 52, 128, 1973.
21. Sinha, R. K., and Walker, P. J. Jr., Removal of sulfur from coal by air oxidation at 350-450°C: v. 51, 1972.
22. Sinha, R. K., and Walker, P. L. Jr., Desulfurization of coals and chars by treatment in various atmospheres between 400 and 600°C: Fuel, v. 51, 329-331, 1972.
23. Given, P. H., and Jones, J. R., Attempted removal of sulfur from coal and coke: ACS, Division of Fuel Chemistry, Preprints, v. 8, no. 3, 185-191, 1964.
24. Smith, G. A., The effects of heat and pressure on the sulfur compounds in coal: Jour. Chem. Mett. Mining Soc., South Africa, no. 42, 149-168, 1941.
25. McKinley, J. B., and Henke, A. M., Desulfurization of coal: U.S. Patent 2,726,148, 1955.

26. Blum, I., and Cindea-Munteau, V., Desulfurization of coals at low temperatures by gaseous desulfurization agents: Acad. Rep. Populace Rimine, Inst. Energet., Studii Cercetari Energet., v. 11, 325-343, 1961.
27. Abel, W. T., Zulkoaki, M., and Gaurtlett, G. J., Dry separation of pyrite from coal: Industrial Energy Engineering, v. 11, no. 3, 342-347, 1972.
28. Meyers, R. A., Hauiersma, J. W., Laud, J. S., and Kraft, M. L., Desulfurization of coal: Science, v. 177, 1187-1188, 1972.
29. Meyers, R. A., Pyritic sulfur removal from coal using a solution containing Fe^{+++} : Ger. Offen. 2,207,491, 1972.
30. Hamersma, J. W., Kraft, M. L., Koutsoukos, E. P., and Meyers, R. A., Chemical removal of pyritic sulfur from coal: Am. Chem. Soc., Div. of Fuel Chem., Preprint, vol. 17, no. 2, 1-14, 1972.
31. Mayland, B. J., Pebble heater adapted to coal gasification: U.S. Patent 2,657,501, 1953.
32. Mukai, S., Araki, Y., Konishi, M., and Otomura, K., Desulfurization of coal with some oxidizing agents: Nenryo Kyohai-shi, v. 48, no. 512, 905-910, 1969.
33. Meyers, R. A., Laud, J. D., and Flegal, C. A., Chemical removal of nitrogen and sulfur from coal: U.S. Natl. Tech. Inform. Serv., v. 72, no. 3, 189, 1972.
34. Meyers, R. A., Solvent extraction of organic sulfur and nitrogen compounds from coal: Ger. Offen. 2,108,786, 1971.
35. Kawinski, V. S., Removal of organic sulfur from coals: Khim. Tverd. Topl., v. 4, 143-5, 1972.
36. Winkler, J., Desulfurization of coal-oil mixtures by attrition grinding with activated iron powder: ACS, Division of Fuel Chemistry, Preprints, v. 12, no. 4, 19-28, 1968.
37. Fohlen, J. L., Desulfurization of coal-distillation products: French Patent 853,404, 1940.
38. Manmohan, R., and Goswami, M. N., Actions of different catalysts on desulfurization of Assam coal: Science and Culture, v. 19, 151-152, 1953.
39. Ouchi, K., Imuta, K., and Yamashita, Y., Catalysts for the depolymerization of mature coals: Fuel, v. 52, 156-157, 1973.

40. Hill, G. R., Experimental energies and entropies of activation - Their significance in reaction mechanism and rate prediction for bituminous coal dissolution: Fuel, v. 45, no. 4, 329-340, 1966.
41. Charlot, L. A., The kinetics of thermal dissolution of a Utah bituminous coal: M.S. thesis, U. of Utah, 1963.
42. Juntgen, H., Van Heek, K. H., and Klein, J., Comparative investigations into the kinetics of gasification with steam or hydrogen and conclusions for gasifier design: Gordon Research Conference on Coal Science, New Hampton School, New Hampton, New Hampshire, July 1973.
43. Vestal, M. L., and Johnson, W. H., Chemistry and kinetics of the hydrodesulfurization of coal: Am. Chem. Soc., Div. of Fuel Chem., Preprint, v. 14, no. 1, 1-11, 1970.
44. Blackwood, J. D., and McCarthy, D. J., The mechanism of hydrogenation of coal to methane: Australian Jour. of Chemistry, ch. 19, 797-813, 1966.
45. Curran, G. P., Struck, R. T., and Gorin, E., The mechanism of hydrogen transfer process to coal and coal extract: Symposium on Pyrolysis Reactions of Fossil Fuels, Pittsburgh, Penn., ACS, v. 10, no. 2, 1966.
46. Potzieter, H. G. J., Kinetics of conversion of tetralin during hydrogenation of coal: Fuel, v. 52, 134, 1973.
47. Liebeberg, B. J., and Potzieter, H. G. J., The uncatalysed hydrogenation of coal: Fuel, v. 52, 134, 1973.
48. Kirk, M. C. Jr., and Seitzer, W. H., Coal hydrogenation process: U.S. Patent 3,594,303, 1971.
49. Orechkin, D. B., On the role of reduction processes in the early stages of the thermal decomposition of coal: Akad. Nauk. SSSR, Trudy Vostochno-Sibirskogs Filiala, Seriya Khimicheskaya, v. 3, 105-126, 1955.

Evaluation of Catalysts for Hydrodesulfurization and Liquefaction of Coal

Walter Kawa, Sam Friedman, W. R. K. Wu, L. V. Frank, and P. M. YavorskyU.S. Department of the Interior
Bureau of Mines, 4800 Forbes Avenue
Pittsburgh, Pennsylvania 15213

INTRODUCTION

A novel process called the Synthoil process is being developed by the Bureau of Mines for converting coals into low-sulfur nonpolluting fuel oil by hydrodesulfurization (HDS). Development of the process to commercial scale would provide electric power plants with clean fuel derived from abundant high-sulfur coals presently unacceptable as fuels because of air quality standards.

In the Synthoil process, coal slurried in recycle oil is transported by a high-velocity, turbulent-flow of hydrogen through a reactor containing a fixed-bed of pelleted catalyst (1).¹ The coal reacts with hydrogen and probably with hydrogen donor compounds and is rapidly liquefied and desulfurized in a single stage. Reactions occur in the liquid phase, but the mixture also includes a gas phase and both organic and inorganic solid phases. High turbulence in the reactor serves to minimize the influence of interparticle mass transfer on reaction rates, while short reaction times and the moderate temperatures used tend to keep hydrogen consumption at a minimum.

Much work has been done recently on catalysts for coal hydroliquefaction and desulfurization, particularly on catalysts used in an ebullated or highly fluidized state. However, most of the work has been proprietary and there are no published data that would assist researchers in the selection of the best existing catalysts or guide the way to the design of new catalysts. This study was undertaken to provide a basis for selecting the best catalyst for use in the Synthoil process. Catalysts were prepared by impregnating commercial supports with compounds of metals known to be active in coal hydrogenation. These and a number of commercial HDS catalysts were then tested in a batch nonflow reactor to evaluate compositions and physical properties with regard to activities for coal conversion to oil and sulfur removal.

EXPERIMENTAL

Hydrogenation Feed Stocks

Pittsburgh-seam high-volatile A bituminous (hvab) coal from the Bureau's experimental mine at Bruceton, Pennsylvania was used in most hydrogenation tests of catalyst activities. One test was made with Indiana #5 hvbb coal. Both coals were pulverized to minus 60 mesh, and the hvab coal was dried in air at 70° C for 20 hours prior to use. As shown in table 1, sulfur contents of the coals were 1.1 and 3.5 percent by weight for the hvab and hvbb coals, respectively. About 60 percent of the sulfur in both coals was organic.

Also shown in table 1 are analyses of topped high-temperature coal tar used as a vehicle oil in hydrogenation experiments. The tar was produced in a commercial slot-type coke oven and consisted of about 15 percent by weight of material insoluble in benzene and 85 percent of benzene-soluble oil (asphaltene plus pentane-soluble oil).

¹ Underlined numbers in parentheses refer to the list of references at the end of this report.

Catalyst Descriptions and Preparation

Screening tests were made with five commercial catalysts and with 74 catalysts prepared by impregnating 17 commercial supports with compounds of Mo, Sn, Ni, Co, and Fe both singly and in combination. In addition, one catalyst was prepared by impregnating Sn on a commercial Co-Mo catalyst.

Descriptions of all catalysts used are given in table 2. Most of the support analyses are manufacturer's data whereas most of the surface areas and pore volumes listed were determined at this laboratory. Surface areas were measured by the BET method using low-temperature nitrogen. Pore volumes of supports were determined by a water retention method, and pore volumes of commercial catalysts were determined by low-temperature adsorption of nitrogen. Pores measured by these methods have diameters above 10 to 14 Å. Average pore diameters were calculated from pore volume and surface area data by determining the diameter of a cylinder having the indicated volume and area. Physical properties of impregnated catalysts listed in table 2 are values for supports before addition of metallic hydrogenation components.

Commercial catalysts tested included two Co-Mo and two Ni-Mo catalysts on alumina supports. A fifth commercial catalyst consisted of Fe on alumina. All had high surface areas and relatively small pores.

Support materials were selected so as to cover wide ranges of compositions, areas, and pore volumes in order to evaluate these properties. Alumina contents were 3.1 to 99.3 percent and silica contents were 0.1 to 96.0 percent. Three contained silicon carbide as the principal component. The supports could be classified as either high-surface area (55 to 425 m²/g) or low-surface area (0.04 to 1.23 m²/g) materials.

Metal compounds used in impregnations were (NH₄Mo₇O₂₄·4H₂O, SnCl₂·2H₂O, Ni(NO₃)₂·6H₂O, Co(NO₃)₂·6H₂O, and FeSO₄·7H₂O. When impregnating a single component, the required amount of metal compound was dissolved in a solvent, and the solution was added dropwise to 200 to 300 g of predried support while stirring constantly under a nitrogen atmosphere. Mo, Ni, Co, and Fe compounds were dissolved in water while stannous chloride was dissolved in aqueous ethanol. Solution volumes equalled support pore volumes plus a several percent excess to allow for handling losses. An impregnation was completed by drying the catalyst to constant weight at 70° C under nitrogen.

Co-Mo catalysts 78, 79, 80, 81, and 82 were prepared by the same single impregnation method using a solution containing both Co and Mo. Following impregnation, catalysts 79 and 81 were calcined in air at 600° C for about 8 hours.

Sn and Mo in catalysts 83 and 84 were impregnated stepwise. In preparing 83, the procedure consisted of adding ammonium molybdate and drying, then adding stannous chloride in aqueous ethanol and re-drying. Catalyst 84 was prepared by a three-step procedure. One-third of the Sn in dilute aqueous HCl and one-third of the Mo in water were combined and added to the support. After drying, the procedure was repeated two more times.

All catalysts except 2 and 10 were presulfided in the batch hydrogenation reactor (before charging with coal and vehicle oil) for 4 hours at 260° C with a gaseous mixture that initially was composed of 15 percent H₂S and 85 percent H₂. Sulfiding of single component catalysts averaged more than 90 percent of amounts needed to form MoS₂, SnS, NiS, CoS, and FeS. The average for multi-component catalysts was more than 75 percent. Actual forms of metal sulfides were not determined.

Hydrogenation Equipment and Procedures

The hydrogenation reactor was a 1.2-liter batch autoclave that was placed in a horizontal position and rotated during an experiment. A detailed description of the vessel and accessory equipment has been published (2).

Charges were contained in a glass liner that fitted closely to the autoclave wall. The charge in most experiments was 50 g of coal, 75 g of tar, and 50 cc of catalyst. A constant catalyst volume was used so that the fluidity of the catalyst-reactant mixture and, hence, the degree of mixing would be nearly the same in all experiments. In addition, catalyst external surface areas would not differ greatly. The amount of catalyst 2 charged was 25 cc, and in experiments with catalysts 79 and 81, charges consisted of 25 g of coal, 37.5 g of tar and 25 cc of catalyst.

After charging, the autoclave was purged of air and pressurized to about 1,900 psi with electrolytic hydrogen from commercial cylinders. Hydrogen charge weights which averaged 9.8 g were determined from prior calibrations of hydrogen weight vs charge pressure for the autoclaves used. Rotation was started and the autoclave was heated to 400° C in about 55 minutes. Pressure increased to about 4,000 psi. After 30 minutes at 400° C, the autoclave was cooled to room temperature at a somewhat slower rate.

Gases were depressurized, scrubbed to remove CO₂ and H₂S, metered and analyzed. Light oil and water were then removed by vacuum distillation to about 110° C and 2 to 3 mm of Hg. Solids and higher-boiling liquids remaining in the autoclave were washed out with benzene and separated by hot benzene extraction into insoluble and soluble fractions. Insolubles were further separated by screening into a fraction of fines consisting mostly of coal- and tar-derived solids and a fraction consisting of pellets of used catalyst. Fines included small but undetermined amounts of catalyst, while the pellets contained coal- and tar-derived solids in their pores in amounts up to about 15 percent depending on the porosity of the catalyst. Benzene solubles were separated into fractions insoluble and soluble in n-pentane. Both fractions of solids and all organic liquid fractions were analyzed for sulfur. The weight of organic benzene insolubles in the fines was calculated as the difference between the weights of the fines and ash in the fines. An estimate of the weight of organic benzene insolubles in used catalyst pellets was made on the basis of the carbon and hydrogen content of the pellets.

An autoclave was weighed on a bullion balance to within + 0.1 g before charging with hydrogen, after depressurizing, and after vacuum distilling. From these weighings and known weights of all materials charged, accurate weights for groups of products were determined as follows: (1) Gases and vapors depressurized, (2) vacuum distillate, and (3) solids and heavy liquids. Actual recoveries were adjusted (normalized) to correspond to the weights of these groups of products by assuming that losses (or gains) in each group of products were distributed among the components of that group in the same proportions as actual recoveries. Adjustments made to normalize recoveries averaged about 2 percent of the total charge.

In the hydrogenation data shown in table 3, product distributions are expressed as weight-percent of moisture- and ash-free (maf) charge. Organic benzene insolubles are the sum of organic insolubles in the fines and in the used catalyst. Asphaltene is oil soluble in benzene but insoluble in pentane. The pentane-soluble oil in table 3 includes pentane-soluble oil recovered in the benzene extraction step and light oil recovered by vacuum distillation, while benzene-soluble oil is the sum of asphaltene and pentane-soluble oil. Conversion of organic benzene insolubles is the difference between organic benzene insolubles charged (maf coal plus insolubles in the tar) and organic benzene insolubles recovered expressed as percent of organic benzene insolubles charged.

Results for seven of the experiments listed in table 3 are average values of duplicate tests. Average differences in yields of benzene-soluble oil in these duplicates was 2.3 percent and the sulfur contents of the oils differed by an average of 0.04 percent.

RESULTS AND DISCUSSION

Of primary interest in hydrogenation tests were catalyst activities for coal liquefaction as measured by oil production and for desulfurization as indicated by the sulfur content of the product oil. The total amount of sulfur removed was the preferred indicator of desulfurization activity but total sulfur removal from coal and tar could not be determined accurately. Coal- and tar-derived solids and the used catalyst both contained sulfur and it was not possible to clearly distinguish between the two. Coal conversions were not reported but can be estimated from the hydrogenation results shown in table 3 by assuming there was no conversion of insolubles in the tar. This assumption is probably justifiable for most experiments by results of batch experiments made with tar and an active Co-Mo catalyst in the absence of coal at 4,000 psi and 425° C. Conversions of insolubles were negligible.

The mild conditions used in this study (30 minutes at 400° C) were chosen so that moderate levels of liquefaction and desulfurization would be obtained with good catalysts, and consequently higher as well as lower activities of other catalysts could be readily discerned.

The feed composition provided one of the base comparison points needed for evaluation of hydrogenation results. When Pittsburgh coal was used, the maf feed contained 52 percent benzene-soluble oil (hereafter called oil) that originated with the tar used as vehicle oil. This oil contained 0.56 percent sulfur, while the total maf feed contained 0.64 percent sulfur.

As shown by the hydrogenation results of the first experiment in table 3, some HDS occurs without an added catalyst. The oil yield of 60 percent represented a net production of 8 percent, and the oil contained 0.06 percent less sulfur than oil in the feed. Total sulfur removal was 24 percent. These results provided a second set of base data for comparison purposes.

Commercial Catalysts

The most effective pelleted catalyst tested based on activities for both oil production and desulfurization was catalyst No. 1, a silica-promoted Co-Mo on alumina (Harschaw 0402T).² Oil containing 0.15 percent sulfur was produced in a yield of 80 percent. Estimated coal conversion was 78 percent. After these results were obtained, the objective in developing new catalysts became one of trying to get results superior to those obtained with 0402T. Catalyst 0402T has been used in all recent Synthoil pilot plant experiments. Catalyst 2 consisted of 25 cc of 0402T or half the standard charge. The experiment with catalyst 2 showed that there was a response to a change in catalyst concentration between 25 and 50 cc and indicates that 50 cc probably does not constitute an excess of catalyst.

The effect of presulfiding 0402T can be seen by comparing results with catalyst 1 and catalyst 3 which was not presulfided. Catalyst 3 was considerably less effective and, hence, presulfiding is clearly desirable in batch tests. Apparently in-situ activation does not occur quickly enough to reach maximum activity in a batch reactor where only the initial activity can be tested. In continuous flow experiments with a fixed bed of catalyst, presulfiding was found to be detrimental to steady state catalyst activity (3).

² Reference to specific brands of materials is made for identification only and does not imply endorsement by the Bureau of Mines.

Catalyst 4 consisted of Co-Mo 0402T pulverized to minus 200 mesh before presulfiding. The use of smaller catalyst particles resulted in increased sulfur removal and a small but possibly insignificant increase in oil production. This effect of a decrease in catalyst particle size indicates the desulfurization reaction is retarded or possibly controlled by intraparticle diffusion. This result is entirely reasonable in view of the numerous instances of diffusion retardation reported in HDS studies of high-molecular weight petroleum fractions (4). It was found, for example, that in the HDS of residual oils in an ebullating bed reactor, decreasing the size of catalyst particles increased the rate of desulfurization (5). However, the use of small catalyst particles to lessen diffusion retardation in a fixed-bed reactor such as is used in the Synthoil process would be impractical because of the resultant higher pressure drop across the bed and the increased risk of flow and temperature control problems.

An experiment was made with catalyst 0402T (No. 5 in table 3) to determine its effectiveness for HDS of a high-sulfur coal--Indiana #5 hvbb coal containing 3.4 percent sulfur. The catalyst proved to be highly effective for liquefaction and desulfurization in the batch reactor, and later was found to be very effective in the HDS of the same coal in a continuous-flow fixed-bed reactor (6).

Commercial HDS catalysts 6 (Co-Mo), 7 (Ni-Mo), and 8 (Ni-Mo) were as effective as catalyst 0402T for desulfurization, but catalyst 0402T produced 12 percent more oil than catalyst 6, and 3 percent more than the Ni-Mo catalysts. Even though the Ni-Mo catalysts were somewhat less effective than catalyst 0402T in these batch tests, final selection of one for use in a large scale Synthoil plant would depend on their aging and regeneration characteristics. Catalyst 9 (Fe on alumina) was moderately active for oil production but ineffective for sulfur removal.

High-Surface Area Impregnated Catalysts

Supports for catalysts 10 through 30 were three high-surface area aluminas containing small amounts of silica. The test with catalyst 10, which consisted of UOP alumina without an added hydrogenation component, showed that high-surface area alumina has no activity. Results were virtually the same as in the experiment with coal and tar alone (first experiment in table 3). In experiments with 5 percent Mo, Sn, Ni, Co, or Fe impregnated on these aluminas, there were no differences in results that were clearly attributable to the support properties shown in table 2. The results did show that when these metals are used as single components on high area aluminas, Mo is the best catalyst for sulfur removal and Sn is the best catalyst for the conversion of coal to oil. Fairly high oil yields were also obtained with Mo and Ni.

Mo and Sn concentrations were investigated with catalysts 11-16, 20, and 21 using 1, 5, and 10 percent on UOP and ALCOA H-151 aluminas. As the Mo concentration was increased, the desulfurization activity also increased but did not approach the activity of catalyst 0402T. Higher levels of desulfurization could probably be obtained with higher concentrations, but with 14 percent or more of Mo, complete coverage of the support surface with a monolayer of MoS_2 could occur with consequent loss of any catalytic contribution of the surface toward sulfur removal. Oil production increased with increasing Mo concentration to 5 percent, but a further increase was of no benefit. Sn catalysts were highly effective for oil production at all concentrations used, but desulfurization activities were poor and decreased as the Sn concentration increased. Supported Mo or Sn used as single components do not appear to be promising coal HDS catalyst candidates.

Catalysts 31 and 32 contained 5 percent Mo on silica-alumina supports that had the same composition but wide differences in surface areas (80 and 425 M^2/g) and some differences in pore volumes and average pore diameters. Hydrogenation results with

these catalysts were similar indicating little or no effect of their differences in physical properties. However, desulfurization activities of these silica-alumina-supported catalysts were lower than activities of alumina-supported catalysts containing 5 percent Mo.

Low-Surface Area Catalysts

Supports for catalysts 33-77 all had low surface areas. They had widely different compositions, pore volumes that ranged from 0.07 to 0.56 cc/g, and average pore diameters that were two to three orders of magnitude larger than those of the high-surface area supports. Whereas all high-surface area catalysts contained less than the amounts of metals needed for a monomolecular layer after sulfiding, the low-surface area catalysts (except for No. 42) contained metals in amounts that could provide from 50 to 1500 layers of metal sulfides. It is therefore likely that in experiments with the low-surface area catalysts, support surfaces were completely covered and had no catalytic or promotional effect on reactions.

Catalysts 33-41 contained 5 percent of impregnated metals. Although their desulfurization activities were very poor (catalyst 34 may be an exception), high oil yields of 80 to 84 percent were obtained with three of the catalysts. This is evidence that a high level of activity for oil production requires neither a high-surface area catalyst nor the availability of a support surface. On the other hand, the low levels of sulfur removal indicate that a high activity for desulfurization may require (in addition to the metal component surface) access to the support surface or a high area or both.

Catalysts 43-77 were impregnated with 1 percent of the metal components. Support combinations AELT-AEHT, SELT-SEHT, and CELT-CEHT were pairs having identical compositions but differing in areas and porosities. Comparisons of hydrogenation results with supports having the same compositions showed no consistent trends attributable to differences in areas or porosities. The most significant features of the experiments were the consistently high yields of oil obtained with Sn catalysts and the low average level of desulfurization with all metal components. Oil yields of 80 percent were obtained in two experiments with Sn catalysts. Thus, in addition to not requiring high surface areas, high metal concentrations are also not required for high coal conversions when Sn is used.

To determine whether the desulfurization activity of a low-surface area catalyst would increase if the support surface was not completely covered, catalyst 42 was prepared using less than 0.002 percent Mo. Fractional coverage of the surface of catalyst 42 was approximately equal to that of catalyst 12 containing 5 percent Mo on UOP alumina. Catalyst 42 was ineffective for oil production but was apparently more active for sulfur removal than catalyst 43 which contained 1 percent Mo on the same support. In fact the 0.36 percent sulfur in the oil was lower than the sulfur content of oil obtained with any low-surface area catalyst containing 1 percent of metal. This result strongly suggests that Mo-catalyzed desulfurization reactions of coal are promoted by the surface of an acidic support. The result is consistent with findings in several recent studies of the mechanism of HDS of thiophene compounds wherein it was reported that the reactions include steps occurring at acid sites on catalyst surfaces (4).

Multicomponent Catalysts

The effectiveness of UOP and H-151 aluminas as supports for Co-Mo catalysts was investigated with catalysts 78-81. These contained Co and Mo in the same percentages as catalyst No. 1 (0402T). Catalysts 78 and 80 were not calcined before sulfiding and were less active than catalyst 1. Catalysts 79 and 81 were calcined

before sulfiding but were otherwise identical to 78 and 80, respectively. Both of the calcined catalysts showed higher activities for oil production but only 79 showed improved desulfurization activity. Activities of 79 were virtually equal to those of catalyst 1 indicating that the UOP alumina is highly suitable as a support. Calcination is widely recognized as a beneficial activation step for HDS catalysts and is generally a part of commercial preparation procedures. Activity increases presumably are the results of improved dispersions of Co and Mo and interactions of Co, Mo, and the support that occur during calcination. Structural studies have indicated that Mo becomes distributed in a monolayer and that part of the Co is converted to a form comparable to that in CoAl_2O_4 . In a recent investigation using electron spin resonance spectra, it was reported that this form of Co persists even after sulfiding (7).

Catalyst 82, containing 2.4 percent Co and 10 percent Mo on a low-surface area support, was ineffective for coal liquefaction and only moderately active for desulfurization. Hydrogenation results with this catalyst showed that the amounts and proportion of Co and Mo used are not the only properties that determine the desulfurization activity of Co-Mo catalysts. The experiment provided additional evidence that a high surface area and accessibility of the support surface may also be important.

Catalysts 83 and 84 were prepared to investigate combinations of Sn and Mo, the best metal component for liquefaction and the best metal component for desulfurization when used singly. The support was a high-surface area alumina. Procedures used in preparing 83 and 84 differed but caused no significant differences in hydrogenation results. Both catalysts produced oil in the high yields obtained when Sn was used alone, but less sulfur was removed than when Mo was used alone. Catalysts 83 and 84 offered no overall advantage.

Catalyst 85 represented an attempt to increase the liquefaction activity of Co-Mo catalyst 0402T by addition of 5 percent Sn. The activity of catalyst 85 for oil production was equal to that of Sn when used alone, but the addition of Sn decreased the activity of catalyst 0402T for sulfur removal. Final assessment of the Sn-Co-Mo combination will require experimentation with other compositions and preparation procedures.

SUMMARY

Based on activities for both liquefaction and desulfurization of coal, the best catalyst tested in this batch study was a commercial high-surface area silica-promoted catalyst containing 2.4 percent Co and 10 percent Mo on an alumina support. This catalyst has been used in all recent experiments in the Bureau of Mines' Synthoil pilot plant. The increased desulfurization that resulted when this catalyst was pulverized indicated that the sulfur removal reactions were diffusion hindered.

Experiments with Mo, Sn, Ni, Co, and Fe impregnated as single components on high- and low-surface area supports showed that Mo catalysts were best for sulfur removal and Sn catalysts were best for conversion of coal to oil. Single component catalysts did not appear to be promising for combined liquefaction and desulfurization.

Maximum desulfurization activity apparently requires a high-surface area catalyst and results from a combination of the catalytic activity of supported metal components and the promotional effect of the support surface. High desulfurization activities were achieved only when less than a monolayer of metal component was deposited on the support. Even with a low-surface area support, the application of less than a monolayer increased the desulfurization activity.

A high surface area or high metal concentration is not essential for high conversions of coal to oil. High oil yields were obtained with several low-surface area catalysts, and, in the case of Sn, with only 1.0 percent of supported metal component.

Sn-Mo and Sn-Co-Mo combinations were not highly effective, but final assessment of these combinations will require further experimentation.

REFERENCES

1. Akhtar, Sayeed, Sam Friedman, and P. M. Yavorsky. Process for Hydrodesulfurization of Coal in a Turbulent-Flow Fixed-Bed Reactor. Paper presented at the 71st Nat. Meeting, AIChE, Dallas, Texas, Feb. 20-23, 1972. (Preprints available.)
2. Hawk, C. O., and R. W. Hiteshue. Hydrogenating Coal in the Batch Autoclave, BuMines Bull. 622, 1965, 42 pp.
3. Yavorsky, P. M., Sayeed Akhtar, and Sam Friedman. Process Developments: Fixed-Bed Catalysis of Coal to Fuel Oil. Paper presented at the 65th Annual Meeting, AIChE, New York, N.Y., Nov. 26-30, 1972. (Preprints available.)
4. Schuman, S. C., and Harold Shalit. Hydrodesulfurization, Catalysis Reviews, v. 4, No. 2, 1970, pp. 245-318.
5. Mounce, William, and R. S. Rubin. H-Oil Desulfurization of Residual Oil, 68th Nat. Meeting, AIChE, Houston, Texas, Feb. 28-March 4, 1971, Preprint 20a.
6. Akhtar, Sayeed, Sam Friedman, and P. M. Yavorsky. Low-Sulfur Fuel Oil From Coal, BuMines TPR #35, 1971, 11 pp.
7. Lo Jacono, M., J. L. Verbeek, and G. C. A. Schuit. Magnetic and Spectroscopic Investigations on Cobalt-Alumina and Cobalt-Molybdenum-Alumina, J. of Catalysis, v. 29, No. 3, June 1973, pp. 463-474.

TABLE 1.- Analyses of feed materials
Basis: percent by weight

Material	Pittsburgh- seam hvab coal	Indiana #5 hvbb coal	High- temp. coal tar
Proximate analysis, as received			
Moisture	0.5	6.1	0.0
Ash	6.0	8.9	0.04
Volatile matter	35.8	38.6	-
Fixed carbon	57.7	46.4	-
Ultimate analysis, moisture-free			
Ash	6.0	9.5	0.04
Hydrogen	5.2	4.9	4.9
Carbon	78.2	71.4	92.8
Nitrogen	1.5	1.5	1.1
Oxygen (by difference)	8.0	9.2	0.56
Sulfur	1.1	3.5	0.6
as sulfate	0.04	0.38	-
as pyrite	0.39	1.00	-
as organic	0.67	2.12	0.6
Solvent analysis			
Benzene insolubles			15.1
Asphaltene			39.8
Oil, n-pentane-soluble			45.1

TABLE 2.- Catalysts used in coal hydrogenation tests

Cat. No.	Catalyst or support supplier and supplier's identification	Particle description	Pore vol., cc/g	Sur-face area, m ² /g	AVG pore dia., Å	Support composition, wt pct			Wt of metal com-pound + support, wt%	Wt. of catalyst charged, g
						Al ₂ O ₃	SiO ₂	Other		
<u>Commercial Catalysts</u>										
1	Harshaw 0402T	1/8-in. tablet	0.40	200	80	Major	5.0	-	2.4 Co, 10.0 Mo	57.7
2	do.	do.	do.	do.	do.	do.	do.	do.	do.	27.0
3	do.	do.	do.	do.	do.	do.	do.	do.	do.	52.1
4	do.	-200 mesh	do.	do.	do.	do.	do.	do.	do.	57.7
5	do.	do.	do.	do.	do.	do.	do.	do.	do.	56.2
6	Grace-Davison SMR 7-3776	1/8-in. tablet	0.53	310	68	Major	-	-	3.2 Co, 10.8 Mo	33.6
	DHS-2	1/16-in. extrudate	0.57	170	135	Major	-	-	2.5 Ni, 10.0 Mo	41.5
7	American Cyanamid AERO HDS-3A	1/8-in. extrudate	0.49	130	150	Major	-	-	3.0 Ni, 12.0 Mo	40.5
8	American Cyanamid AERO HDS-9A	1/8-in. extrudate	0.21	55	155	Major	-	-	12.4 Fe	64.7
9	Strem Chemical 26-272	1/8-in. tablet	0.21	55	155	Major	-	-	12.4 Fe	64.7
<u>Bureau-Prepared Impregnated Catalysts</u>										
10	DOP	1/16-in. sphere	1.15	170	270	91.2	0.7	-	None	25.7
11	do.	do.	do.	do.	do.	do.	do.	do.	1 Mo	27.8
12	do.	do.	do.	do.	do.	do.	do.	do.	5 Mo	30.5
13	do.	do.	do.	do.	do.	do.	do.	do.	10 Mo	32.8
14	do.	do.	do.	do.	do.	do.	do.	do.	1 Sn	28.0
15	do.	do.	do.	do.	do.	do.	do.	do.	5 Sn	29.6
16	do.	do.	do.	do.	do.	do.	do.	do.	10 Sn	35.1
17	do.	do.	do.	do.	do.	do.	do.	do.	5 Ni	30.4
18	do.	do.	do.	do.	do.	do.	do.	do.	5 Co	33.5
19	do.	do.	do.	do.	do.	do.	do.	do.	5 Fe	31.4

1 Charged 25 cc.

2 Not presulfided.

3 Indiana #5 hvbb coal.

TABLE 2.- Catalysts used in coal hydrogenation tests (Cont.)

Cat. No.	Catalyst or support supplier and supplier's identification	Particle description	Pore vol., cc/g	Sur-face area, m ² /g	Avg pore dia., A	Support composition, wt pct			Wt of metal compound + support, wt% g	Wt of catalyst charged, g
						Al ₂ O ₃	SiO ₂	Other		
20	ALCOA H-151	1/8-in. sphere	0.46	290	63	90.0	1.7	-	1 Mo	45.7
21	-----	do.	do.	do.	do.	do.	do.	do.	5 Mo	50.6
22	-----	do.	do.	do.	do.	do.	do.	do.	5 Sn	48.4
23	-----	do.	do.	do.	do.	do.	do.	do.	5 Ni	56.4
24	-----	do.	do.	do.	do.	do.	do.	do.	5 Co	58.6
25	-----	do.	do.	do.	do.	do.	do.	do.	5 Fe	53.6
26	ALCOA F-1	8 x 12 mesh	0.52	230	90	92.0	0.1	-	5 Mo	57.2
27	-----	do.	do.	do.	do.	do.	do.	do.	5 Sn	56.8
28	-----	do.	do.	do.	do.	do.	do.	do.	5 Ni	62.0
29	-----	do.	do.	do.	do.	do.	do.	do.	5 Co	60.9
30	-----	do.	do.	do.	do.	do.	do.	do.	5 Fe	60.0
31	Houdry 511 CP	4-mm tablet	0.60	80	300	12.4	87.3	0.25 Na ₂ O	5 Mo	38.6
32	Houdry 24 CP	4-mm tablet	0.88	425	83	12.4	87.3	do.	5 Mo	32.7
33	Norton SA 101	1/8-in. tablet	0.27	0.13	8.3 x 10 ⁴	90.4	8.5	-	5 Mo	77.5
34	-----	do.	do.	do.	do.	do.	do.	do.	5 Sn	79.9
35	-----	do.	do.	do.	do.	do.	do.	do.	5 Ni	71.8
36	-----	do.	do.	do.	do.	do.	do.	do.	5 Co	66.3
37	-----	do.	do.	do.	do.	do.	do.	do.	5 Fe	69.5
38	Norton BC 132	1/8-in. tablet	0.31	0.04	31 x 10 ⁴	4.7	28.5	65.8 SiC	5 Mo	58.9
39	Norton LA 956	1/8-in. tablet	0.22	0.04	22 x 10 ⁴	99.3	0.4	-	5 Mo	72.3
40	Norton SA 5209	3/17-in. sphere	0.32	0.37	3.5 x 10 ⁴	87.0	11.7	-	5 Mo	54.7
41	Norton BS 131	1/8-in. tablet	0.28	1.23	0.9 x 10 ⁴	3.1	96.0	-	5 Mo	56.8
42	Carborundum AELT	1/8-in. tablet	0.17	0.11	6.2 x 10 ⁴	72.0	21.8	-	0.002 Mo	72.5
43	-----	do.	do.	do.	do.	do.	do.	do.	1 Mo	72.8
44	-----	do.	do.	do.	do.	do.	do.	do.	1 Sn	77.9
45	-----	do.	do.	do.	do.	do.	do.	do.	1 Ni	76.8
46	-----	do.	do.	do.	do.	do.	do.	do.	1 Co	76.9
47	-----	do.	do.	do.	do.	do.	do.	do.	1 Fe	73.7
48	Carborundum AEHT	1/8-in. tablet	0.41	0.08	21 x 10 ⁴	72.0	21.8	-	1 Mo	48.6
49	-----	do.	do.	do.	do.	do.	do.	do.	1 Sn	52.1
50	-----	do.	do.	do.	do.	do.	do.	do.	1 Ni	49.3
51	-----	do.	do.	do.	do.	do.	do.	do.	1 Co	50.4
52	-----	do.	do.	do.	do.	do.	do.	do.	1 Fe	51.0

TABLE 2.- Catalysts used in coal hydrogenation tests (Cont.)

Cat. No.	Catalyst or support supplier and supplier's identification	Particle description	Pore vol., cc/g	Sur-face area, m ² /g	Avg pore dia., Å	Support composition, wt pct			Wt of Metal compound + support, wt%		Wt of catalyst charged, g
						Al ₂ O ₃	SiO ₂	Other	Wt of metal compound	Wt support	
53	Carborundum SELT	1/8-in. tablet	0.37	0.23	6.4 x 10 ⁴	5.8	93.1	-	1 Mo		47.4
54	-----	-----	-----	-----	-----	-----	-----	-----	1 Sn		49.0
55	-----	-----	-----	-----	-----	-----	-----	-----	1 Ni		47.9
56	-----	-----	-----	-----	-----	-----	-----	-----	1 Co		46.2
57	-----	-----	-----	-----	-----	-----	-----	-----	1 Fe		48.2
58	Carborundum SEHT	1/8-in. tablet	0.56	0.70	3.2 x 10 ⁴	5.8	93.1	-	1 Mo		37.7
59	-----	-----	-----	-----	-----	-----	-----	-----	1 Sn		40.2
60	-----	-----	-----	-----	-----	-----	-----	-----	1 Ni		39.7
61	-----	-----	-----	-----	-----	-----	-----	-----	1 Co		40.2
62	-----	-----	-----	-----	-----	-----	-----	-----	1 Fe		38.4
63	Carborundum CELT	1/8-in. tablet	0.21	0.04	21 x 10 ⁴	11.2	26.9	58.6 SiC	1 Mo		64.0
64	-----	-----	-----	-----	-----	-----	-----	-----	1 Sn		61.0
65	-----	-----	-----	-----	-----	-----	-----	-----	1 Ni		61.8
66	-----	-----	-----	-----	-----	-----	-----	-----	1 Co		60.7
67	-----	-----	-----	-----	-----	-----	-----	-----	1 Fe		61.8
68	Carborundum CEHT	1/8-in. tablet	0.30	0.13	9.2 x 10 ⁴	11.2	26.9	58.6 SiC	1 Mo		54.6
69	-----	-----	-----	-----	-----	-----	-----	-----	1 Sn		56.0
70	-----	-----	-----	-----	-----	-----	-----	-----	1 Ni		54.2
71	-----	-----	-----	-----	-----	-----	-----	-----	1 Co		55.6
72	-----	-----	-----	-----	-----	-----	-----	-----	1 Fe		52.8
73	Norton BA 307	3/16-in. sphere	0.07	0.06	4.7 x 10 ⁴	92.7	6.0	-	1 Mo		89.0
74	-----	-----	-----	-----	-----	-----	-----	-----	1 Sn		91.8
75	-----	-----	-----	-----	-----	-----	-----	-----	1 Ni		93.5
76	-----	-----	-----	-----	-----	-----	-----	-----	1 Co		94.9
77	-----	-----	-----	-----	-----	-----	-----	-----	1 Fe		91.7
78	UOP	1/16-in. sphere	1.15	170	270	91.2	0.7	-	2.4 Co, 10 Mo		35.6
79	Same as catalyst 78 except catalyst calcined before sulfiding and 25 cc charged										17.8
80	ALCOA H-151	1/8-in. sphere	0.46	290	63	90.0	1.7	-	2.4 Co, 10 Mo		56.8
81	Same as catalyst 80 except catalyst calcined before sulfiding and 25 cc charged										28.4
82	Carborundum SELT	1/8-in. tablet	0.37	0.23	6.4 x 10 ⁴	5.8	93.1	-	2.4 Co, 10 Mo		47.4
83	UOP	1/16-in. sphere	1.15	170	270	91.2	0.7	-	5 Sn, 10 Mo		36.8
84	-----	-----	-----	-----	-----	-----	-----	-----			41.0
85	Harshaw 0402T	1/8-in. tablet	0.40	200	80	Major	5.0	-	5 Sn, 2.4 Co, 10 Mo		62.0

⁴ Impregnated in 2 steps.⁵ Impregnated in 3 steps.⁶ Sn impregnated on Harshaw Co-Mo 0402T.

TABLE 3.- Hydrogenation results
 Charge: 50 g coal, 75 g vehicle oil, 50 cc catalyst
 Conditions: 4,000 psi, 400° C, 30 minutes at temperature

Hydro- genation components Cat. and conc., No. wt pct	Conv. of organic benzene insols. charged, wt pct	Distribution of products, wt pct of moisture- and ash-free charge				Sulfur content of products, wt pct			
		Organic benzene insols.	As- phal- tene	Pentane soluble oil	Hydro- carbon gases	Benzene soluble oil	As- phal- tene	Pentane soluble oil	Benzene insols.
No catalyst used		36	36	24	0.6	0.50	0.53	0.46	0.88
1 2.4 Co, 10 Mo	63	18	27	53	1.8	0.15	0.21	0.13	2.01
2 do.	52	23	34	40	2.2	0.25	0.34	0.18	1.66
3 do.	39	29	31	37	1.4	0.28	0.33	0.24	1.14
4 do.	73	13	30	52	2.2	0.11	0.13	0.10	-
5 do.	74	12	28	53	2.8	0.24	0.32	0.20	4.2
6 3.2 Co, 10.8 Mo	44	27	22	47	1.1	0.16	0.34	0.07	-
7 2.5 Ni, 10 Mo	57	20	23	54	1.4	0.16	0.26	0.12	2.3
8 3.0 Ni, 12 Mo	57	21	24	53	1.8	0.14	0.28	0.08	1.6
9 12.4 Fe	49	25	40	32	1.4	0.45	0.51	0.37	1.34
10 None	20	38	30	28	1.0	0.49	0.53	0.45	0.86
11 1 Mo	50	24	27	46	2.1	0.35	0.43	0.31	-
12 5 Mo	64	17	34	45	1.0	0.32	0.34	0.30	1.93
13 10 Mo	64	17	30	50	1.1	0.27	0.33	0.24	-
14 1 Sn	77	11	36	48	1.7	0.36	0.43	0.30	-
15 5 Sn	80	9	36	52	2.4	0.39	0.43	0.36	-
16 10 Sn	71	14	29	55	1.9	0.45	0.55	0.34	-
17 5 Ni	68	15	36	44	1.4	0.35	0.36	0.34	2.03
18 5 Co	56	21	35	40	0.7	0.40	0.48	0.32	1.70
19 5 Fe	49	24	39	34	1.6	0.41	0.48	0.32	1.85

1 Charged 25 cc of catalyst.

2 Catalyst was not preulfidated.

3

Experiment made with Indiana #5 hvbb coal.

TABLE 3.- Hydrogenation results (Cont.)

Cat. and conc., No. wt pct	Hydro- genation components wt pct	Conv. of organic benzene insols. charged, wt pct	Distribution of products, wt pct of moisture- and ash-free charge						Sulfur content of products, wt pct					
			Total		Pentane soluble oil		Hydro- carbon gases		Benzene soluble oil		As- phal- tene		Benzene soluble oil	
			Organic benzene insols.	oil, benzene soluble	As- phal- tene	Pentane soluble oil	Hydro- carbon gases	Hydro- carbon gases	Benzene soluble oil	As- phal- tene	Pentane soluble oil	Benzene insols.		
20	1 Mo	44	26	70	28	42	2.2	0.31	0.47	0.21	-	-		
21	5 Mo	66	16	81	29	52	1.5	0.26	0.32	0.23	2.63	2.63		
22	5 Sn	50	24	73	33	40	1.2	0.47	0.54	0.41	1.42	1.42		
23	5 Ni	63	18	77	35	42	1.2	0.32	0.39	0.29	-	-		
24	5 Co	56	21	74	38	36	1.0	0.36	0.39	0.32	1.81	1.81		
25	5 Fe	55	21	74	39	35	1.1	0.46	0.52	0.40	-	-		
26	5 Mo	62	18	79	33	46	1.3	0.25	0.28	0.23	-	-		
27	5 Sn	74	12	83	33	50	2.1	0.40	0.52	0.31	-	-		
28	5 Ni	64	17	78	44	34	1.9	0.39	0.41	0.37	-	-		
29	5 Co	48	25	73	39	34	1.1	0.40	0.46	0.34	-	-		
30	5 Fe	42	28	69	33	36	0.9	0.45	0.55	0.37	-	-		
31	5 Mo	58	20	80	41	39	1.5	0.37	0.45	0.28	1.60	1.60		
32	5 Mo	58	20	77	37	40	2.3	0.36	0.42	0.31	1.49	1.49		
33	5 Mo	64	17	81	40	41	1.4	0.42	0.50	0.34	-	-		
34	5 Sn	72	14	84	40	44	2.0	0.32	0.37	0.27	2.9	2.9		
35	5 Ni	64	17	80	54	26	0.9	0.49	0.51	0.44	-	-		
36	5 Co	46	26	71	39	32	1.1	0.45	0.53	0.34	-	-		
37	5 Fe	45	29	70	35	35	1.6	0.42	0.50	0.33	4.2	4.2		
38	5 Mo	34	32	64	34	30	1.8	0.44	0.50	0.38	-	-		
39	5 Mo	43	27	71	38	33	1.2	0.44	0.46	0.41	2.15	2.15		
40	5 Mo	19	39	58	31	27	0.8	0.54	0.59	0.49	1.71	1.71		
41	5 Mo	43	27	69	32	37	1.4	0.44	0.50	0.39	1.66	1.66		
42	0.002 Mo	30	33	62	32	30	1.0	0.36	0.49	0.22	1.08	1.08		
43	1 Mo	32	32	64	33	31	1.4	0.44	0.47	0.41	1.26	1.26		
44	1 Sn	63	18	80	42	38	1.1	0.44	0.51	0.36	1.67	1.67		
45	1 Ni	35	31	66	36	30	1.2	0.46	0.50	0.41	1.11	1.11		
46	1 Co	35	31	66	40	26	0.6	0.47	0.50	0.39	1.07	1.07		
47	1 Fe	33	32	64	33	31	0.8	0.49	0.52	0.45	1.18	1.18		
48	1 Mo	27	35	62	34	28	0.7	0.51	0.55	0.46	0.95	0.95		
49	1 Sn	61	18	80	43	37	0.9	0.44	0.48	0.39	1.34	1.34		
50	1 Ni	31	33	66	40	26	0.7	0.45	0.49	0.40	1.08	1.08		
51	1 Co	35	31	67	37	30	0.4	0.47	0.57	0.35	1.15	1.15		
52	1 Fe	42	28	70	38	32	1.0	0.43	0.49	0.36	1.21	1.21		

TABLE 3.- Hydrogenation results (Cont.)

Cat. and conc., wt pct	Hydro- genation components	Conv. of organic benzene insols. charged, wt pct	Distribution of products,					Sulfur content of products, wt pct				
			wt pct of moisture- and ash-free charge	Total oil, benzene soluble	As- phal- tene	Pentane soluble oil	Hydro- carbon gases	Benzene soluble oil	As- phal- tene	Pentane soluble oil	Benzene insols.	
53	1 Mo	60	19	78	39	39	1.2	0.43	0.45	0.40	1.04	
54	1 Sn	52	23	75	41	34	1.2	0.46	0.52	0.40	1.41	
55	1 Ni	50	24	72	41	31	1.2	0.42	0.49	0.34	1.41	
56	1 Co	55	22	76	45	31	1.3	0.43	0.47	0.36	1.44	
57	1 Fe	26	35	62	31	31	0.5	0.51	0.53	0.48	1.02	
58	1 Mo	46	26	72	39	33	1.2	0.44	0.51	0.36	1.09	
59	1 Sn	54	22	75	36	39	1.0	0.38	0.50	0.28	-	
60	1 Ni	54	22	75	47	28	1.4	0.42	0.45	0.36	1.11	
61	1 Co	56	21	75	38	37	1.2	0.43	0.49	0.36	-	
62	1 Fe	46	26	72	35	37	1.3	0.44	0.48	0.40	1.29	
63	1 Mo	33	32	65	35	30	0.7	0.51	0.58	0.44	1.22	
64	1 Sn	49	24	74	36	38	1.4	0.51	0.59	0.44	1.37	
65	1 Ni	42	28	71	40	31	1.8	0.41	0.45	0.36	1.16	
66	1 Co	42	28	69	39	30	1.2	0.47	0.53	0.39	1.23	
67	1 Fe	37	30	70	40	30	0.5	0.48	0.56	0.38	1.23	
68	1 Mo	47	25	72	38	34	1.3	0.44	0.48	0.39	1.19	
69	1 Sn	51	23	74	37	37	1.2	0.50	0.59	0.41	1.40	
70	1 Ni	32	33	64	33	31	1.3	0.46	0.50	0.42	1.18	
71	1 Co	25	36	62	36	26	0.7	0.53	0.59	0.44	0.94	
72	1 Fe	41	28	69	39	30	1.4	0.48	0.53	0.41	1.14	
73	1 Mo	47	25	71	33	38	0.9	0.38	0.48	0.29	1.51	
74	1 Sn	54	22	76	34	42	1.6	0.48	0.58	0.40	1.40	
75	1 Ni	29	34	62	35	27	1.4	0.48	0.55	0.40	1.35	
76	1 Co	38	29	67	32	35	0.8	0.47	0.54	0.41	1.66	
77	1 Fe	44	27	71	40	31	1.0	0.43	0.50	0.34	1.75	
78	2.4 Co, 10 Mo	42	28	68	33	35	1.6	0.23	0.28	0.18	-	
79	do.	69	15	79	35	44	1.4	0.18	0.26	0.12	2.5	
80	do.	58	20	76	27	49	1.5	0.22	0.37	0.13	-	
81	do.	63	18	78	34	44	1.6	0.24	0.31	0.18	3.1	
82	do.	37	30	65	33	32	0.9	0.35	0.38	0.31	3.3	
83	5 Sn, 10 Mo	78	11	85	33	52	1.5	0.33	0.39	0.29	-	
84	5 Sn, 10 Mo.	77	11	86	25	61	1.8	0.31	0.37	0.29	-	
85	5 Sn, 2.4 Co, 10 Mo	67	16	83	31	52	1.8	0.36	0.24	0.29	3.3	

Organic Sulfur Compounds in Coal Hydrogenation Products

Sayeed Akhtar, A. G. Sharkey, Jr., J. L. Shultz, and P. M. Yavorsky

U.S. Department of the Interior
Bureau of Mines, 4800 Forbes Avenue
Pittsburgh, Pennsylvania 15213

INTRODUCTION

In the Bureau of Mines Synthoil process for converting coal to low-sulfur fuel oil, a slurry of coal in recycled oil is hydrodesulfurized in a turbulent-flow, fixed-bed reactor packed with pellets of Co-Mo/SiO₂-Al₂O₃ catalyst (1,2,3).¹ At 450° C and 2,000-4,000 psi, the coal is converted to a liquid, and sulfur is eliminated as H₂S. Of the two principal forms of sulfur in coal, the pyritic sulfur is eliminated completely while 60-80 percent of the organic sulfur is eliminated. In a previous experiment to determine the role of the catalyst in hydrodesulfurization, coal slurry was hydrotreated in a reactor packed with glass pellets. At 450° C and 2,000-4,000 psi, the pyritic sulfur was eliminated completely, but only 10-20 percent of the organic sulfur was eliminated. Clearly, the catalyst's role is in the elimination of organic sulfur. To facilitate the search for effective coal hydrodesulfurization catalysts, the organic sulfur compounds formed in the hydrogenation of coal have now been identified, and qualitative information on their relative ease of decomposition by Co-Mo/SiO₂-Al₂O₃ catalyst has been obtained.

EXPERIMENTAL

Fifty g samples of coals were hydrogenated for one hour in a rotating autoclave at 450° C and 4,000 psi. No vehicle oil or catalyst was added. The products were separated into light oil, heavy oil, asphaltene, and benzene insoluble fractions by conventional methods. The oils and asphaltene were analyzed for sulfur compounds with a Dupont 21 110B high-resolution mass spectrometer.² The spectra represented the portions of the samples vaporized at 300° C and 10⁻⁶ torr. Under these conditions, 100 percent of the light oils, about 60 percent of the heavy oils, and 55 percent of the asphaltenes vaporized.

The relative ease of decomposition of the organic sulfur compounds was determined by conducting 5-pass hydrodesulfurization experiments in the continuous fixed-bed reactor of the Synthoil process(3). The feed for the first pass was a slurry of coal in high-temperature tar while the feeds for the subsequent passes were the gross liquid products (liquid products + unreacted solids) from the preceding pass. The gross liquid products from each pass were sampled and analyzed for sulfur compounds by high-resolution mass spectrometry.

RESULTS AND DISCUSSION

The analyses of the Indiana #5 coal and the Homestead mine, Kentucky, coal used in this work are given in table 1. The Indiana #5 coal contained 3.4 percent sulfur, about two-thirds of which was organic, while the Kentucky coal contained 4.6 percent sulfur, about one-third of which was organic.

¹ Underlined numbers in parentheses refer to the list of references at the end of this report.

² Reference to a specific make of equipment is done to facilitate understanding and does not imply endorsement by the Bureau of Mines.

Hydrogenation of Coal Without Catalyst

The analysis of the products from the hydrogenation of coal without catalyst is given in table 2. About 94 percent of the Indiana #5 coal and 91 percent of the Kentucky coal were converted to benzene solubles and gases. The light and heavy oils together amounted to about 50 percent of the products and the asphaltenes to about 20 percent. The high conversion of coal may be noted. Although no catalyst was added, catalysis by coal ash or a product of the reaction may be involved.

Organic Sulfur Compounds in the Products of Hydrogenation

The organic sulfur compounds corresponding to the empirical formulas derived from high-resolution mass spectrometric data for the products of coal hydrogenation are given in table 3. In the products from Indiana #5 coal, 3 sulfur compounds were found in the light oil, 9 in the heavy oil, and none in the asphaltene. The asphaltene spectrum was not sufficiently resolved to identify sulfur compounds. In the products from Kentucky coal, 2 sulfur compounds were found in the light oil, 5 in the heavy oil, and 2 in the asphaltene both of which were also present in the heavy oil. Only 4 sulfur compounds were common to the products from the two coals. The most noteworthy feature about the compounds listed in table 3 is that, with the exception of diallyl sulfide, all are thiophene derivatives. The structural formula of the compounds shown in table 4 illustrate the relationship. Although organic sulfur in coal is believed to occur in several other forms in addition to thiophene, namely thiol, thioether, disulfide, and γ -thiopyrone (4), degradation sulfur compounds from them were not detected. Clearly, they were unstable at the experimental condition and decomposed without any externally added hydrodesulfurization catalyst.

Relative Ease of Decomposition of the Organic Sulfur Compounds by Co-Mo/SiO₂-Al₂O₃ Catalyst

Slurries of the Indiana #5 coal in high-temperature tar were hydrodesulfurized in multiple-pass experiments at 2,000 psi and 4,000 psi (see Experimental). Samples of the products from successive passes were analyzed for sulfur compounds. The results are presented in table 5. At 2,000 psi, the first pass product contained only 3 sulfur compounds: benzothiophene, dibenzothiophene, and naphthobenzothiophene. The second pass product also contained the three sulfur compounds but at lower concentrations. The third, fourth, and fifth pass products contained only benzothiophene and dibenzothiophene; naphthobenzothiophene was no longer detectable. At 4,000 psi, the first pass product contained a measurable concentration of dibenzothiophene and a trace of benzothiophene. The second, third, and fourth pass products contained progressively decreasing concentrations of dibenzothiophene and traces of benzothiophene. The results show that amongst the sulfur compounds formed in the hydrogenation of coal, the most difficult to decompose is dibenzothiophene followed by benzothiophene and naphthobenzothiophene. The remaining sulfur compounds of table 3 decompose readily compared to these three.

SUMMARY AND CONCLUSIONS

Bituminous coals from Indiana #5 seam and Homestead mine, Kentucky, were hydrogenated in a batch autoclave at 450° C and 4,000 psi without adding any catalyst. In one hour more than 90 percent of the coals were converted to benzene soluble liquids and gases. The liquid products contained 14 organic sulfur compounds, 13 of them thiophene derivatives. Their relative ease of decomposition was determined by repetitive hydrodesulfurization of coal slurries with Co-Mo/SiO₂-Al₂O₃ catalyst. Dibenzothiophene is most difficult to decompose, followed by benzothiophene and naphthobenzothiophene.

ACKNOWLEDGMENT

We are thankful to Walter Kawa for conducting the batch hydrogenation of coal, and to Dr. Leslie Reggel for assisting with the nomenclature of the organic sulfur compounds.

REFERENCES

1. Yavorsky, Paul M., Sayeed Akhtar, and Sam Friedman. Process Developments: Fixed-Bed Catalysis of Coal to Fuel Oil, presented at the 65th Annual AIChE meeting, Nov. 26-30, 1972, New York, N.Y.
2. Akhtar, Sayeed, Sam Friedman, and Paul M. Yavorsky. Low-Sulfur Liquid Fuels From Coal, presented at Symposium on Quality of Synthetic Fuels, ACS, April 9-14, 1972, Boston, Mass.
3. Akhtar, Sayeed, Sam Friedman, and Paul M. Yavorsky. Process for Hydrodesulfurization of Coal in a Turbulent-Flow, Fixed-Bed Reactor, presented at the 71st National meeting of the AIChE, Feb. 20-23, 1972, Dallas, Texas.
4. Given, P. H. and W. F. Wyss. The Chemistry of Sulfur in Coal. BCURA Monthly Bulletin, v. XXV, No. 5, May 1961, p. 166.

TABLE 1.- Analysis of coals, as received

	<u>Hvbb</u> <u>Indiana #5</u> <u>coal</u>	<u>Hvab</u> <u>Kentucky</u> <u>coal</u>
<u>Proximate Analysis, Wt Pct</u>		
Moisture	6.1	2.9
Ash	8.9	16.9
Volatile matter	38.6	36.5
Fixed carbon	46.4	43.7
<u>Ultimate Analysis, Wt Pct</u>		
Moisture	6.1	2.9
Ash	8.9	16.9
Carbon	67.0	63.4
Hydrogen	5.3	4.8
Nitrogen	1.4	1.3
Oxygen, by difference	7.9	6.1
Sulfur	3.4	4.6
as sulfate	0.37	0.13
as pyrite	0.98	3.03
as organic	2.07	1.44
<u>Calorific value, Btu/lb</u>	11,750	11,500

TABLE 2.- Analysis of the products of coal hydrogenation,
wt pct of moisture- and ash-free coal

	From Indiana #5 Coal	From Kentucky Coal
Light oils (Distillates to 105° C at 2-3 mm Hg)	17.4	13
Heavy oils (Solubles in benzene and n-pentane)	30.6	34
Asphaltenes (Soluble in benzene but in- soluble in n-pentane)	20.3	18
Organic benzene insolubles	5.8	9
Total	74.1	74
Balance (gaseous hydrocarbons, H ₂ S, NH ₃ , CO, CO ₂ , H ₂ O from make-water)	25.9	26

TABLE 3.- Organic sulfur compounds in the products of coal hydrogenation

	<u>Michigan No. 6</u>			Kentucky Coal		
	<u>m/e</u>	<u>Mol. Form.</u>	<u>Identification</u> ¹	<u>m/e</u>	<u>Mol. Form.</u>	<u>Identification</u> ¹
Light oil	134	C ₈ H ₆ S	Benzothiophene	98	C ₅ H ₆ S	Methylthiophene
	148	C ₉ H ₈ S	Methylbenzothiophene	114	C ₆ H ₁₀ S	Diallylsulfide
	162	C ₁₀ H ₁₀ S	Dimethylbenzothiophene			
Heavy oil	98	C ₅ H ₆ S	Methylthiophene	208	C ₁₄ H ₈ S	Benzo[def]dibenzothiophene
	138	C ₈ H ₁₀ S	Tetrahydrobenzothiophene	234	C ₁₆ H ₁₀ S	Naphthobenzothiophene
	174	C ₁₁ H ₁₀ S	Benzylthiophene	248	C ₁₇ H ₁₂ S	Methylnaphthobenzothiophene
	184	C ₁₂ H ₈ S	Dibenzothiophene	284	C ₂₀ H ₁₂ S	Dinaphthothiophene
	198	C ₁₃ H ₁₀ S	Methyldibenzothiophene	298	C ₂₁ H ₁₄ S	Methyldinaphthothiophene
	208	C ₁₄ H ₈ S	Benzo[def]dibenzo- thiophene			
	234	C ₁₆ H ₁₀ S	Naphthobenzothiophene			
	248	C ₁₇ H ₁₂ S	Methylnaphthobenzothiophene			
	284	C ₂₀ H ₁₂ S	Dinaphthothiophene			
Asphaltenes	<u>Spectrum not well resolved</u>			234	C ₁₆ H ₁₀ S	Naphthobenzothiophene
				284	C ₂₀ H ₁₂ S	Dinaphthothiophene

¹ Based upon molecular formula determined by high-resolution mass spectrometry. Other isomeric forms possible in some instances.

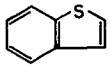
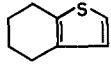
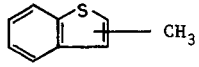
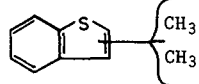
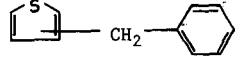
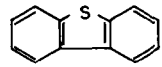
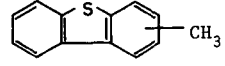
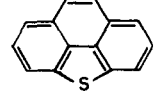
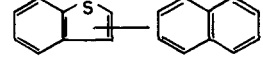
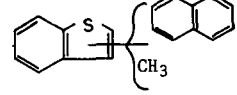
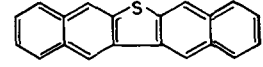
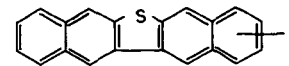
98	C_5H_6S		Methylthiophene
134	C_8H_6S		Benzothiophene
138	$C_8H_{10}S$		Tetrahydrobenzothiophene
148	C_9H_8S		Methylbenzothiophene
162	$C_{10}H_{10}S$		Dimethylbenzothiophene
174	$C_{11}H_{10}S$		Benzylthiophene
184	$C_{12}H_8S$		Dibenzothiophene
198	$C_{13}H_{10}S$		Methyl dibenzothiophene
208	$C_{14}H_8S$		Benzo[def]dibenzothiophene
234	$C_{16}H_{10}S$		Naphthobenzothiophene
248	$C_{17}H_{12}S$		Methyl naphthobenzothiophene
284	$C_{20}H_{12}S$		Dinaphthothiophene
298	$C_{21}H_{14}S$		Methyl dinaphthothiophene

TABLE 4.- Structural formulas of the organic sulfur compounds

TABLE 5.- Sulfur compounds in the products from
multi-pass hydrogenation of Indiana #5
coal with Co-Mo/SiO₂-Al₂O₃ catalyst

A. Operating pressure: 2,000 psi

<u>Compound</u>	<u>Concentration, as percent of ionization</u>				
	<u>I Pass</u>	<u>II Pass</u>	<u>III Pass</u>	<u>IV Pass</u>	<u>V Pass</u>
Benzothiophene	0.26	0.15	0.13	0.12	0.04
Dibenzothiophene	1.67	0.70	0.70	0.49	0.27
Naphthobenzothiophene	0.09	0.02	None	None	None

B. Operating pressure: 4,000 psi

<u>Compound</u>	<u>Concentration, as percent of ionization</u>			
	<u>I Pass</u>	<u>II Pass</u>	<u>III Pass</u>	<u>IV Pass</u> ¹
Benzothiophene	trace	trace	trace	trace
Dibenzothiophene	0.30	0.17	0.08	0.07

¹ Only 4 passes were conducted at 4,000 psi.

Low Sulfur Synthetic Crude Oil from Coal

M.I. Greene, L.J. Scotti, J.F. Jones

FMC Corporation
Princeton, New JerseyABSTRACT

Project COED (Char-Oil-Energy Development) was initiated in 1962 when the Office of Coal Research, Department of the Interior, contracted with the FMC Corporation to develop a process for upgrading coal to a synthetic crude oil (syncrude), a salable gaseous product and char. Successful operation of bench scale units led to the design, construction and operation of a 36 ton-per-day pilot plant at the FMC Corporation Chemical Research and Development Center in Princeton, New Jersey. The pilot plant has operated successfully since July, 1970.

The COED process consists of pyrolyzing pulverized, dried coal in a series of fluidized bed reactors. The oil vapors in the pyrolysis off-gases are condensed using a direct water quench. The oils are separated from the water, dried and filtered with a pressurized, rotary-drum precoat filter. Filtration removes carbonaceous dust from the pyrolysis oil prior to hydrotreating in a fixed-bed catalytic reactor containing commercial nickel-molybdenum catalyst. Hydrotreating at reaction conditions of 2500 psig and 750°F produces a low sulfur syncrude from the heavier oils recovered from the pyrolysis of coal. The syncrude can be used as a feedstock to a refinery or burned as a No. 4 fuel oil. Utilization of the syncrude for these purposes is presented here.

PYROLYSIS SECTION

A schematic of the COED process is shown in Figure 1. The dried and crushed coal is heated to successively higher temperatures in a series of fluidized beds. In each bed, a fraction of the volatile matter of the coal is released. The temperature of each bed is selected to be just below the maximum temperature to which the coal can be heated without agglomerating and defluidizing the bed. Typical operating temperatures of the fluidized beds are 600, 850, 1000 and 1600°F respectively. The number of stages and the operating temperature vary with the type of coal processed. Heat for the process is generated by burning some of the char in the fourth stage and then using the hot gases and hot recycle char as the source of heat for the other reactors. These hot fluidizing gases pass countercurrent to the char flow and collect volatile matter from the coal which is released as oil vapors and light hydrocarbon gases.

The pyrolysis recovery system is outlined in Figure 2. The product gas leaving the second stage reactor at 850°F is directly quenched with by-product water from the process. The condensed oil and water are separated in a decanter with the water recycled for cooling operations. The collected COED pyrolysis oil containing char fines is dried and filtered in a pressurized, rotary-drum precoat filter where solids are removed to give a filtrate with less than 0.1 weight percent solids. The filtered oil is the feed to the hydrotreating section of the pilot plant.

HYDROTREATING SECTION

The hydrotreating section is shown in Figure 3. The oil feed system to the hydrotreating section is kept at 250-300°F to keep the oil pumpable. This oil is pumped to 2500-3000 psig with plunger pumps

and mixed in a packed vessel (guard chamber) with hot recycle gas. The recycle gas has been superheated in a convective type furnace to a temperature that results in an oil-gas mixture temperature in the guard chamber of 700-750°F. The guard chamber serves several functions:

1. Provides for a direct contact heat transfer zone thereby eliminating the need for preheating the COED pyrolysis oil in small preheater tubes;
2. Allows for the partial removal of contaminants such as metals and coke thereby extending the life of the catalyst beds;
3. Minimizes system pressure drop losses by utilizing a high free volume packing material for the accumulation of coke and metal deposits.

The guard chamber effluents pass downflow through the reactor vessel containing two fixed-beds of nickel molybdate catalyst. The catalyst used in the pilot plant is American Cyanamid's Aero HDS-3 series, which contain 3.0 percent NiO and 15 percent MoO₃ on an alumina support. Both the 1/16-inch and 1/8-inch extrudates are used. The reactor vessel consists of a 12-inch diameter pipe, 25 feet long, with provision for an 8-foot catalyst bed in the upper section and a 12-foot catalyst bed in the lower section. Recycle hydrogen quench is provided between reactor stages to maintain the desired bed temperature profiles. High hydrogen-to-oil ratios (40M to 80M SCF/bbl) are used in the pilot plant for two reasons: (1) as a heat transfer agent to provide the sensible heat necessary to bring the COED oil to reaction temperatures and (2) as a diluent to control the temperature rises in the catalyst beds due to the exothermic heats of reaction. In the commercial unit, the high hydrogen-to-oil ratios can be reduced by using liquid product recycle as the diluent. For example, at 15,000 SCF per barrel fresh COED oil, liquid product recycle rates of 0.7 volumes recycle per volume fresh oil will result in an acceptable reactor temperature profile. Furthermore, this liquid recycle will decrease the concentration of metals in the feed to the reactors and thereby help to disperse the deposition of these metals more uniformly through the catalyst beds. Hydrogen is consumed by reacting with the sulfur, nitrogen, oxygen and the unsaturated hydrocarbons in the oil. Recycle hydrogen purity is controlled by purging a portion of the recycle hydrogen stream. Make-up hydrogen is fed on demand by a pressure controller to maintain the system pressure. The reactor effluents are cooled and liquid products recovered in two stages of heat exchange and flash vaporization. The syncrude is the liquid product mixture from the two flash drums.

Typical properties of the oil feed to hydrotreating are shown in Table 1. The filtered pyrolysis oil must be hydrotreated in order to remove contaminants such as sulfur, nitrogen and oxygen. At the same time that these contaminants are removed, the viscosity, pour point and API gravity of the oil are upgraded. Successful hydrotreating operations have been carried out with pyrolysis oils derived from Colorado Bear, Utah King, Wyoming Big Horn and Illinois No. 6-seam coals. The former two coals are representative of low sulfur, Western, high volatile B bituminous coals. Wyoming Big Horn is representative of a low sulfur, Western, sub-bituminous coal. Illinois No. 6-seam coal is a C bituminous coal. Typical hydrotreating operating conditions are shown in Table 2.

The COED process produces a full distillate range syncrude - 100°F to 900°F - which is suitable as either a refinery feedstock or

as a source of various fuel and chemical products. Various synthetic fuels can be derived from fractionation and further processing of syncrude cuts. The properties of the various syncrude products presented are based mostly on one representative sample of a full-range syncrude derived from Illinois No. 6-seam coal.

FUEL TYPES AND YIELDS

Typical yields, distillation data and hydrocarbon type analyses of four syncrudes are shown in Table 3. Syncrudes derived from Western coals result in much higher paraffinic (24% vs. 10%) content and lower aromatic content (34% vs. 48%) than the Illinois type coals. The distillation fractions shown were chosen to simulate the following fuel types:

IBP-180°F	Fuel Gas
180-390°F	Gasoline
390-525°F	Jet Fuel
	Diesel Fuel
390-650°F	No. 2 Oil
390-EP	No. 4 Oil
	Stationary Turbine Oil
650-EP	No. 6 Oil

Although the fuel fractions from COED syncrude do not meet all the ASTM specifications, they do meet the basic requirements. Additional refining and processing will, in most cases, result in a finished product meeting all the required specifications. When the specifications are not met, syncrude fuels can be blended with petroleum fuels to meet the desired specifications. Alternatively, new specifications can be generated for the syncrude fuels such that these fuels can be adapted to existing furnaces and engines. A typical refinery product slate when feeding on an Illinois No. 6-seam syncrude is shown in Table 4. The maximum product yields occur in the middle distillate range which amounts to about 50 volume percent of the COED syncrude.

EXPERIMENTAL EVALUATION OF SYNCRUDE

FMC Corporation subcontracted with AtlanticRichfieldCompany (ARCO) to evaluate a COED syncrude derived from an Illinois No. 6-seam coal as a potential refinery feedstock. The studies were performed in laboratory and pilot plant equipment and included:

1. Fractionation of the full range syncrude
2. Hydrogen pretreatment and reforming of the naphtha fraction of syncrude
3. Evaluation of middle distillate fractions as jet, diesel, home heating and industrial heating fuels
4. Fluid catalytic cracking of the residual fraction of syncrude
5. Hydrocracking of the residual fraction of syncrude.

The detailed processing sequence used by ARCO is outlined in Figure 4. In some cases, particular fuels from syncrude fail to meet some of the ASTM specifications but these fuels are still valuable as blending feedstocks with available specification petroleum-derived fuels. The required blending ratios can be determined from existing correlations when actual experimental data is not available. The major specification not

achieved is API gravity owing to the high aromaticity of the coal-derived oil. In this case, an on-specification fuel blend is confidently obtained by volumetric blending of the syncrude fuel with the petroleum fuel. The following is a summary of the experimental evaluations performed by ARCO.

Naphtha Evaluation

Naphthas derived from syncrude contain about 73 percent naphthenes, 7 percent paraffins and 20 percent aromatics with about 100 ppm each of sulfur and nitrogen. The high naphthenic content results in excellent reformer feedstock once the sulfur and nitrogen impurities are removed to prevent poisoning the noble metal reforming catalyst. A hydrogen pretreatment is therefore required to obtain a clean reformer feedstock. The reforming operation with this feedstock results in extremely low aging rates compared to processing conventional petroleum naphthas. The reformate produced had better than 100 Research Octane Number Clear (RONC) and resulted in a material with 80 percent aromatics content.

Middle Distillate Evaluation

The middle distillate range of COED syncrude is highly aromatic and consequently does not have all the desired properties of jet and diesel fuel. However, hydroprocessing of these fractions results in obtaining reasonable product quality, such that middle distillates derived from syncrude can be blended with available petroleum distillates to make a specification fuel. More severe hydrotreatment of the syncrude middle distillates results in acceptable diesel fuels, No. 4 oils, stationary turbine fuels and No. 2 oils with little or no blending necessary.

Cracking of Residuum

Hydrogen pretreatment of the 650°F to end point fraction of syncrude is required prior to fluid catalytic cracking (FCC) and fixed-bed hydrocracking operations. This is necessary to protect the cracking catalysts from deactivators such as nitrogen and polynuclear aromatics. With both the FCC and hydrocracking operations, additional fuel gas, naphthas and middle distillates are produced from the residual fraction of syncrude. The residuum from the cracking operations of the 650°F to end point fraction of syncrude can be used as a very low sulfur No. 6 fuel oil.

PROPERTIES OF SYNCRUDE FUELS

Gasoline

After reducing the sulfur content of the COED naphthas to 1-2 ppm, the catalyst aging rates for reforming the COED naphthas are extremely low compared to those with petroleum-derived naphthas. This should allow reforming operations for producing high octane reformates to be carried out without the need for severe, high pressure pretreatment. Hydrogen production and C₅ to end point (C₅+) yields from COED naphthas were extremely high compared to conventional petroleum reforming. C₅+ reformate yields were in excess of 90 volume percent with Research Octane Number Clear levels between 99 and 102.

Additional naphtha feedstocks for reforming are produced by fluid catalytic cracking and fixed-bed hydrocracking of the 650°F to end point fraction of syncrude. Table 5 shows a summary of yields and type analyses

of naphthas derived from syncrude. It can be seen from the table that syncrude is an excellent source of high octane material for either the leaded or unleaded gasoline pool. In a typical refinery feeding on syncrude, approximately 34 volume percent of the syncrude feedstock can be converted to acceptable, low sulfur, high octane gasoline.

Fuel Oils

The full range syncrude, the middle distillate fractions and the residual fraction of syncrude can be used either as straight run fuels or as blending fuels with conventional petroleum fuels. The properties of ASTM No. 2, No. 4 and No. 6 fuel oils are compared with various syncrude fractions in Table 6.

The 350-End Point fraction of syncrude was burned as fuel oil in a laboratory burner test. The stack gas emissions were extremely low and the fuel closely resembled that of a No. 2 grade oil. Particular significance of the emissions tests as outlined in Table 7 is the reduction in particulate emissions compared to that of a typical asphaltic No. 4 residual fuel. SO_x , NO_x and hydrocarbons emissions are also appreciably lower for syncrude. This fuel oil fraction was also determined to be an acceptable No. 4 oil as regards storage stability. Syncrude was stable with regard to the production of insoluble sludges and varnish as shown in Table 8. Even after exposure to air at 150°F for two months, only moderate deterioration occurred. The ASTM compatibility ratings indicate that there is no problem involving precipitation of insoluble sludges when blending with paraffinic straight run diluents such as might be done at dockside when blending to meet marine diesel quality.

Engine Fuel

Engine fuels such as JP-5 jet fuel and No. 4-D diesel fuel can be derived from syncrude but with additional hydroprocessing required. The middle distillate fractions of syncrude, in particular, the 390-525°F fraction and the 390-650°F fractions, are applicable to these types of fuels. One of the key factors regarding the quality of engine fuels is the degree of aromaticity which adversely affects such properties as smoke point, luminometer number, specific gravity and cetane number. Middle distillate fractions of syncrude are higher in aromatics than petroleum distillates and are, therefore, unsuitable as engine fuels. However, severe hydrotreatment can result in enough saturation to decrease the aromatics level to less than a few percent. Comparisons of ASTM specification jet and diesel fuels respectively with various middle distillates derived from an Illinois No. 6 syncrude are shown in Tables 9 and 10. The last column on each table lists properties of a middle distillate fraction derived from syncrude that was hydroprocessed in a bench-scale unit. Although all specifications were not achieved, other hydroprocessing conditions might result in a satisfactory JP-5 jet fuel or diesel fuel product. In either case, the syncrude products, with their exceedingly low sulfur content, should serve as suitable blending fuels with conventional petroleum fuels. Yields and aromatics levels for syncrudes from four different coals are shown in Table 11. Western coals, such as Utah King, result in syncrude middle distillate fractions with less than half the aromatics content of middle distillates derived from Illinois No. 6 syncrude. These oils should indeed be more suitable for engine fuel production and would most assuredly result in less severe hydroprocessing conditions necessary to meet fuel specifications.

CONCLUSIONS

The COED process has been successfully demonstrated on a pilot-plant scale resulting in the upgrading of coal to three salable products--gas, char and a low sulfur synthetic crude oil. The syncrude can be further processed in a refinery to produce more valuable products such as gasoline and chemicals. Alternately, the raw syncrude can be fractionated into a range of fuel products suitable for straight run usage or as blending fuels with conventional petroleum fuels. The extremely low sulfur content of syncrude products, when the latter are used as blending stocks, has the resultant effect of upgrading the value of available high sulfur petroleum fuels. The value of syncrude on a dollar per barrel basis when utilized in a petroleum refinery is presently being determined by Chem Systems, Inc.

ACKNOWLEDGMENT

The authors acknowledge the guidance and support from the Office of Coal Research. Their contributions of technical support and funding have helped make the COED pilot plant operations a success. Additional acknowledgment is given to the AtlanticRichfieldCompany and the American Oil Company for their technical expertise in their laboratory evaluation of the COED syncrude product.

FIGURE 1

COED COAL PYROLYSIS

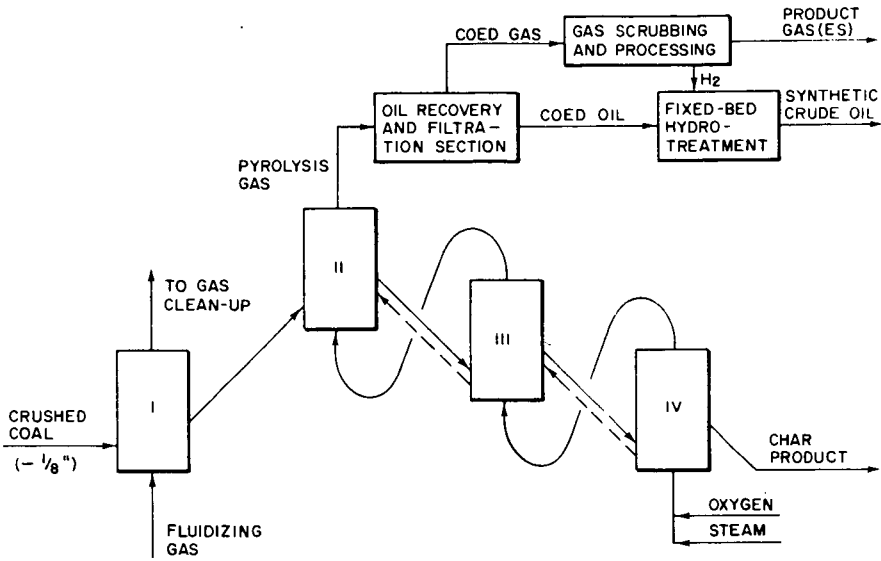


FIGURE 2

COED OIL RECOVERY SYSTEM

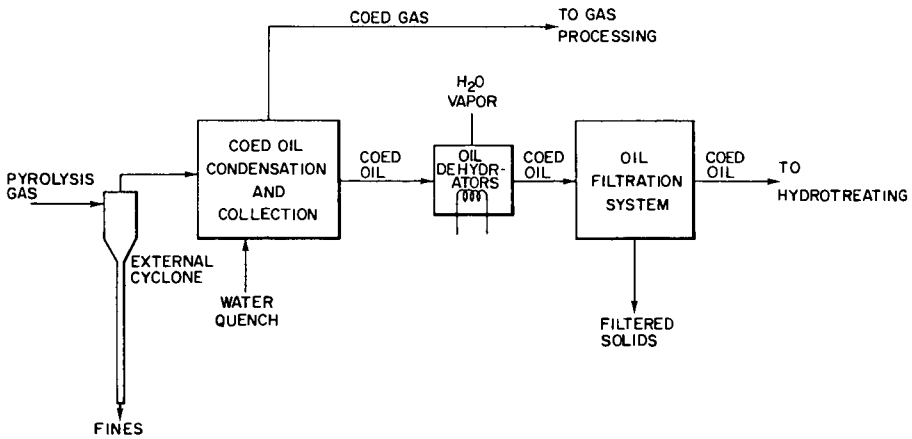
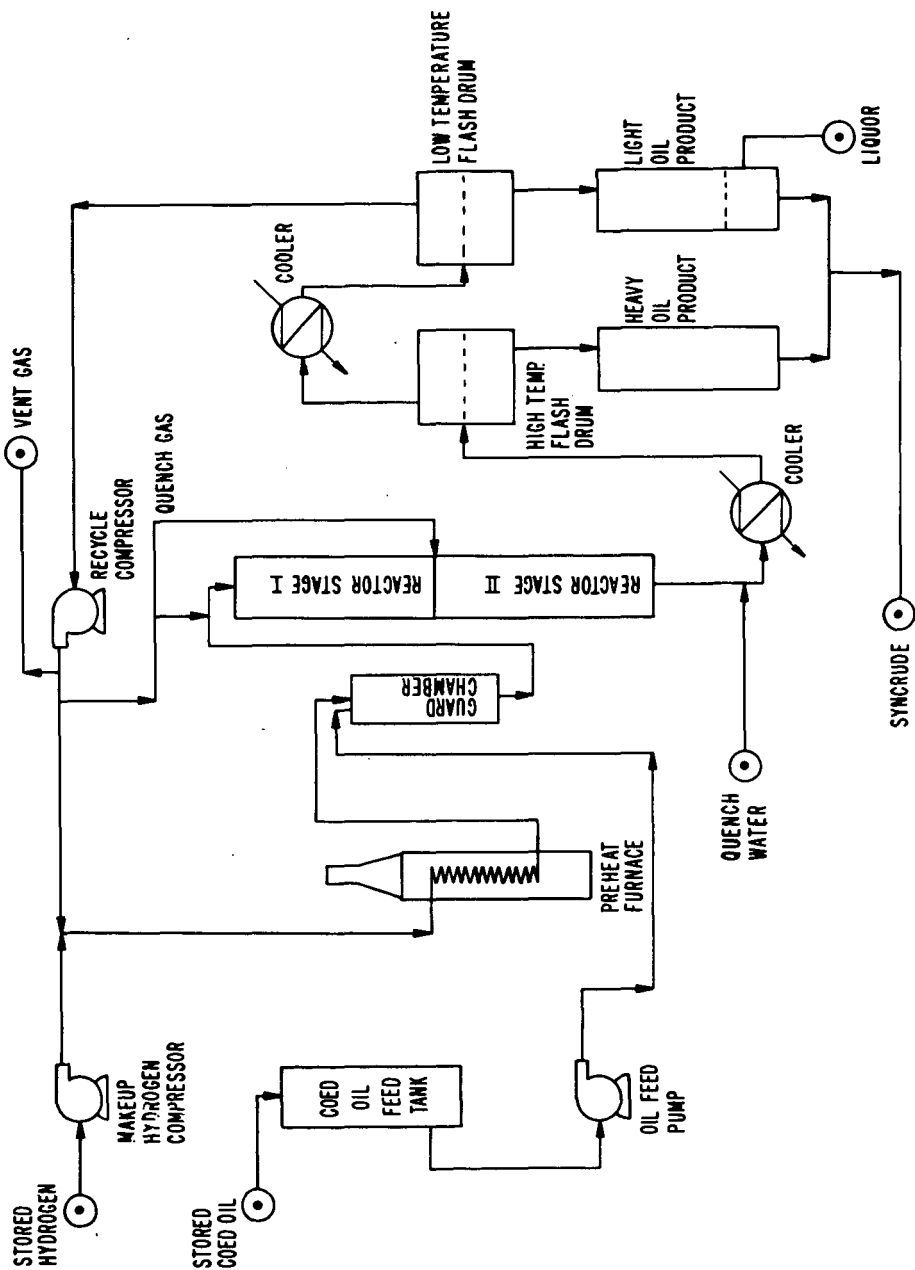


FIGURE 3
SCHEMATIC OF HYDROTREATING SECTION



PROCESSING SEQUENCE

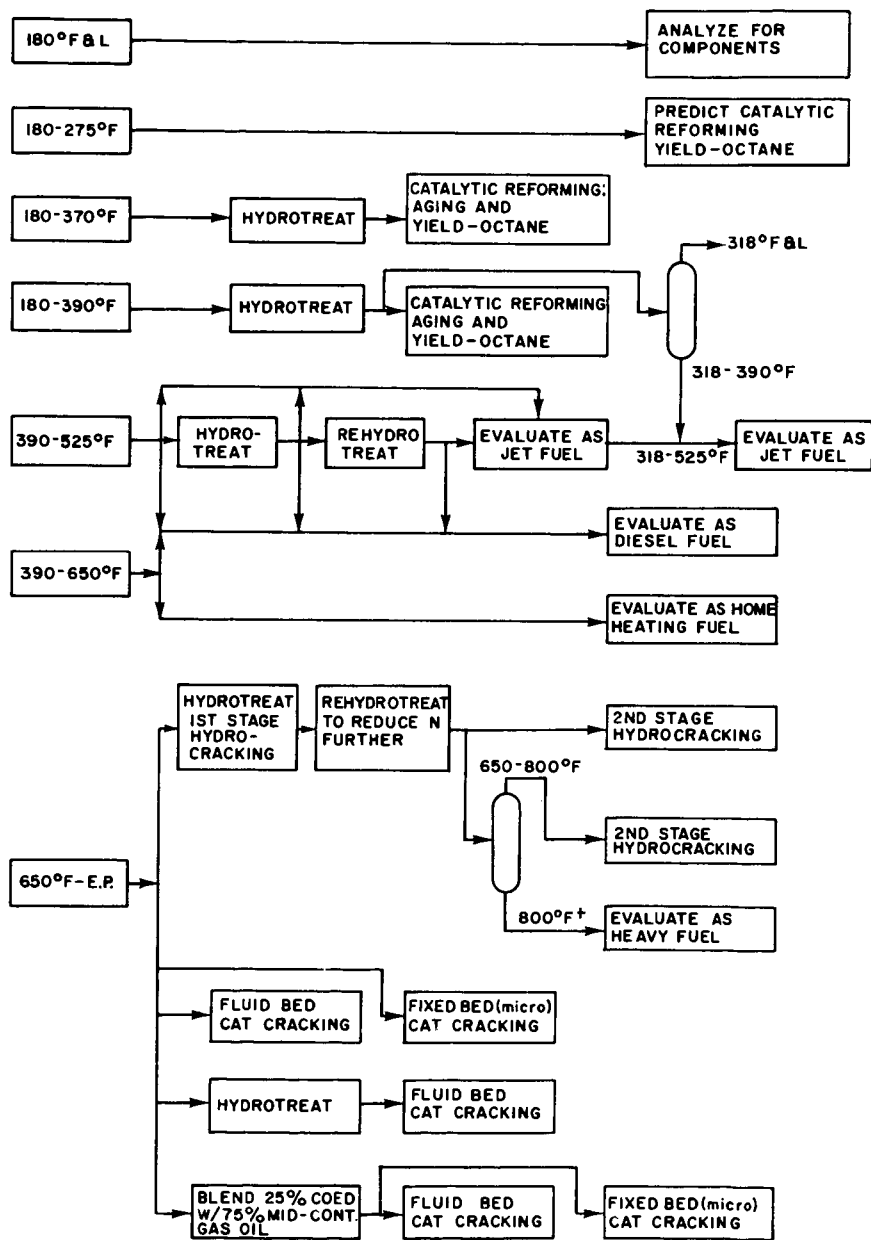


TABLE 1

Typical Properties of Hydrotreating Feed Oils

Coal Source	Colorado	Utah	Wyoming	Illinois
	Bear	King	Big Horn	No. 6-Seam
<u>Properties of Derived Oil</u>				
<u>Elemental Analysis</u>				
Weight & dry				
Carbon	83.6	83.7	82.7	80.5
Hydrogen	8.3	8.6	8.0	7.0
Nitrogen	1.1	1.0	1.0	1.2
Sulfur	0.4	0.2	0.6	2.0
Oxygen	6.6	6.5	7.5	9.2
Ash	0.0	0.0	0.2	0.1
API Gravity, 60°F	-4	-3.5	-4	-4
Moisture, Weight %	0.2	0.1	0.4	0.2
Pour Point, °F	108	130	120	115
Viscosity, SUS 210°F	1090	390	228	1333

TABLE 2TYPICAL PILOT PLANT HYDROTREATING OPERATING CONDITIONS

Illinois No. 6-seam Coal Derived Oil

Catalyst:	NiMo on Alumina extrudates
Pressure:	1750-2500 psig
Temperature:	700-800°F
Space Velocity:	0.3-0.6 lb. oil/hr./lb catalyst
Gas Recycle Rate:	40M to 80M SCF/bbl
Gas Recycle Concentration:	90-95% H ₂
Hydrogen Consumption:	3500 SCF/bbl

TABLE 3

COED SyncrudesTypical Yield, Distillation Data and Hydrocarbon Type Analyses

<u>Coal Source</u>	<u>Illinois No. 6</u>	<u>Colorado Bear</u>	<u>Utah King</u>
Hydrocarbon Type Analysis, Lvol %			
Paraffins	10.4	(2)	23.7
Olefins	NIL	(2)	NIL
Napththenes	41.4	(2)	42.2
Aromatics	48.2	(2)	34.1
API Gravity, 60°F	28.6	24.4	28.5
ASTM Distillation, °F			
Initial Boiling Point (IBP)	108	200	260
50% distilled	465	540	562
End Point (EP) (1)	746	840	868
Fractionation			
Yields, wt. %			
IBP-180°F	2.5	0	0
180-390°F	30.2	28.0	5.0
390-525°F	26.7	22.0	35.0
390-650°F	51.0	50.0	65.0
650-EP	16.2	22.0	30.0
390-EP	67.2	72.0	95.0

(1) 95% except for Illinois No. 6 which is 98%

(2) Componential analyses not available

TABLE 4

COED SYNCRUDE

Typical Refinery Product Slate

Basis: 100 bbl. of Syncrude from Illinois No. 6-seam coal

<u>Fraction</u>	<u>Yields, bbl.</u>		<u>End Use</u>
	<u>FCC (1)</u>	<u>HC (2)</u>	
Hydrogen, SCF	18000	6000	Hydrocracking
Initial Boiling Point-180°F	10.0	8.5	Liquefied Petroleum Gas, Refinery Gas
180-390°F	33.8	34.5	Gasoline
390-650°F	51.6	52.1	Middle Distillate Fuels (Jet, Diesel, No. 2)
650-End Point	2.8	3.1	Residual Fuel (No. 6)

- (1) With Fluid Catalytic Cracking operation on 650-end point fraction of syncrude.
- (2) With Hydrocracking operation on 650-800°F fraction of syncrude.

TABLE 5

COED NAPHTHAS

Source: Syncrude From Illinois No. 6-Seam Coal

Hydrocarbon Type Analysis, Liquid Volume %, Basis COED Syncrude	Raw Naphtha	Pretreated Reformer Feedstock	Reformate (1) (C ₅ +)	Cat (2) Naphthas	Hydrocracked (3) Naphthas
Paraffins	2.3	2.3	3.3	2.3	1.1
Naphthenes	23.7	24.4	1.6	2.3	4.5
BTX (6) and Alkylbenzenes	6.6	6.3	25.7	1.6	0.2
Indans/Tetralins	0.7	0.3	NIL	NIL	0
Olefins	NIL	0	0	2.0	0
API Gravity, 60°F	44	44	34	50	50.6
Sulfur, ppm	93	<1	<1	10	<10
Research Octane No. clear	70	--	99.5	87.4	100 (4)
Research Octane No. leaded	--	--	--	96.4	--
<u>Yields, Basis COED Syncrude</u>					
H ₂ (SCF/bbl. Syncrude)	--	-100	+1500	--	--
C ₅ + (Liquid Volume %)	33.3	33.3	30.6	8.0	4.9 (5)

228

- (1) Gasoline produced by reforming 180-390°F fraction of syncrude.
- (2) Gasoline produced by fluid catalytic cracking of 650-end point fraction of syncrude.
- (3) Naphthas produced by hydrocracking 650-end point fraction of syncrude.
- (4) Predicted RONC for hydrocracked naphtha after reforming over platinum catalyst.
- (5) Predicted yield of hydrocracked naphtha reformate product.
- (6) Benzene, Toluene, Xylene

TABLE 6

SYNCRUDE FUEL OILS

Comparisons with ASTM Specifications

Test	350-End Point Fraction	ASTM No.4	390-650°F Fraction	ASTM No.2	650-End Point Fraction	ASTM No.6
Flash Point, °F	160	130 min.	215	100 min.	400	150 min.
Pour Point, °F	+25	20 max.	-70	20 max.	70	---
Ash, Weight %	0.007	0.10 max.	0.0	---	---	---
Sulfur, Weight %	0.16	0.30 max.	0.004	0.30 max.	0.07	---
Water & Sediment, %	0.10	0.5 max.	---	0.05 max.	---	2.0 max.
Gravity, °API, 60°F	18.4	---	22.5	30 min.	11.2	---
Viscosity, SUS 100°F	52.5	45-125	39.3	32.6-37.9	---	900-9000
Carbon Residue (1)	0.4	---	---	0.35 max.	1.13	---
ASTM Distillation, °F						
Initial Boiling Point	354	---	436	---	557	---
10% distilled	409	---	459	460 max.	705	---
90% distilled	780	---	586	540-640 max.	870	---
End Point	---	---	613	660 max.	---	---

(1) Conradson Carbon Residue Test, ASTM D-189

TABLE 7
COED SYNCRUDE
Fuel Oil Stability Test

	<u>Fresh</u>	<u>Stored (1)</u>
ASTM D-2781 Compatibility Rating (2)	2	2-3
0.8 μ Millipore Filter Residue, Weight %	0.01	0.01, 0.03
ASTM D-1661 Thermal Stability Rating	1-2	2

-
- (1) Two months at 150°F, vented to air.
- (2) As mixed with equal volumes of 350-650°F petroleum distillate. Same rating was observed with 100% coal liquid. Spot No. 2 is defined as "Faint or poorly defined inner ring"; No. 3 is "Well defined, thin, inner ring, only slightly darker than the background." A No. 3 rating or above indicates that a fuel may cause problems in field applications.

TABLE 8
SYNCRUDE FUEL OILS
390-End Point Fraction of Syncrude
Emissions Levels Measurements

<u>Test</u>	<u>Result</u>	<u>Typical No. 4 Residual Fuel</u>
Particulates, lbs./100 gal.	4.6	19.2
Gaseous Contaminants, ppm		
SO _x	60	490
NO _x	53	95
CO	4.5	6.0
HC	3.0	7.1

Test Conditions

Fuel was burned in a small industrial burner firing a 1.5 million Btu/hr. boiler. Stack gas is controlled at 12.5% CO₂, approximately equivalent to 25% excess air and stack temperature is held at 500°F to 510°F.

TABLE 9

COED SYNCRUDE

Comparison of JP-5 Jet Fuel Specifications with Syncrude

<u>Properties</u>	<u>JP-5</u>	<u>390-525°F Fractions</u>	
		<u>As Distilled</u>	<u>2 Stage HDS (1)</u>
ASTM 10% Distillation point, °F	400 maximum	436	412
ASTM Distillation End point, °F	550 maximum	530	526
Gravity, °API, 60°F	36-48	25.7	33.2
Sulfur, Weight %	0.4 maximum	0.007	0.001
Freezing Point, °F	-51 maximum	<-70 (2)	<-80 (2)
Net Heating Value, Btu/lb.	18300 minimum	18070 (2)	18390 (2)
Aniline Gravity Product (3)	4500 minimum	1490	4501
Aromatics, Liquid Volume %	25 maximum	60.7	0 - 5
Olefins, Liquid Volume %	5 maximum	0	0
Smoke Point (4)	19 minimum	10	22
Luminometer Number (5)	50 minimum	20.4 (2)	43.6 (2)
Flash Point	140 minimum	186	156
Copper Corrosion Test (6)	1	1	---

(1) After hydroprocessing of 390-525°F syncrude fraction.

(2) Calculated

(3) A measure of the aromaticity of an oil.

(4) A measure of the smoke and soot-producing characteristics of jet fuels.

(5) A measure of the flame temperature of jet fuels.

(6) A measure of the corrosiveness of oil to copper, a "1" designation indicates slight tarnish.

TABLE 10

COED SYNCRUDE

Comparison of Diesel Fuel Specifications with Syncrude Middle Distillates

Properties	ASTM-No. 4-D Specifications	As Distilled			390-525°F Fraction 2 Stage HDS (l)
		390-650°F	525-650°F	390-525°F	
Pour Point, °F	0 Maximum	-70	-20	<-80	<-80
Flash Point, °F	130 Minimum	215	300	186	156
Sulfur, Weight %	Legal	<.001	<.001	.007	<.001
ASTM Distillation, °F					
10% distilled	460 Maximum	459	562	436	412
50% distilled	--	(5)	588	455	437
90% distilled	620 Maximum	586	626	494	483
100% distilled	660 Maximum	613	(5)	530	(5)
Gravity, °API, 60°F	33 - 37	22.5	19	25.7	33.2
Cetane Number (3)	30 Minimum	18	24	23.0	>30 (2)
Aniline Point, °C (4)	--	(5)	(5)	14.3	58.2
Aromatics, Liquid Volume %	--	(5)	(5)	58.3	5.2

233

- (1) After hydroprocessing of 390-525°F fraction of syncrude.
- (2) Estimated
- (3) A measure of the ignition quality of diesel fuel.
- (4) A measure of the aromaticity of oil.
- (5) Not measured.

TABLE 11

COED SYNCRUDE

Middle Distillate Fractions

<u>Syncrude Source</u>	<u>Yields, Liquid Volume</u> <u>390-525°F Fraction</u>	<u>& Basis Syncrude</u> <u>390-650°F Fraction</u>	<u>Gravity</u> <u>°API, 60°F(1)</u>	<u>Liquid Volume &</u> <u>Aromatics (1)</u>
Colorado Bear	25	47	30.1	45.1
Utah King	40	75	33.0	29.8
Illinois No. 6-seam	24	51	25.7	60.7

(1) For 390-525°F fraction of syncrude only.

COAL LIQUEFACTION IN A SLURRY SYSTEM, S. A. Qader, G. Haider, W. H. Wiser, Department of Mining, Metallurgical and Fuels Engineering, University of Utah, Salt Lake City, Utah 84112.

Coal impregnated with catalysts was slurried with a coal derived oil and liquefied in a stirred tank reactor in the temperature range 425-475°C under hydrogen pressure of 3000-4000 psi. Coal conversions of 90-95 percent were obtained and oils containing 0.6-0.9 percent sulfur were produced from coals containing 2.1-3.5 percent sulfur. The catalytic activity varied in the order stannous chloride > ammonium molybdate > zinc chloride. However, ammonium molybdate was found to have better selectivity and product obtained with stannous chloride was found to be of better quality. Regenerability of the spent catalysts was found to be poor.

SOLVENT REFINING OF COAL - A PROGRESS REPORT. W. B. Harrison and E. L. Huffman,
Southern Services, Inc., P. O. Box 2625, Birmingham, Alabama 35202

In collaboration with other investor-owned electric utilities which are members of the Edison Electric Institute, Southern Services has constructed and is now operating a 6 ton per day pilot plant for further developing the solvent refining process for coal. The principal purpose is to produce a "clean" utility fuel from coal such that abundant domestic reserves can be utilized in a manner compatible with environmental regulations. The process first involves dissolving coal in a coal-derived solvent (anthracene oil) under elevated temperature and pressure in a hydrogen atmosphere. The undissolved matter, containing pyritic sulfur, is then separated from the coal solution, and the organic sulfur is partly removed as hydrogen sulfide. Solvent is recovered from the remaining coal solution and recycled, leaving a fuel product which can be used directly as a hot liquid, or cooled and handled as a solid. This project is dedicated to studies for improving the solid separation and the product solidification steps of the process, and operating experience gained is expected to be useful to the larger pilot plant (50 tons per day) being constructed by Pittsburg and Midway Coal Mining Company under sponsorship of the Office of Coal Research, featuring the same basic process.